# ROLE OF OCRL1-DEPENDENT SIGNALING ABNORMALITIES AND MUTATION HETEROGENEITY IN LOWE SYNDROME CELLULAR PHENOTYPES

by

**Swetha Ramadesikan**

**A Dissertation**

*Submitted to the Faculty of Purdue University*

*In Partial Fulfillment of the Requirements for the degree of*

**Doctor of Philosophy**


Department of Biological Sciences

West Lafayette, Indiana

August 2020

**THE PURDUE UNIVERSITY GRADUATE SCHOOL**

**STATEMENT OF COMMITTEE APPROVAL**

**Dr. R. Claudio Aguilar, Major Professor**

Dept. of Biological Sciences

**Dr. Donna Fekete**

Dept. of Biological Sciences

**Dr. Philip Low**

Dept. of Chemistry

**Dr. Donald Ready**

Dept. of Biological Sciences

**Approved by:**

Dr. Janice Evans

*Dedicated to Appa and Claudio- You both inspire me every day with your never-ending enthusiasm for science and life.*

# ACKNOWLEDGMENTS

A PhD is intellectually and emotionally demanding, yet a rewarding experience. And it takes a village to help you through it. Bear with me, as I acknowledge my village who played a significant part in my journey. For something as monumental as this moment, a mere thank you will not suffice, so read on.

My parents, both doctors, were kind but firm, constantly telling me to 'do well in school' and that became the cornerstone of most of my childhood. Despite growing up in the midst of copious amounts of science and medicine at home, I was not immediately taken to the field but it took many years of slow but steady liking before I decided to major in Bioengineering. Soon, I identified areas of biology that fascinated me, thanks to Dr. Thiagarajan Raman, a kind professor at SASTRA whose classes I still wish I could go back to. However, it took me a while before I decided to pursue graduate school. The Dean at SASTA University, Dr. Vaidhyasubramaniam Sethuraman must be credited for the 'stern' but well-intentioned encouragement he gave me to apply to a semester abroad program. The rest, as they say, is history? To both, I will be grateful for spotting me and nudging me towards a life-changing experience.

I am also grateful to my first research mentor, Dr. Venkata Sabbisetti for pushing me into the deep end of the pool when it came to research, with a lot of faith and confidence. The lessons I learnt from him and the Bonventre lab, during my semester abroad program and the year after have been invaluable.

The past 7 years in Purdue, most of which I spent in Claudio's lab have left a deep impression in my life. I am not one for superlatives, for I am certain that I will continuously be shaped by my environment, my experiences and the people I meet during my lifetime. However, working with Claudio will remain *THE MOST* profound, life-changing experience I never imagined I would have. I remember, as clear as day, the series of emails I exchanged with him back in Spring 2013, requesting an appointment during my campus visit and subsequently being invited to have lunch with the lab. The warmth I felt at the table back in April 2013 continues to remain the same till date. Over the course of my stay in the lab, Claudio has been an integral part of my support system, both professionally and personally. He and Claudia have been outstanding 'parents' for all of us who have left our homes and moved away to pursue our PhDs!

As a mentor and advisor, he has ALWAYS had time for me and everyone in the lab, despite his many commitments. But more importantly, his ability to engage with us outside of science has been something I have thoroughly enjoyed throughout my time in the lab. Lunches were always the time of the day I looked forward to, because of Claudio's stories- his quick wit and humor is something that never tired any of us! I will terribly miss our chats on world politics, economics, culture, society, art, movies and all the random anecdotes we have exchanged over the years! He is a rare gem in the world of science, and I am honored to have been his student. I hope to be at least half as smart, personable, kind and generous as Claudio in the years to come.

I've also been fortunate to have an involved committee made up of Drs. Donna Fekete, Donald Ready, Phil Low and Claudio Aguilar. They asked the hard but right questions, pushing my envelope each time we met and were encouraging me to think of the larger scientific question. Dr. Fekete, particularly, is someone I have always looked up to, since my neurobiology class with her. I will value her involvement in my personal growth as a scientist and her readiness to support all co-curricular activities I participated in during my stay in Purdue.

Besides Claudio, I am eternally indebted to Dr. Kayalvizhi Madhivanan, a former graduate student in the lab. She mentored me as a rotation student and after I joined the Aguilar lab. I will always cherish the time I spent with Kayal where she taught me all she had about Lowe Syndrome, cell biology and became one of my closest friends and mentors. She and Claudio take the credit for transforming me from a timid student with potential into an intelligent, self-confident and fearless scientist.

Claudia, our lab manager has been the supportive pillar holding our lab together and ensuring it runs smoothly. Besides, her presence every morning as I walked in, eased my mind, especially during my early years as I tried to settle into my new surroundings. Dr. Wen-Chieh Hsieh, another former graduate student was also a pleasure to work with. He was a machine, working on multiple projects but always had a patient ear for all my questions. Recently, Jennifer Lee, who joined our lab to continue some of the projects I was a part of is a great addition to our lab. Hardworking, smart and relentless, I am certain she is going to carry forward the Aguilar lab legacy of Lowe Syndrome research. In addition, all the Aguilar lab members who have come and gone or have become recent members have been very good colleagues, making our lab a very enjoyable and conducive environment. I have also been fortunate to train several undergraduate students in the lab. Particularly, Tom Holman, Connor Tebbe, Swetha Sarma and Lisi Skiba have not only been

fantastic and productive researchers, helping me manage multiple projects but a pleasure to work with!

International students who leave their home and move to another country are often plagued with bouts of loneliness, a constant sense of lack of belonging, a never-ending longing to establish a sense of home. While I was lucky to never truly be homesick, I have often wondered how I will find my footing in a small college town in the Midwest. Shelli Taylor, our sweet secretary was a mainstay in my graduate experience. She was always the cheerful and welcoming person in our building who provided comfort for many of us, including me. Speaking to her, even for a few minutes, was soothing and made everything feel better.

Purdue has not only been my home for the past 7 years but has also given my some of my closest friends. Without my friends from Biology- Dr. Vishak Raman, Dr. Alix McCloskey, Kaushik Muralidharan, Dr. Patrick Schweikert and Dr. Thu Cao, grad school would have been an unfulfilling and dull experience. The much-needed coffees (and often something stronger!), venting and soul-searching sessions I have had with you guys will be terribly missed. You guys inspired me to do better and well and I will always be thankful for your friendship.

Saranya Radhakrishnan (Sara) and Kaushik Muralidharan (Kau) have gone above and beyond for me since the day I have known them. To call them family would be an understatement. I am glad to have shared my biggest life-changing moments as well as simple evening dinners with you two. My two biggest cheerleaders and pillars of support in life, your friendship means the world to me and I will be eternally grateful for all you have done and continue to do for me. Shambhavi, Upas, Bharath, Vat, Ganesh, Adharsh are also an integral part of my friend circle here. The countless years spent with all of you makes leaving Purdue so much harder than I imagined. Vat, working in your room the past 4 months has been a tremendous blessing in disguise! Thank you!

Friends from undergrad, Srinath, Sarada, Kripa, Akhi and Ramp, you have been rock solid. Despite how 2020 turned out with canceled defenses, graduation ceremonies and what not, I could not be more thrilled for some of you to participate in my online defense!

As a child, I may not have been entirely appreciative of my parents. I assumed that being an only child, my parents would always remain a core part of my life. And not surprisingly, they have been very supportive through all of this. Though this is typical of (all?) parents, I am also aware of their quiet but unwavering acceptance of who I have become today. They have embraced me,

and truly supported all my life decisions. Over the years, I have also come to recognize that not everyone has this privilege of having understanding and supportive parents like mine. I hope to be as brave and independent as my mother, as smart, driven and fun as my father one day. As for my family in the US, I am thankful for Priya, Anand and the kids whose home was a refuge from the grad school grind. I will miss my Thanksgiving tradition with you guys.

Finally, I owe a lot of my successes and who I have become to Aditya Raghunathan (Adi)- someone I met by chance during the first few weeks of college. From being the supportive boyfriend and now husband, Adi has been everything I have needed over the past 7 years. He may not know or admit it, but his levelheadedness through the decade of knowing me has always had me in awe. While he may not always understand the grind of grad school, his friendship and kindness are the most genuine I have ever experienced. At the risk of sounding poetic, he has been with me through every high and low in my adult life and there is no one else I would want to share these moments with. Even though the road has not been always smooth, his patience through these years are unmatchable and I will be eternally grateful for him sticking around even in my darkest moments.

To quote a cute bear from the A.A Milne children's series, " The smallest things hold the biggest place in our hearts". Adi, the smallest things you did for me over the years and continue to do so (though I may not admit to them often) hold the most room in my heart. I am glad to have experienced this grad school journey with you. I look forward to see what the future holds for us!

# TABLE OF CONTENTS

LIST OF TABLES ..... 11
LIST OF FIGURES ..... 12
ABSTRACT ..... 14
CHAPTER 1. INTRODUCTION ..... 16
1.1 Phosphatidyl inositol phosphates ..... 16
1.2 Phosphatidyl inositol 5' phosphatases ..... 17
1.3 Ocrl1 ..... 27
1.3.1 Domain architecture and interactions of Ocrl1 ..... 28
1.3.2 Functions of Ocrl1 ..... 31
1.4 Inpp5E ..... 37
1.4.1 Domain architecture and interactions of Inpp5E ..... 37
1.4.2 Functions of Inpp5E ..... 38
1.5 Diseases associated with Inpp5E ..... 42
1.5.1 Clinical characteristics of Joubert Syndrome ..... 43
1.5.2 Genotype-phenotype correlation between *INPP5E* mutations causing Joubert Syndrome and MORM ..... 45
1.6 Diseases associated with Ocrl1 ..... 46
1.7 Genotype and phenotype correlation between *OCRL1* mutations causing Lowe Syndrome and Dent-2 disease ..... 49
1.8 Gap in knowledge in LS research ..... 57
1.9 Introduction to thesis study ..... 58
CHAPTER 2. LOWE SYNDROME PATIENT CELLS DISPLAY MTOR- AND RHOGTPASE-DEPENDENT PHENOTYPES ALLEVIATED BY RAPAMYCIN AND STATINS ..... 61
2.1 Abstract ..... 61
2.2 Introduction ..... 62
2.3 Results ..... 64
2.3.1 RhoGTPase modulators affect LS spreading/FPU phenotype severity. ..... 64
2.3.2 Statins alleviate LS membrane remodeling phenotypes ..... 68

2.3.3 Statins alter RhoGTPase signaling, but had no effect on LS ciliogenesis phenotype 71
2.3.4 LS cells exhibited adhesion and spreading defects alleviated by statins ..... 71
2.3.5 Rapamycin mitigates PC assembly defects in LS patient cells. ..... 78
2.3.6 LS cells display constitutive activation of the mTOR pathway that can be mitigated by rapamycin ..... 79
2.3.7 Rosuvastatin/rapamycin combination mitigated both membrane remodeling and PC assembly phenotypes. ..... 83
2.4 Discussion ..... 84
2.4.1 How do deficiencies in Ocrl1 function trigger these phenotypes? ..... 85
2.4.2 How do cellular phenotypes translate into patient symptoms? ..... 88
2.4.3 Therapeutic Perspectives ..... 89
2.5 Materials and methods ..... 92
2.5.1 Reagents ..... 92
2.5.2 Cells and culture conditions ..... 92
2.5.3 Pharmacological treatments and viability/toxicity assessment ..... 93
2.5.4 Cell Spreading Assays ..... 93
2.5.5 Confocal microscopy ..... 94
2.5.6 Fluid shear stress assays ..... 95
2.5.7 Fluid phase uptake assay ..... 95
2.5.8 Ciliogenesis assays ..... 96
2.5.9 Indirect immunofluorescence for lysosomes ..... 96
2.5.10 Western blotting ..... 96
2.5.11 Statistical analysis ..... 97
CHAPTER 3. LOWE SYNDROME CELLULAR PHENOTYPES ARE DIFFERENTIALLY AFFECTED BY SPECIFIC *OCRL1* PATIENT MUTATIONS ..... 100
3.1 Abstract ..... 100
3.2 Introduction ..... 101
3.3 Results ..... 103
3.3.1 Ocrl1 mutants differentially affect cell spreading and ciliogenesis in kidney epithelial cells ..... 105

3.3.2 Mutations affecting different domains result in unique mutant protein behaviors and novel cellular phenotypes specific to the domain ..... 111
3.3.3 Subset of *OCRL1* mutations affecting phosphatase domain likely cause a conformational change in catalytic domain of mutant protein ..... 123
3.3.4 Subset of non-catalytic phosphatase domain mutants can regain cellular and biochemical function upon treatment with 4-phenyl butyric acid, a chemical chaperone .. 129
3.3.5 Lack of Ocrl1 PH domain results in protein mis-localization but sustains Ocrl1's C-terminus specific functions ..... 131
3.4 Discussion ..... 134
3.5 Materials and methods ..... 140
3.5.1 Reagents and constructs ..... 140
3.5.2 Cells and culture conditions ..... 140
3.5.3 Preparation of stable cell lines ..... 140
3.5.4 Drug treatments ..... 141
3.5.5 Transfections ..... 141
3.5.6 Cell Spreading Assays: ..... 141
3.5.7 Ciliogenesis assays ..... 142
3.5.8 Indirect immunofluorescence and fluorescence microscopy ..... 142
3.5.9 Protein purification ..... 143
3.5.10 Malachite green phosphatase assays ..... 143
3.5.11 Statistical analysis ..... 144
CHAPTER 4. CONCLUSIONS AND DISCUSSION ..... 146
REFERENCES ..... 151
VITA ..... 178

# LIST OF TABLES

Table 1.1 Mammalian 5' phosphatases, their substrates and associated human diseases ..... 18

Table 2.1 Adhesion and spreading rates of normal, LS and LS cells treated with Rosuvastatin . 77

Table 2.2 Pharmacological agents used in this study ..... 98

Table 2.3 List of antibodies used in this study..... 99

Table 3.1 Statistical analysis of cell spreading in cells expressing $Ocrl1^{WT}$ vs. phosphatase mutants ..... 107

Table 3.2 Statistical analysis of cell spreading in cells expressing $Ocrl1^{WT}$ vs. ASH-RhoGAP mutants..... 109

Table 3.3 List of antibodies used in this study..... 145

Table 3.4 List of plasmids used in this study..... 145

# LIST OF FIGURES

Figure 1.1 CLUSTALW sequence alignment of phosphatase domains of all mammalian 5' phosphatases ..... 23

Figure 1.2 Domain organization of human Ocrl1, Inpp5B and Inpp5E ..... 27

Figure 1.3 Ocrl1 and its protein interaction partners ..... 29

Figure 1.4 LS-causing *OCRL1* mutations affecting different domains of Ocrl1 ..... 51

Figure 1.5 Mapping of LS causing *OCRL1* missense mutations in the catalytic domain ..... 53

Figure 1.6 Dent-2 disease-causing *OCRL1* mutations affecting different domains ..... 55

Figure 2.1 LS cell spreading phenotype is affected by RhoGTPase modulators. ..... 66

Figure 2.2 Ocrl1-deficiency triggers a cell spreading phenotype in cells of different origin. ..... 67

Figure 2.3 Statins ameliorate LS membrane remodeling phenotypes. ..... 70

Figure 2.4 Ocrl1-deficient cells display adhesion defects. ..... 72

Figure 2.5 LS patient cells are sensitive to fluid shear stress. ..... 73

Figure 2.6 LS patient and HK2 KO cells exhibit focal adhesion defects. ..... 75

Figure 2.7 LS patient cells display a cell spreading delay independent of their adhesion phenotype. ..... 78

Figure 2.8 Rapamycin rescues ciliogenesis defects in LS patient cells. ..... 79

Figure 2.9 LS patient cells display hyperactivation of the mTOR signaling pathway. ..... 82

Figure 2.10 Absence of Ocrl1 led to autolysosome deficiencies in human kidney HK2 cells that can be rescued by the mTOR inhibitors rapamycin and WYE. ..... 83

Figure 2.11 Treatment with combination of rapamycin and rosuvastatin ameliorate both ciliogenesis and spreading phenotypes in LS patient cells. ..... 84

Figure 2.12 Working model for LS phenotype development as a consequence of lack of Ocrl1 activity ..... 92

Figure 3.1 Dual function of Ocrl1 and mutations used in the study ..... 104

Figure 3.2 Ocrl1 phosphatase domain mutants are differentially impaired for cell spreading activity. ..... 106

Figure 3.3 Ocrl1 ASH-RhoGAP domain mutants are modestly affected for cell spreading activity. ..... 107

Figure 3.4 Ocrl1 phosphatase domain mutants are differentially impaired for cilia formation. 110

Figure 3.5 Ocrl1 ASH-RhoGAP domain mutants are differentially impaired for cilia formation. ..... 111

Figure 3.6 ASH-RhoGAP domain mutants exhibit enrichment or accumulation at the centriole under steady state conditions. ..... 113

Figure 3.7 Stable expression of Ocrl1$^{I768N}$ in HK2 KO cells also results in centriole accumulation under steady state conditions. ..... 116

Figure 3.8 Transient expression of phosphatase domain mutants produces TGN fragmentation. ..... 118

Figure 3.9 Stably expressed phosphatase domain mutants also induce TGN fragmentation. .... 122

Figure 3.10 Mapping and molecular dynamics of *OCRL1* missense mutations in the phosphatase domain..... 125

Figure 3.11 Ocrl1 catalytic and non-catalytic phosphatase domain mutants are impaired for 5' phosphatase activity. ..... 128

Figure 3.12 4-phenyl butyric acid (4-PBA) reverts TGN fragmentation and restores 5' phosphatase activity in a dose-dependent manner..... 130

Figure 3.13 Representation of the proposed alternative Ocrl1 transcript. ..... 132

Figure 3.14 Truncation of Ocrl1 PH domain results in nuclear mis-localization of protein. ..... 133

Figure 3.15 Ocrl1 PH domain truncation results in cell spreading defect. ..... 134

Figure 3.16 Heterogenous consequences and cellular phenotypes produced by LS-causing *OCRL1* mutations. ..... 139

Figure 4.1 Genotype-dependent heterogeneity in Lowe Syndrome cellular manifestations. ..... 150

# ABSTRACT

Lowe Syndrome (LS) is a lethal developmental disease characterized by mental retardation, cataracts at birth and kidney dysfunction. LS children unfortunately die by adolescence from renal failure. The gene responsible for the disease (*OCRL1*) encodes an inositol 5' phosphatase Ocrl1. In addition to its 5' phosphatase domain, this protein has other domains that allow protein-protein interactions, facilitating diverse sub-cellular distribution and functions. LS patient cells lacking Ocrl1 display defects in cell spreading, ciliogenesis and vesicle trafficking. Currently the mechanisms underlying these cellular defects are not known, and hence no LS-specific therapies exist.

We have uncovered the mechanisms underlying two LS-specific cellular phenotypes- namely cell spreading and ciliogenesis and identified 2 FDA-approved candidates- statins and rapamycin that could revert these abnormalities. We found that Ocrl1-deficient cells exhibit hyperactivation in mTOR signaling, resulting in ciliogenesis as well as autophagy defects, which were rescued by administering rapamycin. We also identified a novel RhoGTPase signaling-dependent cell adhesion defect in LS patient cells which resulted in focal adhesion abnormalities and sensitivity to fluid shear stress (critical for kidney function). Both RhoGTPase signaling dependent cell spreading and adhesion defects were corrected by treatment with statins.

Importantly, over 200 unique mutations in *OCRL1* cause LS and patients demonstrate heterogeneity in symptoms. However, the correlation between genotype and cellular phenotypes is unknown. We have determined that different *OCRL1* patient mutations have a differential impact on the two cellular phenotypes described above. Mutants exhibit behavior, sub-cellular distribution and cellular phenotypes unique to the domain and relevant to LS pathogenesis. We also propose that a subset of non-catalytic phosphatase domain mutations are conformationally affecting the protein, suggesting that LS has a conformational disease component. Importantly, we tested an FDA-approved drug, 4-phenyl butyric acid (4-PBA), used as a therapeutic in conformational diseases and found that it could revert phenotypes and restore the catalytic activity of these mutants. These findings collectively contribute to provide the cellular basis for LS patient heterogeneity as well as to propose a conformational disease component for LS (allowing the use of chemical chaperones as a therapeutic strategy for a subset of LS patients). Together, we hope

that these studies will help lay the foundation of better prognosis and tailoring personalized therapeutic strategies for LS patients.

# CHAPTER 1. INTRODUCTION

## 1.1 Phosphatidyl inositol phosphates

Phosphatidyl inositol phosphates (PPIs) or phosphoinositides are lipids that are derived from phosphorylation at different positions on the inositol ring. PPIs are found in the inner leaflet of the membrane, facing the cytosol (Dickson & Hille, 2019). On the inositol ring, a phosphate can be added to the hydroxyl (-OH) group at $C_3$, $C_4$ or $C_5$ position by phosphatidyl inositol kinases (PI kinases). This modification is reversible and can be removed by phosphatidyl inositol phosphatases (PI phosphatases) (Dickson & Hille, 2019).

From the activity of a variety of phosphatidyl inositol kinases and phosphatases arises 7 unique PPI species including PI, PI3P, PI4P, PI(3,4)$P_2$, PI(3,5)$P_2$, PI(4,5)$P_2$ and PI (3,4,5)$P_3$ (Madhivanan K, 2016). Though these lipids are enriched in specific intracellular compartments (Madhivanan K, 2016), it is not uncommon to find them mixed on the same membranes (Di Paolo & De Camilli, 2006). In addition to providing compartmental identity (Balla, 2013), their heterogenous distribution, along with their tightly regulated levels make them suitable for mediating different signaling pathways (Di Paolo & De Camilli, 2006) by recruiting specific proteins to those membranes to initiate a signaling cascade (Balla, 2013).

PPIs comprise less than 2% of the phospholipids (Di Paolo & De Camilli, 2006). After PI, PI(4,5)$P_2$ is the most abundant, comprising of nearly 1% of all phosphoinositides (Dickson & Hille, 2019). PI(4,5)$P_2$ is enriched at the plasma membrane (Madhivanan K, 2016) and is produced as a result of sequential phosphorylation of PI by PI-4' kinase and PI-5' kinase (Balla, 2013; Dickson & Hille, 2019). They are hydrolyzed by PI phosphatases such as PI 4'-phosphatase or PI 5'-phosphatase. PI(4,5)$P_2$ levels are also modulated at the plasma membrane by other lipid hydrolyzing enzymes such as phospholipase C (PLC), in response to activation of G-protein coupled receptors (GPCRs) (Balla, 2013; Dickson & Hille, 2019; Madhivanan K, 2016).

PI(4,5)$P_2$ is an important phospholipid and is involved in many cellular processes including phagocytosis, pinocytosis and clathrin-mediated endocytosis (Czech, 2000). PI(4,5)$P_2$ is also essential for reorganization of the actin cytoskeleton, membrane trafficking and regulated exocytosis (Czech, 2000). It also serves as precursor to generate second messengers such as

inositol triphosphate ($IP_3$) and diacyl glycerol (DAG) that subsequently activate other signaling pathways (Czech, 2000).

Given the diversity and importance of PI(4,5)$P_2$'s functions in cellular physiology, it is critical that PI(4,5)$P_2$ levels are always maintained tightly. Dysfunction in any of the PI(4,5)$P_2$-regulating enzymes, be it PI 5'-kinases or PI 5'-phosphatases results in its aberrant accumulation. Mutations in genes that encode PI 5'-phosphatases, result in multiple diseases such as Lowe Syndrome, Dent-2 disease, Joubert Syndrome, MORM, Parkinson's disease and are also implicated in cancers (Jennifer M. Dyson, Fedele, Davies, Becanovic, & Mitchell, 2012; Sandra Hakim, Bertucci, Conduit, Vuong, & Mitchell, 2012; Lisa M. Ooms et al., 2009) (Table.1.1). It is, therefore, essential to understand how these enzymes function to maintain PI(4,5)$P_2$ levels and examine the molecular mechanisms underlying the diseases they cause, when affected.

The next section will cover PI 5'-phosphatases and focus on comparing enzymes Ocrl1 and Inpp5E, which are implicated in diseases Lowe Syndrome and Joubert Syndrome respectively.

## 1.2 Phosphatidyl inositol 5' phosphatases

Phosphatidyl inositol- 5'phosphatases (PI 5'-phosphatases) are enzymes that remove a phosphate group from the hydroxy group on the $C_5$ position of the inositol ring. Their lipid substrates include PI(3,5)$P_2$, PI(4,5)$P_2$ and PI(3,4,5)$P_3$ (Balla, 2013). There are 10 mammalian and 4 yeast phosphatidyl inositol 5' phosphatases (Jennifer M. Dyson et al., 2012).

The 5' phosphatases are classified into 4 groups based on the substrates they preferentially act on (Balla, 2013). Group I enzymes comprises of Inpp5A and hydrolyze only water-soluble inositol (Ins) polyphosphates including Ins(1,4,5)$P_3$ and Ins(1,3,4,5)$P_4$. Group II enzymes comprises of Ocrl1, Inpp5B, SKIP, Inpp5J, Synaptojanin 1 and Synaptojanin 2. These enzymes hydrolyze both soluble inositol phosphates and phosphatidyl inositols. Group III enzymes comprise of SHIP1 and SHIP2 and hydrolyze phosphates at the $D_3$ position on inositol ring while Group IV enzymes comprise of Inpp5E which preferentially hydrolyze PI(3,4,5)$P_3$ and to an extent PI(4,5)$P_2$. (Table 1.1)

**Table 1.1 Mammalian 5' phosphatases, their substrates and associated human diseases**

| Group | Enzyme | Other names | Substrate | Diseases associated with loss of function |
|---|---|---|---|---|
| Type I | INPP5A | | $Ins(1,4,5)P_3$[1,2] and $Ins(1,3,4,5)P_4$[1] | • Leukemia[3]<br>• Cancer[4], Squamous cell carcinoma[5,6]<br>• Glioma[7]<br>• Glioblastoma[8]<br>• Ataxia and cerebellar degeneration[9,10]<br>• Cognitive defects[11]<br>• Skin lesions[12] |
| Type II | INPP5B | Type II inositol 5' phosphatase | $PI(4,5)P_2$ & $PI(3,4,5)P_3$[13], $Ins(1,4,5)P_3$ and Ins $(1,3,4,5)P_4$[14,15] | |

Table 1.1 continued

| | | | | |
|---|---|---|---|---|
| Type II (continued) | OCRL1 | INPP5F | $PI(4,5)P_2$[16], $Ins(1,4,5)P_3$[17], $Ins(1,3,4,5)P_4$[17] | • Lowe Syndrome[18]<br>• Dent-2 disease[19]<br>• Glioblastoma multiforme[8] |
| | Synaptojanin-1 | | $PI(3,4,5)P_3$ and $PI(4,5)P_2$[20,21,22] $Ins(1,4,5)P3$[23,24] | • Parkinsons[25]<br>• Down Syndrome[26]<br>• Epileptic encephalopathy[27] |
| | Synaptojanin-2 | | $PI(3,4,5)P_3$ and $PI(4,5)P_2$[28,29] | • Hearing Loss[30] |
| | SKIP | INPP5K | $PI(4,5)P_2$[31] and $PI(3,4,5)P_3$[32] | • Congenital muscular dystrophy, cataracts and intellectual disability[33,34]<br>• Congenital cataracts[35] |



19

Table 1.1 continued

| | | | | |
|---|---|---|---|---|
| Type II (continued) | INPP5J | Type II INPP5A, PIPP | $PI(4,5)P_2$, $Ins(1,4,5)P_3$, $Ins(1,3,4,5)P_4$[36] $PI(3,4,5)P_3$[37] | • Breast cancer[38] |
| Type III | SHIP1 | INPP5D | $Ins(1,3,4,5)P_4$ $PI(3,4,5)P_3$[39] $Ins(1,2,3,4,5)P_5$ and $Ins(2,3,4,5)P_4$[40] | • Myeloproliferative-like syndrome[41,42,43]<br>• Crohn's disease[44,45,46]<br>• Inflammatory bowel disease[47,46]<br>• Leukemia[48] |
| | SHIP2 | INPPL1 | $Ins(1,3,4,5)P_4$ $PI(3,4,5)P_3$[49,50] | • Opsismodysplasia[51,52,53]<br>• Lymphedema[54] |
| Type IV | INPP5E | Pharbin | $PI(3,4,5)P_3$, $PI(4,5)P_2$[55], $PI(3,5)P_2$[56] | • Joubert Syndrome[57,58]<br>• MORM[58]<br>• Polycystic kidney disease[59] |

Table 1.1 continued

| |
|---|
| 1- (Laxminarayan, Chan, Tetaz, Bird, & Mitchell, 1994), 2- (De Smedt et al., 1997), 3- (Mengubas et al., 1994), 4- (Speed, Little, Hayman, & Mitchell, 1996), 5- (Patel et al., 2018), 6- (Sekulic et al., 2010), 7- (Milinkovic et al., 2013), 8- (Waugh, 2016), 9- (Yang, Sachs, & Nystuen, 2015), 10- (Q. Liu et al., 2020), 11- (Marioni et al., 2018), 12- (Seow et al., 2015), 13- (Jefferson & Majerus, 1995), 14- (Mitchell, Connolly, & Majerus, 1989), 15- (Matzaris, Jackson, Laxminarayan, Speed, & Mitchell, 1994), 16- (X. Zhang, Jefferson, Auethavekiat, & Majerus, 1995), 17- (Ross, Jefferson, Mitchell, & Majerus, 1991), 18- (Attree et al., 1992a), 19- (Hoopes et al., 2005), 20- (S. Guo, Stolz, Lemrow, & York, 1999), 21- (Whisstock et al., 2000), 22- (Tsujishita, Guo, Stolz, York, & Hurley, 2001), 23- (McPherson et al., 1996), 24- (Chung et al., 1997), 25- (Drouet & Lesage, 2014), 26- (Voronov et al., 2008), 27- (Hardies et al., 2016), 28- (Nemoto, Arribas, Haffner, & DeCamilli, 1997), 29- (Khvotchev & Südhof, 1998), 30- (Manji et al., 2011), 31- (Schmid, Wise, Mitchell, Nussbaum, & Woscholski, 2004), 32- (Ijuin et al., 2000), 33- (Osborn et al., 2017), 34- (Wiessner et al., 2017), 35- (Yousaf, Sheikh, Riazuddin, Waryah, & Ahmed, 2018), 36- (Mochizuki & Takenawa, 1999), 37- (L. M. Ooms et al., 2006), 38- (L. M. Ooms et al., 2015), 39- (Damen et al., 1996), 40- (Nelson et al., 2020), 41- (Helgason et al., 2000), 42- (Leung, Tarasenko, & Bolland, 2009), 43- (Ghansah et al., 2004), 44- (Kerr, Park, Maubert, & Engelman, 2011), 45- (Somasundaram et al., 2017), 46- (Fernandes et al., 2018), 47- (Maxwell et al., 2014), 48- (Brauer et al., 2012), 49- (Lioubin et al., 1996), 50- (Pesesse et al., 1998), 51- (Ghosh et al., 2017), 52- (Fradet & Fitzgerald, 2017), 53- (M. P. Thomas, Erneux, & Potter, 2017), 54- (Agollah et al., 2014), 55- (Kisseleva, Wilson, & Majerus, 2000), 56- (Kong et al., 2000), 57- (Bielas et al., 2009), 58- (Jacoby et al., 2009), 59- (S. Hakim et al., 2016) |

All PI 5'-phosphatases are $Mg^{2+}$-dependent enzymes belonging to the apurinic/apyrimidic endonuclease family (Jennifer M. Dyson et al., 2012). They all contain roughly a 300 amino acid catalytic domain with two signature catalytic consensus regions FWXGDXN(F/Y)R and (R/N)XP(S/A)W(C/T)DR(I/V)L which helps in hydrolysis of substrates (Jefferson & Majerus, 1996). In addition. Whisstock et al. (Whisstock et al., 2000) identified 4 more conserved motifs TWN, GXQE, NXH and SDHXPV (where X is any amino acid) that are required for catalytic activity (Fig.1.1). Structural and biochemical studies using yeast and mammalian 5' phosphatase domains have determined the role of these motifs in functions including substrate recognition and specificity, lipid binding, metal ion coordination and 5-phosphate hydrolysis (Jefferson & Majerus, 1996; Mills et al., 2016; L. Tresaugues et al., 2014; Tsujishita et al., 2001; Whisstock et al., 2000). The 6 conserved motifs required for 5' phosphatase activity is highlighted in green in the alignment of all the mammalian 5' phosphatases (Fig.1.1). Additional amino acids predicted to aid in lipid interaction for Ocrl1 and Inpp5B are highlighted in yellow (Fig.1.1).

```
|Q5T1B5|INPP5A_HUMAN/8-385          PGTAVLLVTANVGSLFDDPENL-----QKNWLREFYQV--------VHTHKPHFMALHCQE   48

|Q9NRR6|INPP5E_HUMAN/297-599       RNVALFVATWNMQGQKELP------PSLDEFLLP-----------AEADYAQDLYVIGVQE   44

|Q92835|SHIP1_HUMAN/402-718        DMITIFIGTWNMGNAPPP-------KKITSWFLSKGQ--GKTRDDSADYIPHDIYVIGTQE   52
|O15357|SHIP2_HUMAN/422-735        DMISVFIGTWNMGSVPPP-------KNVTSWFTSKGL--GKTLDEVTVTIPHDIYVFGTQE   52

|Q9BT40|SKIP_HUMAN/12-326          RRLSIHVVTWNVASAAPP-------LDLSDLL----QLNN-----RN--LNLDIYVIGLQE   43
|Q15735|INPP5J_HUMAN/421-736       PGFRITVVTWNVGTAMPP-------DDVTSLL----HLGG-----GDDSDGADMIAIGLQE   45
|O15056|SYNJ2_HUMAN/528-870        KRIRIAMGTWNVNGGKQFRSNVLRTAELTDWLLDSPQLSGATDSQD-DSSPADIFAVGFEE   60
|J3KPK1|SYNJ1_HUMAN/526-869        KKIRVCVGTWNVNGGKQFRSIAFKNQTLTDWLLDAPKLAGIQEFQDKRSKPTDIFAIGFEE   61
|P32019|INPP5B_HUMAN/343-644       QNFRFFAGTYNVNGQSPK-------ECLRLWLSN-------------GIQAPDVYCVGFQE   41
|UPI0007DC791C|OCRL_HUMAN/238-539 QTFRFFVGTWNVNGQSPD-------SGLEPWLNC-------------DPNPPDIYCIGFQE   41


|Q5T1B5|INPP5A_HUMAN/8-385          FGGKNYEASMSHVDKFVKELLSSDAMKEYNRARVYLDENYKSQEHFTALGSFY---FLH    104

|Q9NRR6|INPP5E_HUMAN/297-599       G----------------------CSDR----REWETRL---QETLGP----HYVLLSS    69

|SHIP1_HUMAN/402-718              D----------------------PLSE----KEWLEIL---KHSLQEITSVTFKTVAI    81
|O15357|SHIP2_HUMAN/422-735        N----------------------SVGD----REWLDLL---RGGLKELTDLDYRPIAM    81

|Q9BT40|SKIP_HUMAN/12-326          LNSGIIS-------------LLSDAAFN----DSWSSFL---MDVLSP---LSFIKVSH    79
|Q15735|INPP5J_HUMAN/421-736       VNSMLNK-------------RLKDALFT----DQWSELF---MDALGP---FNFVLVSS    81
|O15056|SYNJ2_HUMAN/528-870        MVELSAG------------NIVNASTTNK----KMWGEQL---QKAISR--SHRYILLTS    99
|J3KPK1|SYNJ1_HUMAN/526-869        MVELNAG------------NIVSASTTNQ----KLWAVEL---QKTISR--DNKYVLLAS    100
|P32019|INPP5B_HUMAN/343-644       L-DLSKE------------AFFFHDTPKE----EEWFKAV---SEGLHP--DAKYAKVKL    79
|UPI0007DC791C|OCRL_HUMAN/238-539 L-DLSTE------------AFFYFESVKE----QEWSMAV---ERGLHS--KAKYKKVQL    79


|Q5T1B5|INPP5A_HUMAN/8-385          ESLKNIYQFDFKAKKYRKVAGKEIYSDTLESTPMLEKEKFPQDYFPECKWSRKGFIRTRW    164

|Q9NRR6|INPP5E_HUMAN/297-599       AAHGVLYMSLFIR-RDLIWFCSEVECSTVT-------------TRIVSQIKTKGALGISF    115

|Q92835|SHIP1_HUMAN/402-718        HTLWNIRIVVLAK-PEHENRISHICTDNVK-------------TGIANTLGNKGAVGVSF    127
|O15357|SHIP2_HUMAN/422-735        QSLWNIKVAVLVK-PEHENRISHVSTSSVK-------------TGIANTLGNKGAVGVSF    127

|Q9BT40|SKIP_HUMAN/12-326          VRMQGILLLVFAK-YQHLPYIQILSTKSTP-------------TGLFGYWGNKGGVNICL    125
|Q15735|INPP5J_HUMAN/421-736       VRMQGVILLLFAK-YYHLPFLRDVQTDCTR-------------TGLGGYWGNKGGVSVRL    127
```

**Figure 1.1 CLUSTALW sequence alignment of phosphatase domains of all mammalian 5' phosphatases**

Figure 1.1 continued

```
|O15056|SYNJ2_HUMAN/528-870        AQLVGVCLYIFVR-PYHVPFIRDVAIDTVK-------------TGMGGKAGNKGAVGIRF    145
|J3KPK1|SYNJ1_HUMAN/526-869        EQLVGVCLFVFIR-PQHAPFIRDVAVDTVK-------------TGMGGATGNKGAVAIRM    146
|P32019|INPP5B_HUMAN/343-644       IRLVGIMLLLYVK-QEHAAYISEVEAETVG-------------TGIMGRMGNKGGVAIRF    125
|UPI0007DC791C|OCRL_HUMAN/238-539 VRLVGMMLLIFAR-KDQCRYIRDIATETVG-------------TGIMGKMGNKGGVAVRF    125


|Q5T1B5|INPP5A_HUMAN/8-385         CIADCAFDLVNIHLFHDASNLVAWETSPSVYSGIRHK--------ALGYVLDRIIDQRFE    216

|Q9NRR6|INPP5E_HUMAN/297-599       TFFGTSFLFITSHFTSGDGKVAERL---LDYTRTVQALVLPRNVPDTNPYRSSAADVTTR    172

|Q92835|SHIP1_HUMAN/402-718        MFNGTSLGFVNSHLTSGSEKKLRRN---QNYMNILRFLALGDK--KLS-----PFNITHR    177
|O15357|SHIP2_HUMAN/422-735        MFNGTSFGFVNCHLTSGNEKTARRN---QNYLDILRLLSLGDR--QLN-----AFDISLR    177

|Q9BT40|SKIP_HUMAN/12-326          KLYGYYVSIINCHLPPHISNNYQRL---EHFDRILEMQNCEGR----D-----IPNI-LD    172
|Q15735|INPP5J_HUMAN/421-736       AAFGHMLCFLNCHLPAHMDKAEQRK---DNFQTILSLQQFQGP----G-----AQGI-LD    174
|O15056|SYNJ2_HUMAN/528-870        QFHSTSFCFICSHLTAGQSQVKERN---EDYKEITQKLCFPMG----------RNV-FS    190
|J3KPK1|SYNJ1_HUMAN/526-869        LFHTTSLCFVCSHFAAGQSQVKERN---EDFIEIARKLSFPMG----------RML-FS    191
|P32019|INPP5B_HUMAN/343-644       QFHNTSICVVNSHLAAHIEEYERRN---QDYKDICSRMQFCQPDPSLP-----PLTI-SN    176
|UPI0007DC791C|OCRL_HUMAN/238-539 VFHNTTFCIVNSHLAAHVEDFERRN---QDYKDICARMSFVVPNQTLP-----QLNI-MK    176


|Q5T1B5|INPP5A_HUMAN/8-385         KVSYFVFGDFNFRLDSKSVVETLCTKATMQTVRAADTNEVVKLIFRESDNDRKVMLQLEK    276

|Q9NRR6|INPP5E_HUMAN/297-599       FDEVFWFGDFNFRLSGGRTVVD----------------ALLCQGLV---VDVPALLQ---    210

|Q92835|SHIP1_HUMAN/402-718        FTHLFWFGDLNYRVDLPTWEAE----------------TIIQKIKQ---QQYADLLS---    215
|O15357|SHIP2_HUMAN/422-735        FTHLFWFGDLNYRLDMDIQ-------------------EILNYISR---KEFEPLLR---    212

|Q9BT40|SKIP_HUMAN/12-326          HDLIIWFGDMNFRIEDFGL--H----------------FVRESIKN---RCYGGLWE---    208
|Q15735|INPP5J_HUMAN/421-736       HDLVFWFGDLNFRIESYDL--H----------------FVKFAIDS---DQLHQLWE---    210
|O15056|SYNJ2_HUMAN/528-870        HDYVFWCGDFNYRIDLT-Y--E----------------EVFYFVKR---QDWKKLLE---    225
|J3KPK1|SYNJ1_HUMAN/526-869        HDYVFWCGDFNYRIDLP-N--E----------------EVKELIRQ---QNWDSLIA---    226
|P32019|INPP5B_HUMAN/343-644       HDVILWLGDLNYRIEELDV--E----------------KVKKLIEE---KDFQMLYA---    212
|UPI0007DC791C|OCRL_HUMAN/238-539 HEVVIWLGDLNYRLCMPDA--N----------------EVKSLINK---KDLQRLLK---    212


|Q5T1B5|INPP5A_HUMAN/8-385         KLFDYFNQEVFRDNNGTALLEFDKELSVFKDRLYELDISFPPSYPYSEDARQG-------    329

|Q9NRR6|INPP5E_HUMAN/297-599       -----HDQLIREMRKGSIF-----------KGFQEPDIHFLPSYKFDIGKDTY-------    247
|Q92835|SHIP1_HUMAN/402-718        -----HDQLLTERREQKVF-----------LHFEEEEITFAPTYRFERLTRDKYAYTKQK    259
```



24

Figure 1.1 continued

```
|O15357|SHIP2_HUMAN/422-735        -----VDQLNLEREKHKVF----------LRFSEEEISFPPTYRYERGSRDTYAWHKQK    256

|Q9BT40|SKIP_HUMAN/12-326          -----KDQLSIAKKHDPLL----------REFQEGRLLFPPTYKFDRNSNDY-------    245
|Q15735|INPP5J_HUMAN/421-736       -----KDQLNMAKNTWPIL----------KGFQEGPLNFAPTFKFDVGTNKY-------    247
|O15056|SYNJ2_HUMAN/528-870        -----FDQLQLQKSSGKIF----------KDFHEGAINFGPTYKYDVGSAAY-------    262
|J3KPK1|SYNJ1_HUMAN/526-869        -----GDQLINQKNAGQVF----------RGFLEGKVTFAPTYKYDLFSDDY-------    263
|P32019|INPP5B_HUMAN/343-644       -----YDQLKIQVAAKTVF----------EGFTEGELTFQPTYKYDTGSDDW-------    249
|UPI0007DC791C|OCRL_HUMAN/238-539  -----FDQLNIQRTQKKAF----------VDFNEGEIKFIPTYKYDSKTDRW-------    249


|Q5T1B5|INPP5A_HUMAN/8-385         EQYMNTRCPAWCDRILMSPSAKEL--------------------VLRVSVCCPSPGHRGM    369

|Q9NRR6|INPP5E_HUMAN/297-599       DSTSKQRTPSYTDRVLYRSRHKG-------------------------DICPVSYSSCPG    282

|Q92835|SHIP1_HUMAN/402-718        ATGMKYNLPSWCDRVLWKSYPLV-------------------------HVVCQSYGSTSD    294
|O15357|SHIP2_HUMAN/422-735        PTGVRTNVPSWCDRILWKSYPET-------------------------HIICNSYGCTDD    291

|Q9BT40|SKIP_HUMAN/12-326          DTSEKKRKPAWTDRILWRLKRQPCAGPDTP-----------IPPASHFSLSLRGYSSHMT    294
|Q15735|INPP5J_HUMAN/421-736       DTSAKKRKPAWTDRILWKVKA-PGGGPSPS-----------GRKSHRLQVTQHSYRSHME    295
|O15056|SYNJ2_HUMAN/528-870        DTSDKCRTPAWTDRVLWWRKKHPFDKTAGELNLLDSDLDVDTKVRHTWSPGALQYYGRAE    322
|J3KPK1|SYNJ1_HUMAN/526-869        DTSEKCRTPAWTDRVLWRRRKWPFDRSAEDLDLLNASFQDESKILYTWTPGTLLHYGRAE    323
|P32019|INPP5B_HUMAN/343-644       DTSEKCRAPAWCDRILWKGKNI---------------------------TQLSYQSHMA    281
|UPI0007DC791C|OCRL_HUMAN/238-539  DSSGKCRVPAWCDRILWRGTNV---------------------------NQLNYRSHME    281


|Q5T1B5|INPP5A_HUMAN/8-385         WSAGS-----GLAQ---------     378

|Q9NRR6|INPP5E_HUMAN/297-599       IKTSDHRPVYGLFRVKVRPGR--     303

|Q92835|SHIP1_HUMAN/402-718        IMTSDHSPVFATFEAGVTSQFVS     317
|O15357|SHIP2_HUMAN/422-735        IVTSDHSPVFGTFEVGVTSQFIS     314

|Q9BT40|SKIP_HUMAN/12-326          YGISDHKPVSGTFDLELKPLV--     315
|Q15735|INPP5J_HUMAN/421-736       YTVSDHKPVAAQFLLQFAFRD--     316
|O15056|SYNJ2_HUMAN/528-870        LQASDHRPVLAIVEVEVQEVD--     343
|J3KPK1|SYNJ1_HUMAN/526-869        LKTSDHRPVVALIDIDIFEVE--     344
|P32019|INPP5B_HUMAN/343-644       LKTSDHKPVSSVFDIGVRVVN--     302
|UPI0007DC791C|OCRL_HUMAN/238-539  LKTSDHKPVSALFHIGVKVVD--     302
```

**IPPc consensus motifs [9, 10, 13]**
**Lipid chain interacting motifs in Ocrl1 and Inpp5B [13]**



25

Many of these enzymes possess accessory domains such as Proline rich domain (PRD; Inpp5E and Inpp5J), RhoGAP domain (Ocrl1 and Inpp5B), SH2 domain (SHIP1 and SHIP2), ASH domain (Inpp5b and Ocrl1) and SAC domain (Synaptojanin1/2) that help in protein localization and interaction with other cellular partners or membranes (Balla, 2013).

Further, alternative splicing produces many isoforms for each of these enzymes that have distinct subcellular localization and non-overlapping function, resulting in little or no redundancy (Madhivanan K, 2016). Phosphatases play critical role in regulating homeostasis, hematopoietic function, embryonic development, neuronal, ocular and kidney function, vesicle recycling and trafficking and actin cytoskeletal reorganization (Jennifer M. Dyson et al., 2012; Lisa M. Ooms et al., 2009).

As expected, these enzymes are involved in many cellular processes, often targeting similar substrates, suggesting overlapping function. However, mutations in genes encoding these 5' phosphatases result in many debilitating diseases, summarized in Table 1.1, indicating that these enzymes cannot compensate for each other's function. This may be likely due to a unique spatio-temporal localization of these enzymes within the same cells or even their differential tissue distribution. Nonetheless, the diseases share some similarities in terms of organs affected and/or their cellular phenotypes. Examining the similarities and differences between these enzymes and the cellular and symptom manifestation of the diseases they produce when affected will allow us to better understand pathogenesis of these 5' phosphatase-related diseases.

Section 1.3-1.8 will be dedicated towards comparing specifically Ocrl1, Inpp5B and Inpp5E. Ocrl1 when mutated, leads to in Lowe Syndrome, (a ciliopathy-like disease) while Inpp5E when mutated leads to Joubert Syndrome (a classical ciliopathy). These enzymes share some similarities in function as well cellular phenotypes they trigger when deficient. Interestingly, the two diseases produced as a result of mutations in *OCRL1* and *INPP5E* also share many similarities including cellular defects, heterogeneity in genotypes and patient phenotypes.

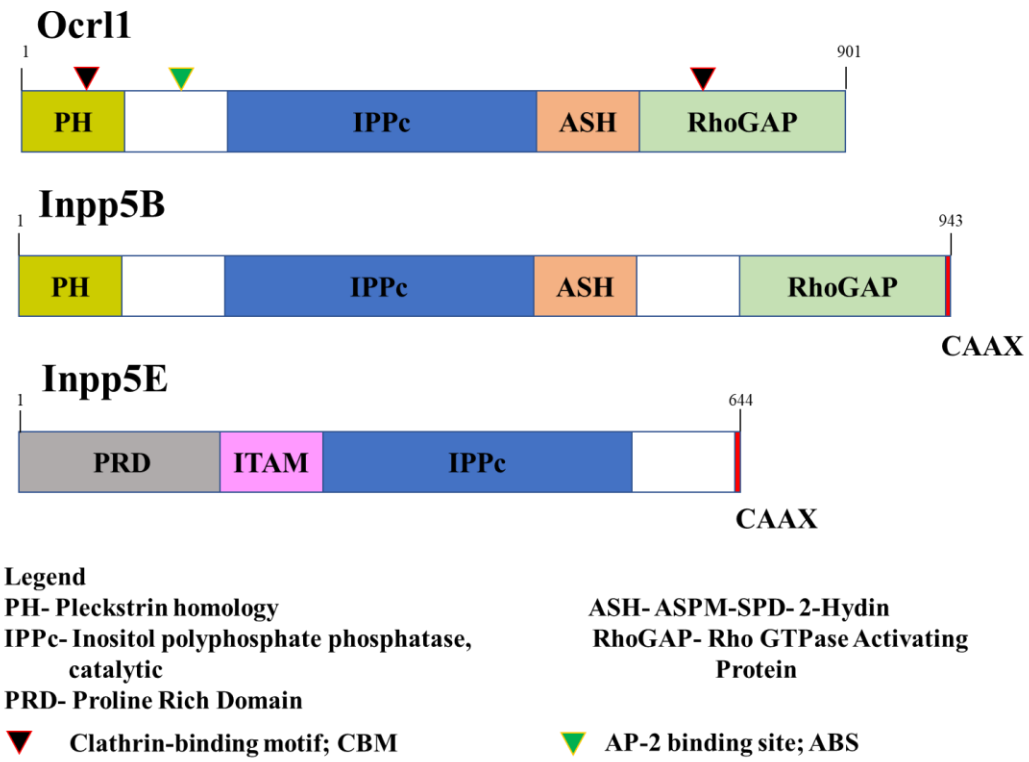


**Figure 1.2 Domain organization of human Ocrl1, Inpp5B and Inpp5E**

## 1.3 Ocrl1

Ocrl1 (EC 3.1.3.36; EC- Enzyme Commission number) is a type II PI 5' phosphatase with specificity for lipids PI(4,5)$P_2$ and PI(3,4,5)$P_3$ (Suchy, Olivos-Glander, & Nussabaum, 1995; X. Zhang et al., 1995). This enzyme is encoded by the gene *OCRL1*, found on the X-chromosome. Mutations in the *OCRL1* gene causes a rare X-linked congenital disease known as Lowe Syndrome (LS) or Oculo-Cerebro-Renal syndrome of Lowe (OCRL) (Attree et al., 1992b) as well as Dent-2 disease, a milder form of LS (Hoopes et al., 2005). LS has a signature clinical triad of symptoms namely, congenital cataracts, hypotonia and mental retardation as well as renal dysfunction (M. Loi, 2006). However, the symptoms and organ involvement can vary between patients. Dent-2 patients on other hand, almost exclusively present with renal dysfunction with mild to no neurological symptoms (sometimes these symptoms set in later during the patient's life) and no ocular defects, except corneal opacities (Bökenkamp & Ludwig, 2016). It is still unclear how mutations in the same gene result in two diseases, with a small subset of common symptoms, but overall have a different clinical presentation and prognosis.

Ocrl1 and its paralog Inpp5B (EC 3.1.3.36) (also known as 75 KDa Inositol Polyphosphate-5-Phosphatase) share similar protein architecture and have some redundancy in function (Lowe, 2005) (Fig.1.2). However, these enzymes have differential tissue expression in humans (Janne et al., 1998) and exhibit some unique characteristics.

While Ocrl1 is ubiquitously expressed across all human tissue types, Inpp5B has relatively lower expression in brain, eyes and kidneys (Janne et al., 1998). In mice (*Mus musculus*), however, both Ocrl1 and Inpp5B are equally enriched in all tissue types (Janne et al., 1998). As a result, mice models of LS do not phenocopy human manifestations including congenital cataracts, hypotonia and renal dysfunction (Janne et al., 1998). A double knockout of *ocrl1* and *inpp5b* resulted in embryonic lethality, suggesting functional redundancy. In addition, there are also differences in human and murine *INPP5B* transcription and splicing mechanisms (Bothwell, Farber, Hoagland, & Nussbaum, 2010). In order to overcome these species-specific compensatory mechanisms, a 'humanized' mouse model has been created. Here both murine *ocrl1* and *inpp5b* are knocked out and a human copy of *INPP5B* is expressed which resulted renal tubular dysfunction in the mice (Bothwell et al., 2011). Zebrafish (*Danio rerio*) Ocrl1 is more similar to human Ocrl1 and deletion of *ocrl1* in zebrafish can recapitulate LS symptoms (B. G. Coon et al., 2012; Gliozzi et al., 2020; Ramirez et al., 2012). These are currently the two higher eukaryotic models used in LS research.

### 1.3.1 Domain architecture and interactions of Ocrl1

Ocrl1 and Inpp5B contain four major domains: N- terminus PH (Pleckstrin Homology), central 5-phosphatase, C-terminus ASH (ASPM-SPD2-Hydin) and a RhoGAP (Rho GTPase Activating Protein) domain (Fig.1.2).

Though structurally similar, the PH domains of Ocrl1 and Inpp5B are different at the sequence level (Coon et al., 2009; Mao et al., 2009). Unlike other lipid-binding PH domains, no lipid interactions have been identified for the PH domains of Ocrl1 and Inpp5B (Mao et al., 2009). The PH domain of Ocrl1 contains a clathrin binding motif (CBM), as well as an assembly protein 2 (AP2) binding site (ABS) (ABS is present in the linker region indicated by the white box between PH and phosphatase domain, Fig.1.2 & 1.3). These two binding sites, are however, absent in Inpp5B, resulting in some functional differences between these two proteins.

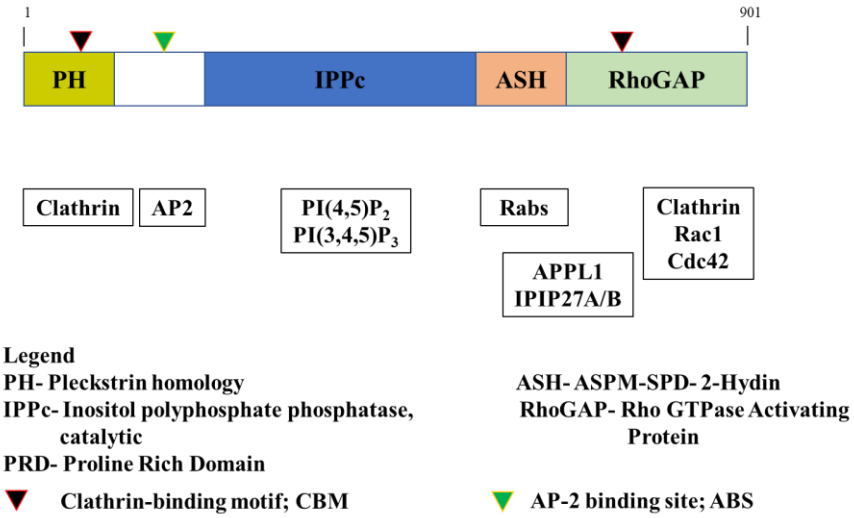


**Figure 1.3 Ocrl1 and its protein interaction partners**

The flexible linker region (white box following PH domain in Fig.12 & 1.3) connects to the central catalytic domain. Weber et al. 2009 (Weber, Ragaz, & Hilbi, 2009) demonstrated that Ocrl1 interacted with the Legionella effector LpnE via its N-terminus (amino acids 1-236). Recent studies have demonstrated that this occurs via the poly proline patch in the linker region between amino acids 170-185 (Voth et al., 2019). Whether this is indicative of other undiscovered interaction partners that associate with the linker region remains to be determined.

The Ocrl1 phosphatase domain bears high conservation with other 5' phosphatases (see Fig.1.1) in the consensus sequences required for its phosphatase activity (Conduit, Dyson, & Mitchell, 2012; L. Tresaugues et al., 2014). In addition, it also contains other conserved regions involved in substrate binding and protein folding (L. Tresaugues et al., 2014; Tsujishita et al., 2001; Whisstock et al., 2000). Nearly 50% of LS-causing mutations in *OCRL1* affect the phosphatase domain (Conduit et al., 2012; Hichri et al., 2011).

Proteins, including Ocrl1, which localize to the cilia or centrosome contain an ASH domain (Ponting, 2006). Ocrl1 was demonstrated to be involved in the formation and maintenance of the primary cilia, revolutionizing our understanding of the cell biology of this disease (Brian G. Coon et al., 2012; Luo, West, et al., 2012; Rbaibi et al., 2012). In addition, in the ASH domain of Ocrl1 lies a Rab-binding site through which Ocrl1 binds several Rabs (with highest affinity for Rab8a) (Fukuda, Kanno, Ishibashi, & Itoh, 2008; Hagemann, Hou, Goody, Itzen, & Erdmann, 2012; Hou et al., 2011) and this interaction plays a critical role in ciliogenesis (Brian G. Coon et al., 2012;

Luo, West, et al., 2012). Though both Inpp5B and Ocrl1 bind Rabs for their targeting to the *trans*-Golgi network (TGN) and *cis*-Golgi network (CGN) respectively, Rabs involved in this process differs for the paralogs (Hyvola et al., 2006; Williams, Choudhury, McKenzie, & Lowe, 2007).

The RhoGAP-like domain which is C-terminal to the ASH domain does not exhibit Rho-GAP activity due to a substitution of the catalytic arginine with glutamine (Lowe, 2005), but it can interact with the RhoGTPases Rac1 and Cdc42 (Faucherre et al., 2005; Faucherre et al., 2003b).

ASH and RhoGAP-like domains are interdependent on each other for their folding as well as interaction with endosomal proteins containing F&H domains, namely, APPL1, IPIP27A and B (also known as Ses1 and Ses2) (Erdmann et al., 2007; Swan, Tomasini, Pirruccello, Lunardi, & De Camilli, 2010).

The RhoGAP domain of Ocrl1 contains a second CBM which Inpp5B lacks. Ocrl1 undergoes alternative splicing, producing two isoforms- long isoform (isoform a) and the short isoform (isoform b) lacking 8 amino acids that follow the second CBM. The shorter isoform is ubiquitously expressed, while the long isoform is exclusively enriched in the nervous tissue (Lowe, 2005). The presence of 8 additional amino acids in the longer isoform results in this isoform to have higher affinity for clathrin (Rawshan Choudhury, Noakes, McKenzie, Kox, & Lowe, 2009).

Ocrl1 localizes to various compartments in the cell, mediated by different protein interactions. It is enriched at the TGN (Dressman, Olivos-Glander, Nussbaum, & Suchy, 2000). In addition, Ocrl1 also is found at endocytic and secretory compartments, and late-stage clathrin coated structures (Erdmann et al., 2007). While Rac binding was thought to mediate its localization at TGN (Faucherre et al., 2005) , it is believed that Rab interaction is necessary for localization to all the above mentioned compartments (R. Choudhury et al., 2005; Hyvola et al., 2006). For example, some of the Ocrl1-Rab interactions that are required for localization include Rab5 for early endosomes (Erdmann et al., 2007), Rab 35 for recycling endosomes(Dambournet et al., 2011), Rab1, Rab6 for TGN (Hyvola et al., 2006). Interestingly, *in vitro* studies show that Ocrl1 phosphatase activity requires Rab interaction (Hyvola et al., 2006). Rab8 is required for Ocrl1's localization at the ciliary base (Brian G. Coon et al., 2012; Hyvola et al., 2006). This transient interaction also aids in cargo delivery (Brian G. Coon et al., 2012). Further, Ocrl1-mediated delivery of cargo to the cilia is also dependent on endocytic proteins IPIP27A/B (Brian G. Coon et al., 2012). In contrast, Ocrl1's membrane ruffle localization occurs via its binding to activated Rac1 (Faucherre et al., 2005).

### 1.3.2 Functions of Ocrl1

Actin cytoskeleton

Absence of Ocrl1 results in defect in actin remodeling, a process critical for many physiological events such as phagocytosis, cytokinesis, membrane trafficking and cell migration. As a result, Ocrl1 loss also leads to defects in the aforementioned processes. For instance, in LS patient fibroblasts, there is an accumulation of $PI(4,5)P_2$ in the absence of Ocrl1 (Suchy & Nussbaum, 2002). This resulted in punctate actin structures that colocalize actin severing protein gelsolin (Suchy & Nussbaum, 2002) and actin "tails" in endosomes (Ueno, Falkenburger, Pohlmeyer, & Inoue, 2011). Decrease in $PI(4,5)P_2$ levels initiates actin depolymerization. Increase in $PI(4,5)P_2$ inhibits actin depolymerization resulting in aberrant structures (Suchy & Nussbaum, 2002).

Alternatively, errors in actin remodeling maybe linked to abnormal RhoGTPase signaling (discussed under 'vesicle trafficking and membrane remodeling') observed in Ocrl1-deficient cells (Lasne et al., 2010; Madhivanan, Mukherjee, & Aguilar, 2012).

Vesicle trafficking

Ocrl1 participates in vesicle trafficking predominantly through its interactions with Rabs, clathrin and AP2. Deficiency or absence of Ocrl1 function resulted in defects in endosome-to-TGN trafficking, recycling to the plasma membrane which consequently led to enlarged endosomes with cargo accumulation (R. Choudhury et al., 2005; van Rahden et al., 2012; Vicinanza et al., 2011). Additionally, Mannose-6-Phosphate receptor (M6PR), (responsible for delivering lysosomal hydrolases from TGN to the lysosome) usually traffics between the TGN and late endosomes, was mis-sorted to the plasma membrane in the absence of Ocrl1 (Vicinanza et al., 2011), causing extracellular secretion of lysosomal enzymes (Cui et al., 2010; A. J. Ungewickell & Majerus, 1999; Vicinanza et al., 2011). Coincidentally, LS patients also exhibit an increased secretion of lysosomal enzymes in urine (Bökenkamp & Ludwig, 2016; A. J. Ungewickell & Majerus, 1999).

Further, while some studies reported no defects in the endocytosis of cargo such as uptake of Transferrin (Tf), Epidermal growth factor (EGF) and Low Density Lipoprotein (LDL) receptors (Coon et al., 2009; van Rahden et al., 2012), other studies indicated abnormal internalization caused due to defects in actin remodeling in the absence of Ocrl1 (R. Nandez et al., 2014).

Another important finding observed proximal tubule cells obtained from LS patients was reduced expression of the multi-ligand receptor megalin at the cell surface, caused due to defective recycling of this receptor from endosomes to plasma membrane (Festa et al., 2019; Vicinanza et al., 2011). In alignment with this, LS children have lesser megalin shedding in urine (Suruda et al., 2017). Megalin is a receptor for low molecular weight proteins, albumin and lysosomal hydrolases (Bökenkamp & Ludwig, 2016). Importantly, deficiency in urinary megalin has been implicated in proximal tubule dysfunction (Norden et al., 2002). Therefore, this is the likely explanation underlying the characteristic LMW proteinuria of LS patients (Vicinanza et al., 2011) . This Ocrl1-specific phenotype was also confirmed by in human proximal tubule kidney epithelial (HK2) and Madin Darby canine kidney (MDCK) kidney cell lines upon knockdown (KD) of Ocrl1 (Vicinanza et al., 2011).

This study demonstrated accumulation of $PI(4,5)P_2$ on endosomes in the absence of Ocr1 (Vicinanza et al., 2011). This was accompanied by actin enrichment that was dependent on the actin nucleating factor N-WASP. Reversal of these phenotypes was observed by reintroducing Ocrl1 with intact catalytic activity, or by the use of pharmacological agents of actin depolymerization or upon overexpression of a constitutively active form of the actin severing protein cofilin (Vicinanza et al., 2011). Interestingly, Rac activation deficiencies were also reported in LS patient fibroblasts (Madhivanan et al., 2012) and that this activation lies downstream of Ocrl1 (Madhivanan et al., 2012; van Rahden et al., 2012). At the same time, this Rac activation was also upstream of cofilin activation which suggested that Ocrl1 mediated-Rac activation is necessary modifying actin for endosomes to TGN trafficking (van Rahden et al., 2012).

Ocrl1 ASH-RhoGAP domain recruits endocytic proteins IPIP27 A and B to early and recycling endosomes (Noakes, Lee, & Lowe, 2011; Michelle Pirruccello, Laura E. Swan, Ewa Folta-Stogniew, & Pietro De Camilli, 2011). Knockdown of IPIPs resulted in defects in trafficking of Tf receptor, Shiga toxin (StxB) and Cation-independent M6PR (CI-M6PR) trafficking, accompanied by ligand retention in endosomes (Noakes et al., 2011). The mechanism underlying this however is unclear.

Ocrl1 has also been implicated in autophagosomal-lysosomal fusion (De Leo et al., 2016). Nutrient depletion (resulting in autophagy induction) in HK2 cells resulted in the recruitment of Ocrl1 to lysosomes in a clathrin and AP2 dependent manner, while Inpp5B was unable to do so

(De Leo et al., 2016). However, LS patient proximal tubule cells from LS patients Ocrl1-depleted HK2 cells showed an upregulation of lysosomal genes, enlarged lysosomes containing $PI(4,5)P_2$, as well enlarged autophagosomes indicating dysfunction in the pathway. Ocrl1 was then demonstrated to be recruited on lysosomal surfaces upon autophagy induction, to limit $PI(4,5)P_2$ levels on the membrane, a critical step necessary for autophagosomal-lysosomal fusion (De Leo et al., 2016).

The humanized LS mouse model also exhibited in $PI(4,5)P_2$ accumulation on lysosomes, defects in lysosomal dynamics including loss in proteolytic activity due to lack maturation of lysosomal enzymes. Using EGFR, this study demonstrated that loss of Ocrl1 perturbed the traffic of cargo from the plasma membrane to lysosome, revealing a new role for Ocrl1 in the endo-lysosomal pathway (Festa et al., 2019).

Cytokinesis

Absence of Ocrl1 leads to cytokinesis defects in Drosophila and in mammalian cells (Dambournet et al., 2011; El Kadhi, Roubinet, Solinet, Emery, & Carreno, 2011). In Drosophila, this caused regression of the cleavage furrow and produced multi-nucleated cells. Abnormal levels of $PI(4,5)P_2$ on endo membranes resulted in the mistargeting of the cytokinesis machinery to these structures (El Kadhi et al., 2011). Recent studies in *Drosophila melanogaster* supports this finding by demonstrating that $PI(4,5)P_2$ build up in the absence of Ocrl1 can be corrected if an atypical phospholipase C protein is overexpressed to help hydrolyze the lipid (Mondin et al., 2019). This reversed $PI(4,5)P_2$ accumulation on endosomal structures as well as rescued phenotypes in a LS zebrafish model (Mondin et al., 2019).

In Ocrl1-deficient mammalian cells, the accumulation of $PI(4,5)P_2$ on intercellular bridges inhibited actin depolymerization, thereby halting scission of the dividing cells at the last stage of cytokinesis. LS patient fibroblasts also displayed the cytokinesis abscission defect (El Kadhi et al., 2011). Gliozzi et al. (Gliozzi et al., 2020) also showed that kidney proximal tubule epithelial cells lacking Ocr1l exhibited higher multinucleated cells as well as lengthened the duration of cell division.

Organogenesis

Hsieh et al. (Hsieh, Ramadesikan, Fekete, & Aguilar, 2018) demonstrated that Six2, a transcription factor important for generation and maintenance of kidney proximal tubule cells was mislocalized in kidney-differentiated cells produced from LS patient derived induced pluripotent

stem cells (iPSCs). This defect was also recapitulated in HK2 KO cells. Similarly, Barnes et al. (Barnes et al., 2018) found aberrant actin structures in neuronal cells derived from LS patient iPSCs, indicating that these cellular phenotypes may contribute to overall organogenesis of kidney and brain respectively as well as homeostasis.

Phagocytosis

A role of Ocrl1 in phagocytosis was demonstrated in *Dictyostelium discoideum* Ocrl1 homolog Dd5P4, which when eliminated resulted in phagocytic cup closure failure (Loovers et al., 2007) and later recapitulated in mammalian cells lacking Ocrl1 (Bohdanowicz, Balkin, De Camilli, & Grinstein, 2012; Marion et al., 2012). Upon recruitment by Rab5 and APPL1, Ocrl1 is transported to the phagocytic cup in AP1-containing vesicles (Bohdanowicz et al., 2012; Marion et al., 2012). At the phagocytic cup, Ocrl1 catalytic activity helps limit $PI(4,5)P_2$ levels which will lead to cessation of actin polymerization, a critical requirement for closure of phagocytic cup. Loss of Ocrl1 also led to Akt hyperactivation due to the accumulation of $PI(3,4,5)P_3$ caused as a result of excess $PI(4,5)P_2$ present on the membrane (Loovers et al., 2007).

Membrane remodeling

Ocrl1 deficiency caused defects in fluid phase uptake, cell spreading and migration-processes that rely on the remodeling of cell membrane (Coon et al., 2009). Abnormalities in fluid phase uptake (determined by decreased uptake of fluorescently labeled dextran) was observed in LS fibroblasts compared to normal cells (Coon et al., 2009) as well as in the pronephros of the LS zebrafish model (Oltrabella et al., 2015). A similar defect was noted in animal models of Dent disease, another kidney-related disease (Piwon, Gunther, Schwake, Bosl, & Jentsch, 2000). Taken together, it suggests that fluid phase uptake defects may contribute to the renal pathophysiology observed in LS and Dent-2 disease.

Cell migration and spreading

Absence of Ocrl1 also produced cell migration defects in LS patient fibroblasts as observed in wound-healing and trans-well migration assays (Coon et al., 2009). Loss of Ocrl1 also led to defects in cell spreading on fibronectin extracellular matrix. Cells were rounded or had irregular shapes indicating a defect in isotropic spreading on the matrix (Coon et al., 2009). Further, migration defects of neural crest cells (NCCs) and melanophores were observed in the LS zebrafish model (Brian G. Coon et al., 2012). The NCC migration defect consequently led to an abnormal

pattern cranial cartilage and may explain the facial dysmorphology observed in patients and in *ocrl1* morphant fish (Brian G. Coon et al., 2012).

Ocrl1 is found at the leading edge of migrating cells and at membrane ruffles along with activated Rac (Faucherre et al., 2005). Though Ocrl1's RhoGAP domain lacks GAP activity, it binds to both activated and inactivated forms of Rac1 (Faucherre et al., 2003a). Hyperactivated RhoA signaling was detected LS patient blood platelets (Lasne et al., 2010) leading to LS to be classified as a bleeding disorder. Additionally, deficient Rac activation has also been reported in LS patient fibroblasts (Madhivanan et al., 2012) in addition to Rho hyperactivation (van Rahden et al., 2012) . The abnormal cell migration and cell spreading seen in patient cells is primarily caused by this Rho/Rac imbalance (Coon et al., 2009).

The catalytic activity of Ocrl1 and its interaction with the endocytic machinery (clathrin and AP2) are both required for its role in cell migration and spreading (Coon et al., 2009). Since Inpp5B does not interact with the endocytic machinery, this is thought to be the reason why the 5' phosphatase also could not rescue these defects (Coon et al., 2009). Like Ocrl1, other 5' phosphatases SKIP and SHIP2 have also been found to localize at membrane ruffles and mediate cell migration on fibronectin (Ramos et al., 2020) but it is not known if they can compensate Ocrl1's role in these processes.

Ciliogenesis

Ocrl1 partially localizes to the ciliary base and in the axoneme in some cell types during ciliogenesis (Brian G. Coon et al., 2012; Luo, West, et al., 2012; Rbaibi et al., 2012). LS fibroblasts, as well as Ocrl1 KD in mouse NIH3T3 fibroblasts and human retinal pigmented epithelial (RPE) cells showed a reduction in cilia formation and length (Brian G. Coon et al., 2012; Luo, West, et al., 2012) as well as $PI(4,5)P_2$ accumulation in the cilia (Prosseda et al., 2017). Recker et al. (F. Recker et al., 2015) demonstrated that fibroblasts obtained from 28 LS patients also exhibited ciliogenesis defects. However, increase in ciliary length was observed in Ocrl1 KD in MDCK cells (Rbaibi et al., 2012).

Like other ciliopathy zebrafish models and LS patients, Ocrl1-deficient fish had underdeveloped eyes and brain, laterality defects, cystic kidneys and facial dysmorphology (Brian G. Coon et al., 2012; Luo, West, et al., 2012). In addition, *ocrl1* morphant zebrafish Kuppfer's vesicle and pronephros had defective cilia (Brian G. Coon et al., 2012; Luo, West, et al., 2012; Rbaibi et al., 2012). Recently, Gliozzi et al.(Gliozzi et al., 2020), demonstrated a shortening of the

proximal tubules in the LS zebrafish model that was attributed to a defect in cytokinesis. In addition, these fish also presented with low molecular weight proteinuria, as observed in patients. This paper suggested that the shortening of proximal tubule was responsible for the excretion defects. This supports the clinical observations that LS is characterized primarily by renal tubulopathy (Bökenkamp & Ludwig, 2016).

Despite the ciliary membrane being uninterrupted from the plasma membrane, its composition is distinct in terms of the lipids and membrane receptors (Madhivanan K, 2016). This unique compartmental identity is maintained primarily by vesicle trafficking and it is critical to sustain it to allow ciliary function (Madhivanan & Aguilar, 2014). Vesicle trafficking to cilia occurs through 2 major routes- directly from TGN to base, mediated by Rab8 positive recycling endosomes; or via an indirect pathway from the plasma membrane, via Rab5-APPL1-IPIP27A/B endocytic axis to the ciliary base (Brian G. Coon et al., 2012) . Ocrl1 interacts with both Rab5 and 8, and Ocrl1 loss caused reduced ciliary traffic of cargo rhodopsin, via both pathways (Brian G. Coon et al., 2012). It is likely both pathways merge at the base of the cilia and operate to deliver specific cargo required for the building and maintenance of cilia (Brian G. Coon et al., 2012). Importantly, Coon et al. (Brian G. Coon et al., 2012) study showed that Ocrl1's participation in ciliogenesis is mediated via its phosphatase activity and ASH-RhoGAP domain with no necessity for the N-terminal PH domain.

Lowe Syndrome as a Ciliopathy-like disease

Abnormalities in ciliary structure or function results in a family of diseases called ciliopathies (Reiter & Leroux, 2017). Often, these diseases have multi-organ involvement (Reiter & Leroux, 2017). So far, more than 150 proteins have been implicated in ciliopathies (Reiter & Leroux, 2017). The discovery of ciliogenesis abnormalities in LS (Brian G. Coon et al., 2012) catapulted the disease from an orphan status to a ciliopathy or ciliopathy-like disease. This is extremely significant for many reasons. First, LS has been demonstrated to share similarities with other ciliopathies including characteristic multi-organ involvement , particularly eyes, kidney and brain. Second, the categorization of LS as a ciliopathy allows researchers to be able to study LS pathogenesis with a new perspective, including borrowing and testing hypotheses from other ciliopathy diseases. Discoveries made in LS may also contribute to the vast field of ciliopathies and help understand other diseases in the family. Finally, this will also help open therapeutic

avenues for LS that lacks a cure. Specifically, ciliopathy-specific drugs can be tested or repurposed as a candidate therapeutic against LS.

## 1.4 Inpp5E

Inpp5E (EC 3.1.3.36) is a type IV PI- 5' phosphatase whose substrates include $PI(3,4,5)P_3$ (highest affinity) $PI(4,5)P_2$, (Kisseleva et al., 2000) and $PI(3,5)P_2$ (Kong et al., 2000; Segawa et al., 2014). Inpp5E is encoded by the gene *INPP5E* located on chromosome 9. Inpp5E is required for embryogenesis (Jacoby et al., 2009) and is expressed highly in the brain (abundant especially in hypothalamus) pancreas, testis and spleen (Kisseleva et al., 2000). Mutations in *INPP5E* causes an autosomal recessive disorder called Joubert Syndrome (JS), a ciliopathy(Bielas et al., 2009; Jacoby et al., 2009) and MORM disease. JS disease is characterized by a midbrain malformation known as 'molar tooth sign', polydactyly, retinal degeneration and mental retardation. Mice and zebrafish models with absent or abnormal Inpp5E function recapitulate phenotypes observed in JS patients (Bielas et al., 2009; Jacoby et al., 2009; Luo, Lu, & Sun, 2012). Recently, Inpp5E has also been shown to be implicated in polycystic kidney disease (S. Hakim et al., 2016) with zebrafish models of the disease recapitulating patient phenotypes such as cilia defects and cystic kidneys (S. Hakim et al., 2016; Xu et al., 2017).

### 1.4.1 Domain architecture and interactions of Inpp5E

Inpp5E contains an N-terminus proline rich domain (PRD) with 13 PxxP consensus sequences, two Immunoreceptor Tyrosine-Associated Motif (ITAMs), a central catalytic 5' phosphatase domain and a C-terminus CAAX box that gets prenylated for membrane anchoring. A splice variant (lacking 34 amino acids) of Inpp5E is also present, which lacks the ITAMs (Kisseleva et al., 2000; Kong et al., 2000). (Fig.1.2)

Inpp5E undergoes tyrosine-phosphorylation by activated insulin receptor (Bertelli et al., 2006) and Ser/Thr-phosphorylation by Aurora kinase A (AurKA) (Plotnikova et al., 2015). It also interacts with insulin receptor substrate 2 (IRS2) (Bertelli et al., 2006; Bertelli et al., 2013). Inpp5E associates with the p85 subunit of PI3K and through its catalytic activity, hydrolyzes $PI(3,4,5)P_3$, and thereby negatively regulates Akt pathway (Bertelli et al., 2006; Bertelli et al., 2013). This underscores its critical role in modulating insulin signaling in cells (Bertelli et al., 2013).

Via its N-terminal proline-rich domain, Inpp5E localizes to the Golgi (Kong et al., 2000). It has also shown to bind to Rabs; namely Rab20, a GTPase found at the Golgi- and phagosome (Fukuda et al., 2008). This is unlike Ocrl1 that interacts with a multitude of Rabs via its ASH domain (Fukuda et al., 2008). Curiously, Inpp5E preferentially binds GDP-bound form of Rab20, an interaction that facilitates into localization at the Golgi (Fukuda et al., 2008). The physiological relevance of this interaction is yet to be determined. It is speculated that Inpp5E contains a Rab-binding site at its N-terminal PRD (Fukuda et al., 2008).

Using tandem affinity purification with Inpp5E as bait, Humbert et al. (Humbert et al., 2012) demonstrated that Inpp5E interacts with several ciliary proteins such as CEP164, 14-3-3ε/γ and RUVBL1, RUVBL2. While the first two proteins are either involved in cilia formation or localize at the cilia, the significance of RUVBL1 and 2 in ciliary function is still unknown (Humbert et al., 2012). These results however indicate that Inpp5E is involved in the overall process of forming and or maintain cilia. Overall, under steady state conditions, Inpp5E is enriched at the Golgi (Kong et al., 2000) which during starvation, it is found to localize at the cilia (Bielas et al., 2009; J. M. Dyson et al., 2017; Jacoby et al., 2009; Luo, Lu, et al., 2012).

Inpp5E's ciliary localization is mediated by the presence of a conserved FDRELYL sequence, instead of the conventional ciliary localization motif that is also present in the protein. (Humbert et al., 2012). GTPase Arl13B helps recruit Inpp5E to the cilia via this sequence in a PDE6D dependent manner. PDE6D is phosphodiesterase and prenyl-binding protein that complexes with Inpp5E (through mechanisms still unclear) at the CAAX box (Humbert et al., 2012). Interestingly, absence of PDE6D has also been linked to Joubert Syndrome as well as induces a mis-localization of Inpp5E (S. Thomas et al., 2014).

### 1.4.2 Functions of Inpp5E

PI3K/Akt signaling

Inpp5E binds to the p85 subunit of PI- 3' kinase (PI3K) and inhibits its signaling (Bertelli et al., 2006). Its phosphatase activity against PI(3,4,5)$P_3$ synergises with the inhibition of p85 resulting in decrease in PI(3,4,5)$P_3$, thereby also inhibiting the PI3K/AKT signaling pathway. Conversely, Inpp5E-deficient cells have high levels of PI(3,4,5)$P_3$ (Bielas et al., 2009) and increased phospho-Akt levels (S. Hakim et al., 2016; Plotnikova et al., 2015). Cells expressing Inpp5E mutants display hyperactivated Akt (Bielas et al., 2009).

Due its effect on the PI3K/AKT pathway, Inpp5E influences many cellular processes. For example, Inpp5E it reduces the anti-apoptotic effects on PI3K/Akt signaling. Overexpression of Inpp5E resulted in increase in apoptotic cells while prolonged exposure to high levels of Inpp5E induced cell growth arrest, suggesting a tumor-suppressive role for this enzyme (Kisseleva, Cao, & Majerus, 2002).

Insulin signaling and glucose homeostasis

Activation of insulin receptor, by insulin leads to the turning on of the PI3K/AKT pathway. This pathway is essential for cell survival and metabolic signaling. Through its catalytic activity, Inpp5E is predicted to limit the availability of $PI(3,4,5)P_3$ therefore counteracting insulin signaling (Bertelli et al., 2006). The hypothalamus is the primary region in the central nervous system (CNS) that regulates insulin signaling (Bertelli et al., 2006). Inpp5E participates in growth factor signaling, by limiting basal levels of $PI(3,4,5)P_3$ in the hypothalamus and consequentially, its response to insulin stimulation (Bertelli et al., 2006; Bertelli et al., 2013; Wang, Ijuin, Itoh, & Takenawa, 2011). Not surprisingly, Inpp5E is abundantly expressed in the hypothalamus and is tyrosine phosphorylated by the insulin receptor. Physiological consequences of these signaling events include CNS-mediated reduction in food intake (dependent on insulin) and glucose homeostasis (Bertelli et al., 2006; Bertelli et al., 2013). Inpp5E overexpression studies resulted in insulin-resistant diabetes and obesity in mice models, making it a potent target for diabetes and obesity drug therapies (Bertelli et al., 2013).

Phagocytosis

Since $PI(3,5)P_2$ is required for phagocytic cup closure, Inpp5E's enzymatic activity against $PI(3,5)P_2$ inhibits phagocytosis (Horan et al., 2007). Inpp5E also interacts with the phagosome-associated Rab20 (Fukuda et al., 2008). In cells lacking Inpp5E, though recruitment of Rab20 to the phagosome was unaffected, Rab5 and Rab20's retention time was significantly lower (Segawa et al., 2014). This indicated a role for Inpp5E in tethering these Rabs to the phagosome, maybe by mediating the $PI(3,5)P_2$ levels at the membrane. Given that Rab5's removal from phagosome coincides with phagosomal maturation (Fairn & Grinstein, 2012), it is tempting to speculate that Inpp5E, by depleting $PI(3,5)P_2$, maybe delaying the release of Rab5, thereby impairing phagosomal maturation.

Vesicle trafficking

From phylogenetic studies, Cil-1 is a 5' phosphatase in *Caenorhabditis elegans* that is similar to mammalian Inpp5E. Cil-1 facilitates the trafficking of the Transient Receptor Potential-Polycystin (TRPP) complex by modulating $PI(3,5)P_2$ and PI3P levels suggesting that it is plausible that Inpp5E may play a similar role in mammalian cells (Bae, Kim, L'Hernault, & Barr, 2009).

Recently, deficiency of Inpp5E has been shown to impair the fusion of autophagosomes with lysosomes, leading to an accumulation of autophagosomes (Hasegawa et al., 2016; Nakamura, Hasegawa, & Yoshimori, 2016). This study demonstrated a role for Inpp5E in the autophagy pathway by its 5' phosphatase activity on $PI(3,5)P_2$ at lysosomes (Nakamura et al., 2016).

Maintenance of cilia and transition zone

Multiple studies in mice and zebrafish have demonstrated the role of Inpp5E in cilia formation and maintenance (Bielas et al., 2009; Jacoby et al., 2009; Luo, Lu, et al., 2012). In addition, loss of Inpp5E also resulted in Kupffer vesicle as well as melanosome migration defects in inpp5e morphant zebrafish (Luo, Lu, et al., 2012). Recently, Hardee et al. (Hardee et al., 2017) demonstrated that fibroblasts obtained from Joubert syndrome patients also exhibited ciliogenesis defects.

Inpp5E directly interacts with Aurora kinase A (AurkA) (Plotnikova et al., 2015), which results in its phosphorylation by the latter. This leads to an enhancement in its catalytic activity towards $PI(3,4,5)P_3$, particularly in regions such as ciliary base (Plotnikova et al., 2015) (where AurkA localizes (Pugacheva, Jablonski, Hartman, Henske, & Golemis, 2007)). This catalytic activity of Inpp5E is required for maintaining ciliary stability (Plotnikova et al., 2015). Interestingly, AurkA is one of the targets of the Akt signaling pathway (X. Liu et al., 2008) and has been shown to regulate cilia stability by complexing with Histone DeAcetylase 6 (HDAC6) (Pugacheva et al., 2007).

In a zebrafish model of Joubert Syndrome, Inpp5E has also been demonstrated to be important for maintaining lipid segregation in kidney epithelial cells which is necessary for establishing apico-basal polarity (Xu et al., 2017). This polarization is necessary for basal body docking in an ezrin-dependent manner which then allowed ciliogenesis to proceed (Xu et al., 2017).

Sonic Hedgehog (Shh) signaling and tissue patterning

Primary cilia are critical for neural crest cell (NCCs) differentiation and proliferation and this is dependent on the Sonic Hedgehog (Shh) pathway. The cilia in these cells are enriched in PI4P and Inpp5E has been shown to be the key 5' phosphatase that helps maintain high levels of

localized PI4P in the cilia by downregulating $PI(4,5)P_2$ levels. Mice studies have demonstrated that absence of Inpp5E led to hyperactivation of Akt signaling and proliferation (likely due to excess of $PI(3,4,5)P_3$) (Jacoby et al., 2009). Loss of Inpp5E also led to $PI(4,5)P_2$ accumulation at the ciliary tips and not the base (Bielas et al., 2009). Build-up of $PI(4,5)P_2$ recruits the tubby-like protein Tulp3 and its ciliary cargo the GPCRs Gpr161 which negatively regulates Sonic hedgehog (Shh) pathways (S. Mukhopadhyay et al., 2010; Saikat Mukhopadhyay et al., 2013). NCCs isolated from *inpp5e*-null mice exhibited stunted cilia bearing enlarged tips with accumulation of Tulp3 and Gpr161. Consequentially, abolition of Shh signaling was observed in these cells, in spite of Shh ligand stimulation. In addition, no defects were observed in levels or trafficking of Shh proteins (Saikat Mukhopadhyay et al., 2013). Aberrant Shh signaling results in polydactyly and exencephaly are known to be caused by aberrant Shh signaling (Lopez-Rios et al., 2012). Interestingly, polydactyly was observed in *inpp5e* knockout mice (Bielas et al., 2009). These results establish the mechanism by which Inpp5E's phosphatase activity is involved in development and tissue patterning via regulation of Shh signal transduction at the primary cilia (Chavez et al., 2015; Lopez-Rios et al., 2012).

In addition to maintenance of cilia, thereby regulating Shh signaling, Dyson et al. (J. M. Dyson et al., 2017) also demonstrated a role for Inpp5E in maintaining the integrity of the ciliary transition zone (TZ). Ablation of Inpp5E in mice led to defects that were reminiscent of ciliary dysfunction as well as aberrant Hh signaling including cleft palate, polydactyly, delayed ossification of bones, micropthalmos. Embryos also exhibited patterning defects as well as accumulation of $PI(4,5)P_2$ and $PI(3,4,5)P_3$ at ciliary transition zone. Further, activation of Shh signaling in mice lacking Inpp5E, along with the accumulation of Inpp5E substrates resulted in mis-localization of TZ proteins. This subsequently led to lesser Smoothened (Smo) accumulation in the cilia upon Shh activation which could not be rescued by Inpp5E lacking catalytic activity (J. M. Dyson et al., 2017). This reveals a new role of Inpp5E in modulating Shh signaling at the transition zone.

Cell division

Spindle assembly checkpoint (SAC) is a cell cycle checkpoint mechanism by which erratic chromosome segregation is corrected to avoid aneuploidy (Nalepa et al., 2013). Following the identification of Inpp5E as a candidate for a 5'phosphatase that regulated mitosis (Nalepa et al., 2013), Sierra Potchanant et al. (Sierra Potchanant et al., 2017) validated that Inpp5E was essential

for maintaining the SAC during cell cycle. Spindle assembly checkpoint. In cell lines lacking Inpp5E, upon induction of SAC, cells displayed multinucleation, a sign of SAC failure. Further, this ability to escape SAC was due to accumulation of Inpp5E substrate $PI(4,5)P_2$. In addition, loss of Inpp5E also resulted in mitotic defects such as multiple centrosomes as well cytokinesis failure (Sierra Potchanant et al., 2017).

Studies also show that Inpp5E regulates phosphoinositide metabolism inside the cilium, thereby controlling PDGF-PI3K-Akt pathway which mediates cell cycle entry (Bielas et al., 2009).

### 1.5 Diseases associated with Inpp5E

Mutations in *INPP5E* result in two ciliopathies namely, Joubert syndrome (OMIM #213300) and Mental retardation, truncal obesity, retinal dystrophy, and micropenis (MORM) syndrome (OMIM #610156); however, their clinical manifestations are starkly distinct.

*INPP5E* has also been implicated in polycystic kidney disease (S. Hakim et al., 2016) and animal studies have confirmed the presence of renal cysts in the absence of Inpp5E (Dillard et al., 2018; S. Hakim et al., 2016; Xu et al., 2017). Loss of Inpp5E also results in a hyperactivation of mTOR-PI3K-Akt signaling axis, which contributes to the ciliary defects and presence of cystic kidneys (S. Hakim et al., 2016).

MORM was discovered in 2006 (Hampshire et al., 2006) in a Pakistani family with 3 members exhibiting mild to moderate mental retardation, upper obesity, micropenis as well as impaired vision (Hampshire et al., 2006) and thought to be similar to Bardet-Biedl syndrome, another ciliopathy. The gene locus was mapped to chromosome 9. In 2009, *INPP5E* was identified as the gene causing MORM (Bielas et al., 2009). However, not much is known about this disease and it is relatively rare.

Joubert Syndrome (also known as Joubert-Boltshauzer Syndrome; JS) was discovered in the 1968 by Marie Joubert (Joubert, Eisenring, & Andermann, 1968). A rare multigenic disease, nearly 21 genes have been found to cause JS (Valente, Brancati, & Dallapiccola, 2008). All these genes encode ciliary proteins, making JS a ciliopathy (Valente et al., 2008). Depending on the chromosomal location of the gene, the mode of inheritance can be autosomal recessive or X-linked. The prevalence of JS in USA is 1:100,000 (Romani, Micalizzi, & Valente, 2013).

It is a multiorgan disease classified into 6 subgroups, based on the organ involvement (Romani et al., 2013; Valente, Dallapiccola, & Bertini, 2013). Depending on the causative gene,

the clinical presentation is speculated to differ, often involving different organs, making this a phenotypically as well as genotypically heterogenous disease (Romani et al., 2013).

One of the genes implicated in JS is PI- 5' phosphatase encoding *INPP5E* (Bielas et al., 2009). JS caused by *INPP5E* mutations has an autosomal recessive mode of inheritance and accounts for 3% of affected patients (Romani et al., 2013). This section will be focused on reviewing the overall clinical presentation of JS.

### 1.5.1 Clinical characteristics of Joubert Syndrome

Neurological

The hallmark of JS is a unique midbrain-hindbrain malformation called 'molar tooth sign' (MTS). Independent of the gene involved, all JS patients exhibit this MTS during brain imaging, a tell-tale sign accompanying JS diagnosis (Valente, Brancati, Boltshauser, & Dallapiccola, 2013). In addition, hypotonia, cerebellar ataxia, developmental delay is also part of the classic symptoms, accompanied by abnormal ocular movements that provide a diagnosis of JS (Romani et al., 2013; Valente, Brancati, et al., 2013).

Other neuroimaging findings include cerebellar dysplasia, loss of demarcation between cortex and white matter and glial proliferation. Many patients also have varying degrees of intellectual disability (Romani), though it is not necessarily a disease hallmark (Brancati, Dallapiccola, & Valente, 2010). A consequence of neurological dysfunction is breathing difficulties, seen early in 10-15% of patients (Romani et al., 2013).

Some other carrying neurological phenotypes include white matter cysts, hydrocephalus, abnormalities in the corpus callosum and absence of the pituitary gland (Brancati et al., 2010). In small percentages of patients, a characteristic posterior cyst is observed (Brancati et al., 2010; Valente et al., 2008). Abnormal migration defects and cortical organization defects have also been reported. Patients with the above defects present with higher incidence of epilepsy, which is otherwise not observed in JS (Brancati et al., 2010). The severity of neurological compromise is directly correlated to prognosis (Brancati et al., 2010).

Besides the brain, some other affected organs include eyes, kidney, liver, skeleton as well as oro-digital deformities, craniofacial dysmorphology, situs invertus. Patients with all of the above organ manifestations are classified under the sub-group 'pure' JS (Romani et al., 2013).

Ocular (JS+retinal involvement)

Abnormal eye movements including nystagmus and strabismus are observed, as well as retinal abnormalities which eventually progress to retinopathies (due to degeneration of photoreceptor cells (Brancati et al., 2010), resulting in compromised vision (Romani et al., 2013). Patients also exhibit coloboma or a 'hole in the eye' either in one or both eyes and are thought to arise from failure of closure of the fetal fissure (Brancati et al., 2010).

Skeletal (JS+skeletal involvement)

Skeletal involvement includes severe scoliosis and skeletal dysplasia (Romani et al., 2013).

Renal (JS+renal involvement)

25% of JS patients present with renal symptoms (Brancati et al., 2010). Renal manifestations include nephronophthisis, cystic dysplastic kidneys (Romani et al., 2013). Symptoms include irregular thickening of basal membrane of the tubular epithelium, progressive interstitial fibrosis. Patients often are asymptomatic with mild unnoticed signs such as polyuria until they develop chronic renal insufficiency or end stage renal disease by second decade of life (Romani et al., 2013).

Hepatic (JS+hepatic involvement)

Hepatic complications are rare but manifest as congenital liver fibrosis. Symptoms include elevated serum liver enzymes, early onset hepatomegaly (enlarged liver) and in severe cases include liver cirrhosis (Brancati et al., 2010).

Other manifestations

Some rare cases also have congenital heart malformations, situs inversus (Valente et al., 2008).

Physical anomalies (JS+oro-facio-digital involvement)

10-15% JS patients display polydactyly, midline oral and facial defects and categorized as facial dysmorphism including frontal bossing, prominent forehead, ptosis of the eye (drooping eyelid), arched eyebrows and protruding, lobulated tongue (Romani et al., 2013). Some other features include cleft lip and/or palate, notched upper lip and lingual or oral soft tumors (Valente et al., 2008).

*INPP5E* mutations often result in 'pure JS' or 'JS with retinal involvement' (Bielas et al., 2009; Brancati et al., 2010; Hardee et al., 2017; Shetty, Ramdas, Sahni, Mullapudi, & Hegde, 2017), with occasional hepatic involvement (Travaglini et al., 2013). Given the cellular functions of Inpp5E in multiple processes like tissue patterning (via Shh signaling), formation and

maintenance of cilia, and modulating pathways such as PI3K-Akt, mTOR, it is not surprising that *INPP5E* mutations result in a severe form of JS with pleiotropic effects in the body.

### 1.5.2 Genotype-phenotype correlation between *INPP5E* mutations causing Joubert Syndrome and MORM

Despite the involvement of the same gene in both diseases, the heterogeneity in the clinical presentation of Joubert Syndrome and MORM is evident. All *INPP5E* missense mutations causative of Joubert Syndrome map to the region encoding the catalytic domain of the protein. (Bielas et al., 2009; Hardee et al., 2017; Shetty et al., 2017; Travaglini et al., 2013). Although mutated Inpp5E can localize to the cilia, they lack catalytic function. Interestingly, though cells expressing mutated Inpp5E have normal cilia number and morphology, their tips are bulged, and this is believed to be due to accumulation of cargo (Bielas et al., 2009; Jacoby et al., 2009; Travaglini et al., 2013). Further, cells expressing these mutants have unstable cilia and are sensitive to serum, making them more prone to cilia disassembly in these conditions (Bielas et al., 2009). Mice lacking Inpp5E also die early, have renal cysts as well as neurological phenotypes during early development (Bielas et al., 2009; Jacoby et al., 2009). However, no striking ocular defects were observed.

The *INPP5E* mutation Q627X causes MORM syndrome. This nonsense mutation results in the loss of the C-terminus CAAX box, producing a truncated Inpp5E protein. In contrast to Joubert Syndrome-related Inpp5E variants, this mutant Inpp5E was restricted to the base of the cilium, but retained enzymatic activity (Bielas et al., 2009). Despite preservation of catalytic activity, ciliary instability was observed (Bielas et al., 2009).

Interestingly, mutations in *PDE6D* produce renal, ocular and neurological defects in mice, phenocopying defects observed in Inpp5E-deficient mice (S. Thomas et al., 2014). As indicated before, Inpp5E binds to PDE6D via its CAAX box and this is required for its PC localization (S. Thomas et al., 2014) The Inpp5E MORM variant is probably unable to sustain this interaction, hence cannot localize at the cilia. This indicates that Inpp5E-mediated ciliary stability depends on its catalytic function and correct localization to the cilia. Nevertheless, it is unclear why MORM syndrome only presents with a subset of phenotypes observed in Joubert syndrome (such as mental retardation, micropthalmos and retinal degeneration) as well as other unique manifestations like micropenis.

Given the biochemical nature of mutants implicated in both the diseases, it is tempting to suggest that depending on the nature of the mutation and the domain of the protein that is affected, the effect it may have on the behavior of mutant protein is distinct. As a result, this may differently impact cellular phenotypes, thereby eliciting heterogeneity in the clinical manifestations observed in Joubert Syndrome vs. MORM. Indeed, there may be other factors such as genetic modifiers, environment and other mechanisms that may also contribute to the heterogeneity in cellular phenotypes as well as patient symptoms.

### 1.6 Diseases associated with Ocrl1

Mutations in *OCRL1* result into two diseases namely, Lowe Syndrome (LS) (OMIM #309000) and Dent-2 disease (OMIM #300555). Dent-2 disease is considered a milder form of LS (Bokenkamp 2009), in that the renal phenotypes are less severe, and patients do not ex\hibit striking ocular or neurological defects that LS patients have. Further, there is a separation in the location of mutations in *OCRL1* that produce LS vs. Dent-2 disease.

LS (also known as Oculo-cerebro-renal syndrome of Lowe (OCRL) was first described in 1952 by Dr. Charles Lowe and colleagues (LOWE, TERREY, & MacLACHLAN, 1952). It is a rare X-linked condition caused by mutations in the gene *OCRL1* (Attree et al., 1992b; Suchy et al., 1995; X. Zhang et al., 1995). The disease prevalence is 1:500,000 (Mario Loi, 2006).

LS has multi-organ involvement with striking ocular, cerebral and renal symptoms. Children with LS are born with bilateral congenital cataracts, generalized hypotonia and exhibit renal Fanconi-like syndrome as early as 6 months of age (Mario Loi, 2006). These three classical manifestations followed by molecular analysis results in a LS diagnosis. With time, renal symptoms worsen, resulting in kidney failure which is the cause of death. So far, there is no LS-specific cure and majority of treatments only manage symptoms.

Renal

The kidney (particularly proximal tubule) is severely affected in LS. Renal symptoms are consistent with impaired proximal tubule function. Classical features include low molecular weight (LMW) proteinuria which is detected in the first few months after birth, aminoaciduria (wide variety of amino acids seen), albuminuria (Lowe, 2005). Megalin trafficking defects has been attributed to the LMW proteinuria (Vicinanza et al., 2011).

Hypercalciuria and hyperphosphaturia is also noted. It is speculated that loss of Ocrl1 results in impaired Trpv6 (a calcium channel) trafficking (Wu et al., 2012), resulting in hypercalciuria. LS patients also develop nephrocalcinosis/nephrolithiasis (Bokenkamp, Levtchenko, Recker, & Ludwig, 2015), which refers to a generalized deposition of calcium oxalate or phosphate crystals in the kidney. Typically, 98% of the $Ca^{2+}$ filtered by the kidney is reabsorbed by the proximal tubule, by a process called micropinocytosis (Kanlaya, Sintiprungrat, Chaiyarit, & Thongboonkerd, 2013). If this fails, the calcium is hypothesized to either adhere to the proximal tubule cells, forming stones (Kohjimoto, Ebisuno, Tamura, & Ohkawa, 1996a) or may eventually undergo transcytosis and enter the kidney interstitial space (Kohjimoto, Ebisuno, Tamura, & Ohkawa, 1996b). The internalized $Ca2^{+}$ ions are degraded by lysosomes. Multiple groups have demonstrated defective micropinocytosis or 'fluid phase' uptake of cargo in the absence of Ocrl1 in LS fibroblasts (Coon et al., 2009) and LS zebrafish models (Oltrabella et al., 2015) as well as impaired endo-lysosomal fusion (Festa et al., 2019). It is hence hypothesized that nephrocalcinosis could be due to defective micropinocytosis and/or defects in vesicle trafficking.

Excretion of lysosomal hydrolases is noticeable (A. J. Ungewickell & Majerus, 1999) and is thought to contribute to the tubular damage. The mis-trafficking of M6PR, a receptor of lysosomal hydrolases and megalin in the absence of Ocrl1 is predicted to be the underlying cause of lysosomal enzyme excretion (Vicinanza et al., 2011). Renal tubular acidosis is often mild in LS while Dent-2 patients have significant acidosis (Cho et al., 2008). Tubular atrophy (Schramm et al., 2004) is also noticeable. This proximal tubule shortening been confirmed in the LS zebrafish model as well (Gliozzi et al., 2020). Besides these findings, renal Fanconi syndrome also includes glucosuria, which is markedly absent in LS patients (A). Hence, the renal phenotype in LS is Fanconi-like (Kleta, 2008).

Initially renal biopsies are normal, with time, interstitial fibrosis is noticeable. There is a gradual decrease in glomerular filtration rate, indicative of glomerular damage (Zaniew et al., 2018). Patients suffer from progressive renal failure, needing dialysis and end stage renal disease (ESRD) is often cause of death by late adolescence (Mario Loi, 2006). Very few patients have survived until their late 40s-early 50s of age.

Ocular

Besides bilateral cataracts at birth (surgically removed) in all LS patients, glaucoma is seen in 50% of them which is also surgically corrected. Increased intraocular pressure in patients (Na

Luo et al., 2014), may contribute to glaucoma. Cataracts are thought to be result of improper embryonic development (Tripathi, Cibis, & Tripathi, 1986), including migration defects in lens cells. Since Ocrl1 loss results in primary cilia and impairs rhodopsin trafficking to cilia (Brian G. Coon et al., 2012), ciliary dysfunction may also contribute to cataracts.

Patients have deep set eyes, micropthalmos (small eyes) and poor visual acuity, requiring corrective glasses. Patients are aphakic (no lens) due to surgical removal of cataract and possess corneal opacities. There is evidence of corneal scarring and keloids. Additionally, abnormal eye movements, including nystagmus and strabismus is seen (Bokenkamp et al., 2015). Dent-2 disease patients rarely have ocular defects, or develop corneal opacities very late in life (Recker, Heutter, & Ludwig, 2013).

Neurological

One of the striking features is hypotonia in all LS newborns, as well as lack of deep tendon reflexes. There is overall decrease in muscle tone as well as delayed developmental and motor milestones. Nervous system defects are thought to cause the hypotonia although the exacerbated levels of lactate dehydrogenase (and other muscle enzymes) in serum may indicate overall tissue damage and muscle wasting. This elevation of muscle enzymes has been seen in some Dent-2 disease patients as well (Cho et al., 2008). All LS patients exhibit severe intellectual disability. Some patients also have seizures (Leahey, Charnas, & Nussbaum, 1993; Röschinger, Muntau, Rudolph, Roscher, & Kammerer, 2000).

Neurological imaging reveals lesions in the periventricular space and deep white matter. Demyelination is also observed, with cysts in the white matter. Gliosis is present and thought to be due to acidic lysosomal enzyme secretion (Recker et al., 2013).

Behavioral traits of LS patients include aggression, repetitive hand movements, stubbornness and temper tantrums. These children are also diagnosed with obsessive compulsive disorder and tend to self-harm. Dent-2 disease patients do not present with neurological deficits at the time of diagnosis, though develop mild to moderate intellectual disability during later stages of life.

Besides eyes, brain and kidney, there are other manifestations in musculo-skeletal system, bones, skin, oral cavity, hemostasis in addition to notable facial deformities.

Musculo-skeletal

Hypotonia often results in joint hypermobility in patients. Patients also have osteopenia (weak bones) and low mineral density, resulting repeated fractures. This is attributed to low levels

of parathyroid hormone (PTH) and due to the excessive loss of calcium and phosphate. 50% of patients also suffer from scoliosis. Majority of patients have Vitamin-D independent rickets that is also attributed to mineral loss.

Oral cavity

Patients suffer from oral cysts (Peverall, Edkins, Goldblatt, & Murch, 2000; Tsai & O'Donnell, 1997), dental follicles (Ruellas, Pithon, Oliveira, & Oliveira, 2008), gingivitis (Roberts, Blakey, Jacoway, Chen, & Morris, 1994), abnormal dentin formation and malformed teeth (Harrison, Odell, & Sheehy, 1999).

Hemostasis

Lasne et al. (Lasne et al., 2010) identified hemorrhagic events in multiple LS patients as well as long closure times from blood samples, which enabled LS to be classified as a bleeding disorder. Further, there were changes to platelet adhesion behavior as well cell shape. These defects were determined to be due to a hyperactivation in RhoA GTPase signaling (Lasne et al., 2010).

Skin

LS patients have been reported to have skin lesions, benign epidermal cyst as well as cysts in hair follicles. These symptoms are attributed to increased secretion of lysosomal enzymes, resulting in tissue damage or defects in cell polarity seen in the absence of Ocrl1 (Grieve et al., 2011).

Physical features

Children are often in the lower percentile of growth and stature (Brooks & Ahmad, 2009), may be due to growth hormone deficiencies (Dai et al., 2019). Additionally, patients have deep set eyes, frontal bossing, wide forehead (Brooks & Ahmad, 2009).

## 1.7 Genotype and phenotype correlation between *OCRL1* mutations causing Lowe Syndrome and Dent-2 disease

The Human Gene Mutation Database (HMGD), the National Human Genome Research Institute (NHGRI) and ClinVar are some of the most comprehensive databases that estimate nearly 250 unique disease mutations in *OCRL1*. These mutations result in either LS or Dent-2 disease. Although these databases have an extensive list of gene variants, some of them (ex. NHGRI's database) have been retired, and not all authors deposit their novel variants in these servers.

From carefully analyzing these existing lists as well as all literature on *OCRL1*, we estimate that LS-causing *OCRL1* mutations alone are nearly 300 while Dent-2 disease producing mutations are close to 80. In addition, there are other Ocrl1 variants that do not have an associated diagnosis/clinical significance or only are associated with neurodevelopmental disorder.

Here we will focus only on those mutations associated with either LS or Dent-2 disease diagnosis. It must be noted that there is a subset of mutations (particularly affecting phosphatase and ASH-RhoGAP domain) that cause both LS and Dent-2 disease and will be represented in both groups. Further, the exact incidence of mutations is not clearly known since not all LS cases involve genetic testing and not all that do receive a molecular diagnosis are reported.

LS mutations-

Of nearly 300 LS-causing *OCRL1* mutations, less than 10% are in the intronic regions (22/292). The rest (270) are found in regions encoding exons and include missense, nonsense, 'indels' (insertions and deletions) resulting in frameshift or splicing defects as well as gross genomic deletions.

Mutations causing LS predominantly cluster around regions of the gene encoding exons 9-24 (phosphatase through RhoGAP domain), with a concentration in the catalytic domain of the protein (Hichri et al., 2011). Over 50% of mutations (158/270) affect the phosphatase domain, nearly 30% (87/270) affect the ASH-RhoGAP domain, while less than 10% (23/270) affect the PH domain (Fig.1.4).

Even within the domains, there is distinct differences in the type of mutations found in the region. Most of the mutations affecting the PH domain are 'indels', causing frameshifts and premature truncation of protein (19/23) while in the ASH-RhoGAP domain, many mutations (48/88) cause frameshift and premature protein termination as well as splicing defects. Most LS-causing mutations affecting phosphatase domain are missense in nature (80/158), resulting in single amino acid changes (Fig.1.4). This is enough to produce disease. Single nucleotide change nonsense mutations that lead to premature termination of protein are less abundant in all domains of the protein.

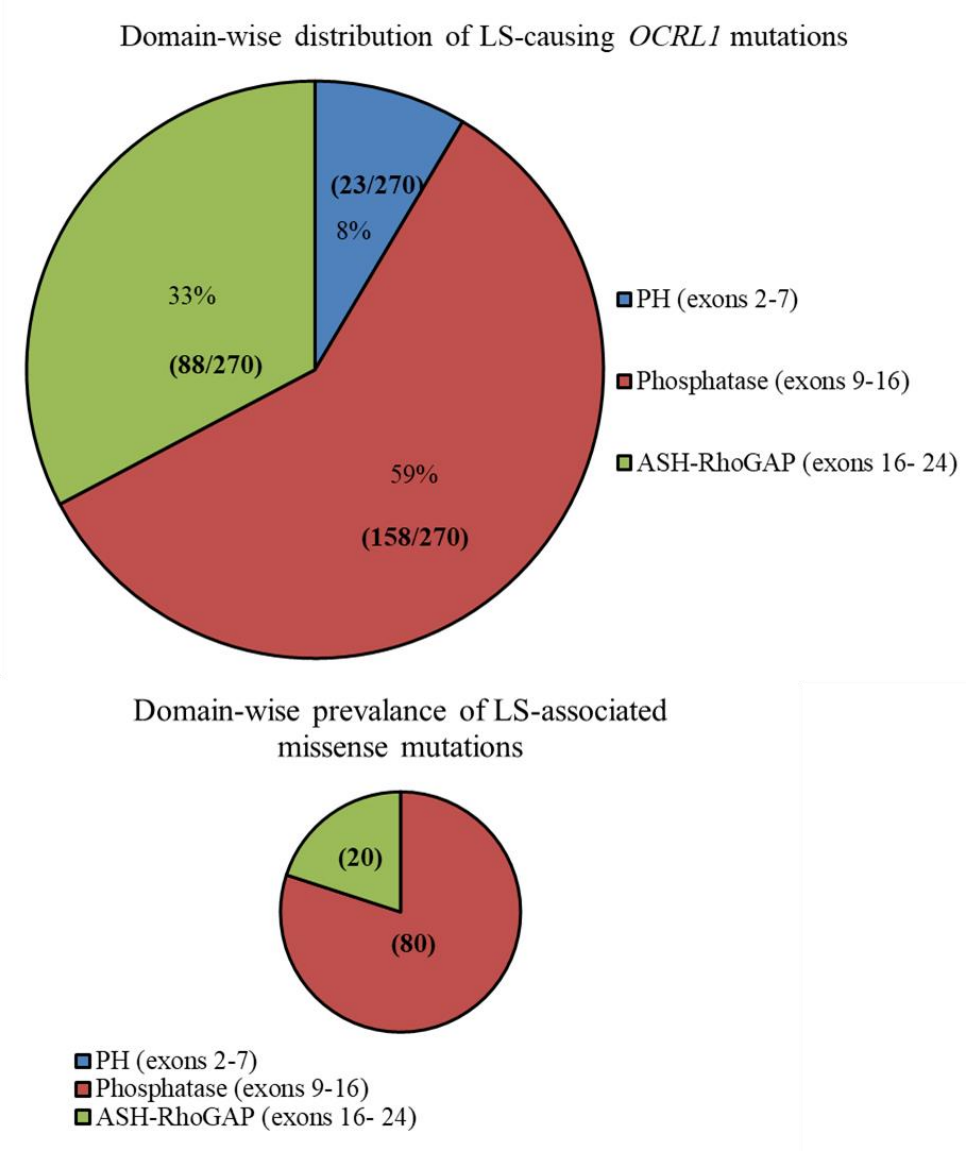


**Figure 1.4 LS-causing *OCRL1* mutations affecting different domains of Ocrl1**

Since the phosphatase domain is the hotspot, especially for missense mutations, the focus of our study is will be on missense mutations affecting this domain. Within the phosphatase domain, incidence of missense mutations is the highest; with 80 unique mutations affecting the catalytic region and accounting for one-third of disease-causing mutations. This region also has high incidence of 'indels' reported (55/158). (Fig. 1.3) Suarez-Artiles et al. (Suarez-Artiles, Perdomo-Ramirez, Ramos-Trujillo, & Claverie-Martin, 2018) performed a splicing analysis of various exons of *OCRL1* and suggested that exons 9, 11, 12, 15, 21, 22 and 23 are considered 'poorly defined' exons since they have a weak 5' or 3' splice site. This may explain why exons encoding

the phosphatase and ASH-RhoGAP domain contain higher percentage of splicing defects resulting in disease.

Importantly, mapping of all LS-causing missense mutations within the phosphatase domain reveals that nearly 50% of existing missense mutations lie outside of the residues essential for substrate binding, interaction with lipids and enzyme function (Fig.1.5). Yet single amino acid changes in regions either not conserved or essential for function leads to disease. This observation has not been reported and the reason why residues that are neither conserved nor essential for catalysis causing disease is currently unknown.

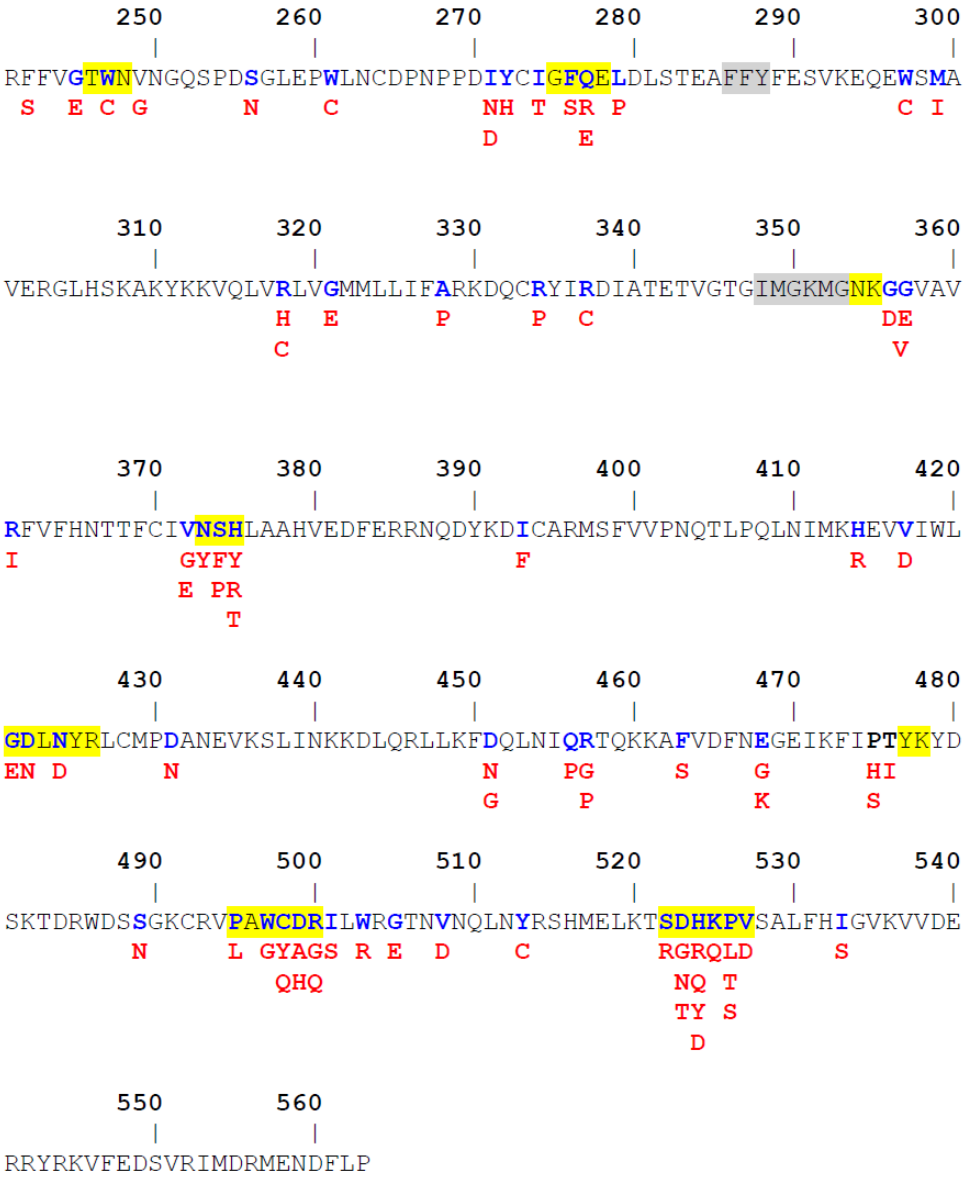


IPPc consensus motifs (Jefferson, et al. 1996, Whisstock, et al. 2000, Tsujishita, et al. 2001, Tresaugeus, et al. 2014, Mills, et al. 2016)

Lipid chain interacting motifs (Tresaugeus, 2014)

**Residues in blue mutated in Lowe Syndrome (LS), change indicated by residues in red**

IPPc- inositol polyphosphate phosphatase, catalytic

**Figure 1.5 Mapping of LS causing *OCRL1* missense mutations in the catalytic domain**

Dent-2 disease mutations-

Dent-2 disease causing *OCRL1* mutations however are found to populate regions encoding exons 1-7 (PH domain and linker region) (Hichri et al., 2011). Compared to LS, nearly 40% of Dent-2 disease causing mutations affect the PH domain. Though mutations affecting the catalytic domain are also present, they occur less frequently compared to LS (Florian Recker et al., 2015). However, we find that 50% of Dent-2 associated mutations still map to the regions encoding the phosphatase domain. It is notable that the actual number of those phosphatase domain mutations are considerably lower compared to those causing LS (37 in Dent-2 vs. 158 in LS). On the contrary, mutations affecting the ASH-RhoGAP domain constitute about 10% of all the mutations (Fig.1.6)

Within the domains, like LS, the distribution of different types of mutations varies. Most of the mutations affecting PH domain are 'indels' (22/27) although a few missense mutations are also present (2/27). Hence it is tempting to speculate that this region may possess unique attributes making them susceptible to 'indels'. (Fig.1.6)

The contribution of missense mutations and 'indels' in the phosphatase domain is comparable to that observed in LS. In the ASH-RhoGAP domain, majority of disease-causing mutations are missense in nature (5/8).

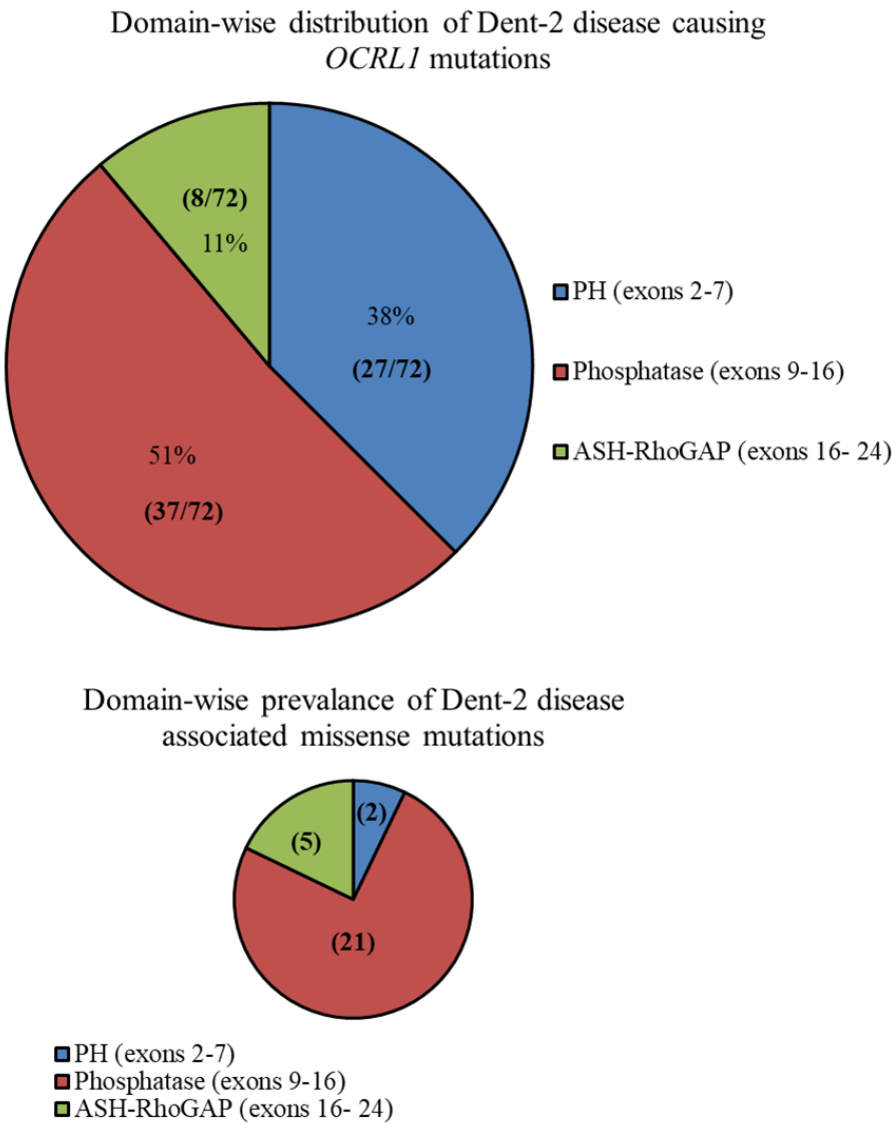


**Figure 1.6 Dent-2 disease-causing *OCRL1* mutations affecting different domains**

Overall, the regions affected by mutations causing LS and Dent-2 disease are distinct. Similarly, the clinical presentation of Dent-2 disease is also different from LS, in that it has renal defects, mild neurological symptoms that manifests later during the lifetime of the patient with little to no ocular phenotypes. Due to this observation, Dent-2 disease has been classified as a milder form of Lowe Syndrome (Bokenkamp et al., 2009).

LS patients are also found to have worse renal function compared to Dent-2 disease patients (Cho et al., 2008; Zaniew et al., 2018). In addition, particularly striking is the presence of renal tubular acidosis in Dent-2 patients which is milder in LS (Cho et al., 2008). In addition, glucosuria

is also observed in some Dent-2 patients (Bokenkamp et al., 2009; Hoopes et al., 2005). The genotype-phenotype correlation as to how *OCRL1* mutations produce differential symptoms resulting in 2 distinct diagnoses is yet to be elucidated. Most importantly, even within LS patients, there is wide spectrum of symptom severity which has no clear explanation so far (Hichri et al., 2011). This makes prognosis challenging and prevents the selection of appropriate therapeutic strategies. As a first step towards addressing this heterogeneity, we must be able to determine at the cellular level, the effect *OCRL1* mutations have on LS cellular phenotypes. So far, such a study has not been undertaken in the field. Based on our existing evidence of the different mutations causing LS, patient symptom heterogeneity and a lack of clear understanding of the relationship between the two aspects, it is proposed that LS is a complex disease both in terms of disease genetics and manifestation.

One of the proposed mechanisms for phenotypic variability amongst LS and Dent-2 patients is that Ocrl1's paralog, Inpp5B may compensate for some of the functions since it shares similar domains as well as interacting partners. And that this ability to compensate may differ across patients, depending on the level of expression in affected tissues (Pirruccello & De Camilli, 2012). While this may partially explain heterogeneity in symptoms, Montjean et al. (Montjean et al., 2015) demonstrated that fibroblasts from Dent-2 disease patients also exhibit defect in ciliogenesis, $PI(4,5)P_2$ accumulation and aberrant actin structures. These defects were independent of Inpp5B expression and the phenotypes were intermediate between control and LS patient fibroblasts. Therefore, this suggests the possibility alternative mechanisms that may contribute to phenotype heterogeneity.

Given that majority of Dent-2 disease causing mutations map to exons 2-7 and result in premature termination of protein, Shrimpton et al. (Shrimpton et al., 2009) proposed that the phenotypic variability observed in Dent-2 patients may be due to the presence of alternative isoforms of Ocrl1 being produced after exon 7. To this end, using bioinformatics tools, they predicted that amino acid methionine 187 (M187) bore the strongest score for being a potential alternative 'start codon', located in exon 8. Further, this study also identified 8 cDNA clones of alternative *OCRL1* transcripts, expressed in different tissue types (particularly brain and eyes) in support of this hypothesis. These transcripts may be preserved despite the truncations in 5' regions of the gene (encoding exons 2-7), as observed in Dent-2 disease. It is speculated that these partial Ocrl1 isoforms may play protective roles in an organ-specific manner thereby leading to a milder

LS phenotype. However, this theory remains to be validated to determine if Dent-2 patients, despite truncations of varying degree in exons 2-7 may indeed be producing alternative gene products using this alternative start site (Shrimpton et al., 2009).

Another aspect that may account for heterogeneity is the effect the mutations may have on mRNA and/or protein expression, biochemical functions and stability. It is important to determine this in order to predict pathogenic potential. It is plausible that some mutations may have a less severe impact of biochemical activity while others may severely hinder Ocrl1's functions. This may contribute to the heterogeneity observed even with LS patients. For example, Hichri et al. demonstrated that over 50% of LS cases in their study had were caused by 'indels' resulting in splicing defects or premature terminations that caused mRNA decay (Hichri et al., 2011).

One must bear in mind that some mutations cause both LS and Dent-2 disease, sometimes even within the same family (Hichri et al., 2011). This highlights the underlying of genetic and/or environmental modifiers that can influence disease manifestation.

## 1.8 Gap in knowledge in LS research

So far, LS has no cure and all patients die from renal failure. There are two critical areas with knowledge gap in LS research.

Effect of patient mutations on LS-specific cellular phenotypes

In order to understand the correlation between genotype and phenotype in patients, it is essential to first determine how mutations that affect the different domains impact the cellular processes Ocrl1 is involved in, particularly those required for renal function. At the cellular level, it has been established that Ocrl1's participation in membrane remodeling (important for renal function) requires its N-terminus and phosphatase domain (Coon et al., 2009), while its role in ciliogenesis (also important for renal function) requires its phosphatase domain and C-terminus (Brian G. Coon et al., 2012). This leads us to hypothesize us that *OCRL1* mutations may differentially affect these processes, depending on the domain they affect.

Importantly, out of the 80 unique missense mutations in the phosphatase domain (which is essential for both cellular processes), 50% of them map to regions non-essential for enzyme function yet result in disease upon being mutated (Fig.1.4). While mutations in residues important for enzyme function may predictably lead to LS, it is still unknown why mutations in non-essential residues cause disease. Although LS patients with mutations in the phosphatase domain are

predicted to have most severe symptoms, we do not know if there are inherent differences in the mechanism of disease manifestation due to mutations in catalytic vs. non-catalytic residues.

Molecular mechanisms underlying LS pathogenesis

Additionally, though many studies have discovered cellular abnormalities that can explain LS patient symptoms (particularly renal and ocular), we do not know the overall signaling pathways that are mis-regulated in the absence of Ocrl1. Hence, studies that can identify the molecular mechanisms underlying cellular phenotypes that contribute to the LS manifestations, particularly the kidney are needed. Such studies can provide us with opportunities to develop novel LS-specific therapeutics that specifically target these aberrant signaling pathways. They can also potentially explain the pleiotropic effects of the lack of Ocrl1.

## 1.9 Introduction to thesis study

Studies by Coon et al. (Brian G. Coon et al., 2012; Coon et al., 2009) demonstrate that Ocrl1's role in membrane remodeling and ciliogenesis occurs via different domains and interactions (N-terminus and C-terminus respectively) and independent of each other. Its phosphatase activity is essential for both processes to occur. Therefore, this indicates that defects in these processes observed in LS cells may be due to two independent signaling pathways.

Multiple groups demonstrated that the membrane remodeling defects are due to a RhoGTPase signaling deficiency (Lasne et al., 2010; Madhivanan et al., 2012). The exact mechanism of how RhoGTPase imbalance results in cell spreading is not understood. Similarly, the mechanisms of cilia defects are not known. Uncovering these pathways may provide novel LS-specific therapeutic opportunities.

Chapter 2 will discuss novel findings on molecular mechanism of membrane remodeling and ciliogenesis defects in LS. We identified previously unnoticed cell adhesion defects and sensitivity to fluid shear stress (critical in renal environment) in LS fibroblasts, that was also confirmed in human proximal tubule epithelial (HK2) cells lacking Ocrl1 (HK2 KO cells). Further, focal adhesion proteins such as pFAK and vinculin were abnormally distributed in LS fibroblasts and HK2 KO cells, providing a molecular basis for these defects. Given these protein complexes not only help tissue organization but overall embryogenesis and neuronal development, these findings will help us better understand LS pathogenesis. These defects are also downstream of the RhoGTPase signaling imbalance.

In addition, the ciliogenesis defects observed in the LS fibroblasts and HK2 KO cells are caused by a hyperactivation of mTOR signaling. Further, patient cells show signs of defects in the autophagy process. In summary, these findings in LS agrees with other renal diseases in which aberrant ciliogenesis and mTOR hyperactivation has been observed.

Importantly, we have identified 2 FDA-approved candidates (discovered by another graduate student in the lab) statins and rapamycin that can revert the membrane remodeling and ciliogenesis phenotypes respectively. These results are consistent with Ocrl1 displaying dual, independent functions towards the two cellular processes. In line with this, none of the candidates could rescue both phenotypes, while combinatorial treatment rescued both defects. Finally, in a zebrafish LS model, preliminary results suggest that the candidate drugs also extend the lifespan of the animals.

In summary, this study demonstrates the identification of molecular mechanisms that underly LS cellular phenotypes as well as provide the first LS-specific therapeutic strategy to rescue cellular phenotypes (Madhivanan K*, Ramadesikan S*, et al. *Equal contributing authors, *Hum. Mol. Gen.,2020*).

Chapter 3 will focus on determining the effect *OCRL1* mutations have on above described cellular phenotypes, namely cell spreading and ciliogenesis. By selecting LS patient mutations that affect different Ocrl1 domains, our findings reveal that these mutants exert differential impact on cellular phenotypes. This depends on the effect the mutation has on resulting Ocrl1 and the protein domain affected. We have also determined that mutations affecting different domains impart specific characteristics to the mutant protein, that may be relevant to LS pathogenesis. These results were also confirmed by creating stable cell lines (HK2 KO background) expressing select Ocrl1 mutants.

Importantly, using a multi-disciplinary approach, we have determined that mutations in two non-catalytic residues within the phosphatase domain (a hotspot for LS mutations) may be conformationally affecting the phosphatase domain, leading to loss of activity and cellular phenotypes. We tested an FDA-approved drug, 4-phenyl butyric acid (4-PBA), used as a chemical chaperone in cystic fibrosis, and found that it could revert phenotypes and catalytic activity of some of these mutants. This is the first study to carefully study the effect of mutations on cellular phenotype and provides evidence for heterogeneity among mutants in their ability to affect cellular processes. It also demonstrates that LS is a conformational disease and provides the first therapeutic strategy to not only revert phenotypes but also restore enzyme function. For the subset

of patients who may bear similar mutations, this would mean that a therapeutic strategy like 4-PBA this may, for the very first time, allow them to use their own enzyme. (Ramadesikan S et al., *in preparation*).

# CHAPTER 2. LOWE SYNDROME PATIENT CELLS DISPLAY MTOR- AND RHOGTPASE-DEPENDENT PHENOTYPES ALLEVIATED BY RAPAMYCIN AND STATINS

**A version of this chapter has been published in Human Molecular Genetics, 2020.**
Citation: Kayalvizhi Madhivanan*, Swetha Ramadesikan*, Wen-Chieh Hsieh, Mariana C Aguilar, Claudia B Hanna, Robert L Bacallao, R Claudio Aguilar, Lowe syndrome patient cells display mTOR- and RhoGTPase-dependent phenotypes alleviated by rapamycin and statins, Human Molecular Genetics, ddaa086, https://doi.org/10.1093/hmg/ddaa086
* Equal contribution

## 2.1 Abstract

Lowe Syndrome (LS) is an X-linked developmental disease characterized by cognitive deficiencies, bilateral congenital cataracts and renal dysfunction. Unfortunately, this disease leads to the early death of affected children often due to kidney failure. Although this condition was first described in the early fifties and the affected gene (*OCRL1*) was identified in the early nineties, its pathophysiological-mechanism is not fully understood and there is no LS-specific cure available to patients.

Here we report two important signaling pathways affected in LS patient cells. While RhoGTPase signaling abnormalities led to adhesion and spreading defects as compared to normal controls, PI3K/mTOR hyperactivation interfered with primary cilia assembly (scenario also observed in other ciliopathies with compromised kidney function).

Importantly, we identified two FDA-approved drugs able to ameliorate these phenotypes. Specifically, statins mitigated adhesion and spreading abnormalities while rapamycin facilitated ciliogenesis in LS patient cells. However, no single drug was able to alleviate both phenotypes. Based on these and other observations, we speculate that Ocrl1 has dual, independent functions supporting proper RhoGTPase and PI3K/mTOR signaling.

Therefore, this study suggest that Ocrl1-deficiency leads to signaling defects likely to require combinatorial drug treatment to suppress patient phenotypes and symptoms.

## 2.2 Introduction

The Oculo-Cerebro-Renal syndrome of Lowe (OCRL) (OMIM #309000) or Lowe Syndrome (LS) is an X-linked disease caused by functional deficiencies of the Inositol 5-phosphatase (EC 3.1.3.36) Ocrl1. LS affected children have poor quality of life and a short life expectancy. Specifically, patients exhibit bilateral cataracts at birth, mental retardation and renal malfunction that often lead to kidney failure and premature death; however, its mechanism is not fully understood. This disease is rare, but it is estimated to affect tens of thousands of children worldwide. Currently there are no LS-specific treatments.

Given its enzymatic activity, lack of Ocrl1 function leads to cellular accumulation of its preferred substrate phosphatidyl-inositol (4, 5) bisphosphate [PI(4, 5)$P_2$] (Mehta, Pietka, & Lowe, 2014). The excess of this important regulatory lipid affects vesicle trafficking (*e.g.*, recycling (R. Choudhury et al., 2005; van Rahden et al., 2012) and signaling (*e.g.*, regulation of actin polymerization (Suchy & Nussbaum, 2002). In addition, Ocrl1 has several interaction partners (Mehta et al., 2014) likely to mediate multiple other functions also predicted to impact trafficking and signaling.

Previously, our lab identified two categories of phenotypes in cells from affected individuals that result from vesicle trafficking and signaling abnormalities that may shed light onto the cellular mechanisms of the disease: Membrane remodeling and cilia phenotypes (Brian G. Coon et al., 2012; Coon et al., 2009; Madhivanan et al., 2012).

*i*) Membrane remodeling phenotypes (Coon et al., 2009): We found that LS patient fibroblasts exhibited significant deficiencies in cell migration, spreading and fluid-phase uptake (FPU) as compared to normal controls. Importantly, these phenotypes have been confirmed *in vivo* (Oltrabella et al., 2015), and were determined to be Ocrl1-specific (*i.e.*, rescued by Ocrl1$^{WT}$, but not by its paralog Inpp5b (Coon et al., 2009). Proper Ocrl1 phosphatase activity or interaction with endocytic machinery components AP2 and clathrin, were required to maintain proper membrane remodeling capabilities (Coon et al., 2009). Since the affected processes depend on RhoGTPase-dependent actin reorganization, we proposed that these phenotypes were caused by a RhoGTPase activation imbalance. Indeed, we and others detected such de-regulation of RhoGTPase signaling (hyperactivation of RhoA and deficient activation of Rac1) in LS patient cells (Lasne et al., 2010; Madhivanan et al., 2012; van Rahden et al., 2012).

*ii*) Primary cilia (PC) assembly phenotypes (Brian G. Coon et al., 2012): We determined that LS patient fibroblasts cannot properly undergo ciliogenesis, leading to a decreased fraction of ciliated cells upon stimulation and to abnormal, shorter PC. This phenotype is also dependent on Ocrl1 and its phosphatase activity; however, Inpp5b can partially mitigate it if overexpressed. In addition, Ocrl1's PC function is *independent* of binding to the endocytic machinery, but instead requires interaction with the endosomal proteins IPIP27/Ses (Brian G. Coon et al., 2012). These differences with phenotypes described in (*i*), suggested that supporting ciliogenesis is a distinct function of Ocrl1 with a RhoGTPase-independent mechanism. In fact, we demonstrated that Ocrl1 participates in the IPIP27-dependent endosome-to-PC vesicle trafficking of cilia-enriched receptors such as rhodopsin (Brian G. Coon et al., 2012). Importantly, other investigators also reported trafficking defects upon Ocrl1 deficiency (including the recycling of the albumin receptor Megalin (Oltrabella et al., 2015; Vicinanza et al., 2011) and the mechanosensory TRPV4 channel (Na Luo et al., 2014)). Further, the discovery that LS involves PC abnormalities (independently confirmed by others (Luo, West, et al., 2012; Rbaibi et al., 2012; Florian Recker et al., 2015)) also opened the possibility of adopting or adapting therapeutic approaches or theoretical concepts from ciliopathies to LS.

Here, we expanded the characterization of the RhoGTPase signaling abnormalities observed in Lowe syndrome patients unveiling a misregulation of the RhoA effector MLCK and we established that RhoA-inhibitors corrected this category of LS phenotypes. Importantly, we have found previously unnoticed RhoGTPase-dependent cell adhesion defects and hyperactivation of the mTOR signaling pathway in patient cells. Importantly, this latter finding further indicate that *LS is similar to other conditions with kidney/cerebral compromise such as Joubert, Morm and Bardet-Biedl syndromes as well as autosomal/recessive polycystic kidney disease, which also show mTOR hyperactivation and are characterized by ciliary phenotypes* (S. Hakim et al., 2016; Ibraghimov-Beskrovnaya & Natoli, 2011; Mekahli et al., 2014; Pema et al., 2016).

We also tested FDA-approved compounds known to affect RhoGTPase signaling and ciliogenesis for their ability to alleviate the easy-to-score cell spreading and PC assembly phenotypes in LS fibroblasts. As a result of this effort we identified the well-known statin drug group as mitigator of the spreading abnormalities and rapamycin as being able to alleviate mTOR signaling hyperactivation and the PC phenotype. The toxicity of these drugs for Lowe syndrome patient cells at selected concentrations was also determined.

Our results are consistent with Ocrl1 displaying dual, independent functions towards two cellular processes: membrane remodeling and ciliogenesis. In agreement with this idea, no compound could rescue both phenotype categories. However, drug-combination treatment was successful at reverting both phenotype types simultaneously.

In summary, based on our findings we propose a new theoretical framework for LS in which Ocrl1-deficiency leads to RhoGTPase-dependent and mTOR-dependent phenotypes, and the prospect of novel therapeutic applications for statins and rapamycin as anti-LS agents.

## 2.3 Results

We and others previously established that Ocrl1 participates in important cellular processes such as membrane remodeling and ciliogenesis (Bohdanowicz et al., 2012; Brian G. Coon et al., 2012; Coon et al., 2009); it was also suggested that this protein has a role in RhoGTPase signaling (Lasne et al., 2010; Madhivanan et al., 2012; van Rahden et al., 2012) and vesicle trafficking (Billcliff et al., 2016; Cauvin et al., 2016; R. Choudhury et al., 2005; Cui et al., 2010; A. Ungewickell, Ward, Ungewickell, & Majerus, 2004; Vicinanza et al., 2011). Nevertheless, a detailed mechanistic study of the causes and consequences of these phenotypes as well as the exploration of strategies to revert such abnormalities was lacking. This work aims to fill-in those gaps.

### 2.3.1 RhoGTPase modulators affect LS spreading/FPU phenotype severity.

LS cells have been shown to exhibit a RhoGTPase activation imbalance; specifically, RhoA hyperactivation and Rac1 signaling deficiency (Lasne et al., 2010; Madhivanan et al., 2012; van Rahden et al., 2012). We hypothesized that an abnormally high RhoA/Rac1 activation ratio causes LS cell spreading/migration/FPU deficiencies. In consequence, we predicted that RhoA inhibitors would ameliorate this LS phenotype, whereas RhoA activators would make it worse. Therefore, we proceeded to monitor the spreading on fibronectin-coated surfaces of cells treated or not with RhoA modulators. Cells were fixed and stained with fluorescently labeled-phalloidin after 30min spreading time at 37°C. Following imaging, cell area measurements were performed as described before (Coon et al., 2009) and in Materials and Methods.

In agreement with our predictions (see above), normal fibroblasts displayed a “LS-like” cell spreading phenotype (Coon et al., 2009) upon treatment with a RhoA activator (Fig.2.1A), while incubation with this chemical worsened the already impaired spreading ability of LS cells (Fig.2.1B). However, the use of a RhoA inhibitor ameliorated the cell spread phenotype (Fig.2.1B). Importantly, these observations were confirmed using cells from another unrelated LS patient (Fig.2.2A) and kidney HK2 and HEK293T OCRL1-/- (K.O.) cells (Fig.2.2B and data not shown, respectively; as compared to their WT counterparts).

These results indicate that the RhoA/Rac1 imbalance in LS cells is the underlying cause of the cell spreading defect; further, it suggested that these phenotypes can be corrected using RhoA inhibitors.

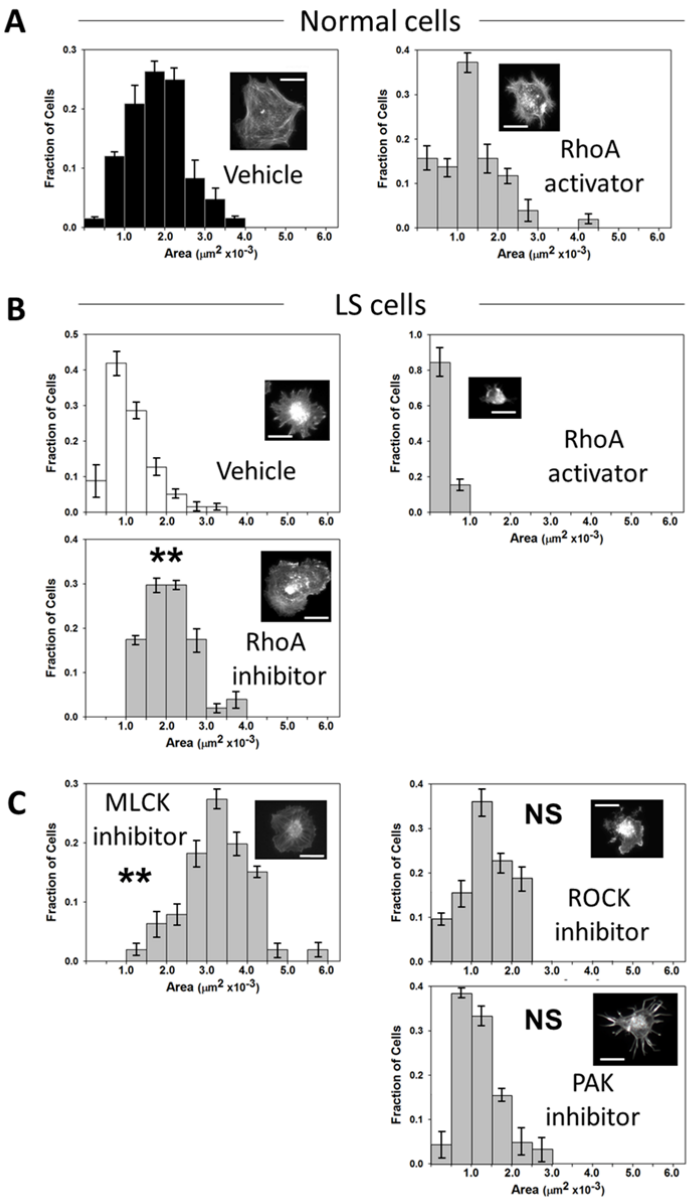


**Figure 2.1 LS cell spreading phenotype is affected by RhoGTPase modulators.**
Normal (A) and LS patient (B) cells were resuspended and treated with vehicle or the indicated pharmacological agent as indicated in materials and methods. N=200 cells (in at least 3 experiments). Insets show examples of stained cells representative of the high frequency groups within each histogram. Scale bar: 10μm. **: p<(0.05/4=0.0125) (Bonferroni correction), KS test. (Data- Dr. Kayalvizhi Madhivanan)

In order to gain insight concerning the RhoA-dependent signaling pathways that trigger this LS phenotype, we used pharmacological inhibitors of two important RhoA-effectors: Rho associated kinase (ROCK) and Myosin Light Chain Kinase (MLCK); while also using an inhibitor

of p21 activated kinase (PAK), which acts downstream of Cdc42/Rac1, as a control (Meshki, Douglas, Hu, Leeman, & Tuluc, 2011; Totsukawa et al., 2000). We found that in contrast to the ROCK-inhibitor fasudil, the MLCK-inhibitor ML-7 was able to mitigate the cell spreading phenotype (Fig.2.1C). These results suggest that RhoA hyperactivation induces cell spreading abnormalities through the RhoA effector MLCK. These observations are in agreement with previous reports that MLC phosphorylation by MLCK is involved in the regulation of actin rearrangement at the cell periphery (Totsukawa et al., 2004; Totsukawa et al., 2000).

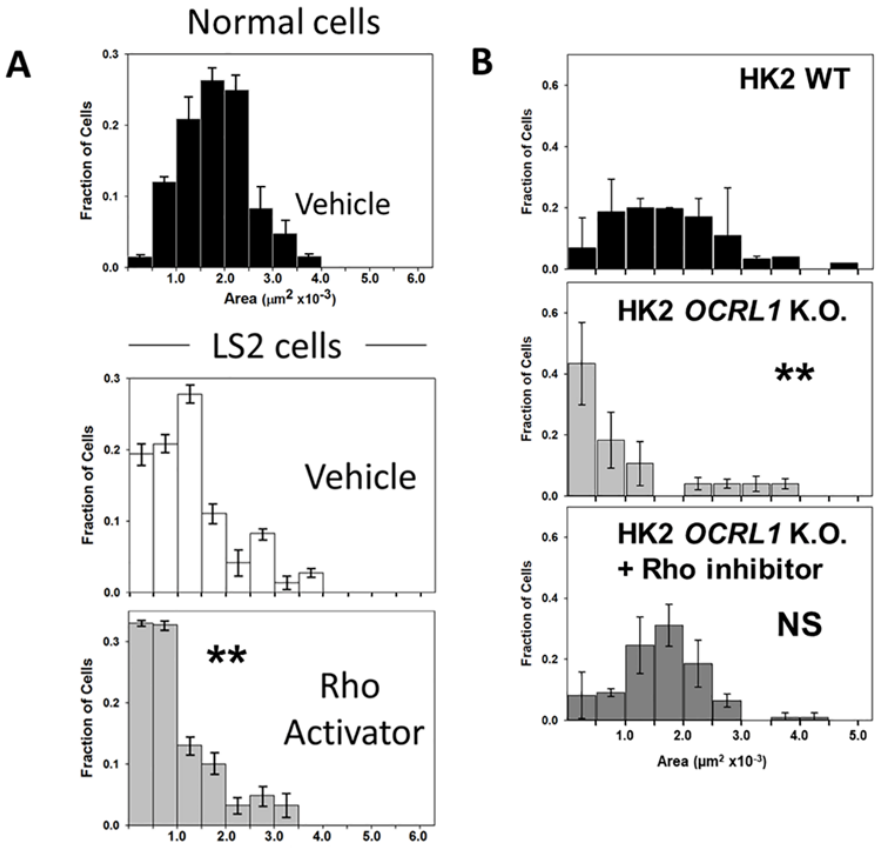


**Figure 2.2 Ocrl1-deficiency triggers a cell spreading phenotype in cells of different origin.** A: LS cells from a patient (LS2) different than the one characterized in Fig.2.1 was treated with the indicated pharmacological agents or vehicle and its cell size distribution was determined as in Fig.2.1 and compared to the one from cells from a normal individual (same as in Fig.2.1). B: Human HK2 kidney cells WT and KO were treated or not with a RhoA inhibitor and cell spreading experiments were conducted as in Fig. 2.1.

### 2.3.2 Statins alleviate LS membrane remodeling phenotypes

Based on the premise that RhoA hyperactivation (and the consequent RhoA-mediated inhibition of Rac1 activation) is the cause of LS membrane remodeling phenotypes, we searched for FDA-approved compounds known to decrease RhoA activation. This strategy was preferred over pharmacologically enhancing signaling by Rac1, as this RhoGTPase has very dynamic, quantitative and spatio-temporal specific activation requirements. In contrast, decreasing the LS-characteristic global RhoA hyperactivation, thereby relieving RhoA-mediated inhibition of Rac1, is predicted to lead to improved Rac1 signaling.

This repurposing/repositioning strategy yielded the statin drug group as suitable candidates for alleviating RhoA hyperactivation-dependent LS phenotypes. Indeed, statins have been shown to be active against RhoA hyperactivation observed, for example, in certain cancers (Zhong et al., 2015). These compounds decrease cholesterol (Cho) biosynthesis by inhibiting 3-hydroxy-3-methylglutaryl coenzyme A (HMG-CoA) reductase (Fig.2.3A and (McFarland et al., 2014)); consequently, they also down-modulate the downstream synthesis of two intermediates (farnesyl-pyrophosphate and geranyl-geranyl-pyrophosphate) required for RhoA prenylation, which in turn is essential for GTPase membrane anchoring and activation (Fig.2.3A).

Therefore, we tested several generation statins (Maji, Shaikh, Solanki, & Gaurav, 2013) including fluvastatin, atorvastatin, pitavastatin and rosuvastatin for their ability to ameliorate LS spreading defects. All statins mitigated to a certain extent the LS spreading phenotype; however, rosuvastatin produced the best results (rosuvastatin > pitavastatin >>> simvastatin and others) in terms of maximizing rescue effect over needed dose and toxicity (Fig.2.3B and data not shown).

Phenotype alleviation was observed following the use of an acute rosuvastatin dose (100uM for 1h), but similar effect was also evident using lower concentrations (1-10uM) sustained over longer periods of time (≥72h; Fig.2.3B). Importantly, the latter usage scheme better emulated current approved treatment conditions with statins that render an effective concentration of free drug in plasma of up to 10μM (Björkhem-Bergman, Lindh, & Bergman, 2011). Following exposure to statins, viability and stress-induced changes in morphology were determined for LS cells (Fig.2.3C). Our results showed that rosuvastatin had minimal toxicity, while other statins including pitavastatin and cerivastatin were substantially toxic (Fig.2.3C, D), it should be noted that the latter was recalled from the market due to severe rhabdomyolysis effects (Maji et al., 2013). In addition, and to monitor the magnitude of the statins' effects on HMG-CoA reductase in LS

cells, we incubated patient fibroblasts in Cho-free media supplemented with vehicle or statins and determined the uptake of fluorescently-labeled Cho. While vehicle-treated cells had normal production of endogenous Cho, the ones exposed to statins (due to their HMG-CoA reductase inhibitory activity) were Cho-depleted at different extent as evidenced by a substantial increase in the uptake of exogenous, fluorescently-labeled Cho (Fig.2.3E). Our results suggested that rosuvastatin in addition to being less toxic at the chronic dose, led to a less acute inhibition of cholesterol biosynthesis (and consequently to a lower demand of exogenous, fluorescent-analog uptake). However, in contrast with the relatively innocuous chronic exposure (10 $\mu$ M for $\geq$72h), we observed that acute doses of rosuvastatin (100 $\mu$ M) induced toxicity when exposure time $\geq$15h (data not shown).

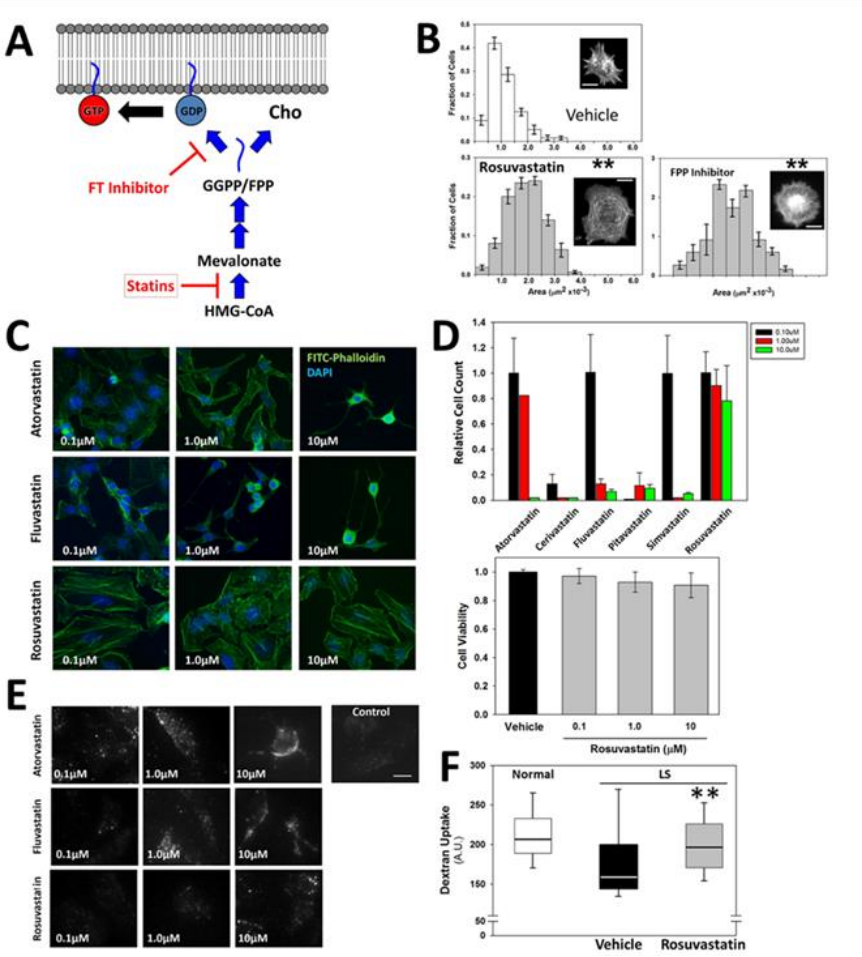


**Figure 2.3 Statins ameliorate LS membrane remodeling phenotypes.**

A. Scheme depicting point of inhibition of the Statins and Farnesyl-Transferase (FT) inhibitors on the mevalonate pathway. Prenylated RhoGTPases are represented as membrane-anchored circles (blue and red for GDP- and GTP-loaded, respectively). HMG-CoA: 3-Hydroxy-3-Methyl-Glutaryl-CoA; GGPP: Geranylgeranyl Pyrophosphate; FPP: Farnesyl Pyrophosphate; Cho: cholesterol. B. Histograms for LS patient cells treated with vehicle or the indicated drug were constructed as described in Materials and methods and in Fig. 1. Insets show examples of stained cells representative of the high frequency groups within each histogram. Scale bar: 10μm. **: p<(0.05/3=0.0167) (Bonferroni correction) by the KS test. C-E. LS patient cells were treated with the indicated statins at the indicated concentration as described in Materials and methods and processed in the following ways: fixed and stained with FITC-phalloidin/DAPI (C), used for viability assays either by staining/cell counting (upper panel) or by MTT assays (lower panel) (D), and for uptake of fluorescent-Cho, with and without (control) statins (E). F. Fluid phase uptake was estimated on Normal and LS cells treated as indicated, incubated with as fluorescent-dextran, fixed, imaged and the fluorescent intensity associated with cells measured using ImageJ software. Statistical significance of the LS fluid-phase uptake phenotype difference between cells treated with vehicle or Rosuvastatin was assessed by using the Wilcoxon test (**: p<0.05). (Data- Dr. Kayalvizhi Madhivanan)

### 2.3.3 Statins alter RhoGTPase signaling, but had no effect on LS ciliogenesis phenotype

Statins inhibit isoprenoid chain biosynthesis ((McFarland et al., 2014), Fig.2.3A); therefore, they impair the prenylation of RhoGTPases and their activation. In consequence, statin treatment is expected to lower all RhoGTPase activation levels. Since LS cells present a RhoA hyperactivation scenario (with consequent low levels of activated Rac1) statin treatment was predicted to primarily affect the sustained activation/prenylation of RhoA relieving the suppression of Rac1 signaling. In fact, statins were able to correct different forms of the membrane remodeling phenotype, i.e., cell spreading and FPU abnormalities (Fig.2.3B,F). Importantly, the cell spreading phenotype observed in cells from another LS patient was also ameliorated by rosuvastatin (data not shown).

Further, using a validated FRET-based biosensor (Itoh et al., 2002), we determined that as expected Rac1 activation levels raised in LS cells upon rosuvastatin treatment (data not shown).

We reasoned that if as predicted (see above and Fig.2.3A), the mechanism by which statins revert LS membrane remodeling phenotypes was by interfering with the biosynthesis of farnesylation intermediates, then a farnesylation inhibitor should also be active for LS membrane remodeling defect mitigation. Indeed, our results indicate that these inhibitors can rescue the cell spreading phenotype of LS patient cells (Fig.2.3B).

Although able to revert LS membrane remodeling defects, statins were unable to mitigate PC assembly defects in LS patient cells (data not shown). This observation further supports the idea that Ocrl1 acts on the cellular processes of membrane remodeling and ciliogenesis via different biochemical pathways.

### 2.3.4 LS cells exhibited adhesion and spreading defects alleviated by statins

To better characterize the LS cell spreading phenotype and statin's suppression mechanism, we proceeded to monitor cell behavior using time-lapse microscopy. Specifically, we performed cell spreading assays of normal and LS cells treated with vehicle or rosuvastatin in real time by continuous imaging using Cytosmart devices (Fig.2.4A) or at regular intervals in Lab-tek chambers (Fig.2.4B) (see Materials and methods). Our results indicate two major differences between normal and LS fibroblasts; cell adhesion and spreading capabilities.

While 80% of normal cells made stable adhesions by 30 minutes, even after 1h a substantial number of LS cells did not adhere or made unstable attachments (Fig.2.4A,B). Analysis of this kinetic data highlighted differences in the rates of adhesion between normal and LS cells (Table 2.1). Further, and in contrast with normal cells, a substantial number of LS fibroblasts established weak adhesions as evidenced by frequent LS cell de-attachments (Fig.2.4B, additional movies available). A similar result was obtained when we used HK2 human proximal tubule cells OCRL1 K.O. as compared to HK2WT cells (Fig.2.4C).

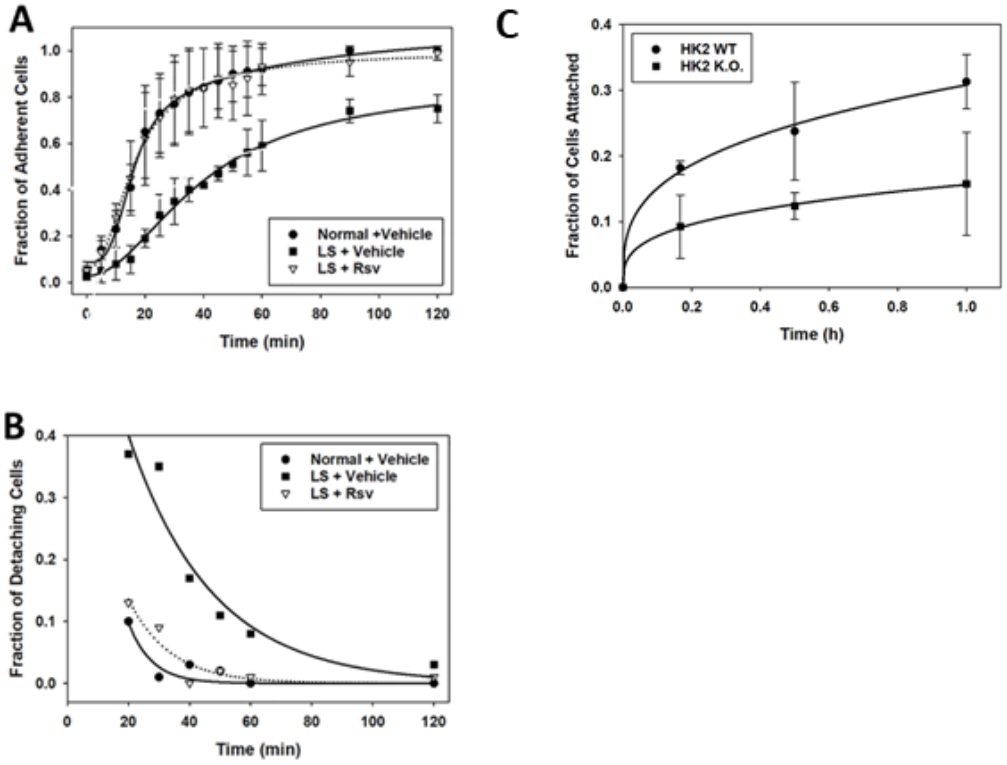


**Figure 2.4 Ocrl1-deficient cells display adhesion defects.**
A-B: Normal and LS patient cells (treated with vehicle or Rosuvastatin, Rsv) were seeded on Fibronectin-coated surfaces. Cells adhered (A) or in suspension (B) were quantified as a function of time, results represent the average of 3 independent experiments. (C) HK2 WT and KO cells were seeded on Fibronectin-coated surfaces and attachment experiments were performed as described in (A).

Although RhoA is required for adhesion and migration (Kaibuchi, Kuroda, & Amano, 1999), Rac1 activation is required for cell adhesion consolidation (Lawson & Burridge, 2014); therefore,

we speculated that the RhoA/Rac1 imbalance was responsible for LS adhesion defects. In fact, normal cells treated with a RhoA-activator to emulate LS signaling unbalance, displayed an increased proportion of de-attaching cells (data not shown). Importantly, rosuvastatin treatment alleviated the LS cell adhesion defect (Fig.2.4A,B). This observation is also consistent with the effect of statins in counteracting RhoA hyper-activation in LS cells, enhancing Rac1 signaling.

Further, we observed that LS cells were more susceptible to de-attachment than normal cells when subjected to fluid sheer stress (FSS) exerted by rinsing with PBS 20min after seeding cells on fibronectin-coated surfaces. Specifically, we monitored cell adhesion by time-lapse microscopy (Fig.2.5A) and by fixing, actin staining and comparing the proportion of attached cells before and after exerting FSS (Fig.2.5B) (see Materials and methods).

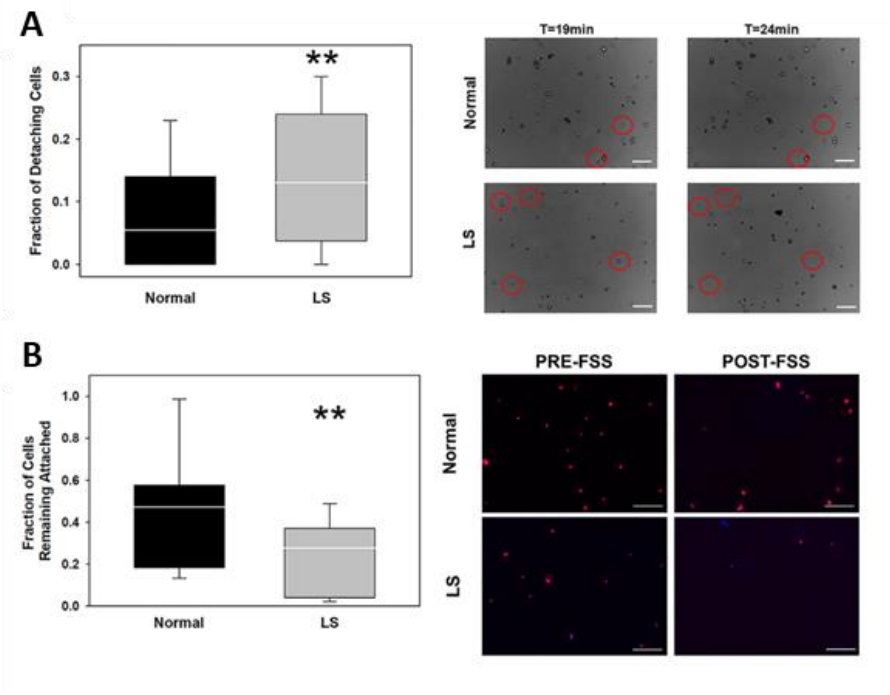


**Figure 2.5 LS patient cells are sensitive to fluid shear stress.**
Normal and LS patient cells were subjected to fluid sheer stress and the fraction of detaching (A) and of cells that remain attached (B) were calculated by analyzing time-lapse microscopy data (A) and fixed/phalloidin-stained samples (B). Differences between Normal and LS distributions were assessed by the Wilcoxon test (**: $p<0.05$).

Interestingly, focal adhesions showed a distinct organization in normal vs. LS cells, with the latter exhibiting less peripherally activated Focal Adhesion Kinase (FAK) as detected by immunofluorescence using an anti-phospho-Tyr397 FAK antibody and this abnormality was also alleviated by incubation with Rosuvastatin (Fig.2.6A). A similar result was observed in HK2 OCRL1-/- as compared to WT cells (Fig.2.6B). Importantly, these abnormalities were also alleviated by incubation with Rosuvastatin (Fig.2.6A, right panel). In addition, we also observed shorter, less mature vinculin-positive structures with decreased anchoring of stress fibers in LS cells (Fig.2.6C).

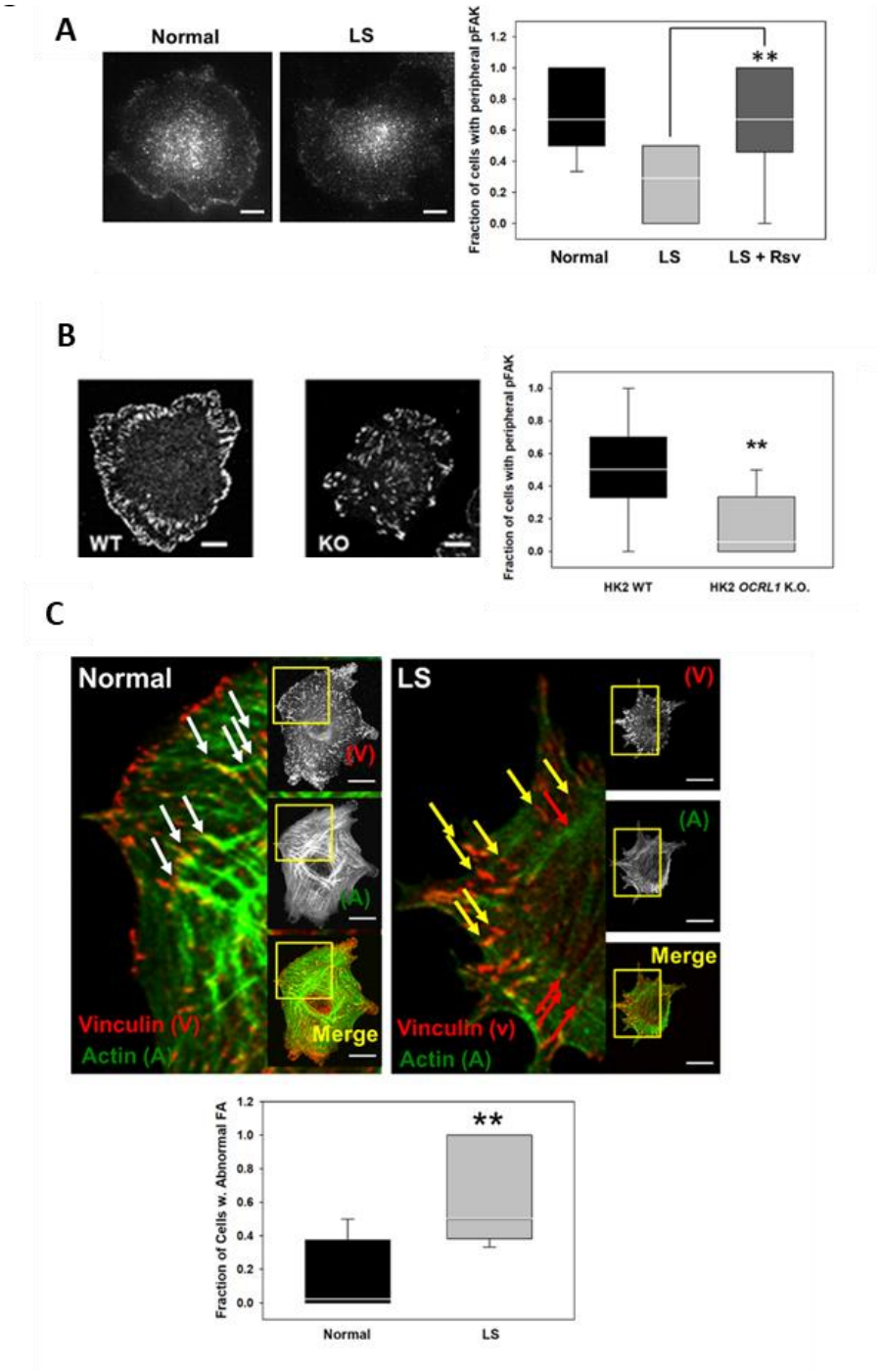


**Figure 2.6 LS patient and HK2 KO cells exhibit focal adhesion defects.**
Status of focal adhesions in Normal and LS patient cells (A) and HK2 WT and KO cells (B) was investigated by immunostaining with anti-phosphorylated FAK. Normal and LS patient cells were immunostained with anti-vinculin (C) antibodies. Cells were imaged and the indicated adhesion structures were quantified as described in Materials methods. White arrows: properly actin-linked vinculin structures; Red arrows: actin filaments disconnected from vinculin structures; Yellow arrows: vinculin-positive adhesions not linked to the actin cytoskeleton. **: $p<0.05$ by the Wilcoxon test. Scale bars: 10μm.

LS cells also took longer to reach a fully spread morphology as compared to their normal counterparts (Fig.2.7, lower panel). Specifically, we used time lapse microscopy to track the spreading status of individual cells by assigning them a "spreading score" (see Materials and Methods and Fig.2.7 , top panel) as a function of spreading time. Briefly, a cell was considered as stably attached when it substantially decreased its x-y movements and needle-like filopodia structures became visible (additional movies available). With these data we computed the time-course of evolution from initial to fully spread morphology of normal vs. LS cells (Table 2.1). Specifically, while conventional spreading assays report a composite of both Rac1-dependent adhesion and spreading defects, time lapse-microscopy allowed the separated evaluation of one from another phenotype.

It should be noted that spreading time T for each cell was computed with respect to the moment in which they were able to stably attach to the fibronectin-coated coverslip. For example, as indicated above, in average it took significantly longer time for LS than normal cells to stably attach (i.e., different attachment time); however, this moment was set to be spreading time T=0. Therefore, the spreading ability of each cell was evaluated independently of their initial adhesion capability. While most normal cells were fully spread; i.e., exhibited no further significant change in spreading area by 2h after attachment, LS fibroblasts took longer or never reached such ultimate spread morphology (Fig.2.7, lower panel). The corresponding rates of spreading were calculated and collected in Table 2.1. Importantly, in agreement with their ability to support Rac1-mediated spreading (Kou, Sartoretto, & Michel, 2009), statins also alleviated this deficiency (Fig.2.7, lower panel).

**Table 2.1 Adhesion and spreading rates of normal, LS and LS cells treated with Rosuvastatin**

| Process | Process Continuous Rate($min^{-1}x10^3$)[a] | | |
|---|---|---|---|
| | **Normal** | **LS** | **LS+Rsv** |
| Adhesion | 41±2 | 17±3** | 35±5 |
| Spreading | 30±2 | 17±2** | 24±2 |

a. Kinetic data from Fig.2.4A (adhesion) and Fig.2.7 lower panel (spreading) were fit using a non-linear regression model to estimate the continuous rates of each process for the indicated samples (see Materials and methods under Statistical analysis). **: indicates a significant difference between LS and Normal rates with $p<0.05$ by the Student's t-test.

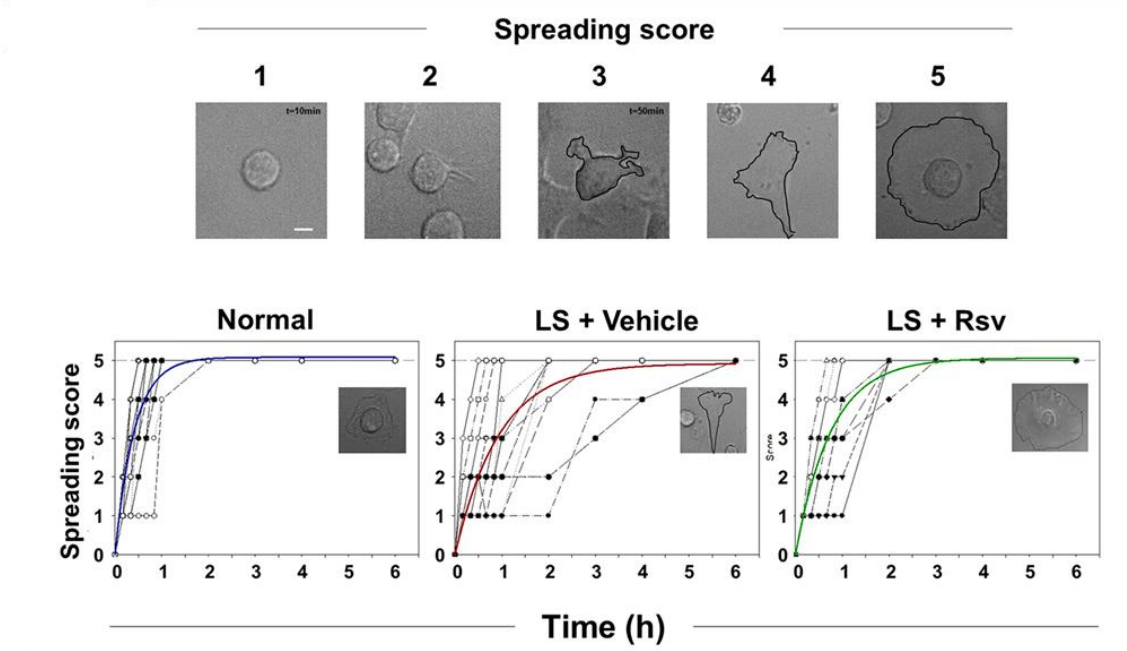


**Figure 2.7 LS patient cells display a cell spreading delay independent of their adhesion phenotype.**

Normal and LS patient cells (treated or not with vehicle or rosuvastatin, Rsv) were seeded on fibronectin-coated surfaces and monitored using time-lapse microscopy. Time=0 was the moment in which the cells stably attach (see main text for details). According to their morphological characteristics, cells were scored following the 1-5 spreading score described in the text and exemplified by DIC images in the upper panel (perimeter of some cells is traced for better visualization). Time required to achieve each score level was recorded for 43-45 cells (note that many trajectories overlap) of each sample in 3 independent experiments and plotted as shown in the lower panels. A regression curve describing overall behavior is included (times required to reach half spreading trajectory are collected in Table I). Examples of the morphologies acquired by fully spread cells are also exemplified in the graph insets. Scale bar: 10µm.

### 2.3.5 Rapamycin mitigates PC assembly defects in LS patient cells.

Since statins could not correct LS ciliogenesis abnormalities, we focused on drugs known to mitigate PC phenotypes in ciliopathies. Rapamycin is currently in clinical trials for the treatment of polycystic kidney disease and has also shown promise against Bardet-Biedel's syndrome (W. E. Braun, Schold, Stephany, Spirko, & Herts, 2014; Shillingford, Leamon, Vlahov, & Weimbs, 2012; Stallone et al., 2012; Tobin et al., 2008); therefore, we tested this drug as candidate for mitigation of LS ciliogenesis defects. Our results showed that LS fibroblasts treated with rapamycin showed a significant increase in the PC length and fraction of ciliated cells in

comparison to the vehicle-treated group (Fig.2.8A). Specifically, we observed PC phenotype alleviation capabilities under both, acute treatment: 100nM for 12h and under a more sustained treatment regime (≥72h) at a concentration compatible with plasma levels yielded by current approved rapamycin treatments, i.e., 10nM (Jimeno et al., 2008) (Fig. 2.8A). The toxicity on LS cells associated with the use of this drug was found to be minimal (Fig. 2.8B).

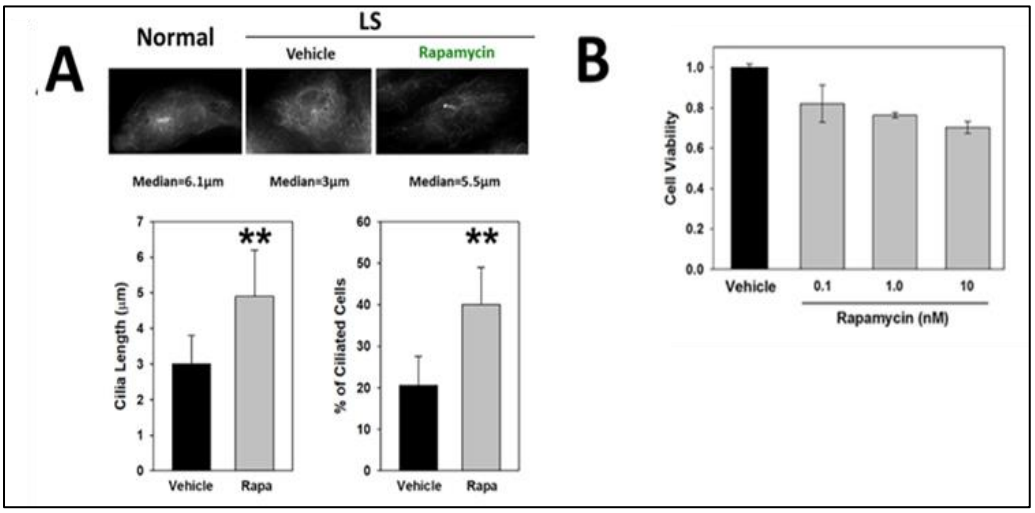


**Figure 2.8 Rapamycin rescues ciliogenesis defects in LS patient cells.**
A. As described before, LS patient cells display primary cilia assembly defects (cilia length and number of ciliated cells under serum-starvation conditions) as compared to their normal counterparts. LS cilia assembly phenotypes were ameliorated by treatment with rapamycin (Rapa). **: $p<0.05$ by the Wilcoxon test. B. LS patient cells showed moderate decrease in cell viability as detected by MTT assays due to rapamycin treatment (at the indicated concentration) as compared vehicle-treated cells.

In addition, we established that rapamycin was unable to alleviate membrane remodeling abnormalities (data not shown); once again, further supporting the idea that membrane remodeling and PC phenotypes are caused by distinct mechanisms.

### 2.3.6 LS cells display constitutive activation of the mTOR pathway that can be mitigated by rapamycin

We previously showed that in LS patient cells PC abnormalities were mechanistically associated with vesicle trafficking defects from the endosome to the PC (Brian G. Coon et al.,

2012). In agreement with this, other cargo trafficking abnormalities (e.g., TRPV4 (Na Luo et al., 2014) M6PR (A. Ungewickell et al., 2004)) have been observed in Ocrl1-deficient cells. Therefore, the ability of rapamycin to rescue the LS PC phenotype is not completely unexpected considering that its target, the mammalian Target Of Rapamycin (mTOR) has been shown to affect vesicle trafficking (Al-Awqati, 2015; Grahammer et al., 2017). Indeed, via SGK1, mTOR is known to stabilize integral membrane proteins (including TRPV4 (E. J. Lee, Shin, S.H, Chun, J, Hyun, S, Kim, & Y, 2010)) at the plasma membrane (Grahammer et al., 2017; Lang, Stournaras, & Alesutan, 2014), decreasing cargo endosomal localization and therefore, impairing trafficking to the PC. In fact, mTOR hyperactivation has been correlated with ciliogenesis abnormalities (Zullo et al., 2010). Since lack of Ocrl1 phosphatase activity is known to lead to PI(4, 5)$P_2$ accumulation (Cui et al., 2010; Prosseda et al., 2017; Vicinanza et al., 2011; X. L. Zhang, Hartz, Philip, Racusen, & Majerus, 1998), and this lipid is the substrate of PI3K, we predicted that this scenario would promote high level of mTOR signaling activation via the PI3K/Akt pathway in LS cells (Fig.2.9A). Further, we hypothesized that rapamycin's ability to ameliorate the LS PC phenotype is due to inhibition of a putative constitutive mTOR activation in LS cells as it has been shown to occur in other ciliopathies (S. Hakim et al., 2016; Mekahli et al., 2014; Pema et al., 2016).

We proceeded to investigate the activation of the Akt and mTOR signaling pathways in LS cells treated or not with rapamycin. Cell lysates were prepared, resolved by SDS-PAGE and the presence of phosphorylated and dephosphorylated key elements of the Akt and mTOR pathways were investigated by Western blotting with specific antibodies (Fig.2.9B).

Our results showed that in contrast to normal cells, the PI3K/Akt pathway was constitutively activated in LS cells as inferred by the presence of Akt phosphorylated at Serine 473 (Fig.2.9B). Importantly, both mTOR protein complexes mTORC1 and mTORC2 were activated in LS above the levels of normal cells (Fig.2.9B) and downstream kinase SGK1 was found to be phosphorylated at serine 422 (Fig. 2.9B), which is consistent with activation of this enzyme (García-Martínez & Alessi, 2008). Band densitometry (followed by normalization by total amount of protein) of least 3 experiments revealed that in LS cells phosphorylated AKT, SGK1 and mTORC1 levels were about twice more abundant than in normal cells (a more modest 20-50% increase was noted for phosphorylated mTORC2) . Similar results were obtained by using HK2 WT and HK2 OCRL1-/-lysates (Fig. 2.9C&D).

As predicted, mTOR and SGK1 activation in LS cells was counteracted by rapamycin treatment (Fig.2.9B); and as expected, activation of the upstream PI3K/Akt pathway was not affected by exposure to this drug. To further confirm that counteracting mTOR pathway hyperactivation was responsible for re-establishing ciliogenesis in LS cells (and not an off-target/side effect of rapamycin) we used different mTOR inhibitors (INK128 and WYE132), that in contrast to rapamycin, act via a non-competitive/allosteric mechanism (Yu et al., 2010; H. Zhang et al., 2015). Importantly, both INK128 and WYE132 were able to decrease mTOR phosphorylation and, very importantly, to rescue ciliogenesis defects in LS cells (Fig.2.9E). In contrast, inhibition of PI3K cIII (this PI3K class is unable to activate mTOR (Jaber et al., 2012; Juhász et al., 2008; Ronan et al., 2014)) with SAR405, did not affect mTOR activation and had no effect on ciliogenesis by LS cells (Fig.2.9E).

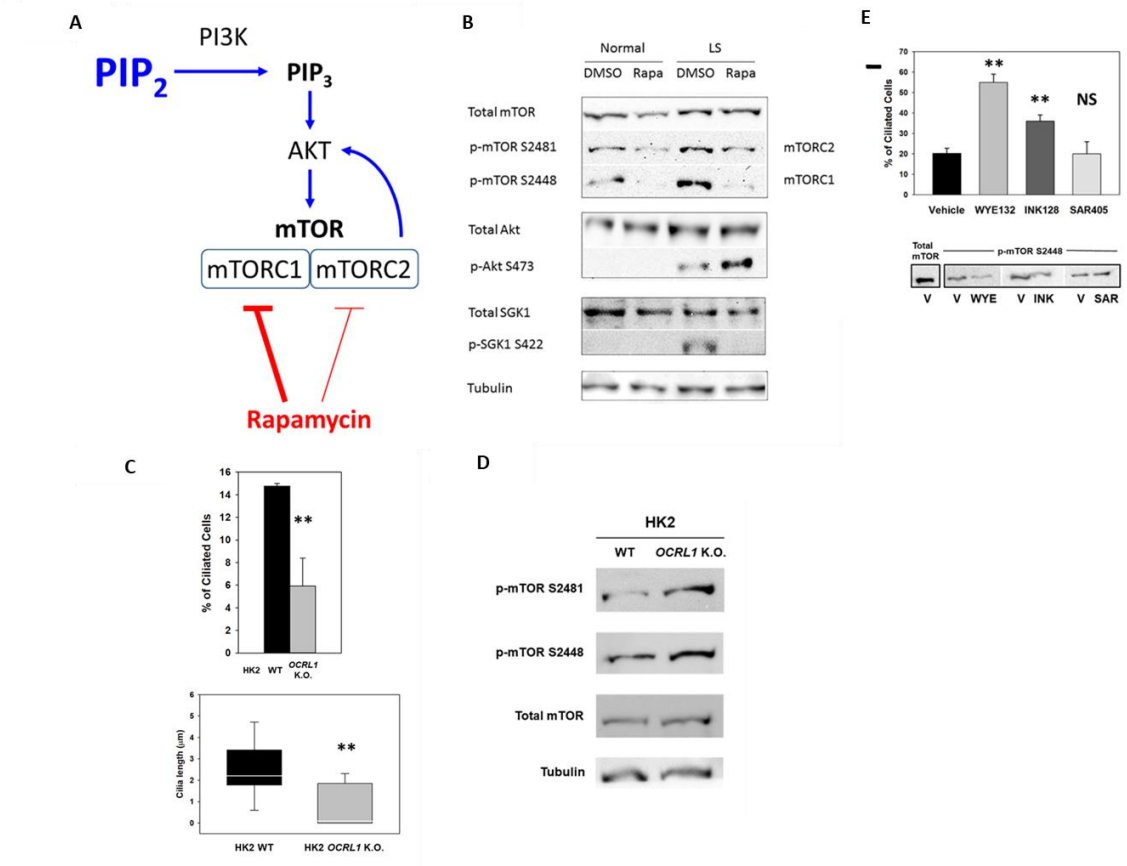


**Figure 2.9 LS patient cells display hyperactivation of the mTOR signaling pathway.** A. Scheme depicting targets of inhibition by rapamycin on the mTOR pathway downstream of $PIP_2$ (PI3K substrate) accumulation typical of LS patient cells. B. Levels of activated (phosphorylated) elements of the PI3K/mTOR pathway were detected by Western blotting with specific antibodies on lysates from normal and LS patient cells treated with vehicle (DMSO) or Rapa. Total protein content of each protein investigated and tubulin (loading control) was also determined. C. HK2 WT or KO cells display cilia defects. D. Levels of activated (phosphorylated) elements of the PI3K/mTOR pathway were detected by Western blotting with specific antibodies on lysates from HK2 WT and KO cells. E. Upper panel: Effect of alternative mTOR inhibitors on the ciliogenesis by LS patient cells as compared to vehicle-treated cells. In contrast to vehicle and SAR405 (inhibitor of the mTOR-independent PI3KcIII), mTOR inhibitors WYE132 and INK128 were able to ameliorate the LS ciliogenesis phenotype. Phenotype. **: p<(0.05/3) (Bonferroni correction) by the student's t-test test. Lower panel: hyperactivation of mTOR was suppressed by mTOR inhibitors WYE132 (WYE) and INK128 (INK), but not by Vehicle (V) or SAR405 (SAR).

Hyperactivation of mTOR is expected to inhibit autophagy, which is of great importance for kidney proximal tubule cells (Havasi & Dong, 2016; Jiang et al., 2012; Kimura et al., 2011; Livingston & Dong, 2014; Takabatake, Kimura, Takahashi, & Isaka, 2014), a subpopulation known to be affected in LS patients (Hsieh et al., 2018; Oltrabella et al., 2015; Florian Recker et

al., 2015). Indeed, we observed that the fraction of cells displaying autolysosomes was substantially decreased in HK2 human proximal tubule OCRL1 K.O. than in WT cells (Fig.2.10). This phenotype was suppressed by treatment of the cells with mTOR inhibitors (Fig.2.10).

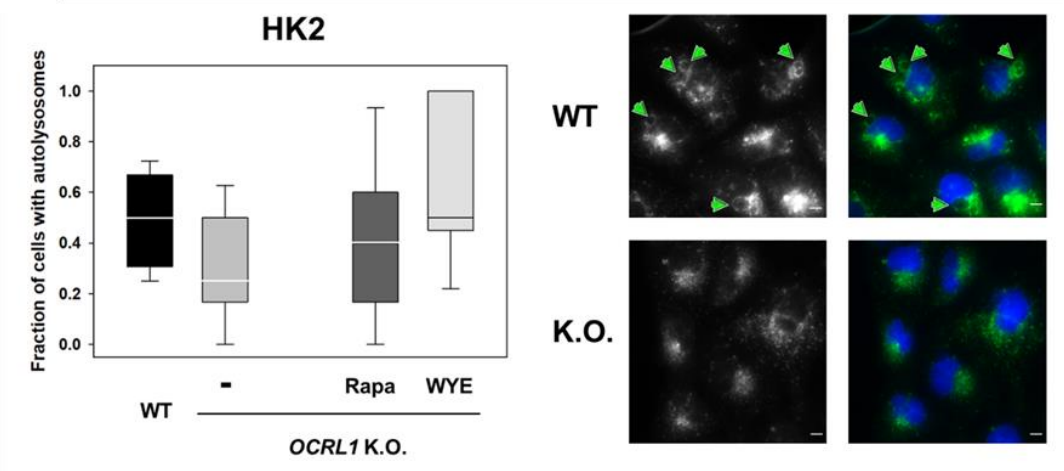


**Figure 2.10 Absence of Ocrl1 led to autolysosome deficiencies in human kidney HK2 cells that can be rescued by the mTOR inhibitors rapamycin and WYE.**
Human HK2 kidney cells WT and OCRL1 K.O. were stained for Lamp2 by immunofluorescence and treated or not with rapamycin (10nM) or WYE (1uM). Fraction of cells displaying these structures were quantified for each experimental group and statistically analyzed using the Wilcoxon test applying the Bonferroni correction for 3 comparisons of 3 OCRL1 K.O. samples vs. their WT counterpart, $p<\alpha=0.05/3=0.016667$ (A); representative images of analyzed cells are shown in panel B, arrows point to some characteristic autolysosomes. Scale bar: 10 µm.

As a whole these results are in agreement with the findings of multiple laboratories showing that pathological conditions characterized by cilia abnormalities (Joubert, Morm, Bardet-Biedl syndromes as well as polycystic kidney disease) display mTOR/PI3K pathway hyperactivation (S. Hakim et al., 2016; Mekahli et al., 2014; Pema et al., 2016). Importantly, in many cases, these ciliogenesis phenotypes were suppressed by administration of rapamycin (S. Hakim et al., 2016).

### 2.3.7 Rosuvastatin/rapamycin combination mitigated both membrane remodeling and PC assembly phenotypes.

Our results suggest that Ocrl1's roles in membrane remodeling and PC assembly are independent and mediated by distinct signaling pathways, RhoGTPase-dependent and mTOR-dependent, respectively. Therefore, we predicted that upon Ocrl1-lack of function, a combination

treatment of LS cells with statins and rapamycin will be needed to simultaneously rescue both phenotypes. In agreement with this prediction, we observed significant rescue of both phenotypes in LS (Ocrl1 NULL) cells incubated with a mix of rosuvastatin and rapamycin (Fig.2.11).

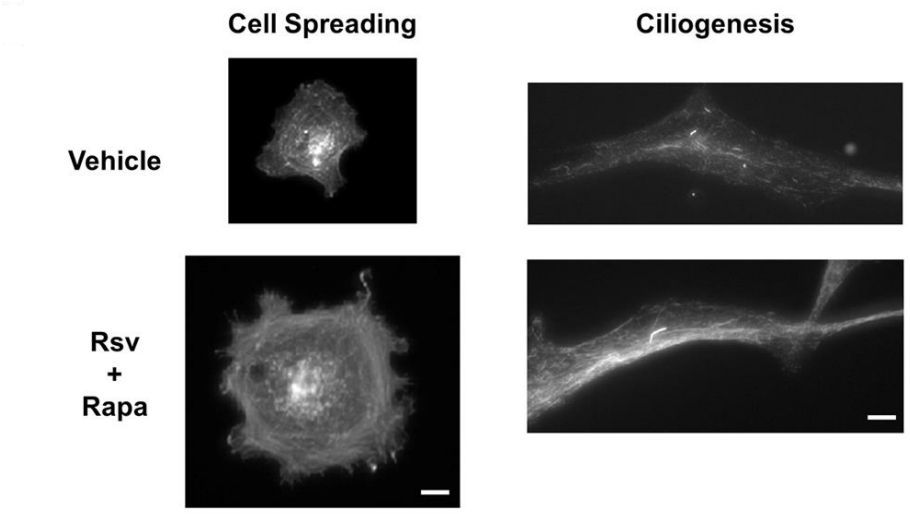


**Figure 2.11 Treatment with combination of rapamycin and rosuvastatin ameliorate both ciliogenesis and spreading phenotypes in LS patient cells.**
LS cells were treated with either Rapa or Rsv or a combination of both and subjected to ciliogenesis and cell spreading assays as described before. (Data- Dr. Kayalvizhi Madhivanan)

## 2.4 Discussion

This study sheds light onto the mechanisms underlying LS and pave the way for the development of therapeutic approaches against this disease. Specifically, here we show that LS patient cells exhibit phenotypes compatible with RhoGTPase signaling imbalance and constitutive activation of the PI3K/Akt and mTOR pathways. In addition, we also found adhesion and RhoA- and MLCK-dependent spreading abnormalities in LS patient cells.

Further, we identified two FDA-approved drug groups capable of alleviating those signaling abnormalities and their phenotypic manifestations in LS patients' and other OCRL1-deficient cells. Interestingly, none of these compounds could individually revert both phenotypes, instead a combination of drugs was necessary for mitigation of all LS cellular defects. This observation further supports the idea that Ocrl1 has at least two independent functional roles in two important cellular processes: membrane remodeling and ciliogenesis. This is in agreement with the fact that

the Ocrl1's molecular requirements to sustain the two above mentioned cellular process categories are very dissimilar. On one hand, Ocrl1 N-terminus-mediated interactions (perhaps mediated via proteins involved in cargo internalization, e.g., AP-2 and clathrin) are required for membrane remodeling, while dispensable for ciliogenesis (Brian G. Coon et al., 2012; Coon et al., 2009). On the other hand, ciliogenesis relies on Ocrl1 C-terminus binding (likely via the endosomal proteins IPIP27/Ses (Brian G. Coon et al., 2012)). Nevertheless, it should be highlighted that Ocrl1's lipid phosphatase activity is required to support both processes (Brian G. Coon et al., 2012; Coon et al., 2009). Further, the ability of the functional homolog Inpp5b to replace the role of Ocrl1 in each process is also different: while this paralog cannot support membrane remodeling (it should be noted that Inpp5b lacks AP-2 and clathrin binding motifs (Coon et al., 2009; Madhivanan, Ramadesikan, & Aguilar, 2015)), it partially alleviates (if overexpressed) the ciliogenesis defect exhibited by Ocrl1-deficient cells (Brian G. Coon et al., 2012). In addition, the processes mentioned above have different mechanistic requirements; whereas membrane remodeling relies on proper RhoGTPase signaling (Warner, Wilson, & Caswell, 2019), ciliogenesis has an important component of vesicle trafficking to the PC (Hsiao, Tuz, & Ferland, 2012; Madhivanan & Aguilar, 2014). Interestingly, the mTOR pathway known to play a role in vesicle trafficking (Al-Awqati, 2015; Grahammer et al., 2017), is also known to be associated with ciliopathies when hyper-activated (Mekahli et al., 2014), and here we show that it is constitutively active in LS patient cells (Fig.2.11B). These observations explain the differential ability of statins (RhoGTPase modulators) and rapamycin (mTOR inhibitor) to mitigate LS phenotypes.

It is important to notice that due to different *OCRL1* mutations and genetic modifiers, patients may exhibit different penetrance of each phenotype category. Therefore, we predict that these variations would make the anti-LS effectivity of each individual drug (or specific combinations) subjective to personalized optimization.

### 2.4.1 How do deficiencies in Ocrl1 function trigger these phenotypes?

RhoGTPase signaling pathways.

The link between Ocrl1 and these pathways is multi-fold: Ocrl1 is a RhoGTPase-binding protein (Faucherre et al., 2003a), a regulatory element in PtdIns signaling (which is intrinsically linked to RhoGTPase regulation (Croisé, Estay-Ahumada, Gasman, & Ory, 2014) and it has been shown to participate in a signaling module involving the RhoGTPase Rac1 (van Rahden et al.,

2012). Further, it should also be kept in mind that, at least during cell migration, Rac1 is activated at endosomes and then recycled to the leading edge (Barbieri, Di Fiore, & Sigismund, 2016; Palamidessi et al., 2008). Since Ocrl1 has been shown to bind both Rac1-GDP (Faucherre et al., 2003a) and AP2/clathrin (R. Choudhury et al., 2005), this protein may link the signaling inactive form of Rac1 to endocytosis and therefore, to activation in endosomes. Ocrl1's phosphatase activity would be required for $PI(4,5)P_2$ turnover and consequently for uncoating (Ramiro Nandez et al., 2014) of these [Rac1-GDP]-containing vesicles; but it is also possible that Ocrl1 would promote $PI(4,5)P_2$ (and $PI(3,4,5)P_3$) production/hydrolysis cycling required for proper Rac1 signaling at the remodeling membrane. Therefore, it is to be expected that Ocrl1-deficiencies would lead to diminished Rac1 signaling and in consequence to RhoA activation; which in turn would lead to Rac1 inactivation/RhoA hypersignaling via a feedback circuit.

Rac1 is responsible for the formation of early initial focal contacts which are finer and localized predominantly at cell periphery while Rho-mediated focal adhesions are morphologically larger and less peripheral (Nobes & Hall, 1995). Rac1 activation is required for cell spreading (Price, Leng, Schwartz, & Bokoch, 1998).

Strikingly in work resembling our own result with Ocrl1-deficient cells, Guo et al. (F. Guo, Debidda, Yang, Williams, & Zheng, 2006) showed that cells lacking Rac1 displayed poorer adhesion and diminished spreading on fibronectin at the 20-30min time point post seeding. Furthermore, Rac1-deficient cells also had defects in forming stable focal complexes at early stages of attachment, while the levels of expression of focal adhesion proteins remained unchanged (F. Guo et al., 2006). In contrast, activated Rac1 mutant (Rac1V12,N33) has been shown to enhance cell adhesion and spreading in an actin-dependent manner (D'Souza-Schorey, Boettner, & Van Aelst, 1998).

We also observed that many of the shorter vinculin-positive structures in LS cells are not linked to the actin cytoskeleton (Fig.2.6C). On the one hand, this uncoupling of the focal adhesion complexes from the actin cytoskeleton may explain the overall disorganized appearance of adhesions in patient cells as compared to normal cells. On the other hand, this abnormality may impair ECM-cell mechano-transduction causing the cells to be unable to respond to external forces, reorganize the actin cytoskeleton and allow the maturation of focal adhesions (Ciobanasu, Faivre, & Le Clainche, 2012; Kuo, 2013).

PI3K/Akt/mTOR signaling pathways.

It has been shown that Ocrl1 deficiency causes $PI(4,5)P_2$ accumulation (Cui et al., 2010; Vicinanza et al., 2011; X. L. Zhang et al., 1998). Since this lipid is the substrate of PI3K, we hypothesize that LS cells will exhibit constitutive activation of the PI3K/Akt pathway that in turn would trigger downstream mTOR signaling. Our data supported this hypothesis showing evidence of activity via both mTORC1 and mTORC2 in LS cell lysates (Fig.2.9B), with the latter expected to exert a positive feedback on the PI3K/Akt pathway (Gan, Wang, Su, & Wu, 2011) and leading to SGK1 activation by phosphorylation (García-Martínez & Alessi, 2008). In fact, we observed the presence of high levels of phosphorylated SGK1 in LS cells as compared to the normal controls. Importantly, this enzyme has been shown to stabilize membrane localization of multiple cargoes (including cilium-localized proteins, such as TRPV4 (Al-Awqati, 2015; E. J. Lee, Shin, S.H, Chun, J, Hyun, S, Kim, & Y, 2010), i.e., impairing their endosome-to-PC transport (a process which involves Ocrl1 (N. Luo et al., 2014)). In fact, constitutive activation of mTOR has been consistently linked to cilia abnormalities (Zullo et al., 2010). It should be noted that although mTORC1 displays substantially higher sensitivity for rapamycin, mTORC2 can also be inhibited by this pharmacological agent (Li, Kim, & Blenis, 2014). Indeed, our results showed that upon rapamycin treatment, mTOR underwent dephosphorylation consistent with inactivation of both mTORC1 and 2 and also exhibited SGK1 dephosphorylation (Fig.2.11B) along with the re-establishment of efficient ciliogenesis of LS cells (Fig.2.9B). In contrast to LS patient cells, an ocrl1-deficient zebrafish line showed no major activation of AKT/mTOR signaling (Ramirez et al., 2012) pointing to inevitable differences between this animal model and the human scenario and/or between the comparison of cellular and whole organismal levels. Along the same lines, and very interestingly, although PC assembly defects have been observed in more than 28 different patients' cells (Brian G. Coon et al., 2012; Florian Recker et al., 2015), cilia abnormalities are milder in LS zebrafish. This latter observation further indicates the strong correlation between the mTOR/AKT signaling susceptibility of the model under study and the magnitude of the cilia defects; i.e., high mTOR activation (humans) leads to substantial ciliogenesis defects, while low/normal mTOR/Akt activation (zebrafish) correlates with mild PC assembly abnormalities.

Recent studies by Hakim et al. (S. Hakim et al., 2016) have demonstrated that renal-specific deletion of INPP5E in mice, the gene which encodes the lipid 5' phosphatase mutated in Joubert and MORM syndromes led to hyperactivation of mTOR/PI3K-Akt signaling. Further, ablation of INPP5E in the kidney also resulted in ciliary loss as observed by others previously (Bielas et al.,

2009). The authors also demonstrated that treatment with rapamycin was able to reduce mTOR hyper signaling (S. Hakim et al., 2016).

mTOR hyperactivation has also been demonstrated in human patients and murine models of Autosomal dominant and recessive polycystic kidney disease (ADPKD and ARPKD, respectively). While the molecular mechanisms that lead to this mTOR hyperactivation in these kidney pathologies is currently under investigation, many pre-clinical studies however, have shown significant success in the use of Rapamycin (or everolimus) as a treatment strategy to reduce cystogenesis (Ibraghimov-Beskrovnaya & Natoli, 2011; Pema et al., 2016).

In addition, the neurological condition known as Tuberous sclerosis complex is also characterized by a mTOR hyperactivation scenario that strongly correlates with the presence of epileptic seizures (Zeng, Xu, Gutmann, & Wong, 2008). Interestingly, LS patients display neurological abnormalities and at least half of them present with seizures.

### 2.4.2 How do cellular phenotypes translate into patient symptoms?

Although highly dependent on cell type and cellular environment, the process of cell spreading, migration and adhesion play crucial roles during embryogenesis; therefore, defects or delays in these processes are predicted to lead to developmental abnormalities. Further, we speculate that both membrane remodeling and ciliogenesis phenotypes contribute to specific LS patient symptoms. For example, either PC or FPU abnormalities are predicted to impact kidney function. On the one hand, the role of the PC in osmo/chemo/mechanosensing, epithelia repair and signaling, explains why the LS ciliogenesis phenotype will affect renal function (Coon et al., 2009; N. Luo et al., 2014). In addition, the underlying vesicle trafficking defect involved in PC phenotype (Brian G. Coon et al., 2012) also affects the steady state distribution of receptors involved in solute reabsorption such as Megalin (Oltrabella et al., 2015; Vicinanza et al., 2011). On the other hand, FPU deficiency will impair quick reabsorption of material from the ultrafiltrate and control of membrane composition. For example, FPU is the major mean of uptake of oxalate crystals by proximal tubule cells (Aggarwal, Narula, Kakkar, & Tandon, 2013). Therefore, one predicted consequence of the FPU phenotype is the generation of kidney stones (nephro-calcinosis/lithiasis), which indeed are often present in LS patients (T. Liu, Yue, Wang, Tong, & Sun, 2015; Tasic et al., 2011). In addition to these defects, a recent study (Gliozzi et al., 2020) has also demonstrated the shortening of proximal tubules in Ocrl1-deficient zebrafish. Taken together, these deficiencies may

cause a severe impact on renal function which may explain the severity of kidney involvement in LS patients.

These phenotypes are also predicted to play a role in LS neurological and eye symptoms. For example, since neurons rely on FPU for synaptic vesicle recycling upon sustained stimulation, abnormalities in this process may contribute to limitations in synaptic plasticity and other functions dependent on synaptic vesicle replenishing (Holt, Cooke, Wu, & Lagnado, 2003). Also, during embryo development, neuron and lens migration defects, as well as abnormalities in PC-dependent planar cell polarity, will lead to neurological and ocular symptoms (E. J. Lee, Shin, S.H, Chun, J, Hyun, S, Kim, & Y, 2010; May-Simera, Nagel-Wolfrum, & Wolfrum, 2017).

It should be noted that in the context of a whole organism the ultimate symptom outcome is determined by multiple layers of complexity. Specifically, organ/tissue characteristics, cell type sensitivity and multiple genetic modifiers may accentuate or alleviate phenotype severity (and may affect drug accessibility/response). Also, although FPU abnormalities do NOT contribute to PC defects (and PC phenotypes do NOT affect FPU), when both abnormalities are present (e.g., in Ocrl1 NULL patients), phenotypes may synergistically act on specific processes in vivo. For example, cell migration defects directly depend on membrane remodeling; however, PC function is required for establishing proper direction of migration in chemo/hapto/duro-taxis gradients typical of in vivo environments (Schneider et al., 2010; Schneider et al., 2005).

### 2.4.3 Therapeutic Perspectives

This study also explored the possibility of using pharmacological agents to counteract LS cellular phenotypes to set up the basis for the development of post-natal treatments against LS that should take a precision medicine approach based on patient-specific variations.

To mitigate RhoA hyperactivation, we relied on the use of statins. These compounds are the most widely prescribed class of drugs for lowering cholesterol during hypercholesterolemia and ischemic heart disease treatment (Davies et al., 2016). Statins act upon the mevalonate pathway (cholesterol synthesis) as small molecule inhibitors of HMG-CoA reductase, preventing mevalonate synthesis and subsequent cholesterol production (Fig.2.3A) (Davies et al., 2016). However, intermediate products of the mevalonate pathway are involved in other cellular processes. Examples include geranylgeranyl pyrophosphate and farnesyl pyrophosphate which are involved in prenylation and hence are required for the activation of RhoGTPases such as RhoA

(Fig.2.3A). In fact, these functions of statins are being exploited as a treatment for HIV infection (Feinstein, Achenbach, Stone, & Lloyd-Jones, 2015) and cancers where RhoA is found hyperactivated (Zhong et al., 2015). In addition, statins have been effectively used against another genetic disease with a neurological component known as Noonan syndrome (Y. S. Lee et al., 2014). Similarly, we demonstrated that treatment with statins could alter the RhoGTPase imbalance and mitigate the membrane remodeling phenotypes exhibited by LS cells.

The use of a farnesyl transferase inhibitor emulated statin's action in rescuing the spreading phenotype (Fig.2.3B); therefore, these observations suggested that RhoA hyperactivation can be inhibited by interference of its prenylation, leading to decreased RhoGTPase membrane anchoring and consequent activation.

Since RhoA is hyperactivated in LS patient cells (Lasne et al., 2010; van Rahden et al., 2012) it makes it the primary target for statin-mediated inhibition. Impairment of prenylation will decrease RhoA activation to a level in which Rac1 inhibition is not complete, allowing Rac1 to signal which in turn will contribute to RhoA inactivation. Although this treatment would lead to lower levels of total membrane-anchored activated RhoGTPases, our studies indicate that a better Rac1/RhoA signaling balance can be acquired.

Rapamycin's and other drugs' capabilities to inhibit mTOR constitutive signaling activation, correlate with their ability to restore normal ciliogenesis in LS patient cells. Nevertheless, it should be noted that only rapamycin is currently approved for use in humans. Interestingly, rapamycin has been shown to counteract phenotypes observed in ciliopathy models (S. Hakim et al., 2016).

Indeed, both statins and rapamycin are currently and successfully used in children to ameliorate conditions such as familial hypercholesterolemia and rejection prophylaxis/autoimmune lymphoproliferative syndrome, respectively (Davies et al., 2016; Teachey, 2012). Therefore, these drugs are prime candidates to be readily and successfully repositioned/repurposed to counteract symptoms in LS. Nevertheless, as mentioned before, the anti-LS efficacy of such drugs would be directly linked to patient specific characteristics such as the nature of the *OCRL1* mutation and genetic modifiers.

We believe that this work has the potential to pave the way to clinical trials. In addition, since previous investigations unveiled that LS shares some characteristics with other genetic diseases such as ciliopathies (Brian G. Coon et al., 2012), these discoveries may also impact patients suffering from other conditions besides LS.

In summary, our results lead us to propose a working model in which Ocrl1 deficiencies cause trafficking and signaling abnormalities (Fig.2.12).

On the one hand, absence of Ocrl1 (or mutations affecting its phosphatase activity) conduce to accumulation of PI(4, 5)$P_2$, which in turn leads to constitutive activation of the PI3K/AKT and mTOR pathways (Fig.2.12). This signaling axis is known to affect the trafficking of cargo (e.g., channels such as TRPV4) to the endosomal compartment and therefore to the PC, ultimately impacting ciliogenesis (Fig.2.12).

On the other hand, lack of Ocrl1 also contributes to general trafficking abnormalities (Brian G. Coon et al., 2012; Vicinanza et al., 2011) and likely to defects in endosomal activation of Rac1 (Fig.2.12). These and other abnormalities yet to be mechanistically established, contribute to a RhoA/Rac1 signaling unbalance scenario (high RhoA- and low Rac1-activation) that conduces to actin re-organization abnormalities (Suchy & Nussbaum, 2002) (Fig.2.12). This RhoGTPase-mediated effect on microfilament cytoskeleton assembly is predicted to be synergic with abnormal control of PI(4, 5)$P_2$-sensitive actin dynamics regulators (Fig.2.12). Lack of proper cytoskeletal control/regulation constitutes the major cause of the membrane remodeling defects observed in LS patient cells (Fig.2.12).

Finally, given their activities down-modulating mTOR and RhoA signaling, this working model provides an explanation for the phenotype alleviating properties of FDA-approved doses of the drugs rapamycin and rosuvastatin (Fig.2.12).

Further studies should be pursued to test/refine this model and to add mechanistic details to it. We speculate that broader models that provide emphasis in the effects of Ocrl1-deficiency on important cellular signaling circuits have the potential to better our understanding of the disease and led us towards viable therapeutics against this terrible disease.

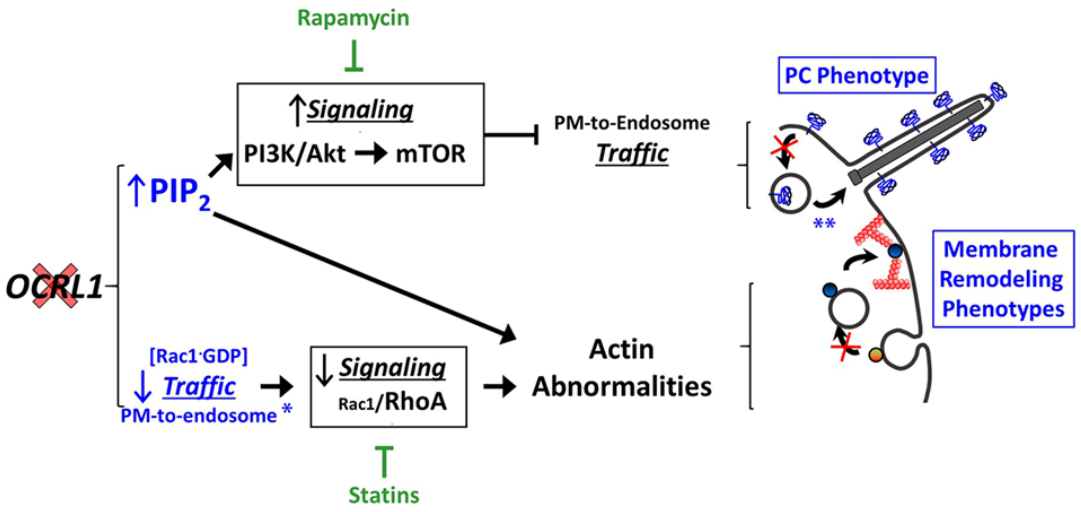


**Figure 2.12 Working model for LS phenotype development as a consequence of lack of Ocrl1 activity.**

Ocrl1 deficiencies would increase the availability of the PI3K substrate PIP2 leading to mTOR hyperactivation and consequently to inhibition of cilia-localized cargo traffic to endosomes and their delivery to the cilia (**: (Coon et al. 2012). Indeed, $PIP_2$ accumulation will also interfere with normal actin dynamics affecting membrane remodeling processes. Ocrl1 abnormal function is also directly linked to vesicle trafficking defects and [Rac1-GDP] requires traffic to endosomes to be activated by the GEF TIAM (*: (75, 76)) and recycle back to the plasma membrane (PM) to promote membrane rearrangements (see text for further details).

## 2.5 Materials and methods

### 2.5.1 Reagents

Materials were purchased from Fisher Scientific (Fairlawn, NJ) or Sigma (St. Louis, MO) unless stated otherwise. The different antibodies used in this study are listed in Table 2.3.

### 2.5.2 Cells and culture conditions

Normal (GM07492) and LS primary dermal fibroblasts (GM01676 and GM03265) were purchased from the NIHGMS Human Genetic Cell Repository (Coriell Institute for Medical Research, Camden, NJ, USA). Cells were cultured in DMEM, Streptomycin/Penicillin, 2mM L-Glutamine and 15% fetal bovine serum (FBS) at 37 ºC in a 5% $CO_2$ incubator. When needed, cells were transferred to fibronectin-coated surfaces (plates or coverslips) prepared by incubation with 10µg/mL Fibronectin for 2h at 37 ºC. Normal human proximal tubule epithelial (HK2) and human

embryonic kidney epithelial 293T (HEK293T) cells obtained from ATCC were grown in DMEM, Streptomycin/Penicillin, 2mM L-Glutamine and 10% fetal bovine serum (FBS) at 37 ºC in a 5% $CO_2$ incubator. *OCRL1*$^{-/-}$ (*OCRL* K.O) HK2 and HEK293T cells were prepared by GenScript Inc. Piscataway, NJ, USA and maintained under same conditions than their normal counterparts.

### 2.5.3 Pharmacological treatments and viability/toxicity assessment

Cells were incubated with the indicated drugs, for the specified times at different concentrations as described, in low serum (0.1%) media to avoid substantial protein-mediated drug sequestration. In addition to cell counting post-treatment, a sample of cells seeded on fibronectin-coated coverslips was fixed and stained with FITC-phalloidin and DAPI for cell morphology inspection. Viability was monitored by performing MTT assays as follows: Following treatment of cells (in triplicates) with indicated drugs at different concentrations for specific times, media was aspirated and replaced with MTT solution (freshly prepared at 0.5mg/ml in complete media) and incubated for 1.5h. Additionally, a blank control with only MTT reagent containing no cells was also prepared. Following incubation, solution was aspirated and MTT was immediately solubilized using 1mL DMSO (per well) by gentle pipetting, Absorbance values of solubilized MTT solution from the different wells were measured at 570nm using a spectrophotometer. Pharmacological compounds used in this study are listed in Table 2.2.

*Cholesterol uptake Assay***:** Was performed using an AbCam kit (ab236212) according to manufacturer instructions.

### 2.5.4 Cell Spreading Assays

We utilized two approaches to monitor cell spreading: 1) *After a predetermined time-point* and 2) *At multiple time points*.

Spreading after a predetermined time-point.

Human dermal fibroblasts (12h after seeding) were treated with the indicated drug (or vehicle) in 0.1% serum for indicated time. After drug treatment, the cells detached from the culture dish using 20mM EDTA (in 1X PBS), centrifuged at 300xg for 5min, resuspended in 1% serum in the presence of drug or vehicle. Cell suspensions were then set in a rotator for 1h before seeding them on fibronectin-coated coverslips for 30min, undisturbed, to allow attachment and spreading.

Following this, coverslips were washed with 1X PBS and fixed in 4% formaldehyde. Rhodamine-Phalloidin was used to stain the actin cytoskeleton of the fixed cells and imaged by epifluorescence microscopy. At least 50 cells were quantified per experiment by tracing and measuring cell areas by using the magic wand tool in ImageJ software.

Spreading at multiple time points.

Human dermal fibroblasts were treated as described above, seeded on fibronectin-coated LabTek chambers and allowed to attach and spread. Cells were imaged at intervals of 10min after seeding for 8h using 20X objective in a Zeiss Axiovert inverted microscope. Number of detaching cells were quantified at every 10min up to the first 1h by using cell counter tool in ImageJ. To determine spreading kinetics, individual cells were tracked in each time lapse image and were scored from 1-5 based on general cell morphology. Briefly, cells that were just attached and looked circular with no protrusions or visible extensions received score 1. Cells with needle-like (filopodia) projections were scored 2, cells with lamellopodia-like extensions were scored 3, cells with more extended lamellopodia-like extensions and increase in cell area were given a score of 4 and a further increase in cell area, often accompanied by isotropic spread morphology was given score of 5.

Alternatively, cells treated as described above and allowed to attach on fibronectin-coated dishes. Immediately after seeding, the cells were imaged with 10X objective simultaneously using up to 3 Cytosmart Imaging Systems (Lonza) at intervals of 30s for 2h. Number of cells attached were quantified at every 10min up to the first 1h using Cell Counter tool in ImageJ software.

### 2.5.5 Confocal microscopy

Cells were prepared as described under *Spreading after a pre-determined time point* and after fixation indirect immunofluorescence was performed using antibodies against phospho-FAK (Y397) or vinculin. Briefly, cells were gently washed with PBS, fixed with 4% formaldehyde-PBS for 10min and permeabilized using 0.25% Triton-X 100 in PBS for 20min, followed by blocking with 5% BSA in PBS for 30min. Cells were also immunostained with Phalloidin-FITC and DAPI to label the actin cytoskeleton and nucleus respectively. Images were acquired at the Indiana O'Brien Center Biological Microscopy (Division of Nephrology, IU School of Medicine) using an Olympus IX81 inverted confocal microscope. A 60X Oil objective (NA 1.42) was used and

randomly selected fields were imaged using constant voltage, gain and intensity for the different groups, as well uniform step size (0.19μm) using sequential image collection mode.

### 2.5.6 Fluid shear stress assays

We utilized two approaches to monitor resistance to Fluid sheer stress (FSS): 1) *After a predetermined time-point* 2) *At multiple time points.*

FSS *after a predetermined time-point.*

Equal number of normal and LS cells were allowed to attach on fibronectin-coated coverslips (22mm x 22mm) as described before. 20min after seeding, one set of coverslips were washed gently washed and immediately fixed using 4% formaldehyde. Another set of coverslips were subjected to fluid shear stress by flushing 1X PBS using a standard wash bottle with spout and then fixed with 4% formaldehyde. Coverslips were then immunostained with Rhodamine-Phalloidin (1:200) to label the actin cytoskeleton and DAPI to label the nucleus. Cells were then imaged by using Axiovert inverted epifluorescence microscope. For each group, 3 random rows were selected on the coverslip and completely imaged from end to end without skipping any field within the row. Attached cells were then counted from each row and the fraction of cells remaining on the coverslips before and after fluid shear stress was calculated.

FSS *at multiple time points.*

Normal and LS fibroblasts were seeded on fibronectin-coated wells and allowed to attach. Immediately after seeding, cells were imaged with 10X objective simultaneously using up to 3 Cytosmart Imaging Systems (Lonza) at intervals of 30s for up to 2h. 20min after seeding, a 1mL pipette tip was used to gently aspirate 1mL of media which was immediately released into the culture dish to produce a sudden fluid shear stress. Number of cells attached before this event (t=19min) and after the shear stress (t=24min) were counted using Cell Counter tool on ImageJ and fraction of cells detaching was calculated.

### 2.5.7 Fluid phase uptake assay

Cells were seeded on glass coverslips for 12h prior to experiments and then treated with the indicated drug or vehicle in 0.1% serum media for the specific amount of time. Cells were treated with 1mg/mL 70kDa dextran-TMR (dissolved in media containing FBS) at 37°C for 20min.

Coverslips were washed extensively with PBS (at 4°C) and fixed. The cells were then imaged and the fluorescence intensity of the dextran-TMR taken up by cells was measured using Image J.

### 2.5.8 Ciliogenesis assays

Cells were grown on coverslips overnight in complete media. Then media was replaced by 0.1% serum DMEM (starvation media) containing vehicle or the drug to induce ciliogenesis for indicated times. Cells were then fixed with 4% formaldehyde (in 1X PBS) and immunostained with anti-acetylated tubulin antibody (Table 2.3). At least 50 cells were imaged for every experiment and repeated at least thrice. The fraction of cells displaying cilia and cilia length were determined described before (Brian G. Coon et al., 2012).

### 2.5.9 Indirect immunofluorescence for lysosomes

Following treatment with drugs, cells were washed and fixed with 4% formaldehyde-PBS for 10min and immunolabeled for LAMP2. Random fields were imaged using Zeiss Axiovert inverted microscope using 40X objective with constant fluorescence exposure times. Cells were scored for the presence or absence of autolysosomes and fraction of cells/field exhibiting these structures was determined.

### 2.5.10 Western blotting

Normal and LS cells were seeded on 100mm plates and grown to 60-70% confluency in complete media. Then media was exchanged to 0.1% serum DMEM media with DMSO or 10nM rapamycin for 12 hrs. The cells were washed twice with ice-cold PBS, collected by scraping cells in 200µl/plate of lysis buffer (25mM HEPES-KOH , pH7.4, 250mM NaCl, 1% Triton-X-100 supplement with phosphatase and protease inhibitors), and lysed by passing the cells 10 times through a 26G1/2 needle. The lysates were centrifuged at 14,000xg for 20min at 4°C, and the supernatant fractions were collected. The samples were analyzed by SDS-PAGE using 7% or 10% poly-acrylamide gels, and transferred to nitro cellulose membranes. The membranes were blocked with 5% skim milk in PBST and immunoblotted with indicated primary and HRP-conjugated secondary antibodies.

### 2.5.11 Statistical analysis

The Kolmogorov-Smirnov (KS) test was used to determine statistical significance of differences between spreading-distribution histograms. While the student's t-test was used to evaluate the significance of differences of normally distributed samples, the Wilcoxon's test was employed when samples were non-normally distributed. The Bonferroni's correction was performed whenever there were multiple comparisons [$\alpha C=p/n$; n being the number of comparisons].

A von Bertalanffy logistic model was adopted to fit the data presented in Fig.2.4A (adhesion) and Fig.2.7 (spreading). The estimated time to achieve half the maximal value of each process ($T_{0.5}$) was obtained and used to calculate their continuous rates (K) according to: $K= -Ln(0.5)/ T_{0.5}$. The associated error $\Delta K$ was estimated using standard rules of error propagation (Taylor, 1997) based on the determined $T_{0.5}$ error ($\Delta T_{0.5}$), according to $\Delta K=K(\Delta T_{0.5}/T_{0.5})$.

**Table 2.2 Pharmacological agents used in this study**

| Compound | Activity | Source | Catalog number | Use (conc/time) |
|---|---|---|---|---|
| Calpeptin | Rho activator | Cytoskeleton, Inc | CN01 | 137.5μM/1h |
| C3 Transferase | Rho inhibitor | Cytoskeleton, Inc | CT04 | 10.5nM/2h (Fibroblasts), 4.2nM/2h (HK2) |
| Fasudil | Rho Kinase | Selleck | S1573 | 10μM/3h |
| PF-3758309 | PAK inhibitor | AdooQ | A11930 | 1-10μM/3-6h |
| ML7 | MLCK inhibitor | Enzo | BML-EI197- | 1μM/6h |
| fluvastatin | HMG-CoA reductase inhibitors | Cayman | 10010337 | 1-100μM/3-6h |
| simvastatin | | Cayman | 10010344 | 1-10μM/8-12h |
| atorvastatin | | Toronto Research Chemicals | A791750 | 1-100μM/3-6h |
| pitavastatin | | Selleck | S1759 | 10μM/12h |
| Rosuvastatin | | Bio Vision | 1955-5 | 100μM/12h or 10-20μM/72h (long-term exposure) |
| FTI276 | Farnesylation | CalBioChem | 344550 | 0.5μM/6h |
| Rapamycin | mTOR inhibitor | Cayman Chemicals | No13346 | 100nM/12h or 10nM/72h (long-term exposure) |
| WYE132 | mTOR inhibitor | BioVision Inc | 2256-500 | 1μM/72h |
| INK128 | mTOR inhibitor | MedKoo | 205495 | 20nM/72h |
| SAR405 | PI3K cIII inhibitor | MedChem | HY12481 | 1μM/72h |

**Table 2.3 List of antibodies used in this study**

| Antigen | Host | Source | Dilution used and application[a] |
|---|---|---|---|
| mTOR (total) | Rabbit | Cell signaling (#2972) | 1:1000 (WB) |
| p-mTOR (S2448) | Rabbit | Cell signaling (#2971) | 1:1000 (WB) |
| p-mTOR (S2481) | Rabbit | Cell signaling (#2974) | 1:1000 (WB) |
| Akt (Total) | Rabbit | Bioss (Bs-0115R) | 1:500 (WB) |
| p-Akt (S473) | Rabbit | Cell signaling (#4058) | 1:1000 (WB) |
| SGK-1 (Total) | Rabbit | Millipore (# 07-315) | 1:100 (WB) |
| p-SGK-1 (S422) | Mouse | Santa Cruz (sc-16745) | 1:100 (WB) |
| Tubulin | Mouse | Biolegend (627903) | 1:500 (WB) |
| Acetylated-Tubulin | Mouse | Sigma Aldrich (6-11B-1) | 1:1000 (IIF) |
| Pericentrin | Rabbit | Abcam (ab4448) | 1:300 (IIF) |
| Vinculin | Mouse | Sigma Aldrich (V9131) | 1:800 (IIF) |
| Phospho-Paxillin | Rabbit | Epitomics (2128-1) | 1:500 (WB) |
| Pan FAK | Rabbit | Santa Cruz (C-20) | 1:500 (WB) |
| Phospho-FAK | Rabbit | Santa Cruz (11765-R) | 1:50 (IIF), 1:500 (WB) |
| LAMP2 | Mouse | Santa cruz (sc-18822) | 1:150 (IIF) |
| a: WB: Western blotting; IIF: Indirect Immuno-Fluorescence. | | | |

# CHAPTER 3. LOWE SYNDROME CELLULAR PHENOTYPES ARE DIFFERENTIALLY AFFECTED BY SPECIFIC *OCRL1* PATIENT MUTATIONS

## 3.1 Abstract

Lowe Syndrome (LS) is a lethal genetic disorder caused by mutations in the *OCRL1* gene, which encodes the lipid 5' phosphatase Ocrl1. Patients exhibit characteristic triad of symptoms including congenital cataracts, low molecular weight proteinuria and mental retardation. Progressive renal dysfunction is the cause of death. Ocrl1 localizes to the *trans*-Golgi network (TGN) and participates in many cellular processes. Over 200 *OCRL1* mutations have been identified in LS, but their impact on cellular processes is unknown. Despite observations of heterogeneity in LS patient symptoms, there is little understanding of the correlation between the genotype of patients and disease and/or cellular phenotypes.

Here, we demonstrate for the first time that different mutations have diverse effects on triggering LS cellular phenotypes. Additionally, mutations in specific domain impart unique characteristics to the resulting mutant protein, including TGN fragmentation as well as centriolar sequestration. Some mutations also conformationally affect the protein, resulting in phenotypes and loss of activity which can be reverted by using an FDA-approved drug, 4-phenyl butyric acid.

This study demonstrates for the first time, the differential effect of LS mutations on cellular phenotypes as well as highlights a conformational disease component for LS. It can provide a framework that can help stratify patients as well as provide better prognosis depending on the nature and location of mutation in the *OCRL1* gene and its effect on the biochemical activity and protein domains of Ocrl1.

## 3.2 Introduction

Lowe Syndrome (LS) (OMIM#30900) is an X-linked genetic disorder caused by mutations in the *OCRL1* gene (Attree et al., 1992b). Affected children suffering from the disease are born with bilateral congenital cataracts and develop neurological and renal symptoms as early as 6 months of age (Mario Loi, 2006; LOWE et al., 1952). Progressive renal dysfunction leads to end stage renal disease and their premature death (Mario Loi, 2006). There are currently no LS-specific therapeutics (Bökenkamp & Ludwig, 2016).

The gene product of *OCRL1* is an inositol 5' phosphatase (EC 3.1.3.36) (Suchy et al., 1995; X. Zhang et al., 1995) that localizes at the *trans*-Golgi network (TGN) (Dressman et al., 2000), endosomes (Erdmann et al., 2007) and transiently at the plasma membrane (Faucherre et al., 2005); with specificity for the signaling lipid phosphatidyl inositol 4,5-bisphophate, $PI(4,5)P_2$ (Suchy et al., 1995; X. Zhang et al., 1995). In addition to its phosphatase domain, Ocrl1 possesses an N-terminal PH domain (Mao et al., 2009) and C-terminal ASH-RhoGAP domains (Erdmann et al., 2007; Ponting, 2006) through which it interacts with several signaling and trafficking proteins in cells, thereby participating in several basic cellular processes including cell migration, cell spreading, actin remodeling, ciliogenesis, vesicle trafficking, cytokinesis and phagocytosis (Bohdanowicz et al., 2012; R. Choudhury et al., 2005; Brian G. Coon et al., 2012; Coon et al., 2009; Dambournet et al., 2011; El Kadhi et al., 2011; Noakes et al., 2011; Suchy & Nussbaum, 2002; van Rahden et al., 2012).

Our lab previously identified LS-specific cellular phenotypes, namely- ***membrane remodeling*** (Coon et al., 2009) (fluid phase uptake, cell migration and spreading) and ***primary cilia assembly*** (Brian G. Coon et al., 2012) abnormalities. Further, we determined that Ocrl1 participates in the above two processes is through determinants spatially segregated within the protein (with the N-terminus involved in membrane remodeling (Coon et al., 2009) and the C-terminus required for cilium assembly (Brian G. Coon et al., 2012)). In contrast, a functional Ocrl1 5'-phosphatase domain is required for both processes to proceed normally (Brian G. Coon et al., 2012; Coon et al., 2009) (Fig.3.1A).

There are over 200 unique LS-causing mutations that have been identified in *OCRL1* (Bökenkamp & Ludwig, 2016; Hichri et al., 2011) and affect all domains of Ocrl1. There is heterogeneity in LS patient symptoms (Bökenkamp & Ludwig, 2016; Hichri et al., 2011), but little is known about the correlation between the genotype of patients and their cellular phenotypes.

Taking this together with the domain-specific involvement of Ocrl1 in various cellular processes, we speculated that Lowe syndrome cellular phenotypes would be differentially affected depending on which domain is affected by the mutation.

Here we demonstrate that different *OCRL1* mutations depending on the domain they affect, have a differential impact on cell spreading and ciliogenesis, thereby proposing cellular basis for LS patient symptom heterogeneity. Based on the domain they affect; mutants possess unique characteristics including differences in localization and protein stability. Importantly, the phosphatase domain mutants tested produced fragmentation of TGN, a phenotype exclusive to this domain. This novel cellular phenotype has been associated with other neurodegenerative diseases (Bexiga & Simpson, 2013). Given LS has a neurological component, we predict that this defect may contribute to disease pathogenesis.

In addition, molecular dynamics analysis on mutations affecting non-catalytic residues of the phosphatase domain predicted conformational changes affecting catalytic regions, thereby explaining the impairment of enzyme activity as well as cellular phenotypes. These results not only explain how mutations affecting non-catalytic residues cause LS but also to propose that some *OCRL1* mutants lead to a conformational/protein misfolding disease scenario.

Importantly, we were able to rescue cellular phenotypes tested as well as enzymatic activity using 4-phenylbutyric acid (4-PBA), an FDA-approved drug that is currently administered as the treatment for cystic fibrosis (as well as in trials for other neurological misfolded protein disorders (Cortez & Sim, 2014)) where it is predicted to function as a molecular chaperone (Rubenstein, Egan, & Zeitlin, 1997).

In summary our results provide the first comprehensive analysis of the effect *OCRL1* mutations on cellular phenotypes likely to impact overall embryogenesis and organ-specific function (ex.kidneys). Our data also establishes a conformational disease component for Lowe Syndrome. Further, the FDA-approved drug 4-phenyl butyric acid (4-PBA) can alleviate phenotypes triggered by conformationally affected Ocrl1 mutants. We believe that this study will provide the framework that can stratify LS patients as well as allow aid in creating tailored therapeutic strategies that would consider the nature, location of mutation in the gene and its effect on the biochemical activity and protein domains of Ocrl1.

## 3.3 Results

LS-causing mutations in *OCRL1* predominantly affect exons 9-23 which encodes the phosphatase and ASH-RhoGAP domain, with less than 10% of mutations affecting the PH domain. The phosphatase domain, however, is a hotspot, with over 50% of mutations mapping to this region (Hichri et al., 2011; Utsch et al., 2006). Though different mutations types are found to cause LS, we decided to focus on the missense mutations in the gene.

In order to cover the spectrum of mutations in gene, we selected mutations that affect the different domains of Ocrl1. As representatives of the ASH-RhoGAP domain, we selected mutations V577E, F668V (ASH domain) and I768N and A861T (RhoGAP domain). Within the phosphatase domain, there are nearly 80 unique missense mutations that cause LS. While many of them map to conserved regions within the domain important for catalysis, substrate specificity and recognition, mutations are also found in residues that are non-catalytic. Therefore, we selected mutations we selected phosphatase mutations H524R (catalytic residue) and D451G and V508D (non-catalytic residues) in order to represent both categories. Since there are no reported LS-causing missense mutations that map to the PH domain, this domain could not be represented in the study (Fig.3.1B).

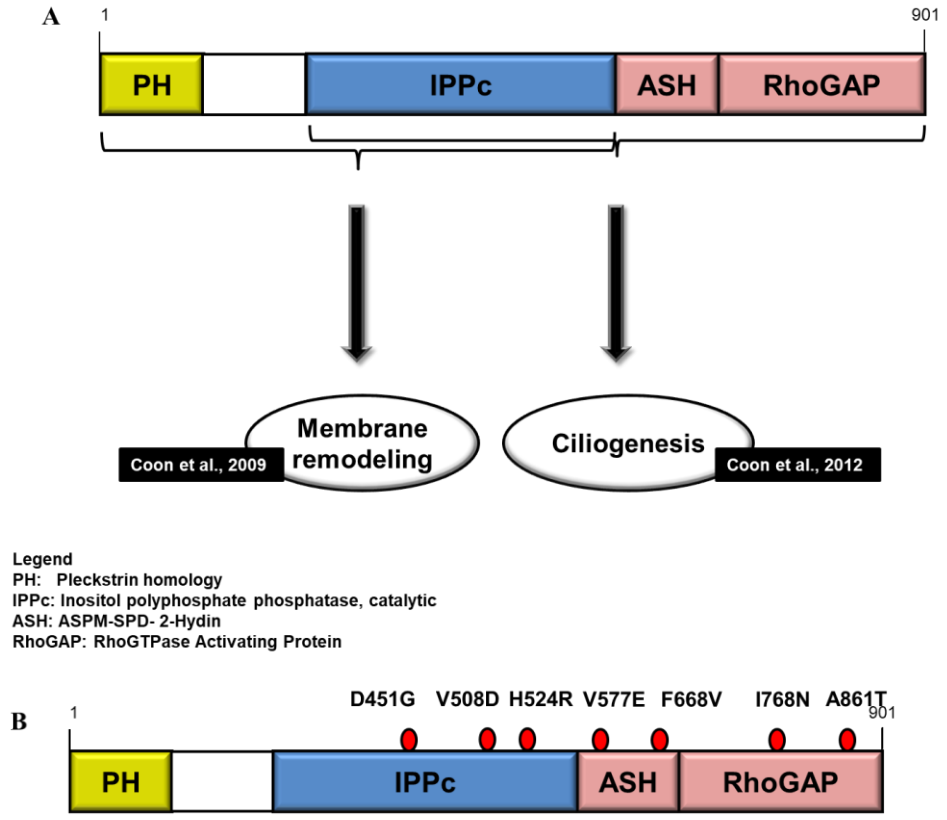


**Figure 3.1 Dual function of Ocrl1 and mutations used in the study**

A: Ocrl1's function in cellular processes is spatially segregated across its different protein domains. B: LS mutations tested in this study mapped on the different Ocrl1 domains they affect.

### 3.3.1 Ocrl1 mutants differentially affect cell spreading and ciliogenesis in kidney epithelial cells

Since renal failure is the cause death in LS patients, we reasoned that it would be critical to determine how patient genotype may affect processes that were critical for renal function. Therefore, we used human embryonic kidney (HEK) epithelial cells lacking *OCRL1* (HEK KO) and selected cell spreading and ciliogenesis as cellular readouts.

Spreading

We transfected the different GFP-tagged WT Ocrl1 or mutants in HEK KO cells and performed standard spreading assays as described before (Coon et al., 2009) and in materials and methods. Briefly, 18h after transfection, cells were lifted and allowed to attach and spread for 30min on fibronectin-coated coverslips. After 30 min of attachment and spreading, cells were fixed with 4% formaldehyde, stained with rhodamine-phalloidin to label the actin cytoskeleton. Random fields with transfected cells were imaged using Zeiss inverted epifluorescence microscope with a 40X objective. Spreading area was measured using magic wand tracing tool in ImageJ and statistical analysis were performed as described in materials and methods.

We found that all phosphatase domain mutants exhibited a smaller cell spreading area compared to $Ocrl1^{WT}$ (Fig.3.2). Due to the comparison of multiple mutants with $Ocrl1^{WT}$ in the KS test, a Bonferroni correction was applied which concluded that a p value $< 0.0167$ to be the accurate significance value (see Materials and methods). The mutants were all significantly affected for cell spreading. Interestingly, though mutations in the phosphatase domain resulted in defects in cell spreading, we also observed a diverse range of severity in the spreading phenotype within mutations affecting one domain. For instance, unlike $Ocrl1^{D451G}$ and $Ocrl1^{H524R}$, $Ocrl1^{V508D}$ was only modestly affected for spreading (~10% reduction in median spreading area compared to WT) (Table 3.1).

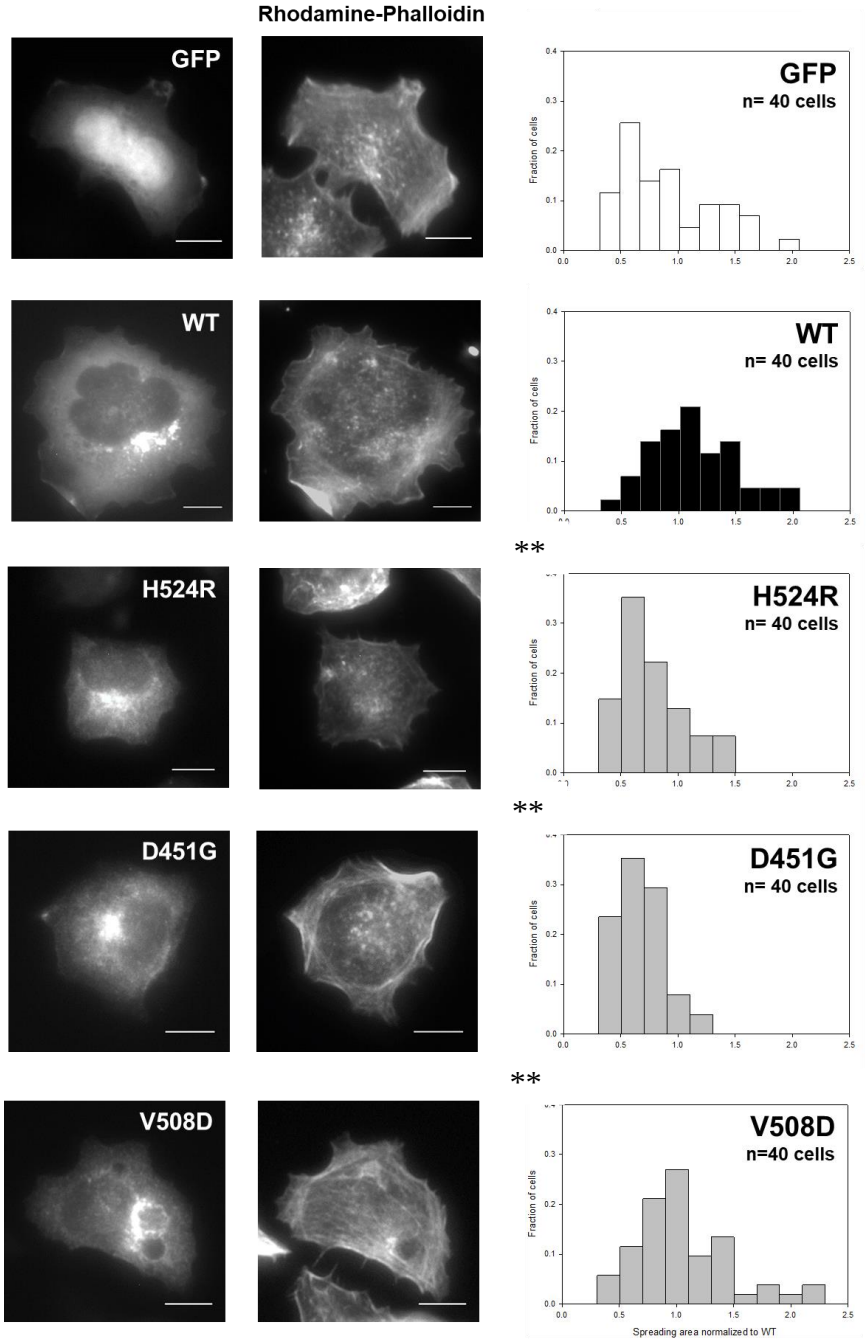


**Figure 3.2 Ocrl1 phosphatase domain mutants are differentially impaired for cell spreading activity.**

HEK KO cells transfected with different Ocrl1 phosphatase mutants were allowed to attach and spread on fibronectin-coated surfaces (See materials and methods). Histograms are from a single representative experiment, n=40 cells. Experiments were repeated at least 3 times, with a total n=120-150 cells. Example of stained cells representative of the high frequency groups within each histogram. Scale bar: 10µm. **p<(0.05/3=0.0167) (Bonferroni correction) using KS test.

**Table 3.1 Statistical analysis of cell spreading in cells expressing Ocrl1$^{WT}$ vs. phosphatase mutants**

| KS test | | |
|---|---|---|
| | **Median** | **p value** |
| **WT** | 1 | |
| **H524R** | 0.67 | <0.0167 |
| **D451G** | 0.79 | <0.0167 |
| **V508D** | 0.91 | <0.0167 |

Based on our demonstration that the ASH-RhoGAP domains of Ocrl1 is not involved in membrane remodeling (Coon et al., 2009), we expected mutations affecting the C-terminus (ASH-RhoGAP) domains to not impact cell spreading processes. Unexpectedly, all ASH-RhoGAP mutants Ocrl1$^{V577E}$,Ocrl1$^{F668V}$,Ocrl1$^{I768N}$ and Ocrl1$^{A861T}$ demonstrated a trend to exhibit smaller spreading area (Fig.3.3, Table 3.2) though it was not statistically significant. Overall, ASH-RhoGAP mutants showed a consistent cell spreading defect, though phosphatase mutants appeared to be more sensitive to this phenotype compared to the former.

Interestingly, we also noticed that the mutants Ocrl1$^{V577E}$,Ocrl1$^{F668V}$,Ocrl1$^{I768N}$ produced a distinct perinuclear punctate structure which was also investigated (Fig.3.3, yellow arrows; see next section).

**Figure 3.3 Ocrl1 ASH-RhoGAP domain mutants are modestly affected for cell spreading activity.**

HEK KO cells transfected with different Ocrl1 ASH-RhoGAP were allowed to attach and spread on fibronectin-coated surfaces (See materials and methods). Histograms are from a single representative experiment, n=40 cells. Experiments were repeated at least 3 times, with a total n=120-150 cells. Example of stained cells representative of the high frequency groups within each histogram. Scale bar: 10μm. **p<(0.05/4=0.0125) (Bonferroni correction) using KS test. Arrowhead indicates centriole accumulation (see Section 3.3.2)

Figure 3.3 continued

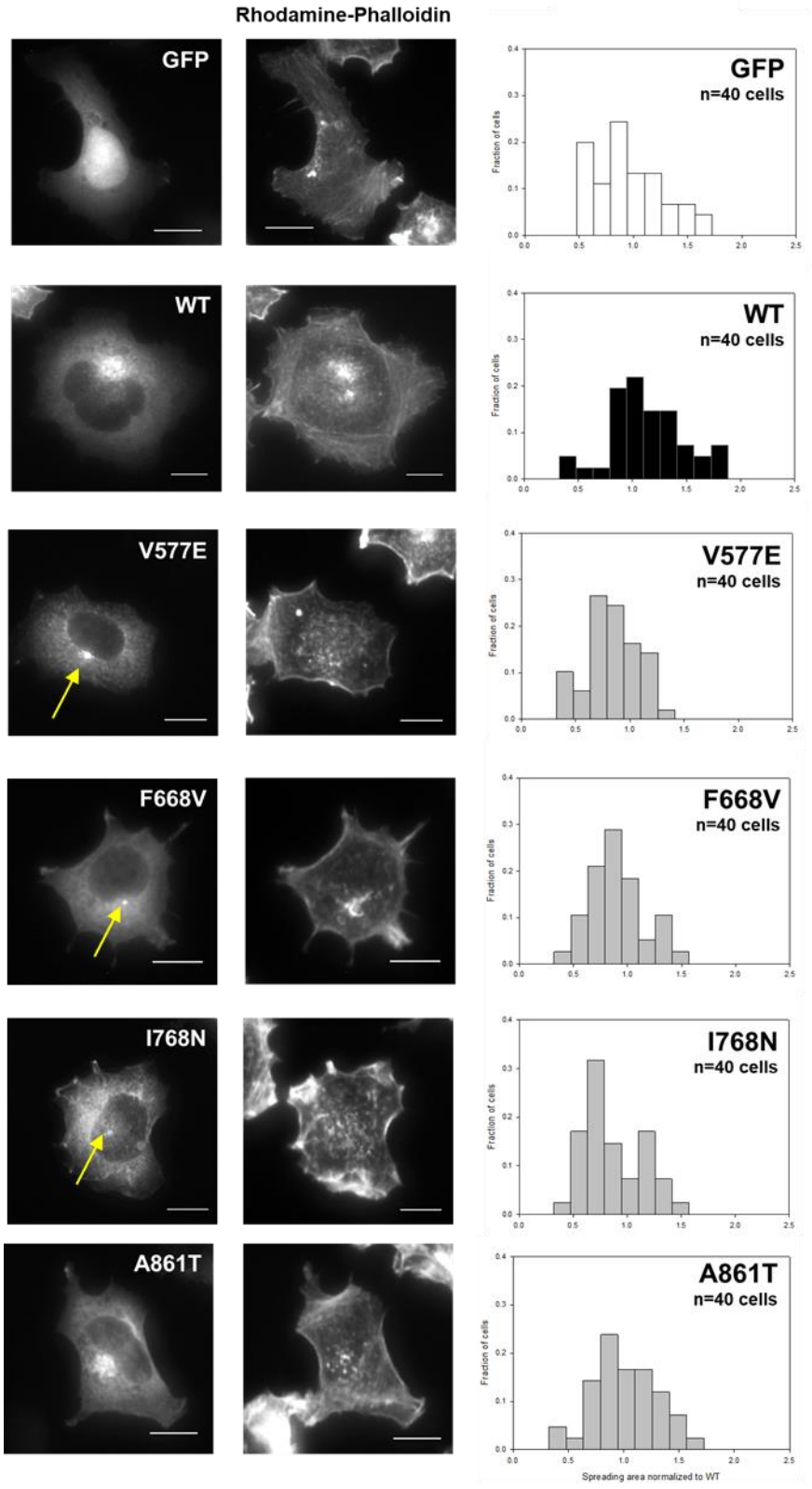

**Table 3.2 Statistical analysis of cell spreading in cells expressing Ocrl1$^{WT}$ vs. ASH-RhoGAP mutants**

| KS test | | |
|---|---|---|
| | **Median** | **p value** |
| **WT** | 1 | |
| **V577E** | 0.85 | <0.05 |
| **F668V** | 0.87 | <0.05 |
| **I768N** | 0.85 | <0.05 |
| **A861T** | 0.85 | <0.05 |

Ciliogenesis

We also tested the impact of Ocrl1 mutants on ciliogenesis by expressing them HEK KO cells. Cells were seeded at ~30-50% confluency, transfected with Ocrl1 mutants and ciliogenesis assays were performed as described previously (Coon et al., 2009). Briefly, 18h after transfection, cells were starved for 24h by replacing with 0.1% FBS media to induce ciliogenesis. Cells were fixed with 4% formaldehyde, followed by indirect immunofluorescence using antibodies against acetylated tubulin (to label primary cilia) and pericentrin-2 (to label centriole; base of cilium). Fields were randomly imaged using Zeiss Axiovert Inverted microscope using 40X objective.

The fraction of Ocrl1 mutant transfected cells forming a cilium was calculated and normalized to the fraction of cilia produced by Ocrl1$^{WT}$-expressing cells from the respective experiment (See materials and methods).

We predicted that LS mutations in phosphatase domain will affect ciliogenesis. Indeed, phosphatase mutants Ocrl1$^{H524R}$ ,Ocrl1$^{D451G}$ ,Ocrl1$^{V508D}$ were affected for ciliogenesis again in varying degrees (Fig.3.4). Ultimately, Ocrl1$^{H524R}$ ,Ocrl1$^{D451G}$ were significantly impaired for this phenotype, though Ocrl1$^{V508D}$ had a reproducible trend to produce fewer cilia than Ocrl1$^{WT}$.

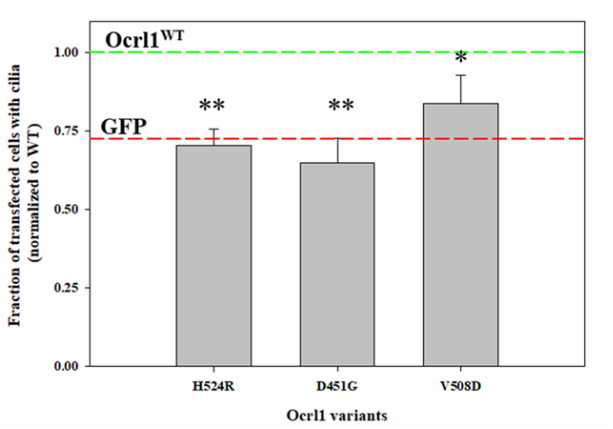


| Unpaired Student's t test | |
|---|---|
| | p value |
| WT | |
| H524R | <0.01 |
| D451G | <0.01 |
| V508D | <0.05 |

**Figure 3.4 Ocrl1 phosphatase domain mutants are differentially impaired for cilia formation.**

Ciliogenesis assays (see Materials and methods) were done with HEK KO cells transfected with different Ocrl1 phosphatase mutants. 20 random fields with at least 50 cells were imaged and fraction of transfected cells with cilia were calculated. This number was normalized to fraction Ocrl1WT cells forming cilia. Each experiment was repeated at least thrice (n=120-150 cells). Scale bar: 10µm. **p<(0.05/3=0.0167) (Bonferroni correction) using Student's t-test, *p<0.05. Red reference line represents fraction of Ocrl1$^{WT}$ expressing cells making cilia, green reference line represents fraction of GFP expressing cells making cilia.

Since Ocrl1's C-terminus was also required for ciliogenesis (Brian G. Coon et al., 2012), we expected that all the ASH-RhoGAP mutants would be affected for ciliogenesis. Mutants Ocrl1$^{V577E}$, Ocrl1$^{F668V}$ and Ocrl1$^{I768N}$ produced fewer cilia, though only Ocrl1$^{I768N}$ was significantly affected for ciliogenesis (Fig.3.5). On the other hand, Ocrl1$^{A861T}$ remained unaffected for cilia formation (Fig.3.5). Like the effect on cell spreading, we observed a trend for phosphatase mutants to have a more striking ciliogenesis defect, compared to mutants of C-terminus (Fig.3.2- 3.5).

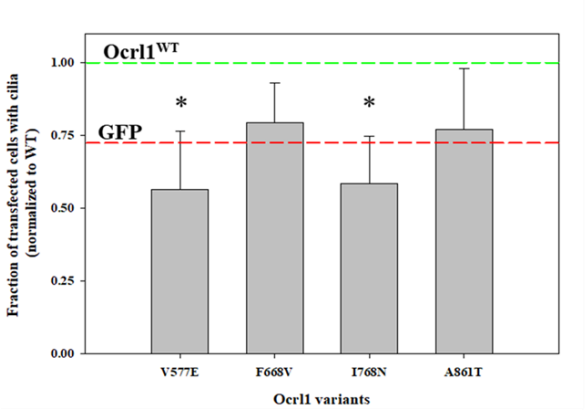


| Unpaired Student's t test | |
|---|---|
| | p value |
| WT | |
| V577E | <0.05 |
| F668V | 0.0597 |
| I768N | <0.05 |
| A861T | NS |

**Figure 3.5 Ocrl1 ASH-RhoGAP domain mutants are differentially impaired for cilia formation.**

Ciliogenesis assays (see Materials and methods) were done with HEK KO cells transfected with different Ocrl1 ASH-RhoGAP mutants. 20 random fields with at least 50 cells were imaged and fraction of transfected cells with cilia were calculated. This number was normalized to fraction Ocrl1WT cells forming cilia. Each experiment was repeated at least thrice (n=120-150 cells). Scale bar: 10µm. **p<(0.05/4=0.0125) (Bonferroni correction) using Student's t-test, *p<0.05. Red reference line represents fraction of Ocrl1$^{WT}$ expressing cells making cilia, green reference line represents fraction of GFP expressing cells making cilia.

### 3.3.2 Mutations affecting different domains result in unique mutant protein behaviors and novel cellular phenotypes specific to the domain

Centriolar accumulation

Transient expression of ASH-RhoGAP mutants Ocrl1V577E, Ocrl1F668V and Ocrl1I768N in HEK KO cells under nutrient-fed conditions (such as those maintained during cell spreading experiments) produced a characteristic perinuclear punctate structure (Fig.3.3, yellow arrows). Therefore, to better determine Ocrl1 localization in different cellular compartments we used human proximal tubule kidney (HK2) epithelial cells lacking *OCRL1* (HK2 KO). Unlike HEK cells, HK2 cells are larger in size and possess a flat morphology. This makes them more suitable to observe intracellular compartments. (All mutant-specific phenotypes validated in HK2 KO cells were also observed in HEK KO cells).

Similar to our observations in HEK KO cells, Ocrl1$^{V577E}$, Ocrl1$^{F668V}$ and Ocrl1$^{I768N}$ produced a punctate perinuclear structure in HK2 KO cells (Fig.3.6, yellow arrows & Ocrl1 panel inset).

Upon starvation, which results in ciliogenesis induction, Ocrl1 has been shown to localize transiently (~25% of the time) at the base of cilium for trafficking of ciliary cargo (Brian G. Coon et al., 2012). Even though the mutants produced this perinuclear punctate structure under steady

state conditions, given the proximity of the centriole to the region where the structure was found, we performed colocalization of these perinuclear dots with the centriole by co-staining cells with an antibody against pericentrin-2 (PC2), a marker of the centriole. We found that Ocrl1$^{V577E}$, Ocrl1$^{F668V}$ and Ocrl1$^{I768N}$ mutant-expressing cells exhibited higher colocalization of perinuclear dot with PC2 (Fig.3.6A&B). Under these conditions, we could not observe Ocrl1$^{WT}$ at the centriole, reiterating its transient localization at the organelle only under ciliogenesis conditions. Ocrl$^{A861T}$ behaved more like Ocrl1$^{WT}$ in that there was no significant observable enrichment at the centriole (Fig.3.6A&B).

Under steady state conditions, GFP by itself has been reported to diffuse into the centriolar space due to its small size (27KDa) (Verdier, Morthorst, & Pedersen, 2016). On the other hand, Ocrl1$^{WT}$ only localizes to this region upon induction of ciliogenesis (Brian G. Coon et al., 2012). The ASH-RhoGAP mutants however displayed a localization to this compartment that was greater than both Ocrl1$^{WT}$ and GFP indicating aberrant behavior. (GFP localization at centriole marked by red reference line in Fig.3.6B).

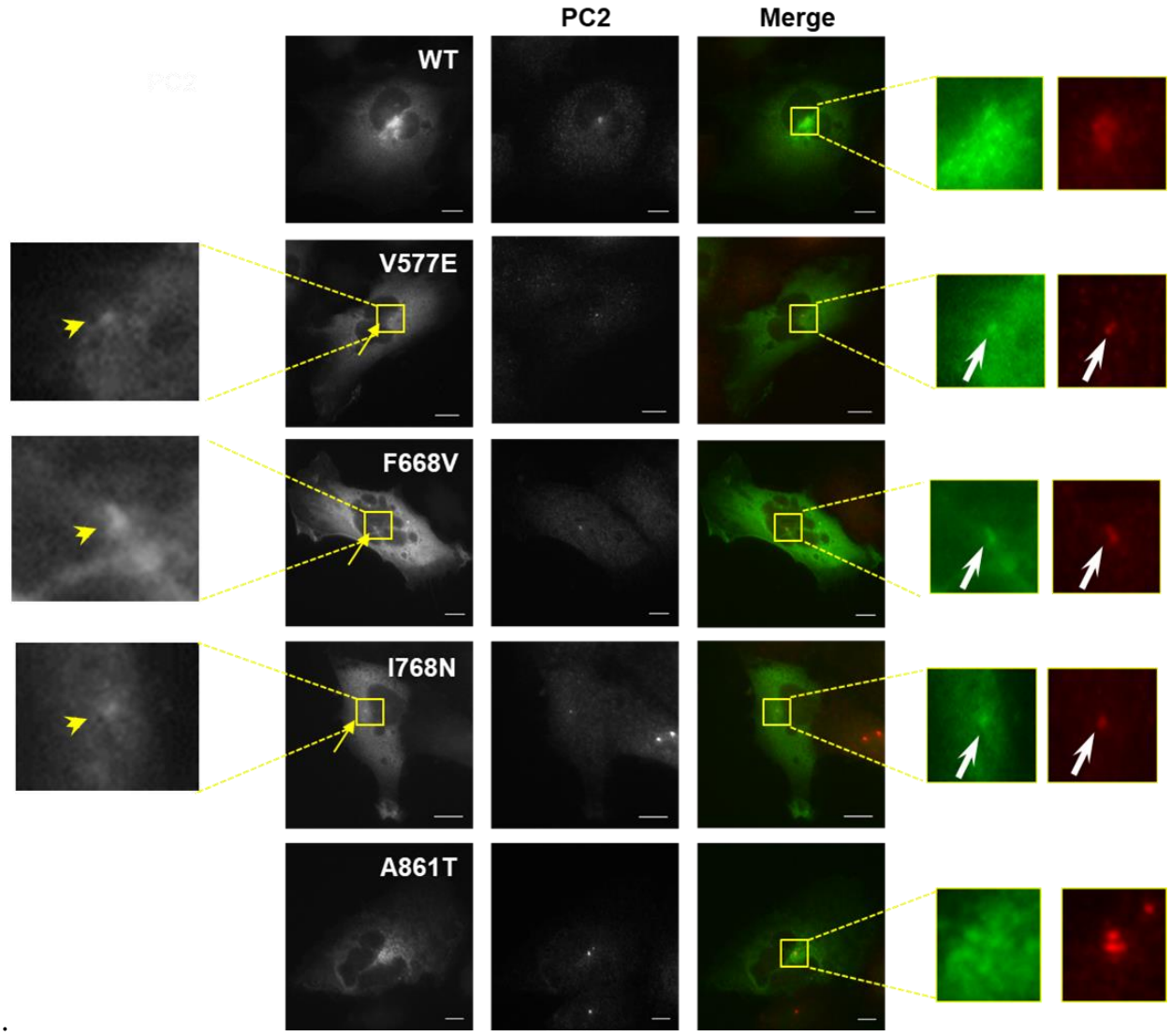


.

**Figure 3.6 ASH-RhoGAP domain mutants exhibit enrichment or accumulation at the centriole under steady state conditions.**

A: HK2 KO cells transiently expressing Ocrl1$^{WT}$ or ASH-RhoGAP mutants (left panel) immunostained for PC-2 (centriole marker; middle panel) (see materials and methods). Yellow arrows indicate Ocrl1 at PC-2 labeled structures. Scale bar: 10µm. B: Transfected cells were randomly imaged from at least 25 fields containing at least 40 cells. Cells with Ocrl1 colocalization to PC-2 were scored and fraction of cells exhibiting colocalization in a field was determined. **p<(0.05/4=0.0125) (Bonferroni correction), *p<0.05 using Wilcoxon test. Box plot of representative experiment. Red reference line indicates enrichment observed in GFP-transfected cells

Figure 3.6 continued

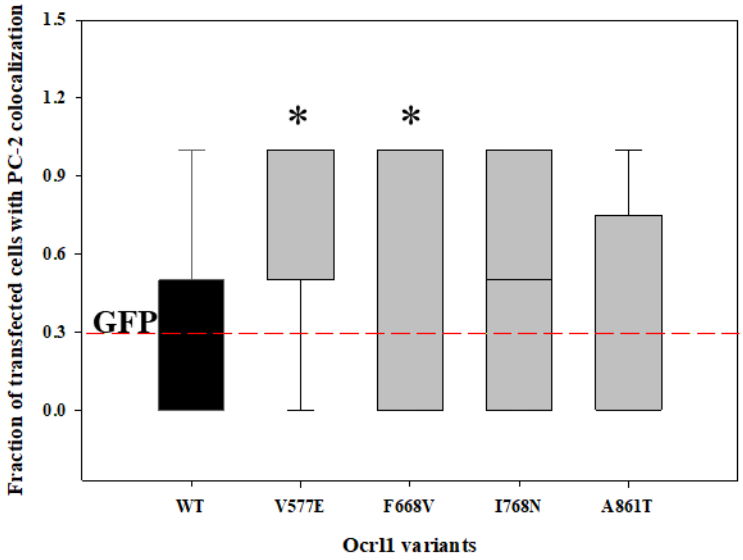


We also analyzed if this association with the centriole was a dose-dependent effect, created by transient overexpression of these mutants. We segregated transfected cells into 'low', 'medium' and 'high' fluorescence groups based on the minimum and maximum fluorescence of the entire population. Over 85% of the cells populated the 'low' fluorescence category indicating that levels of expression of all the mutants were similar. Independent of fluorescence intensity, mutants Ocrl1$^{V577E}$, Ocrl1$^{F668V}$ and Ocrl1$^{I768N}$ were localizing at the centriole (data not shown).

In addition to the centriolar enrichment, ASH-RhoGAP mutants Ocrl1$^{V577E}$, Ocrl1$^{F668V}$ and Ocrl1$^{I768N}$ had an overall diffuse cytosolic appearance in cells and lacked perinuclear TGN enrichment (Fig.3.6A). On the other hand, Ocrl1$^{A861T}$ had a perinuclear localization comparable to Ocrl1WT (Fig.3.6A). Higher levels of expression of all four mutants, compared to Ocrl1WT resulted in mutant protein aggregation (data not shown). Though this may not be representative of a physiological level of expression, it indicated that mutations in the ASH-RhoGAP domains are likely to affect overall protein stability and/or folding.

To recreate a more 'patient-like' scenario, we prepared HK2 KO cells stably expressing Ocrl1$^{I768N}$ (see Materials and methods) to see if the centriolar enrichment was recapitulated. Multiple attempts of producing cell lines stably expressing Ocrl1$^{I768N}$ were unsuccessful. Though we observed GFP-Ocrl1 positive cells in the first 7 days of antibiotic selection, none of them successfully produced clonal populations (even after 3 weeks of antibiotic selection) that could be

isolated and sub-cultured. Therefore, after multiple unsuccessful attempts to prepare these lines, we took an intermediate approach and prepared ‘quasi’ stables where 24h following transfection with plasmid encoding Ocrl1$^{I768N}$, cells were grown on coverslips and subject to antibiotic selection for up to a week. Following 7 days of antibiotic selection, coverslips were fixed and indirect immunofluorescence was performed using antibodies against PC2. Cells stably expressing Ocrl1$^{I768N}$ also showed centriolar accumulation of mutant as observed under transient expression conditions (Fig.3.7). Stable integration of Ocrl1$^{I768N}$ (presumably with lower copy numbers of plasmid) produced diffuse cytosolic distribution of the mutant, that lacked perinuclear enrichment (except centriole accumulation) and did not produce aggregates (Fig. 3.7). This was compatible with our observation of aggregates only under high levels of mutant protein expression.

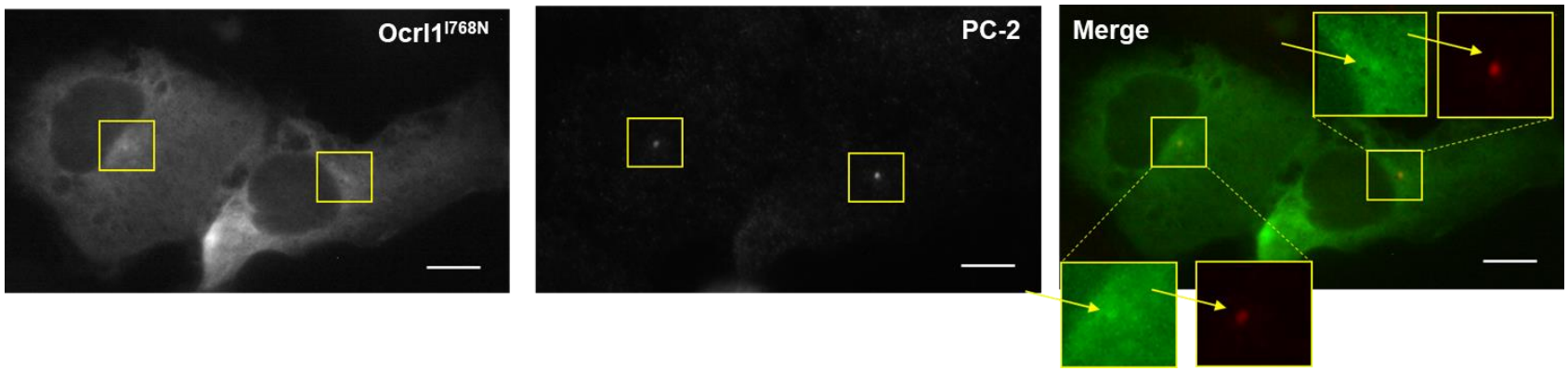


**Figure 3.7 Stable expression of Ocrl1$^{I768N}$ in HK2 KO cells also results in centriole accumulation under steady state conditions.** HK2 KO cells stably expressing Ocrl1$^{I768N}$ immunostained for PC-2 (centriole marker) (see materials and methods). Yellow highlighted region in merged images corresponding to the perinuclear region which was scaled to 2X (inset images) to better visualize Ocrl1 and PC2 colocalization. Yellow arrows indicate Ocrl1 at PC-2 labeled structures. Scale bar: 10µm.

TGN fragmentation

Besides defects in cell spreading and ciliogenesis, we had previously observed that Ocrl1$^{H524R}$ induced fragmentation of the *trans*-Golgi network (TGN) (Coon et al., 2009). This was seen in HeLa cells, as a dominant negative effect (Coon et al., 2009). Similarly, an Ocrl1 truncated variant lacking phosphatase domain also induced the same phenotype (R. Choudhury et al., 2005).

Since non-catalytic mutants (Ocrl1$^{D451G}$ and Ocrl1$^{V508D}$) induced ciliogenesis and cell spreading defects (although in varying degrees) like Ocrl1$^{H524R}$, we also tested their ability to produce TGN fragmentation. When compared to HK2 WT cells, HK2 KO cells themselves showed no TGN fragmentation (data not shown). But when they were transiently transfected with Ocrl1$^{D451G}$ or Ocrl1$^{V508D}$ TGN fragmentation was observed (Fig.3.8A,B). TGN fragmentation was quantified by measuring the area occupied by the TGN with respect to the whole cell area.

During transient transfections, cells often acquire multiple copies of the plasmid. This may result in cellular behaviors that are a consequence of overexpression. To test if this was the case, we also analyzed TGN fragmentation in transfected cells as a function of total fluorescence intensity and found no correlation between the two parameters (data not shown). This suggested that fragmentation of TGN was independent of the levels of mutant Ocrl1 expressed in cells. TGN fragmentation was accompanied by dispersed mutant Ocrl1 in the perinuclear region that colocalized poorly with TGN particles (see Fig.3.8A inset).

**Figure 3.8 Transient expression of phosphatase domain mutants produces TGN fragmentation.**

A: HK2 KO cells transiently transfected with $Ocrl1^{WT}$ (top panel) or $Ocrl1^{D451G}$ (middle panel) or $Ocrl1^{V508D}$ (bottom panel) and immunostained for TGN. Yellow highlighted region in merged images corresponding to the TGN area which was scaled to 4X (magnified image) to better visualize TGN fragmentation. Yellow arrowheads indicate fragmented TGN puncta that lack Ocrl1. White arrows indicate dispersed mutant Ocrl1 lacking TGN colocalization. Scale bar: 10µm. B: At least 40 transfected cells were imaged randomly, per experiment and area occupied by TGN was quantified (See materials and methods). Each experiment was repeated at least thrice with total n=120-150 cells/group. **p<(0.05/2=0.025) (Bonferroni correction) using Wilcoxon test.

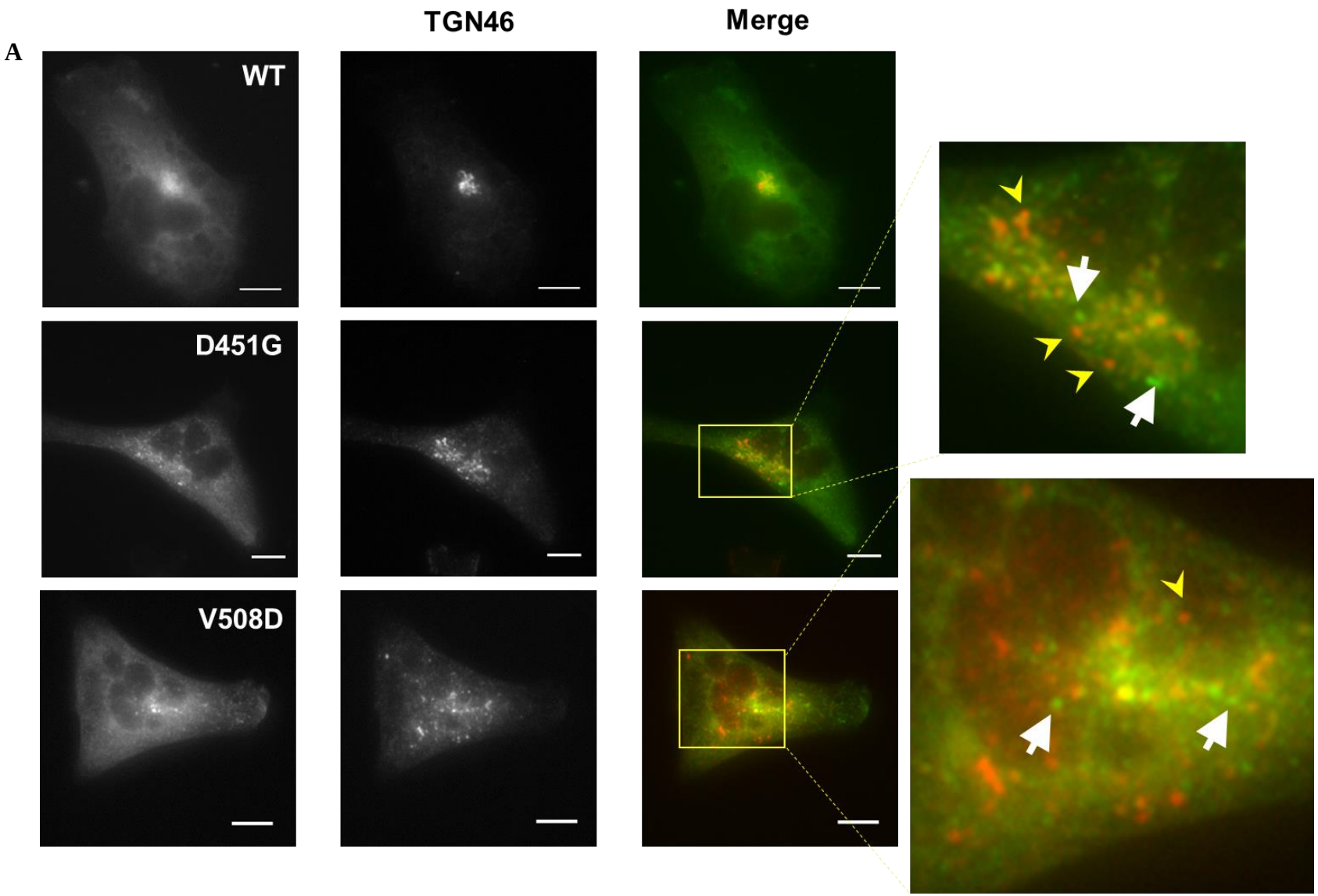
A
TGN46
Merge
WT
D451G
V508D

Figure 3.8 continued

**B**

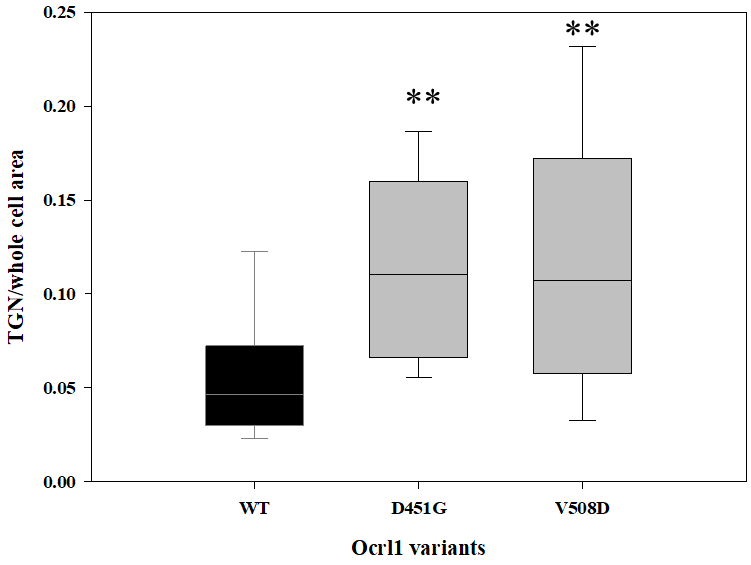


We also created stable HK2 KO cell lines (see Materials and methods) expressing Ocrl1$^{H524R}$ or Ocrl1$^{WT}$. In agreement with our previous observations using transient transfections, stable integration of Ocrl1$^{H524R}$ also led to TGN fragmentation. (Fig.3.9A,B). (Cells with stable plasmid integration were identified by the presence of GFP-tagged Ocrl1).

We also attempted to make stable HK2 KO cell lines expressing Ocrl1$^{D451G}$. Like Ocrl1$^{I768N}$, we could not isolate clones stably expressing Ocrl1$^{D451G}$. Therefore, we used a similar 'quasi' stables approach where 24h following transfection with plasmid encoding Ocrl1$^{D451G}$, cells were grown on coverslips and subject to antibiotic selection for up to a week. Following 7 days of antibiotic selection, coverslips were fixed and indirect immunofluorescence was performed using antibodies against TGN. All GFP-positive cells that survived antibiotic selection were imaged. We found that these 'quasi'-stable cells expressing Ocrl1$^{D451G}$ also showed significant TGN fragmentation (Fig.3.9A&B). Mutant Ocrl1 fragmentation was also recapitulated (data not shown). In both cell lines stably expressing Ocrl1 mutants, the average fluorescence intensity of cells was comparable and within a low and narrow range. These values were compatible with cells expressing low copy numbers of the plasmid. This is the closest we could recapitulate a patient-like scenario, although the exact levels of expression of these two mutants in actual patients bearing these mutations is unknown.

In summary, though we did not observe significant TGN fragmentation in HK2 KO cells, three different phosphatase domain missense mutations, when expressed transiently or stably in cells lacking Ocrl1 produced TGN fragmentation. These results also suggested that presence of some mutants may induce phenotypes that may be more severe than those produced when Ocrl1 is absent.

Golgi fragmentation has been associated with many other neurological disorders including Alzheimer's disease, Parkinson's disease, Huntington's disease, amyotropic lateral sclerosis (ALS), Angelman syndrome, spinal muscular atrophy and epilepsy (Ayala & Colanzi, 2017; Bexiga & Simpson, 2013; Caracci, Fuentealba, & Marzolo, 2019; Martínez-Menárguez, Tomás, Martínez-Martínez, & Martínez-Alonso, 2019). Given that LS patients have neurological symptoms, (Mario Loi, 2006), we envisioned that this cellular defect may be relevant to disease pathogenesis.

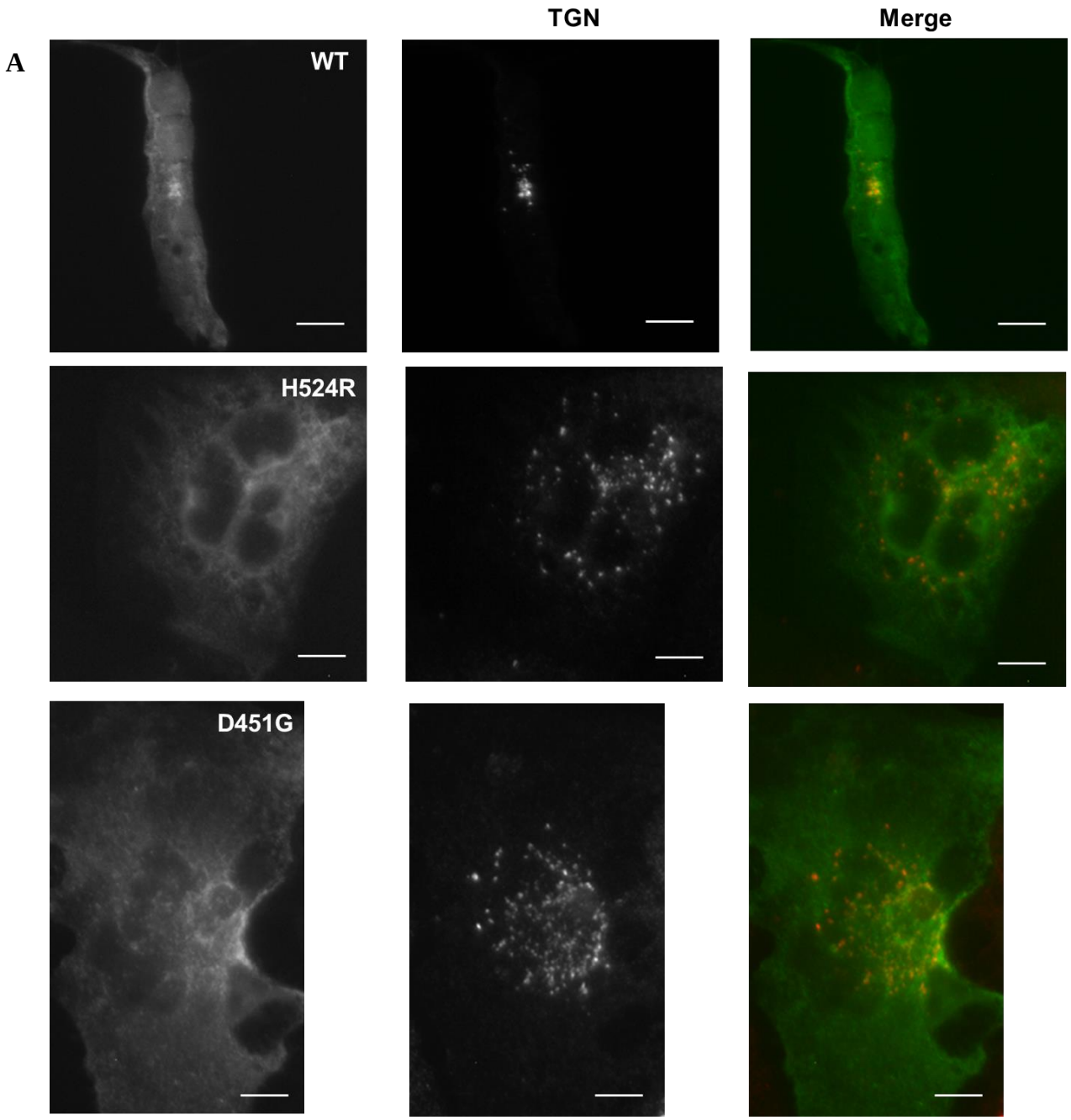


**Figure 3.9 Stably expressed phosphatase domain mutants also induce TGN fragmentation.** A: 'Semi' stable HK2 KO cell lines expression Ocrl1$^{WT}$ (top) or Ocrl1$^{H524R}$ (middle) or Ocrl1$^{D451G}$ (bottom) (see materials and methods) were prepared. All cells stably expressing Ocrl1 variants were imaged and TGN area was quantified (see materials and methods). Scale bar: 10μm. B: TGN fragmentation determined as a function of total cell area. **p<(0.05/2=0.025) (Bonferroni correction) using Wilcoxon test.

Figure 3.9 continued

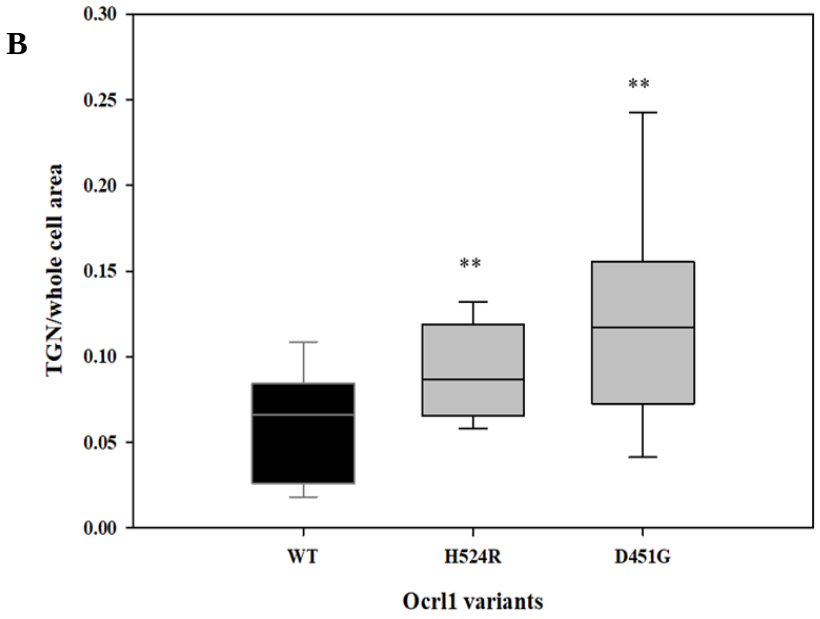


### 3.3.3 Subset of *OCRL1* mutations affecting phosphatase domain likely cause a conformational change in catalytic domain of mutant protein

So far, two out of the three phosphatase domain mutations we tested map to residues that are not essential for phosphatase activity. However, they all produced cellular defects that are linked to lack of phosphatase activity. In order to better understand how three different mutations within the phosphatase domain result in similar cellular phenotypes, we first mapped the mutations within the phosphatase domain (Fig.3.10A).

The phosphatase domain contains 6 conserved motifs essential for 5' phosphatase activity (Jefferson & Majerus, 1996; Tsujishita et al., 2001; Whisstock et al., 2000), as well as other conserved residues recently identified to also play a role in substrate binding as well as lipid chain interactions (Mills et al., 2016; Lionel Tresaugues et al., 2014) (Fig.3.10A, yellow and grey highlighted regions). The mutation H524R affects a critical residue that interacts with the scissile 5' phosphate (Mills et al., 2016; Lionel Tresaugues et al., 2014), and has been demonstrated to abolish phosphatase activity (Lin et al., 1997). On the other hand, D451G and V508D affect residues that are found outside the conserved catalytic motifs within the phosphatase domain, and yet were still affecting cellular functions of Ocrl1 (Fig.3.10A). We hypothesized that *these*

*mutations affected the conformation of the catalytic domain, thereby impairing phosphatase activity.*

Using 3-dimensional molecular dynamics, we modeled the two single residue changes D451G and V508D in the phosphatase domain of Ocrl1 (PDB ID: 4CMN) and our analysis predicted that these two mutations imparted conformation changes in critical catalytic residues. Particularly, D451G mutation was predicted to affect the conformation catalytic residues within and adjacent to the motif $^{421}$GDLNYR$^{426}$ and $^{495}$PAWCDRIL$^{502}$ (Fig.3.10B) while V508D was predicted to affect residues adjacent to the $^{522}$SDHKPV$^{527}$ motif (data not shown).

**Figure 3.10 Mapping and molecular dynamics of *OCRL1* missense mutations in the phosphatase domain.**

A: Mapping of all LS causing *OCRL1* missense mutations in the phosphatase domain, inset highlights location of mutations H524R, D451G and V508D. B: Molecular dynamics prediction of the effect of D451G mutation on Ocrl1 phosphatase domain structure. Ocrl1 phosphatase domain crystal structure (PDB ID: 4CMN) was used to run molecular dynamics simulations. WT (left) domain represented by stick model; blue color represents catalytic residues. Mutation of residue 451 Asp (D) to Gly (G) in this model (right, represented by orange shape fill) resulted in change in the position of catalytic blue residues (listed in white boxes) and acquired new position in red, resulting in overall conformation changes within the phosphatase domain. (Prepared by Dr. R. Claudio Aguilar)

**A**

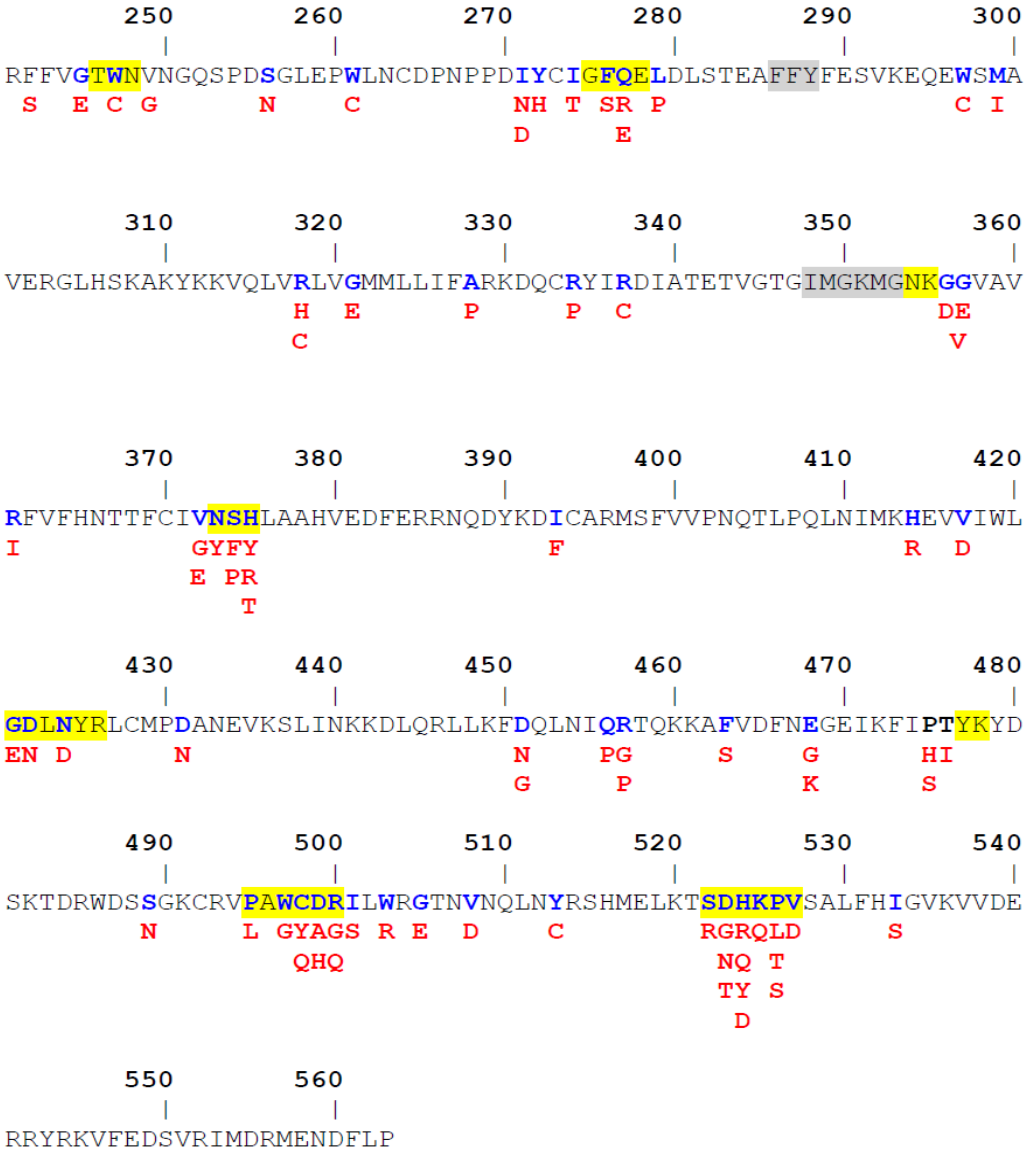


IPPc consensus motifs (Jefferson, et al. 1996, Whisstock, et al. 2000, Tsujishita, et al. 2001, Tresaugeus, et al. 2014, Mills, et al. 2016)

Lipid chain interacting motifs (Tresaugeus, 2014)

**Residues in blue mutated in Lowe Syndrome (LS), change indicated by residues in red**

IPPc- inositol polyphosphate phosphatase, catalytic

Figure 3.10 continued

**B**

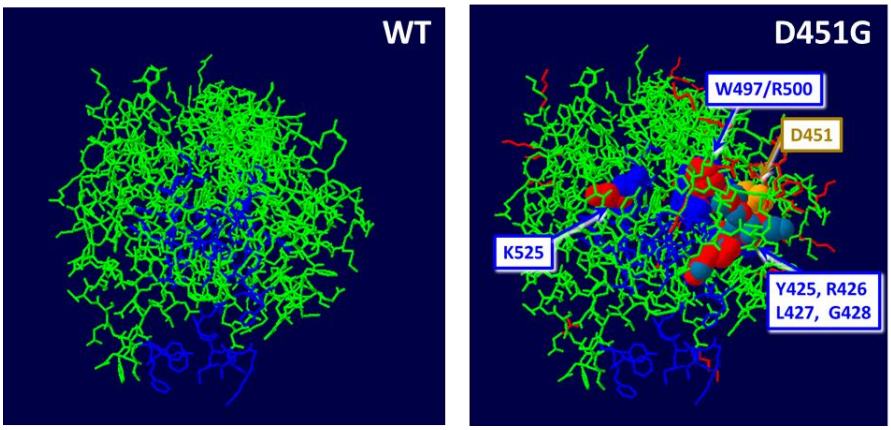


To determine if mutations D451G and V508D affected Ocrl1 phosphatase activity, we performed in vitro malachite green phosphatase assays (Materials and methods) using bacterially purified Ocrl1 catalytic mutants ($Ocrl1^{H524R}$, $Ocrl1^{D451G}$, $Ocrl1^{V508D}$) or $Ocrl1^{WT}$ that was fused to a glutathione S-transferase (GST) tag. $Ocrl1^{H524R}$, as expected lacked phosphatase activity (Fig.3.11, top right panel). Surprisingly, the other two mutants $Ocrl1^{D451G}$ and $Ocrl1^{V508D}$ also lacked enzymatic activity (Fig.3.11, bottom panel), thereby supporting our hypothesis and molecular dynamics predictions.

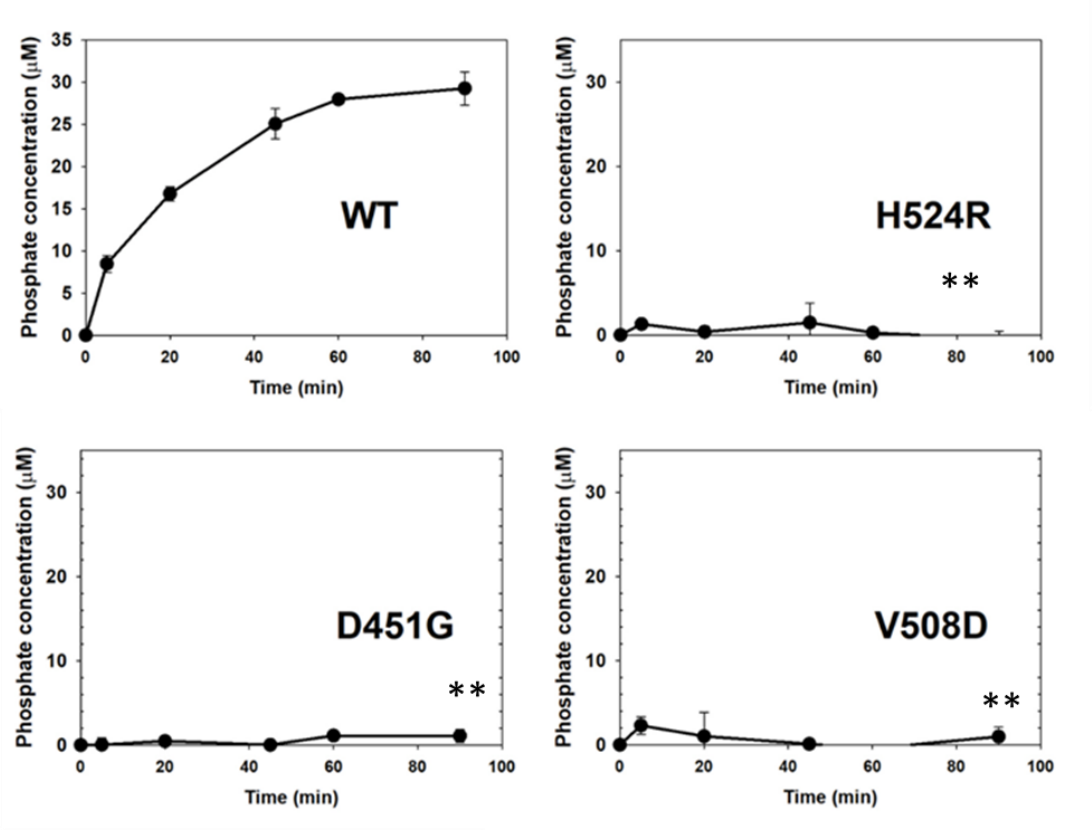


**Figure 3.11 Ocrl1 catalytic and non-catalytic phosphatase domain mutants are impaired for 5' phosphatase activity.**

Bacterially expressed GST-tagged Ocrl1 (amino acids 1-563; encoding PH and phosphatase domain); WT (top panel left) and the different phosphatase mutants were purified (See materials and methods). *In vitro* malachite green phosphatase assays were performed (See materials and methods). Standard curve for each experiment was prepared and free phosphate generated by Ocrl1 variants was calculated. Experiments were done with constant enzyme and substrate concentration, only varying the incubation times of enzyme and substrate (X-axis). All experiments were done in triplicates and repeated at least thrice. **p<(0.05/3=0.0167) (Bonferroni correction) using Student t-test.

Taking these results together with our molecular dynamics predictions, provided a potential mechanism underlying the lack of phosphatase activity in these mutants, thereby explaining the LS-specific cellular phenotypes we observed. Importantly, these findings now suggested that LS had a component of a 'conformational or misfolded protein disease'. A conformational disease is one where mutations in the gene lead to loss of function of the resultant mutant protein, either by affecting synthesis, transport stability, protein folding or its enzymatic activity (Kopito & Ron, 2000). This causes the accumulation of the non-native conformation, rendering loss in function

(Kopito & Ron, 2000). In fact, we mapped all known *OCRL1* missense mutations affecting the phosphatase domain and interestingly, found that ~50% of these mutations affect residues outside of the regions essential for catalysis within the domain (Fig.3.10A).

### 3.3.4 Subset of non-catalytic phosphatase domain mutants can regain cellular and biochemical function upon treatment with 4-phenyl butyric acid, a chemical chaperone

Some well-studied conformational diseases include cystic fibrosis (Kopito & Ron, 2000). In this disease, the gene *CFTR* (encoding a chloride channel) acquires a mutation that leads to the deletion of amino acid phenylalanine at position 508, resulting in CFTR ΔF508 mutant protein. This single mutation is found in almost 70% of the Caucasian patients (Rubenstein et al., 1997), resulting misfolded mutant CFTR protein and subsequent accumulation in the endoplasmic reticulum (ER) As a result, this chloride channel protein does not localize to the cell surface, resulting in partial function, poor regulation of fluid composition in the airway. This produces thick mucus and respiratory difficulties in patients (Rubenstein et al., 1997). Lowering the temperature (thermal stability) or treating with glycerol (a chemical chaperone) helped in releasing this mutant CFTR from the ER as well as restored its function (Rubenstein et al., 1997).

A chemical chaperone is a molecule that is either an osmolyte or a hydrophobic compound that interacts with a protein that is in its non-native conformation, thereby allowing it to fold and stabilize its native conformation (Cortez & Sim, 2014). 4-phenyl butyric acid (4-PBA) is a hydrophobic chemical chaperone that is currently used for treatment of cystic fibrosis (Cortez & Sim, 2014). In addition, it has also shown promise for other conformational diseases such as Parkinsons disease, Alzheimers disease and amylotrophic lateral sclerosis, sickle cell anemia (Cortez & Sim, 2014) and myopathies (C. S. Lee et al., 2017).

Based on the effectiveness of 4-PBA in other conformational disorders, we treated Ocrl1$^{D451G}$ or Ocrl1$^{V508D}$ transfected HK2 KO cells with either vehicle or 5mM 4-PBA (Rubenstein et al., 1997) and used TGN fragmentation as a read-out. Ocrl1-mutant expressing cells treated with 4-PBA had significantly reduced TGN fragmentation compared to vehicle-treated Ocrl1-mutant expressing cells. (Fig.3.12A,B). To determine if this rescue in TGN morphology was due to a direct effect on the phosphatase activity of mutant Ocrl1, we performed *in vitro* malachite green

assays using purified Ocrl1$^{D451G}$ incubated with 4-PBA and found that the drug was also able to restore phosphatase activity of the mutant in a dose-dependent manner (Fig.3.12C).

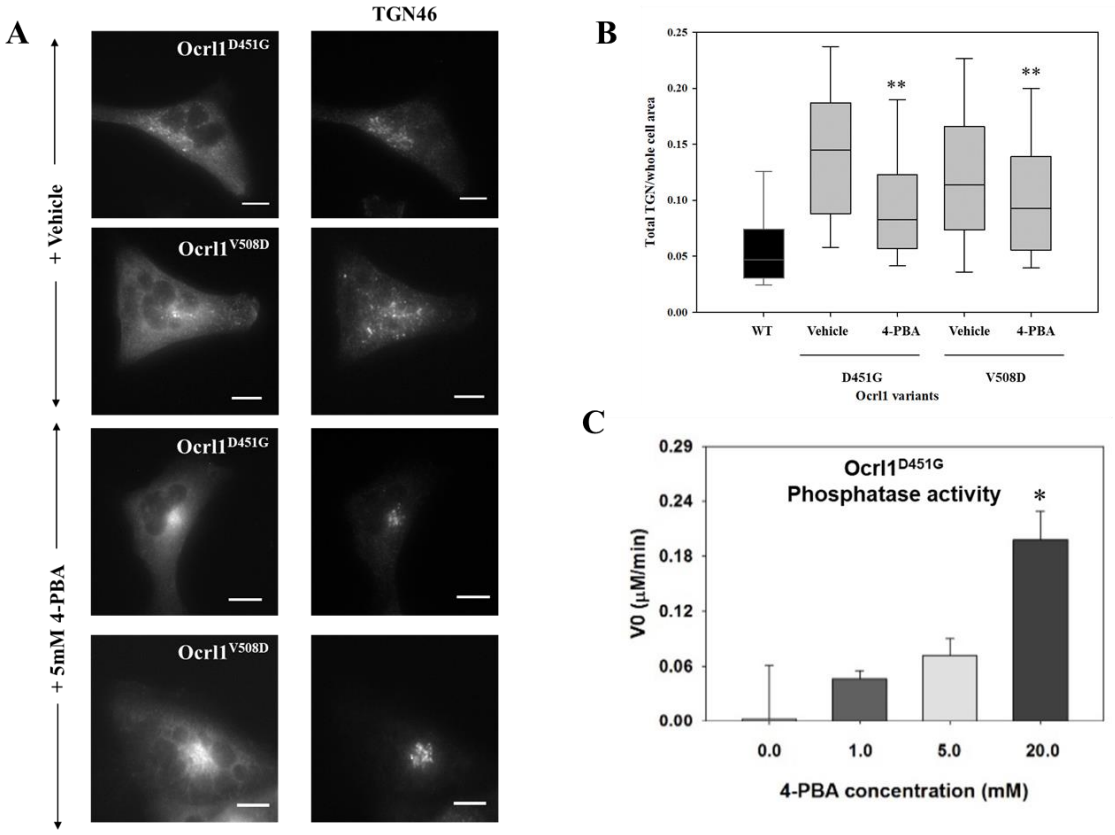


**Figure 3.12 4-phenyl butyric acid (4-PBA) reverts TGN fragmentation and restores 5' phosphatase activity in a dose-dependent manner.**

A: HK2 KO cells transiently transfected with Ocrl1$^{D451G}$ or Ocrl1$^{V508D}$ and treated with vehicle (top panel) or 4-PBA (bottom panel) and immunostained for TGN. Scale bar: 10µm. B: At least 40 transfected cells were imaged randomly, per experiment and area occupied by TGN was quantified (See materials and methods). Each experiment was repeated at least thrice with total n=120-150 cells/group. **p<(0.05/2=0.025) using Wilcoxon test. C: Bacterially purified Ocrl1$^{D451G}$ was incubated with different concentrations of 4-PBA and in vitro malachite green assays were performed. Each experiment was done in triplicates and repeated at least thrice. *p<0.05 using Student's t-test.

Together, these findings strongly suggested a new paradigm for LS pathogenesis- that is caused by '*conformational or misfolded proteins*' and that this phenomenon can be reverted by treatment with 4-PBA. Interestingly, similar to our findings, other studies have demonstrated that 4-PBA can rescue the function of select missense mutants of *BMPR2* and *MCT8* genes in diseases

such as pulmonary arterial hypertension (PAH) and Allan-Herndon-Dudley Syndrome respectively (D. Braun & Schweizer, 2017; Dunmore et al., 2020).

### 3.3.5 Lack of Ocrl1 PH domain results in protein mis-localization but sustains Ocrl1's C-terminus specific functions

As mentioned earlier, *OCRL1* mutations affecting the PH domain are less frequent in occurrence compared to other domains. (~10% of total LS causing mutations). Additionally, the nature of these mutations are mostly nonsense mutations, deletions or insertions that cause frameshift and result in premature truncations and splicing defects. (Bökenkamp & Ludwig, 2016; Hoopes et al., 2005; Shrimpton et al., 2009; Utsch et al., 2006).

However, mutations in *OCRL1* cause another disease called Dent-2 disease (OMIM #300555). Interestingly, majority of Dent-2 disease causing *OCRL1* mutations affect the PH domain (especially exons 2-7) and most of these mutations cause frameshift, resulting in deletions of 5' genomic regions, premature protein termination as well as splicing defects between exons 2-7 (Hichri et al., 2011; Utsch et al., 2006; Zaniew et al., 2018). In spite of the deleterious nature of the Dent-2 disease causing *OCRL1* mutations, Dent-2 disease is characterized by renal symptoms with little to no ocular and neurological involvement; and is therefore classified as a milder form of Lowe Syndrome (Bokenkamp et al., 2009).

Multiple studies have demonstrated phenotype heterogeneity between LS and Dent-2 disease (Cho et al., 2008; Hichri et al., 2011; Shrimpton et al., 2009; Utsch et al., 2006). It is speculated that the segregation of LS vs. Dent-2 disease causing mutations in *OCRL1* may indicate a genotypic correlation to phenotypes observed in patients. Shrimpton et al. (Shrimpton et al., 2009) proposed that premature protein termination within exons 2-7 which frequently seen in Dent-2 disease patients may lead to milder phenotypes if these patients were producing other Ocrl1 variants, whose translation was occurring from a site beyond this region. Using bioinformatic tools, methionine 187 (M187) within exon 8, received the highest score and was predicted a likely candidate as an alternative translation initiation site. In addition, verified cDNA clones encoding regions of Ocr1 (past exon 7) have also been detected, particularly in organs such as brain and eyes (Shrimpton et al., 2009). Taken together, these findings suggested that patients who may carry deletions or truncations that affect the PH domain may still be producing shorter Ocrl1 variants, particularly in brain and eyes that are translated from an alternative methionine (M187 being a

likely candidate) (Shrimpton et al., 2009). Since these variants will likely encode a functional phosphatase and ASH-RhoGAP domain, it may still be able to participate in a subset of cellular functions, thereby producing a milder phenotype only in some organs (Shrimpton et al., 2009). To date, no cellular studies have experimentally tested this hypothesis in cells.

Therefore, we prepared a GFP-tagged N-terminal (Ocrl1$^{\Delta PH}$) truncation variant of Ocrl1, translated from M187 but that lacks amino acids 1-186 (that includes the PH domain) (Fig.3.13). This served two purposes; on one hand, it would allow us to test whether functional product is being produced from M187. On the other hand, it would help better elucidate the role of the PH domain in Ocrl1's localization and function.

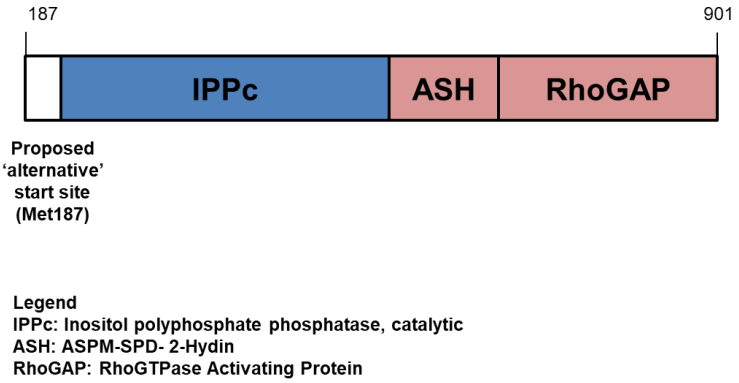


**Figure 3.13 Representation of the proposed alternative Ocrl1 transcript.**

Ocrl1$^{\Delta PH}$ localized to the TGN like Ocrl1$^{WT}$ but surprisingly, it was also enriched in the nucleus (Fig.3.14). Rab-mediated membrane targeting is predicted to be pivotal for Ocrl1's intracellular localization (Hou et al., 2011; Hyvola et al., 2006). Since this is likely preserved in this variant, it was surprising to observe the nuclear mis-localization of this Ocrl1 variant.

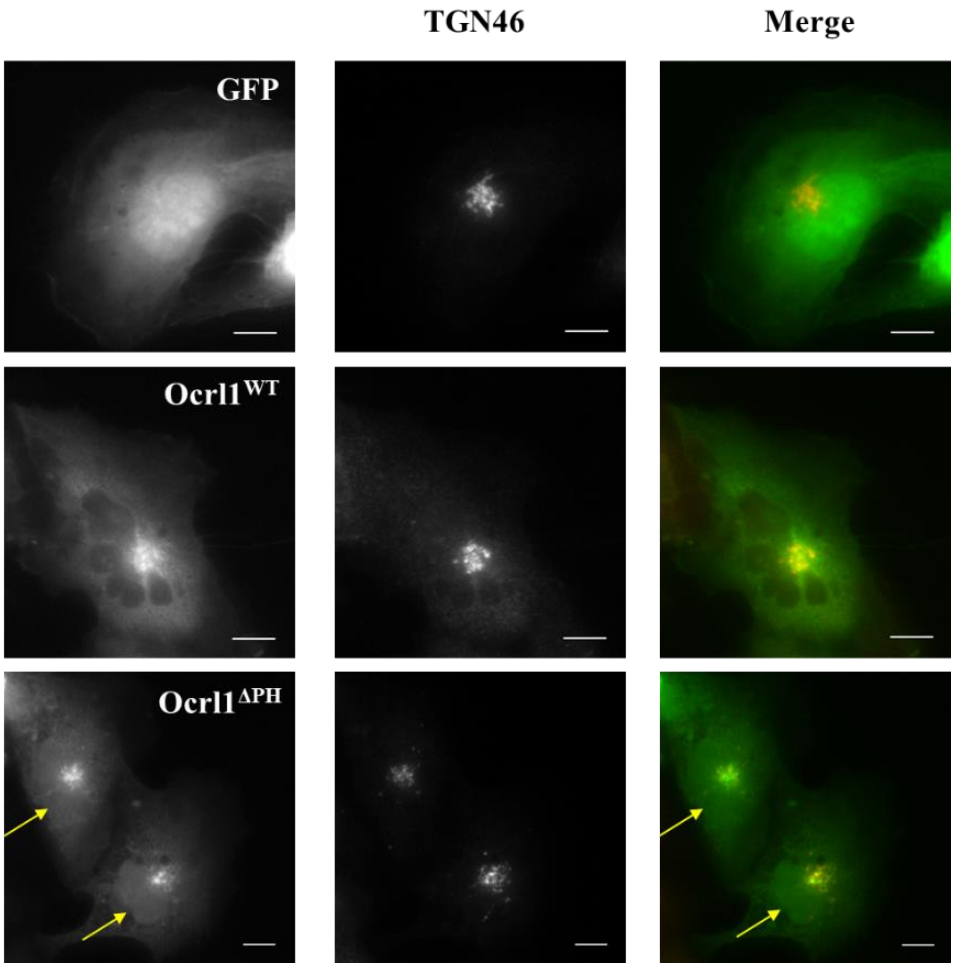


**Figure 3.14 Truncation of Ocrl1 PH domain results in nuclear mis-localization of protein.** HK2 KO cells transiently expressing GFP (top panel), Ocrl1$^{WT}$ (middle panel) or Ocrl1$^{\Delta PH}$ and immunostained for TGN (see materials and methods). Yellow arrows indicate Ocrl1$^{\Delta PH}$ enrichment in the nuclear compartment at PC-2 labeled structures. Scale bar: 10µm.

Next we tested the ability of Ocrl1$^{\Delta PH}$ to participate in cell spreading and ciliogenesis. In line with Ocrl1's N-terminus region being essential for spreading, Ocrl1$^{\Delta PH}$ showed a spreading defect (Fig.3.15). However, Ocrl1$^{\Delta PH}$ was unaffected for ciliogenesis (Fraction of transfected cells with cilia, normalized to Ocrl1WT: 1.05, $p<0.05$ Student's t test), not shown), that can be attributed to the presence of functional phosphatase and ASH-RhoGAP domains. These results suggested that a partially functional Ocrl1 variant can be produced from M187 that could sustain ciliogenesis, although it lacked the ability to facilitate cell spreading. In addition, the aberrant mis-localization of this variant to the nucleus suggested that the N-terminus may be also important for maintaining correct Ocrl1 localization in cells.

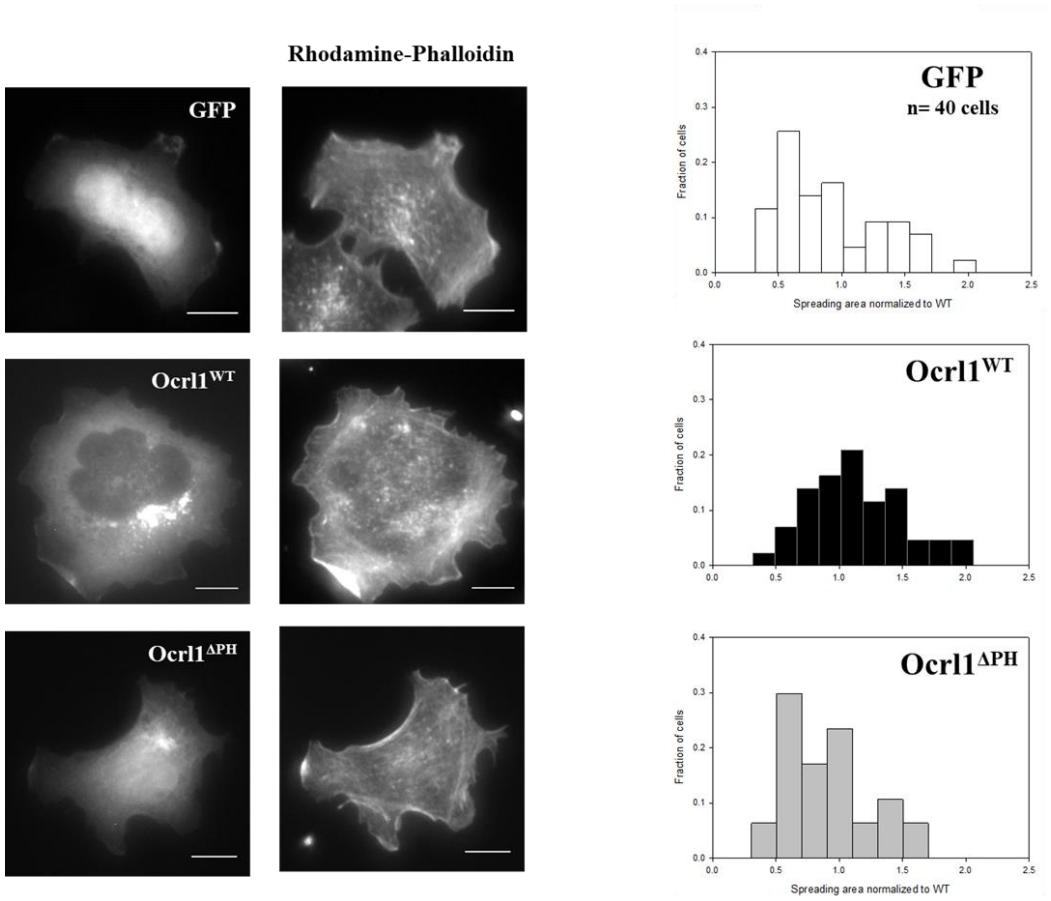


| KS test | | |
|---|---|---|
| | Median | p value |
| WT | 1 | |
| GFP | 0.86 | <0.01 |
| ΔPH | 0.81 | <0.01 |

**Figure 3.15 Ocrl1 PH domain truncation results in cell spreading defect.**

HEK KO cells transfected with GFP (top panel) or Ocrl1$^{WT}$ (middle panel) Ocrl1$^{\Delta PH}$ (bottom panel) were allowed to attach and spread on fibronectin-coated surfaces (See materials and methods). Histograms are from a single representative experiment, n=40 cells. Experiments were repeated at least 3 times, with a total n=120-150 cells. Example of stained cells representative of the high frequency groups within each histogram. Scale bar: 10µm. $p<0.05$ using KS test.

## 3.4 Discussion

In this study, we have found that Ocrl1 mutants differentially impact LS-specific cellular phenotypes namely cell spreading and ciliogenesis. However, contrary to the expectation that only those processes will be impaired, that were associated with the domain affected by the mutation, we found that almost all mutants were producing both spreading and ciliogenesis phenotypes in varying degrees. We also determined that mutants exhibited diverse behaviors in terms of

intracellular localization, protein stability and in some cases produced domain-specific phenotypes. We reasoned that these unique characteristics will influence the role of mutant Ocrl1 in triggering LS cellular and patient phenotypes.

Specifically, we found that ASH-RhoGAP mutants were predominantly diffuse and cytosolic, lacking the WT-typical perinuclear enrichment. For these variants we also observed aggregates with dose-dependent abundance. Indeed, mutations affecting this domain are predicted to be destabilizing in nature, resulting in misfolded and/or degraded products (McCrea et al., 2008; Pirruccello & De Camilli, 2012). Consequentially, this may either result in degradation or aggregation of mutant Ocrl1. Ultimately, if the protein gets eliminated or remains as aggregates, it will fail to be present where it is needed (as observed by us), creating a scenario similar to having 'no Ocrl1'. This may explain why we observed a subtle yet consistent trend for these mutants to display cell spreading defects even though the ASH-RhoGAP domain is primarily involved for ciliogenesis (Brian G. Coon et al., 2012).

At the other end of the spectrum, we have an Ocrl1 predicted variant that lacks its N-terminal PH domain but bears all other regions. This Dent-2 typical variant will be able to undergo Ocrl1-Rab interactions, required for proper intra-cellular localization (Hou et al., 2011; Hyvola et al., 2006). Indeed, like Ocrl1$^{WT}$ this protein was enriched in compartments like TGN; however, we still observed nuclear mis-localization. These observations suggest that the eliminating the PH domain led to the loss of a previously unnoticed localization determinant, that allows the GFP-tag to aberrantly drag/mis-localize at the nucleus. This behavior is typical of free GFP (see Fig.3.14, top panel), but it is not observed in GFP-tagged Ocrl1$^{WT}$ where the protein's strong localization determinants overpower the tag tendency to accumulate in the nucleus. Indeed, this variant lacks the N-terminal region that contains the clathrin binding motif (CBM) as well as the AP2-binding site (ABS), indicating a possible role of clathrin and AP2 interactions for sustaining Ocrl1 localization. Alternatively, this may be revealing the presence of yet to be identified Ocrl1-interaction partners in the N-terminus that play a critical role in maintaining its cellular localization and must be actively pursued. This variant produced cellular phenotypes that were in agreement with the well demonstrated segregation of Ocrl1's functions across the protein domains, however we must consider if the mis-localization in any way contributed to some of the phenotypes in addition to the absence of the PH domain.

Other mutants localized to Ocrl1-specific compartments to some extent, but displayed a pattern significantly different from that of $Ocrl1^{WT}$. Proteins containing ASH domains (including Ocrl1) localize at the centriole and cilia (Ponting, 2006), indeed, is within this region that Ocrl1 contains Rab-binding sites (Hyvola et al., 2006) that during starvation (ciliogenesis-stimulating conditions) contribute to localization to and support the assembly of the primary cilia (Brian G. Coon et al., 2012; Hagemann et al., 2012). However, this enrichment of ASH-RhoGAP mutants at centriole occurred even under steady state conditions (which was not the case for $Ocrl1^{WT}$). Importantly, this was observed even in a Rab-binding mutant $Ocrl1^{F668V}$ suggesting that this phenomenon is likely related to unique properties these mutants may possess.

These mutants also produce aggregates at higher levels of expression. Though this may not necessarily be physiologically compatible, we observed a positive correlation in cells exhibiting aggregates and enrichment at centriole (data not shown). Interestingly, subunits as well as substrates of proteosomal complexes have also been demonstrated to be enriched at the centriole (Vora & Phillips, 2016). Given the proposed unstable nature of ASH-RhoGAP mutants, it is tempting to speculate that this enrichment we observed may be due to these misfolded or unstable proteins being targeted for degradation by the centriole-associated proteasome aka 'aggresome' (Johnston, Ward, & Kopito, 1998; Olzmann, Li, & Chin, 2008; Park et al., 2017) and must be experimentally tested. In fact, many other misfolded protein diseases, mutant protein enrichment has been observed in this compartment (Johnston et al., 1998; Park et al., 2017).

We must also consider the possibility that this aberrant enrichment may interfere with centriolar function. Centrioles serve as the microtubule organizing center a nucleation site for primary cilia, facilitate cargo trafficking to the cilia and participate in cell division (Madhivanan & Aguilar, 2014; Satir, Pedersen, & Christensen, 2010). Therefore, the likelihood of the mutant Ocrl1 accumulation contributing to the ciliogenesis defects observed with these variants cannot be ignored.

Unlike ASH-RhoGAP mutants, the phosphatase mutants (both catalytic and non-catalytic) did not show apparent signs of aggregation and appeared 'perinuclear'. However, they produced TGN fragmentation. A closer observation of phosphatase mutants also revealed that though they appeared like $Ocrl1^{WT}$, TGN fragmentation was often accompanied by dispersion of mutant Ocrl1 in this area and these Ocrl1 puncta colocalized poorly with TGN. This TGN phenotype, also observed in neurological diseases, may be extremely important for LS pathogenesis, given the

neurological component of LS. In addition, TGN fragmentation is often accompanied with dysfunction in the organelle including defects in secretion, trafficking and TGN-dependent post translational modifications (ex. Glycosylation) (Fan et al., 2008). Supporting this prediction, Ocrl1 deficiency has already been shown to cause trafficking defects in LS patient cells (R. Choudhury et al., 2005). In addition, there are also reports of LS patients exhibiting defects in synthesis of heparan sulfate, decreased urinary excretion and sulfation of glycosoamino glycans (Kieras, Houck, French, & Wisniewski, 1984; Wisniewski, Kieras, French, Houck, & Ramos, 1984) , all processes dependent on TGN function (Fan et al., 2008). Given that TGN fragmentation is specific to phosphatase mutants, it might be interesting to determine if the above clinical manifestations are only observed in patients with phosphatase domain mutations.

Besides TGN fragmentation, these mutants produced striking defects in cell spreading and ciliogenesis that was compatible with loss of phosphatase function which we confirmed. However, one of the most critical findings of this work is the conformational disease component of LS based on our analysis of the non-catalytic mutants Ocrl1$^{D451G}$ and Ocrl1$^{V508D}$. This finding now allows us to understand and explain LS pathogenesis from the conformational disease point of view. Second, it opens a new therapeutic avenue for LS, which is the use of chemical chaperones, like 4-PBA that are successful in other conformational diseases like cystic fibrosis (produced by misfolded CFTR protein) (Cortez & Sim, 2014).

In fact, out of the 80 unique missense mutations within the phosphatase domain of Ocrl1, ~50% of the mutations (including D451G and V508D) are affecting non-catalytic residues and yet produce LS. We are actively pursuing studies to expand our understanding of whether these other non-catalytic mutations may behave in a similar manner. Importantly, the ability of 4-PBA to restore Ocrl1 enzymatic activity as well as revert TGN fragmentation suggests that for a subset of LS patients who carry these (and similar) mutations, 4-PBA may allow them to restore the function of their endogenous Ocrl1 enzyme.

In summary, our data shows that mutations have a diverse impact on protein stability as well as localization; which may produce a diverse range of cellular phenotypes, including those unique to specific domains. This generates a considerable degree of heterogeneity in LS cellular phenotypes.

Another very interesting conclusion of this work is that (for reasons yet to be fully understood) in some cases mutated Ocrl1 variants could be worse that the absence of this protein.

Specifically, we found that some cellular phenotypes like TGN fragmentation and cell spreading appear to be more severe in the presence of mutants Ocrl1$^{D451G}$ and Ocrl1$^{H524R}$ (independent of levels of expression) when compared to the complete absence of Ocrl1. One hypothesis to explain these observations is that in addition to impairing cell spreading or TGN maintenance, these mutants may be sequestering other interaction partners in cells, which may contribute to the severity in the phenotypes. This may be yet another reason for cellular phenotype heterogeneity. Nevertheless, it needs to be determined if patients carrying these mutants indeed have specific or more severe clinical manifestations of LS compared to others.

The heterogenous behavior of mutants within a given domain, creates yet another level of complexity when we try to establish a correlation between the genotype and cellular phenotypes of LS. For instance, though Ocrl1$^{V508D}$ exhibited all phosphatase domain-specific defects, the phenotypes induced by this variant were milder in comparison to other mutants within the same domain. Similarly, Ocrl1$^{A861T}$, an ASH-RhoGAP mutant, for reasons unknown, produces only some phenotypes like spreading defects but retains its localization as well as participation in ciliogenesis.

Taking together the various aspects of heterogeneity the mutants presented with, we propose that even though Ocrl1's function is spatially segregated within the protein, we have demonstrated that mutations affecting these domains do not impact its function in the same manner (Fig.3.16). In addition to the domain affected by the mutation, we must consider

1. Effect of mutations on intrinsic properties of mutant Ocrl1 including stability, biochemical interactions and intracellular localization.
2. Mutations in *OCRL1* trigger diverse phenotypes, some of which are common to mutants across different domains, which some are unique to specific Ocrl1 domains.
3. Some phenotypes like TGN fragmentation are exacerbated in the presence of mutant Ocrl1 when compared to having no Ocrl1.

Therefore, the impact of *OCRL1* mutations on LS cellular phenotypes is a composite of all the above factors (Fig.3.16). This is the first study to provide compelling evidence for heterogeneity in LS cellular phenotypes. It is however imperative to keep in mind that how this links to LS patient symptom heterogeneity needs to be directly verified. Along with the vast cellular basis for heterogeneity, genetic modifiers as well as environmental factors may play a role in how these defects manifest in patients.

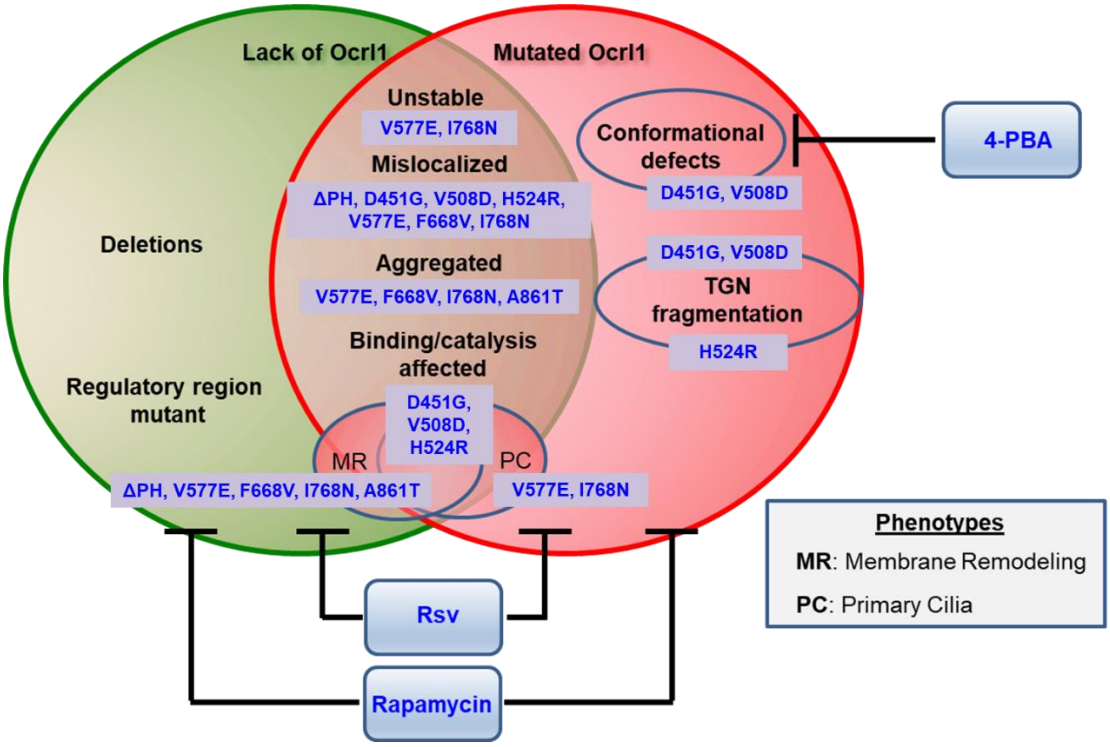


**Figure 3.16 Heterogenous consequences and cellular phenotypes produced by LS-causing *OCRL1* mutations.**

We have also recently identified 2 FDA- approved compounds statin and rapamycin that can revert LS-specific cell spreading (and other membrane remodeling) defects and cilia abnormalities respectively (Madhivanan et al., 2020). Importantly, we found that neither compound could correct the both phenotypes while combinatorial administration was able to rescue both spreading and cilia defects. This reiterates the dual and independent function of Ocrl1 in these two processes (Madhivanan et al., 2020). In addition, our results with 4-PBA provides an additional therapeutic candidate to consider. Therefore, based on our current findings with the different Ocrl1 mutants, we must take into account not just the domain affected by the mutation but also its impact on protein behavior, biochemical properties such as stability or conformation as well as tendency to trigger domain specific phenotypes in addition to other universal LS phenotypes before selecting a therapeutic strategy for LS patients.

## 3.5 Materials and methods

### 3.5.1 Reagents and constructs

All reagents were procured from Fisher Scientific (Fairlawn, NJ) or Sigma Aldrich (St. Louis, MO) unless stated otherwise. Antibodies used in this study are listed in Table 3.1. Site-directed mutagenesis (Agilent Technologies) was performed using pEGFP-c1 hs*OCRL1* (wild-type, isoform b) as template to create the various *OCRL1* constructs used in this study. Plasmid constructs used in this study are listed in Table 3.4.

### 3.5.2 Cells and culture conditions

Normal human proximal tubule epithelial (HK2) and human embryonic kidney epithelial 293T (HEK293T) cells were purchased from ATCC and cultured in DMEM, Streptomycin/Penicillin, 2mM L-Glutamine and 10% fetal bovine serum (FBS). Cells were maintained at 37 ºC in a 5% $CO_2$ incubator. *OCRL1*$^{-/-}$ (*OCRL* KO) HK2 and HEK293T cells were prepared by GenScript Inc. Piscataway, NJ, USA and maintained under identical conditions. Absence of Ocrl1 as well LS-specific phenotypes including cell spreading and ciliogenesis defects were validated in the KO cell lines (Hsieh et al., 2018; Madhivanan et al., 2020).

### 3.5.3 Preparation of stable cell lines

HK2 cells (and HK2 KO) have been immortalized using a plasmid encoding SV40 large T antigen than confers it resistance to G418 (ATCC). However, all plasmids encoding *hsOCRL1* utilize G418 to provide mammalian selection. To overcome the inherent G418 resistance HK2 KO cells exhibit, we co-transfected our plasmid of interest (encoding Ocrl1$^{WT}$ or Ocrl1 mutants) with pTre2Hyg-6XHis vector (uses Hygromycin for mammalian selection) which was used to select for cells that stably integrated plasmid. Plasmids were transfected at 4:1 DNA ratio (1.6µg plasmid of interest: 0.4µg selection plasmid). This was done to ensure that a fraction of cells expressing our plasmid will also express the selectable marker carrying plasmid. 24h after transfection, cells were treated with complete media containing 100µg/ml Hygromycin. Media was replaced every 48h with fresh media containing antibiotic. By 7 days of selection, we observed cells with stably integrated plasmid of interest (observed by GFP fluorescence). Within 2-3 weeks, colonies of stable clones (3/Ocrl1 variant) were identified and isolated using sterile cloning discs. These clones

were sub-cultured over multiple passages and TGN localization of Ocrl1 was confirmed by indirect immunofluorescence.

### 3.5.4 Drug treatments

HK2 KO cells were cultured and transfected as described above. Following transfection, cells were either treated with vehicle (sterile tissue culture grade water) or 5mM 4-phenyl butyric acid (4-PBA) (Millipore Inc, #567616) dissolved in DMEM+ 0.1% FBS media for 6h. For phosphatase assays done in the presence of 4-PBA, 0-20mM of 4-PBA was used.

### 3.5.5 Transfections

Plasmids encoding different Ocrl1 mutants were transfected using Fugene 6 reagent (Promega) according to manufacturer's instructions. Briefly, 4µl of Fugene 6 reagent was added dropwise to 200µl of DMEM media (free of serum and antibiotics) and incubated for 5min at room temperature. Then, 1µg of plasmid DNA was added to this mixture dropwise and incubated for 15min at room temperature to allow complex formation. This mixture was added dropwise to freshly plated cells. Cells were incubated with this mixture for 18h to allow for plasmid uptake and expression following which they were used for different assays.

### 3.5.6 Cell Spreading Assays:

Cells were transfected as described above and grown in complete media up to 18h. Cell confluency was maintained at ~50% to ensure single cell suspensions were obtained prior to spreading assays. 18h post transfection, 20mM EDTA (in 1XPBS) was used to lift cells, pelleted at 100xg for 5min and resuspended in fresh media. Cell suspensions were then set in a rotator for 1 hour before seeding them on 10ug/ml fibronectin-coated coverslips for 30min, undisturbed, to allow attachment and spreading. At 30min, coverslips were gently washed using 1X PBS and fixed in 4% formaldehyde for 10min at room temperature. Actin cytoskeleton were stained with rhodamine–phalloidin (used at 1:200) and imaged by epifluorescence microscopy. At least 40 cells were analyzed per experiment. The magic wand tool in ImageJ software was used to trace the cell boundaries and determine cell areas and perimeter.

In every experiment, spreading area of cells expressing Ocrl1 mutants was normalized to the median area calculated in Ocrl1$^{WT}$-expressing for that respective experiment. Histograms were constructed from the normalized spreading area values and Kolmogorov-Smirnov (KS) test was performed to determine statistical significance.

### 3.5.7 Ciliogenesis assays

Cells were seeded (in complete media) on glass cover slips coated with poly-D-lysine and transfected as described above. Confluency of cells was maintained in such a way that it did not exceed 50% at the time of cilia formation. 18h after transfection, the media was replaced by 0.1% serum DMEM (starvation media) for another 24h to induce ciliogenesis. Cells were washed with 1X PBS, fixed in 4% formaldehyde–PBS for 10min. Indirect immunofluorescence was performed using antibodies against acetylated tubulin antibody (to label cilium) and pericentrin-2 (PC-2; to label centriole) (refer to Table 3.3). 20 random fields, comprising of at least 50 cells were imaged for every experiment and repeated at least thrice.

From all the transfected cells imaged, the fraction of Ocrl1 mutant-transfected cells forming a cilium was calculated. This was normalized to the fraction of cilia produced by Ocrl1$^{WT}$-expressing cells from the respective experiment. The upper limit of fraction of ciliated cells was 1 (represented by HEK KO cells expressing Ocrl1$^{WT}$) while the lower limit of fraction of ciliated cell was 0.7 (HEK KO cells expressing Ocrl1$^{GFP}$). Though we observed variability between experiments, individual experiments were statistically significant.

### 3.5.8 Indirect immunofluorescence and fluorescence microscopy

In all immunofluorescence procedures, antibodies were diluted in DMEM media containing 10% FBS (blocking agent) and 0.1% saponin (permeabilizing agent). Primary antibodies were incubated for 1h at room temperature, washed 2X with PBS. Fluorescent molecule-conjugated secondary antibodies were incubated with cells for 45min in the dark, washed 2X with PBS. Cells were then stained using DAPI to label the nucleus and mounted on pre-cleaned glass slides using Aqua-PolyMount reagent (Polysciences). Following indirect immunofluorescence, coverslips were imaged with constant fluorescence exposure times using a 40X objective on Zeiss Axiovert

inverted microscope. Random fields were imaged to cover the entire coverslip. Exposure times were maintained consistent for all independent experiments.

### 3.5.9 Protein purification

The PH and phosphatase domain of wild-type hsOcrl1 (1-563 residues) was cloned in a pGEX-4T1 plasmid (Clontech) that contains an N-terminus glutathione S-transferase (GST) tag. Using site directed mutagenesis, missense mutations H524R, D451G and V508D were introduced. Plasmids were transformed in Rosetta (DE3) competent cells. Bacterial cultures were grown overnight at 37°C, in LB medium supplemented with 2.5% glucose, 1X ampicillin, and 1X chloramphenicol. The following day, cultures were expanded in super broth media containing 1X ampicillin and 1X chloramphenicol for 3h at 37 °C. Then, cultures were supplemented with 5% glycerol and 0.1 mM IPTG and incubated for 5h at 30 °C.

Cells were harvested by centrifugation (3,000g, 10 min), and pellets were stored at -80 °C until use. Cells were lysed in lysis buffer containing 200mM Tris (pH 7.4), 10% glycerol, 01.% Tween-20, complete EDTA-free protease inhibitor, 1 mg/ml lysozyme was added to resuspend prepared cell pellets. Cells were disrupted by sonication at 50% power for 3 sets of 33 pulses with 30 second breaks in between pulses. Cell debris was removed via centrifugation at 21,500g, 30 min, 4 °C. The supernatant was transferred to tubes containing glutathione resin (Pierce) and incubated at room temperature on a shaker (12rpm) for 2 hours. Beads were washed 4 times with lysis buffer (w/o protease inhibitor and lysozyme). Then, 100mM glutathione (pH 8.0) was added to the tubes containing supernatant and incubated at room temperature on a shaker (12rpm) for 2h to elute the protein. Supernatant (after centrifugation at 1,000g for 2 min) was loaded onto desalting columns (ThermoFisher Scientific, Zeba, 89891), centrifuged (1,000g, 2 min, acceleration: 5) and purified protein was obtained. Protein concentration was estimated using NanoDrop 1000 (ThermoFisher Scientific) and was used immediately for malachite green phosphatase assays.

### 3.5.10 Malachite green phosphatase assays

For phosphatase activity assays, the malachite green phosphate assay kit (Sigma-Aldrich, MAK307) was used. Briefly, in a 384-well plate, 10μl of 2μM of purified Ocrl1 (wildtype and

mutant) was incubated with drug or vehicle for one hour at room temperature, to obtain a final enzyme concentration of 1uM. After treatment,10μl of 50μM PI(4,5)$P_2$ diC8 (Echelon Biosciences, P-4508) was added to wells and incubated for 5 minutes at room temperature in the same buffer as the purified phosphatases, containing 200mM Tris, pH 7.4. To stop enzyme reaction, 20μl of 0.25X malachite green reagent was added to the reaction wells. After 20min of color development, absorbance was measured at 620nm. A standard phosphate curve was prepared (as per manufacturer's instructions) in the enzyme buffer solution to determine the amount of free phosphate released by the enzyme variants tested. Experiments were repeated at least three times and each condition was tested in triplicates. Student's t-test was used to determine statistical significance.

### 3.5.11 Statistical analysis

The Kolmogorov-Smirnov (KS) test was used to calculate statistical significance between spreading-distribution histograms. The student's t-test was used to evaluate the significance of differences of normally distributed samples (ex. for ciliogenesis experiments), while the Wilcoxon's test was employed when samples were non-normally distributed (ex. Estimation of TGN fragmentation and PC-2 colocalization). For all comparisons involving $Ocrl1^{WT}$ and Ocrl1 mutants, the Bonferroni's correction for multiple comparisons was performed whenever applicable [αC=p/n; n being the number of comparisons].

After carefully analyzing each data set distribution the most appropriate representation of data in each case was adopted. These representations included histograms and box plots as they allow to thoroughly examine the data distribution (Weissgerber, Milic, Winham, & Garovic, 2015). When the data presented a normal distribution, a bar graph with standard deviations was used to represent the data.

**Table 3.3 List of antibodies used in this study**

| Antigen | Host | Source | Dilution used and application |
|---|---|---|---|
| Acetylated-Tubulin | Mouse | Sigma Aldrich (6-11B-1) | 1:1000 (IIF) |
| Pericentrin-2 (PC-2) | Rabbit | Abcam (ab4448) | 1:300 (IIF) |
| TGN46 | Rabbit | Thermo Fisher (PA5-23068) | 1:400 (IIF) |
| IIF: Indirect Immuno-Fluorescence | | | |

**Table 3.4 List of plasmids used in this study**

| Construct name | Species | Vector | Source |
|---|---|---|---|
| GFP | | pEGFP-c1 | Clontech |
| $Ocrl1^{WT}$ | *Homo sapiens* (isoform b) | pEGFP-c1 | Coon et al. 2009 |
| $Ocrl1^{H524R}$ | *Homo sapiens* (isoform b) | pEGFP-c1 | Coon et al. 2009 |
| $Ocrl1^{D451G}$ | *Homo sapiens* (isoform b) | pEGFP-c1 | This study |
| $Ocrl1^{V508D}$ | *Homo sapiens* (isoform b) | pEGFP-c1 | This study |
| $Ocrl1^{V577E}$ | *Homo sapiens* (isoform b) | pEGFP-c1 | This study |
| $Ocrl1^{F668V}$ | *Homo sapiens* (isoform b) | pEGFP-c1 | This study |
| $Ocrl1^{I768N}$ | *Homo sapiens* (isoform b) | pEGFP-c1 | This study |
| $Ocrl1^{A861T}$ | *Homo sapiens* (isoform b) | pEGFP-c1 | This study |
| $Ocrl1^{\Delta PH}$ | *Homo sapiens* (isoform b) | pEGFP-c1 | This study |
| pTRe2HygZ | | pTRe2HygZ | Clontech |

# CHAPTER 4. CONCLUSIONS AND DISCUSSION

LS is a devastating congenital disease that currently has no cure. Through cell and animal-based models, we have been able to identify various LS-specific defects caused by the deficiency of the 5' phosphatase activity of Ocrl1. However, mechanisms underlying these phenotypes have not been studied.

This disease affects mainly the eyes, brain and kidney; however, other clinical manifestations such as dental and oral cysts, growth deformities, musculo-skeletal problems including scoliosis, as well as bone-related conditions such as osteopenia have also been observed (Bökenkamp & Ludwig, 2016; Mario Loi, 2006). In addition, patient symptom heterogeneity makes it a complicated disease to provide prognosis for. (Bökenkamp & Ludwig, 2016; Recker et al., 2013).

Nearly 300 *OCRL1* mutations have been identified to cause LS and they are distributed across the gene, although the regions encoding for the catalytic domain are more frequently found affected. Since there is genotypic and phenotypic heterogeneity, LS is a very complex disease. In order to determine if patient symptoms are related to the mutation harbored by the patient, we must determine the effect these mutations have on LS cellular phenotypes.

Ocrl1's participation in two key cellular processes- membrane remodeling and ciliogenesis has been shown to occur independently via the N-terminus and C-terminus of the protein respectively (Brian G. Coon et al., 2012; Coon et al., 2009). However, the phosphatase domain is essential for both processes (Brian G. Coon et al., 2012; Coon et al., 2009). Us and others have previously demonstrated that membrane remodeling defects are produced due to a RhoGTPase-signaling imbalance (Lasne et al., 2010; Madhivanan et al., 2012; Madhivanan et al., 2020; van Rahden et al., 2012). Now, we have identified mTOR signaling hyperactivation to be the underlying cause for ciliogenesis defects (Fig.4.1). Based on these findings, we have identified statins and rapamycin as two candidate compounds that can revert these signaling problems and the cellular phenotypes produced.

Importantly, we have discovered a RhoGTPase-dependent, previously unidentified cell adhesion defect in LS patient cells and proximal tubule kidney cells lacking Ocrl1 (HK2 KO). This consequentially causes abnormal focal adhesion arrangements and diminished resistance to fluid shear stress (Fig.4.1). This phenotype is relevant to renal as well as neurological functions (Essig & Friedlander, 2003; Robles & Gomez, 2006) and was rescued by treatment with statins.

The identification of mTOR hyperactivation also led us to monitor autophagy in Ocrl1-deficient cells (Fig.4.1). Despite the critical role autophagy plays in organs like brain and kidney (Damme, Suntio, Saftig, & Eskelinen, 2015; Takabatake et al., 2014), not much is known about the status of this process in LS. We observed defects in autolysosome morphology in HK2 KO cells that could be rescued by rapamycin treatment. mTOR hyperactivation and autophagy defects are observed in many other renal diseases such as Joubert syndrome and polycystic kidney disease (S. Hakim et al., 2016). Similarly, Rho hyperactivation has also been implicated in deterioration of renal function in diseases like polycystic kidney disease and nephrotic syndrome (Cai et al., 2018; Peng et al., 2008; Sharpe & Hendry, 2003).

We demonstrated that the nephrogenesis- related transcription factor Six2 was mislocalized in kidney cells derived from iPSCs obtained from LS patient cells (Hsieh et al., 2018). This transcription factor is important for maintenance and differentiation of kidney progenitor cells. Following a similar trend, preliminary evidence from the lab suggests that HK2 KO cells exhibit defects in Wnt signaling including hypersensitivity to Wnt agonists leading to increased apoptosis (unpublished data). Given the importance of Wnt signaling in nephrogenesis (Schmidt-Ott & Barasch, 2008), this may be very relevant to LS-related kidney abnormalities and must be pursued.

In summary the discovery of novel cellular deficiencies has expanded our understanding of LS, provided us with an expanded arsenal of theories to explain some of the LS patient symptoms (particularly deteriorating renal function). LS affects thousands of children but has no specific cure so far. Therefore, the identification of therapeutic candidates to counteract LS-specific cellular phenotypes is promising.

While majority of LS research has focused on determining cellular phenotypes produced in the absence of Ocrl1, many of the LS-causing *OCRL1* mutations result in the production of a mutated protein that is expressed in patient cells. The impact of these mutated protein products on cellular phenotypes and its consequences on patient symptoms is unknown. Based on previous studies in the lab (see Chapter 2), we hypothesized that mutations affecting N-terminus regions lead to severe impairment in cell spreading and mutations in the C-terminus will lead to ciliogenesis defects. On the other hand, mutations affecting the phosphatase domain will cause both defects.

Our results show that nearly all mutations trigger defects in both phenotypes. In addition, mutations affecting some domains also produce unique cellular phenotypes such as TGN

fragmentation. Depending on the nature and position of the mutations, patient variants are also differentially impacted for intracellular localization and stability. All of these collectively determine the functionality of the mutant (Fig.4.1). For example, most mutations in the ASH-RhoGAP domain tend to destabilize the protein, leading to misfolding or degradation (Pirruccello & De Camilli, 2012; M. Pirruccello, L. E. Swan, E. Folta-Stogniew, & P. De Camilli, 2011). Compatible with this, these mutants have a cytosolic distribution, lack TGN enrichment and tend to form aggregates at higher levels of mutant expression. This may lead to a scenario close to having "no Ocrl1". This may explain why mutations affecting the C-terminus may also produce spreading abnormalities.

Furthermore, these domain-specific phenotypes include TGN fragmentation (phosphatase mutants) and centriolar accumulation (ASH-RhoGAP mutants) (Fig.4.1). TGN fragmentation has been implicated in neurological diseases (Bexiga & Simpson, 2013); therefore, it is possible that this phenotype may also have a role in the neurological abnormalities observed in LS. It may also be valuable to determine if LS patients with phosphatase domain mutations display more severe neurological impairment.

TGN morphological defects may also affect functions such as trafficking, secretion and protein modifications and can be investigated. This phenotype was observed by us (with $Ocrl1^{H524R}$) (Coon et al., 2009) and another group (with an Ocrl1 variant lacking only the phosphatase domain) (R. Choudhury et al., 2005). Choudhury et al. (R. Choudhury et al., 2005) attributed the observation to defective endosome to TGN trafficking in the absence of functional Ocrl1. However, in LS patient and HK2 cells lacking Ocrl1, we do not observe TGN fragmentation This suggests that though the phenotype may be linked to the domain, it may not entirely be due to lack of activity.

On the other hand, while $Ocrl1^{WT}$ transiently localizes to the centriole upon ciliogenesis induction, it is absent from this region in steady state whereas ASH-RhoGAP mutants enrich at the centriole. This brings up many interesting questions. Is this aberrant localization facilitated by a localization determinant? Although proteins with ASH domain (including Ocrl1) tend to localize at the cilia, the absence of this phenomenon with $Ocrl1^{WT}$ suggests this is an unlikely possibility. Most mutations in the ASH-RhoGAP domain tend to destabilize the protein, leading to misfolding or degradation (Pirruccello & De Camilli, 2012). Compatible with this, these mutants have a cytosolic distribution, lack TGN enrichment and tend to form aggregates at higher levels of mutant expression. The centriole contains a proteosomal machinery, also called 'aggresome' that is known

to facilitate protein degradation (Kopito, 2000; Park et al., 2017). Taken together, it is possible that this enrichment is in fact, an indication of the unstable nature of these mutants. Whether this enrichment is the physiological consequence of proteosomal degradation needs to be determined. In addition, the effect of this phenotype on centriolar function must be considered. If this were to be true, this may contribute to the ciliogenesis defects we observe with these mutants.

Even within mutants, we observed varying degrees of impairments in cellular phenotypes. While we cannot explain these differences yet, a closer structural approach may allow us to frame hypotheses. Importantly, some phenotypes like TGN fragmentation were worse in the presence of mutants when compared to a complete absence of Ocrl1. This may speak to the varying severity of symptoms seen in patients.

Nonetheless, all the mutants we tested may have resulted in an impairment of cell spreading and ciliogenesis, however, the underlying mechanisms driving these phenotypes are likely to be different and depend on various other domain-specific attributes these mutants have.

A very exciting finding that has come out of this work is the possibility of LS having a component of conformational disease (Fig.4.1). This provides new directions for LS research. First, this expands our current understanding of the disease mechanism. Importantly, the use of 4-PBA, a chemical with conformational mutants reverted TGN fragmentation and enzyme activity. This is in agreement with our modeling data and is a promising therapeutic candidate for LS. Structural verification of our molecular dynamics data is necessary to determine what residues are affected. Further, the exact mechanism of 4-PBA chemical chaperone activity in this context needs to be thoroughly studied.

Overall, our results have allowed us to rationally identify and test three FDA-approved compounds as candidate LS therapies. In addition, we have reported and characterized new cellular abnormalities including cell adhesion, autophagy defects as well as TGN fragmentation that may bear a lot of relevance for organ function; particularly in kidney and brain tissue homeostasis. Typically, renal and neurological symptoms manifest early in LS and worsen with time. This indicates that Ocrl1 may be critical for early organ development as well necessary for maintaining homeostasis in these organs. Therefore, how these cellular defects may impact either of these processes can be followed up.

In LS patient cells lacking Ocrl1, we were able to rescue cellular phenotypes and the revert the underlying signaling deficiencies by treating with candidate compounds. The expression of

various Ocrl1 mutants also produces similar cellular phenotypes and this indicates that the underlying signaling deficiencies may be present. Since different mutants (belonging to the same as well as different domains) differentially impact a given phenotype, one can envision tailoring the choice and dose of drug, depending on the mutation. In addition, our studies have established a cellular basis for heterogeneity in LS, revealing that this is a very complex disease not just genotypically but also at the cellular level (Fig.4.1). As a first step towards this, we must test the efficacy of these candidates to rescue phenotypes in the context of various mutants. But extensive studies involving but not restricted to response, efficacy, toxicity and long-term effects must be performed before making such determinations.

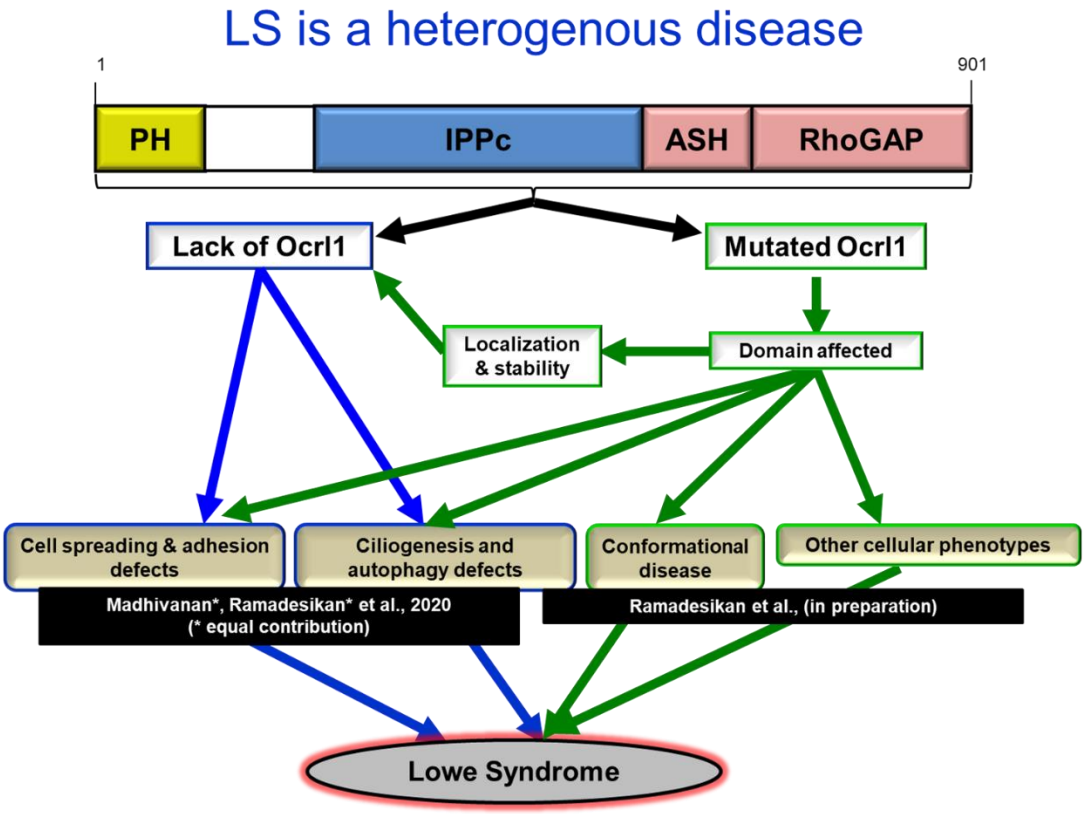


**Figure 4.1 Genotype-dependent heterogeneity in Lowe Syndrome cellular manifestations.**

# REFERENCES


A, B. Novel OCRL mutations in patients with Dent-2 disease.

Aggarwal, K. P., Narula, S., Kakkar, M., & Tandon, C. (2013). Nephrolithiasis: molecular mechanism of renal stone formation and the critical role played by modulators. *Biomed. Res. Int., 2013*, 292953. doi:10.1155/2013/292953

Agollah, G. D., Gonzalez-Garay, M. L., Rasmussen, J. C., Tan, I. C., Aldrich, M. B., Darne, C., . . . Sevick-Muraca, E. M. (2014). Evidence for SH2 domain-containing 5'-inositol phosphatase-2 (SHIP2) contributing to a lymphatic dysfunction. *PLoS One, 9*(11), e112548. doi:10.1371/journal.pone.0112548

Al-Awqati, Q. (2015). Kidney growth and hypertrophy: the role of mTOR and vesicle trafficking. *J Clin Invest, 125*(8), 2267-2270. doi:10.1172/JCI83542

Attree, O., Olivos, I. M., Okabe, I., Bailey, L. C., Nelson, D. L., Lewis, R. A., . . . Nussbaum, R. L. (1992a). THE LOWE OCULOCEREBRORENAL SYNDROME GENE ENCODES A PROTEIN HIGHLY HOMOLOGOUS TO INOSITOL POLYPHOSPHATE-5-PHOSPHATASE. *Nature, 358*(6383). doi:10.1038/358239a0

Attree, O., Olivos, I. M., Okabe, I., Bailey, L. C., Nelson, D. L., Lewis, R. A., . . . Nussbaum, R. L. (1992b). The Lowe's oculocerebrorenal syndrome gene encodes a protein highly homologous to inositol polyphosphate-5-phosphatase. *Nature, 358*(6383), 239-242. doi:10.1038/358239a0

Ayala, I., & Colanzi, A. (2017). Alterations of Golgi organization in Alzheimer's disease: A cause or a consequence? *Tissue Cell, 49*(2 Pt A), 133-140. doi:10.1016/j.tice.2016.11.007

Bae, Y.-K., Kim, E., L'Hernault, S. W., & Barr, M. M. (2009). The CIL-1 PI 5-Phosphatase Localizes TRP Polycystins to Cilia and Activates Sperm in C. elegans. *Current Biology, 19*(19), 1599-1607. doi:10.1016/j.cub.2009.08.045

Balla, T. (2013). Phosphoinositides: Tiny lipids with giant impact on cell regulation. *Physiological Reviews, 93*(3), 1019-1137. doi:10.1152/physrev.00028.2012

Barbieri, E., Di Fiore, P. P., & Sigismund, S. (2016). Endocytic control of signaling at the plasma membrane. *Curr Opin Cell Biol, 39*, 21-27. doi:10.1016/j.ceb.2016.01.012

Barnes, J., Salas, F., Mokhtari, R., Dolstra, H., Pedrosa, E., & Lachman, H. M. (2018). Modeling the neuropsychiatric manifestations of Lowe syndrome using induced pluripotent stem cells: defective F-actin polymerization and WAVE-1 expression in neuronal cells. *Mol Autism, 9*, 44. doi:10.1186/s13229-018-0227-3

Bertelli, D. F., Araujo, E. P., Cesquini, M., Stoppa, G. R., Gasparotto-Contessotto, M., Toyama, M. H., . . . Velloso, L. A. (2006). Phosphoinositide-specific inositol polyphosphate 5-phosphatase IV inhibits inositide trisphosphate accumulation in hypothalamus and regulates food intake and body weight. *Endocrinology, 147*(11), 5385-5399. doi:10.1210/en.2006-0280

Bertelli, D. F., Coope, A., Caricilli, A. M., Prada, P. O., Saad, M. J., Velloso, L. A., & Araujo, E. P. (2013). Inhibition of 72 kDa inositol polyphosphate 5-phosphatase E improves insulin signal transduction in diet-induced obesity. *Journal of Endocrinology, 217*(2), 131-140. doi:10.1530/joe-12-0562

Bexiga, M. G., & Simpson, J. C. (2013). Human diseases associated with form and function of the Golgi complex. *Int J Mol Sci, 14*(9), 18670-18681. doi:10.3390/ijms140918670

Bielas, S. L., Silhavy, J. L., Brancati, F., Kisseleva, M. V., Al-Gazali, L., Sztriha, L., . . . Gleeson, J. G. (2009). Mutations in INPP5E, encoding inositol polyphosphate-5-phosphatase E, link phosphatidyl inositol signaling to the ciliopathies. *Nat Genet, 41*(9), 1032-1036. doi:10.1038/ng.423

Billcliff, P. G., Noakes, C. J., Mehta, Z. B., Yan, G., Mak, L., Woscholski, R., & Lowe, M. (2016). OCRL1 engages with the F-BAR protein pacsin 2 to promote biogenesis of membrane-trafficking intermediates. *Mol Biol Cell, 27*(1), 90-107. doi:10.1091/mbc.E15-06-0329

Björkhem-Bergman, L., Lindh, J. D., & Bergman, P. (2011). What is a relevant statin concentration in cell experiments claiming pleiotropic effects? *Br J Clin Pharmacol, 72*(1), 164-165. doi:10.1111/j.1365-2125.2011.03907.x

Bohdanowicz, M., Balkin, D. M., De Camilli, P., & Grinstein, S. (2012). Recruitment of OCRL and Inpp5B to phagosomes by Rab5 and APPL1 depletes phosphoinositides and attenuates Akt signaling. *Molecular Biology of the Cell, 23*(1), 176-187. doi:10.1091/mbc.E11-06-0489

Bokenkamp, A., Bockenhauer, D., Cheong, H. I., Hoppe, B., Tasic, V., Unwin, R., & Ludwig, M. (2009). Dent-2 Disease: A Mild Variant of Lowe Syndrome. *Journal of Pediatrics, 155*(1), 94-99. doi:10.1016/j.jpeds.2009.01.049

Bokenkamp, A., Levtchenko, E., Recker, F., & Ludwig, M. (2015). Clinical utility gene card for: Lowe syndrome. *European journal of human genetics : EJHG, 23*(6). doi:10.1038/ejhg.2014.177

Bothwell, S. P., Chan, E., Bernardini, I. M., Kuo, Y. M., Gahl, W. A., & Nussbaum, R. L. (2011). Mouse model for Lowe syndrome/Dent Disease 2 renal tubulopathy. *J Am Soc Nephrol, 22*(3), 443-448. doi:10.1681/ASN.2010050565

Bothwell, S. P., Farber, L. W., Hoagland, A., & Nussbaum, R. L. (2010). Species-specific difference in expression and splice-site choice in Inpp5b, an inositol polyphosphate 5-phosphatase paralogous to the enzyme deficient in Lowe Syndrome. *Mamm Genome, 21*(9-10), 458-466. doi:10.1007/s00335-010-9281-7

Brancati, F., Dallapiccola, B., & Valente, E. M. (2010). Joubert Syndrome and related disorders. *Orphanet J Rare Dis, 5*, 20. doi:10.1186/1750-1172-5-20

Brauer, H., Strauss, J., Wegner, W., Müller-Tidow, C., Horstmann, M., & Jücker, M. (2012). Leukemia-associated mutations in SHIP1 inhibit its enzymatic activity, interaction with the GM-CSF receptor and Grb2, and its ability to inactivate PI3K/AKT signaling. *Cell Signal, 24*(11), 2095-2101. doi:10.1016/j.cellsig.2012.07.017

Braun, D., & Schweizer, U. (2017). The Chemical Chaperone Phenylbutyrate Rescues MCT8 Mutations Associated With Milder Phenotypes in Patients With Allan-Herndon-Dudley Syndrome. *Endocrinology, 158*(3), 678-691. doi:10.1210/en.2016-1530

Braun, W. E., Schold, J. D., Stephany, B. R., Spirko, R. A., & Herts, B. R. (2014). Low-Dose Rapamycin ( Sirolimus) Effects in Autosomal Dominant Polycystic Kidney Disease: An Open-Label Randomized Controlled Pilot Study. *Clinical Journal of the American Society of Nephrology, 9*(5), 881-888. doi:10.2215/cjn.02650313

Brooks, J. K., & Ahmad, R. (2009). Oral anomalies associated with the oculocerebrorenal syndrome of Lowe: case report with multiple unerupted teeth and pericoronal radiolucencies. *Oral Surg Oral Med Oral Pathol Oral Radiol Endod, 107*(3), e32-35. doi:10.1016/j.tripleo.2008.11.023

Bökenkamp, A., & Ludwig, M. (2016). The oculocerebrorenal syndrome of Lowe: an update. *Pediatr Nephrol, 31*(12), 2201-2212. doi:10.1007/s00467-016-3343-3

Cai, J., Song, X., Wang, W., Watnick, T., Pei, Y., Qian, F., & Pan, D. (2018). A RhoA-YAP-c-Myc signaling axis promotes the development of polycystic kidney disease. *Genes Dev, 32*(11-12), 781-793. doi:10.1101/gad.315127.118

Caracci, M. O., Fuentealba, L. M., & Marzolo, M. P. (2019). Golgi Complex Dynamics and Its Implication in Prevalent Neurological Disorders. *Front Cell Dev Biol, 7*, 75. doi:10.3389/fcell.2019.00075

Cauvin, C., Rosendale, M., Gupta-Rossi, N., Rocancourt, M., Larraufie, P., Salomon, R., . . . Echard, A. (2016). Rab35 GTPase Triggers Switch-like Recruitment of the Lowe Syndrome Lipid Phosphatase OCRL on Newborn Endosomes. *Curr Biol, 26*(1), 120-128. doi:10.1016/j.cub.2015.11.040

Chavez, M., Ena, S., Van Sande, J., d'Exaerde, A. d. K., Schurmans, S., & Schiffmann, S. N. (2015). Modulation of Ciliary Phosphoinositide Content Regulates Trafficking and Sonic Hedgehog Signaling Output. *Developmental Cell, 34*(3), 338-350.

Cho, H. Y., Lee, B. H., Choi, H. J., Ha, I. S., Choi, Y., & Cheong, H. I. (2008). Renal manifestations of Dent disease and Lowe syndrome. *Pediatr Nephrol, 23*(2), 243-249. doi:10.1007/s00467-007-0686-9

Choudhury, R., Diao, A. P., Zhang, F., Eisenberg, E., Saint-Pol, A., Williams, C., . . . Lowe, M. (2005). Lowe syndrome protein OCRL1 interacts with clathrin and regulates protein trafficking between endosomes and the trans-Golgi network. *Molecular Biology of the Cell, 16*(8). doi:10.1091/mbc.E05-02-0120

Choudhury, R., Noakes, C. J., McKenzie, E., Kox, C., & Lowe, M. (2009). Differential Clathrin Binding and Subcellular Localization of OCRL1 Splice Isoforms. *Journal of Biological Chemistry, 284*(15), 9965-9973. doi:10.1074/jbc.M807442200

Chung, J. K., Sekiya, F., Kang, H. S., Lee, C., Han, J. S., Kim, S. R., . . . Rhee, S. G. (1997). Synaptojanin inhibition of phospholipase D activity by hydrolysis of phosphatidylinositol 4,5-bisphosphate. *J Biol Chem, 272*(25), 15980-15985. doi:10.1074/jbc.272.25.15980

Ciobanasu, C., Faivre, B., & Le Clainche, C. (2012). Actin dynamics associated with focal adhesions. *Int J Cell Biol, 2012*, 941292. doi:10.1155/2012/941292

Conduit, S. E., Dyson, J. M., & Mitchell, C. A. (2012). Inositol polyphosphate 5-phosphatases; new players in the regulation of cilia and ciliopathies. *Febs Letters, 586*(18), 2846-2857. doi:10.1016/j.febslet.2012.07.037

Coon, B. G., Hernandez, V., Madhivanan, K., Mukherjee, D., Hanna, C. B., Barinaga-Rementeria Ramirez, I., . . . Aguilar, R. C. (2012). The Lowe syndrome protein OCRL1 is involved in primary cilia assembly. *Human molecular genetics, 21*(8), 1835-1847.

Coon, B. G., Hernandez, V., Madhivanan, K., Mukherjee, D., Hanna, C. B., Barinaga-Rementeria Ramirez, I., . . . Aguilar, R. C. (2012). The Lowe syndrome protein OCRL1 is involved in primary cilia assembly. *Hum Mol Genet, 21*(8), 1835-1847. doi:10.1093/hmg/ddr615

Coon, B. G., Mukherjee, D., Hanna, C. B., Riese, D. J., II, Lowe, M., & Aguilar, R. C. (2009). Lowe syndrome patient fibroblasts display Ocrl1-specific cell migration defects that cannot be rescued by the homologous Inpp5b phosphatase. *Human Molecular Genetics, 18*(23), 4478-4491. doi:10.1093/hmg/ddp407

Cortez, L., & Sim, V. (2014). The therapeutic potential of chemical chaperones in protein folding diseases. *Prion, 8*(2). doi:10.4161/pri.28938

Croisé, P., Estay-Ahumada, C., Gasman, S., & Ory, S. (2014). Rho GTPases, phosphoinositides, and actin: a tripartite framework for efficient vesicular trafficking. *Small GTPases, 5*, e29469. doi:10.4161/sgtp.29469

Cui, S., Guerriero, C. J., Szalinski, C. M., Kinlough, C. L., Hughey, R. P., & Weisz, O. A. (2010). OCRL1 function in renal epithelial membrane traffic. *American Journal of Physiology-Renal Physiology, 298*(2), 335-345. doi:10.1152/ajprenal.00453.2009

Czech, M. P. (2000). PIP2 and PIP3: complex roles at the cell surface. In *Cell* (Vol. 100, pp. 603-606). United States.

D'Souza-Schorey, C., Boettner, B., & Van Aelst, L. (1998). Rac regulates integrin-mediated spreading and increased adhesion of T lymphocytes. *Mol Cell Biol, 18*(7), 3936-3946.

Dai, C., Wang, L., Li, Y., Zheng, Z., Qian, J., Wang, C., . . . Shan, X. (2019). Lowe syndrome with extremely short stature: growth hormone deficiency may be the pathogeny. *Growth Factors, 37*(3-4), 170-177. doi:10.1080/08977194.2019.1669589

Dambournet, D., Machicoane, M., Chesneau, L., Sachse, M., Rocancourt, M., El Marjou, A., . . . Echard, A. (2011). Rab35 GTPase and OCRL phosphatase remodel lipids and F-actin for successful cytokinesis. *Nature Cell Biology, 13*(8), 981-U245. doi:10.1038/ncb2279

Damen, J. E., Liu, L., Rosten, P., Humphries, R. K., Jefferson, A. B., Majerus, P. W., & Krystal, G. (1996). The 145-kDa protein induced to associate with Shc by multiple cytokines is an inositol tetraphosphate and phosphatidylinositol 3,4,5-triphosphate 5-phosphatase. *Proc Natl Acad Sci U S A, 93*(4), 1689-1693. doi:10.1073/pnas.93.4.1689

Damme, M., Suntio, T., Saftig, P., & Eskelinen, E. L. (2015). Autophagy in neuronal cells: general principles and physiological and pathological functions. *Acta Neuropathol, 129*(3), 337-362. doi:10.1007/s00401-014-1361-4

Davies, J. T., Delfino, S. F., Feinberg, C. E., Johnson, M. F., Nappi, V. L., Olinger, J. T., . . . Swanson, H. I. (2016). Current and Emerging Uses of Statins in Clinical Therapeutics: A Review. *Lipid Insights, 9*, 13-29. doi:10.4137/LPI.S37450

De Leo, M. G., Staiano, L., Vicinanza, M., Luciani, A., Carissimo, A., Mutarelli, M., . . . De Matteis, M. A. (2016). Autophagosome-lysosome fusion triggers a lysosomal response mediated by TLR9 and controlled by OCRL. *Nat Cell Biol, 18*(8), 839-850. doi:10.1038/ncb3386

De Smedt, F., Missiaen, L., Parys, J. B., Vanweyenberg, V., De Smedt, H., & Erneux, C. (1997). Isoprenylated human brain type I inositol 1,4,5-trisphosphate 5-phosphatase controls Ca2+ oscillations induced by ATP in Chinese hamster ovary cells. *J Biol Chem, 272*(28), 17367-17375. doi:10.1074/jbc.272.28.17367

Di Paolo, G., & De Camilli, P. (2006). Phosphoinositides in cell regulation and membrane dynamics. *Nature, 443*(7112), 651-657. doi:10.1038/nature05185

Dickson, E. J., & Hille, B. (2019). Understanding phosphoinositides: rare, dynamic, and essential membrane phospholipids. *Biochem J, 476*(1), 1-23.

Dillard, K. J., Hytönen, M. K., Fischer, D., Tanhuanpää, K., Lehti, M. S., Vainio-Siukola, K., . . . Anttila, M. (2018). A splice site variant in INPP5E causes diffuse cystic renal dysplasia and hepatic fibrosis in dogs. *PLoS One, 13*(9), e0204073. doi:10.1371/journal.pone.0204073

Dressman, M. A., Olivos-Glander, I. M., Nussbaum, R. L., & Suchy, S. F. (2000). Ocrl1, a PtdIns(4,5)P(2) 5-phosphatase, is localized to the trans-Golgi network of fibroblasts and epithelial cells. *J Histochem Cytochem, 48*(2), 179-190.

Drouet, V., & Lesage, S. (2014). Synaptojanin 1 mutation in Parkinson's disease brings further insight into the neuropathological mechanisms. *Biomed Res Int, 2014*, 289728. doi:10.1155/2014/289728

Dunmore, B. J., Yang, X., Crosby, A., Moore, S., Long, L., Huang, C., . . . Morrell, N. W. (2020). 4PBA Restores Signalling of a Cysteine-substituted Mutant BMPR2 Receptor Found in Patients with PAH. *Am J Respir Cell Mol Biol*. doi:10.1165/rcmb.2019-0321OC

Dyson, J. M., Conduit, S. E., Feeney, S. J., Hakim, S., DiTommaso, T., Fulcher, A. J., . . . Mitchell, C. A. (2017). INPP5E regulates phosphoinositide-dependent cilia transition zone function. *J Cell Biol, 216*(1), 247-263. doi:10.1083/jcb.201511055

Dyson, J. M., Fedele, C. G., Davies, E. M., Becanovic, J., & Mitchell, C. A. (2012). Phosphoinositide phosphatases: just as important as the kinases. *Sub-cellular biochemistry, 58*, 215-279. doi:10.1007/978-94-007-3012-0_7

El Kadhi, K. B., Roubinet, C., Solinet, S., Emery, G., & Carreno, S. (2011). The Inositol 5-Phosphatase dOCRL Controls PI(4,5)P2 Homeostasis and Is Necessary for Cytokinesis. *Current Biology, 21*(12), 1074-1079. doi:10.1016/j.cub.2011.05.030

Erdmann, K. S., Mao, Y., McCrea, H. J., Zoncu, R., Lee, S., Paradise, S., . . . De Camillil, P. (2007). A role of the Lowe syndrome protein OCRL in early steps of the endocytic pathway. *Developmental Cell, 13*(3), 377-390. doi:10.1016/j.devcel.2007.08.004

Essig, M., & Friedlander, G. (2003). Shear-stress-responsive signal transduction mechanisms in renal proximal tubule cells. *Curr Opin Nephrol Hypertens, 12*(1), 31-34. doi:10.1097/00041552-200301000-00006

Fairn, G. D., & Grinstein, S. (2012). How nascent phagosomes mature to become phagolysosomes. *Trends Immunol, 33*(8), 397-405. doi:10.1016/j.it.2012.03.003

Fan, J., Hu, Z., Zeng, L., Lu, W., Tang, X., Zhang, J., & Li, T. (2008). Golgi apparatus and neurodegenerative diseases. *Int J Dev Neurosci, 26*(6), 523-534. doi:10.1016/j.ijdevneu.2008.05.006

Faucherre, A., Desbois, P., Nagano, F., Satre, V., Lunardi, J., Gacon, G., & Dorseuil, O. (2005). Lowe syndrome protein Ocrl1 is translocated to membrane ruffles upon Rac GTPase activation: a new perspective on Lowe syndrome pathophysiology. *Human Molecular Genetics, 14*(11), 1441-1448. doi:10.1093/hmg/ddi153

Faucherre, A., Desbois, P., Satre, V., Lunardi, J., Dorseuil, O., & Gacon, G. (2003a). Lowe syndrome protein OCRL1 interacts with Rac GTPase in the trans-Golgi network. *Human Molecular Genetics, 12*(19). doi:10.1093/hmg/ddg250

Faucherre, A., Desbois, P., Satre, V., Lunardi, J., Dorseuil, O., & Gacon, G. (2003b). Lowe syndrome protein OCRL1 interacts with Rac GTPase in the trans-Golgi network. *Human Molecular Genetics, 12*(19), 2449-2456. doi:10.1093/hmg/ddg250

Feinstein, M. J., Achenbach, C. J., Stone, N. J., & Lloyd-Jones, D. M. (2015). A Systematic Review of the Usefulness of Statin Therapy in HIV-Infected Patients. *Am J Cardiol, 115*(12), 1760-1766. doi:10.1016/j.amjcard.2015.03.025

Fernandes, S., Srivastava, N., Sudan, R., Middleton, F. A., Shergill, A. K., Ryan, J. C., & Kerr, W. G. (2018). SHIP1 Deficiency in Inflammatory Bowel Disease Is Associated With Severe Crohn's Disease and Peripheral T Cell Reduction. *Front Immunol, 9*, 1100. doi:10.3389/fimmu.2018.01100

Festa, B. P., Berquez, M., Gassama, A., Amrein, I., Ismail, H. M., Samardzija, M., . . . Devuyst, O. (2019). OCRL deficiency impairs endolysosomal function in a humanized mouse model for Lowe syndrome and Dent disease. *Hum Mol Genet, 28*(12), 1931-1946. doi:10.1093/hmg/ddy449

Fradet, A., & Fitzgerald, J. (2017). INPPL1 gene mutations in opsismodysplasia. *J Hum Genet, 62*(2), 135-140. doi:10.1038/jhg.2016.119

Fukuda, M., Kanno, E., Ishibashi, K., & Itoh, T. (2008). Large scale screening for novel Rab effectors reveals unexpected broad Rab binding specificity. *Molecular & Cellular Proteomics, 7*(6), 1031-1042. doi:10.1074/mcp.M700569-MCP200

Gan, X., Wang, J., Su, B., & Wu, D. (2011). Evidence for direct activation of mTORC2 kinase activity by phosphatidylinositol 3,4,5-trisphosphate. *J Biol Chem, 286*(13), 10998-11002. doi:10.1074/jbc.M110.195016

García-Martínez, J. M., & Alessi, D. R. (2008). mTOR complex 2 (mTORC2) controls hydrophobic motif phosphorylation and activation of serum- and glucocorticoid-induced protein kinase 1 (SGK1). *Biochem J, 416*(3), 375-385. doi:10.1042/BJ20081668

Ghansah, T., Paraiso, K. H., Highfill, S., Desponts, C., May, S., McIntosh, J. K., . . . Kerr, W. G. (2004). Expansion of myeloid suppressor cells in SHIP-deficient mice represses allogeneic T cell responses. *J Immunol, 173*(12), 7324-7330. doi:10.4049/jimmunol.173.12.7324

Ghosh, S., Huber, C., Siour, Q., Sousa, S. B., Wright, M., Cormier-Daire, V., & Erneux, C. (2017). Fibroblasts derived from patients with opsismodysplasia display SHIP2-specific cell migration and adhesion defects. *Hum Mutat, 38*(12), 1731-1739. doi:10.1002/humu.23321

Gliozzi, M. L., Espiritu, E. B., Shipman, K. E., Rbaibi, Y., Long, K. R., Roy, N., . . . Weisz, O. A. (2020). Effects of Proximal Tubule Shortening on Protein Excretion in a Lowe Syndrome Model. *J Am Soc Nephrol, 31*(1), 67-83. doi:10.1681/ASN.2019020125

Grahammer, F., Ramakrishnan, S. K., Rinschen, M. M., Larionov, A. A., Syed, M., Khatib, H., . . . Theilig, F. (2017). mTOR Regulates Endocytosis and Nutrient Transport in Proximal Tubular Cells. *J Am Soc Nephrol, 28*(1), 230-241. doi:10.1681/ASN.2015111224

Grieve, A. G., Daniels, R. D., Sanchez-Heras, E., Hayes, M. J., Moss, S. E., Matter, K., . . . Levine, T. P. (2011). Lowe Syndrome protein OCRL1 supports maturation of polarized epithelial cells. *PLoS One, 6*(8), e24044. doi:10.1371/journal.pone.0024044

Guo, F., Debidda, M., Yang, L., Williams, D. A., & Zheng, Y. (2006). Genetic Deletion of Rac1 GTPase Reveals Its Critical Role in Actin Stress Fiber Formation and Focal Adhesion Complex Assembly. *Journal of Biological Chemistry, 281*(27), 18652-18659. doi:10.1074/jbc.M603508200

Guo, S., Stolz, L. E., Lemrow, S. M., & York, J. D. (1999). SAC1-like domains of yeast SAC1, INP52, and INP53 and of human synaptojanin encode polyphosphoinositide phosphatases. *J Biol Chem, 274*(19), 12990-12995. doi:10.1074/jbc.274.19.12990

Hagemann, N., Hou, X., Goody, R. S., Itzen, A., & Erdmann, K. S. (2012). Crystal structure of the Rab binding domain of OCRL1 in complex with Rab8 and functional implications of the OCRL1/Rab8 module for Lowe syndrome. *Small GTPases, 3*(2), 107-110. doi:10.4161/sgtp.19380

Hakim, S., Bertucci, M. C., Conduit, S. E., Vuong, D. L., & Mitchell, C. A. (2012). Inositol Polyphosphate Phosphatases in Human Disease. *Phosphoinositides and Disease, 362*, 246-314. doi:10.1007/978-94-007-5025-8_12

Hakim, S., Dyson, J. M., Feeney, S. J., Davies, E. M., Sriratana, A., Koenig, M. N., . . . Mitchell, C. A. (2016). Inpp5e suppresses polycystic kidney disease via inhibition of PI3K/Akt-dependent mTORC1 signaling. *Hum Mol Genet, 25*(11), 2295-2313. doi:10.1093/hmg/ddw097

Hampshire, D. J., Ayub, M., Springell, K., Roberts, E., Jafri, H., Rashid, Y., . . . Woods, C. G. (2006). MORM syndrome (mental retardation, truncal obesity, retinal dystrophy and micropenis), a new autosomal recessive disorder, links to 9q34. *Eur J Hum Genet, 14*(5), 543-548. doi:10.1038/sj.ejhg.5201577

Hardee, I., Soldatos, A., Davids, M., Vilboux, T., Toro, C., David, K. L., . . . Malicdan, M. C. V. (2017). Defective ciliogenesis in INPP5E-related Joubert syndrome. *Am J Med Genet A, 173*(12), 3231-3237. doi:10.1002/ajmg.a.38376

Hardies, K., Cai, Y., Jardel, C., Jansen, A. C., Cao, M., May, P., . . . Consortium, A. w. g. o. t. E. R. (2016). Loss of SYNJ1 dual phosphatase activity leads to early onset refractory seizures and progressive neurological decline. *Brain, 139*(Pt 9), 2420-2430. doi:10.1093/brain/aww180

Harrison, M., Odell, E. W., & Sheehy, E. C. (1999). Dental findings in Lowe syndrome. *Pediatr Dent, 21*(7), 425-428.

Hasegawa, J., Iwamoto, R., Otomo, T., Nezu, A., Hamasaki, M., & Yoshimori, T. (2016). Autophagosome-lysosome fusion in neurons requires INPP5E, a protein associated with Joubert syndrome. *EMBO J, 35*(17), 1853-1867. doi:10.15252/embj.201593148

Havasi, A., & Dong, Z. (2016). Autophagy and Tubular Cell Death in the Kidney. *Semin Nephrol, 36*(3), 174-188.

Helgason, C. D., Kalberer, C. P., Damen, J. E., Chappel, S. M., Pineault, N., Krystal, G., & Humphries, R. K. (2000). A dual role for Src homology 2 domain-containing inositol-5-phosphatase (SHIP) in immunity: aberrant development and enhanced function of b lymphocytes in ship -/- mice. *J Exp Med, 191*(5), 781-794. doi:10.1084/jem.191.5.781

Hichri, H., Rendu, J., Monnier, N., Coutton, C., Dorseuil, O., Poussou, R. V., . . . Lunardi, J. (2011). From Lowe Syndrome to Dent Disease: Correlations between Mutations of the OCRL1 Gene and Clinical and Biochemical Phenotypes. *Human Mutation, 32*(4), 379-388. doi:10.1002/humu.21391

Holt, M., Cooke, A., Wu, M. M., & Lagnado, L. (2003). Bulk membrane retrieval in the synaptic terminal of retinal bipolar cells. *J Neurosci, 23*(4), 1329-1339.

Hoopes, R. R., Shrimpton, A. E., Knohl, S. J., Hueber, P., Hoppe, B., Matyus, J., . . . Scheinman, S. J. (2005). Dent disease with mutations in OCRL1. *American Journal of Human Genetics, 76*(2), 260-267. doi:10.1086/427887

Horan, K. A., Watanabe, K.-i., Kong, A. M., Bailey, C. G., Rasko, J. E. J., Sasaki, T., & Mitchell, C. A. (2007). Regulation of Fc gamma R-stimulated phagocytosis by the 72-kDa inositol polyphosphate 5-phosphatase: SHIP1, but not the 72-kDa 5-phosphatase, regulates complement receptor 3-mediated phagocytosis by differential recruitment of these 5-phosphatases to the phagocytic cup. *Blood, 110*(13), 4480-4491. doi:10.1182/blood-2007-02-073874

Hou, X., Hagemann, N., Schoebel, S., Blankenfeldt, W., Goody, R. S., Erdmann, K. S., & Itzen, A. (2011). A structural basis for Lowe syndrome caused by mutations in the Rab-binding domain of OCRL1. *Embo Journal, 30*(8), 1659-1670. doi:10.1038/emboj.2011.60

Hsiao, Y. C., Tuz, K., & Ferland, R. J. (2012). Trafficking in and to the primary cilium. *Cilia, 1*(1), 4. doi:10.1186/2046-2530-1-4

Hsieh, W. C., Ramadesikan, S., Fekete, D., & Aguilar, R. C. (2018). Kidney-differentiated cells derived from Lowe Syndrome patient's iPSCs show ciliogenesis defects and Six2 retention at the Golgi complex. *PLoS One, 13*(2), e0192635. doi:10.1371/journal.pone.0192635

Humbert, M. C., Weihbrecht, K., Searby, C. C., Li, Y., Pope, R. M., Sheffield, V. C., & Seo, S. (2012). ARL13B, PDE6D, and CEP164 form a functional network for INPP5E ciliary targeting. *Proc Natl Acad Sci U S A, 109*(48), 19691-19696. doi:10.1073/pnas.1210916109

Hyvola, N., Diao, A., McKenzie, E., Skippen, A., Cockcroft, S., & Lowe, M. (2006). Membrane targeting and activation of the Lowe syndrome protein OCRL1 by rab GTPases. *Embo Journal, 25*(16), 3750-3761. doi:10.1038/sj.emboj.7601274

Ibraghimov-Beskrovnaya, O., & Natoli, T. A. (2011). mTOR signaling in polycystic kidney disease. *Trends Mol Med, 17*(11), 625-633. doi:10.1016/j.molmed.2011.06.003

Ijuin, T., Mochizuki, Y., Fukami, K., Funaki, M., Asano, T., & Takenawa, T. (2000). Identification and characterization of a novel inositol polyphosphate 5-phosphatase. *J Biol Chem, 275*(15), 10870-10875. doi:10.1074/jbc.275.15.10870

Itoh, R. E., Kurokawa, K., Ohba, Y., Yoshizaki, H., Mochizuki, N., & Matsuda, M. (2002). Activation of rac and cdc42 video imaged by fluorescent resonance energy transfer-based single-molecule probes in the membrane of living cells. *Mol Cell Biol, 22*(18), 6582-6591.

Jaber, N., Dou, Z., Chen, J. S., Catanzaro, J., Jiang, Y. P., Ballou, L. M., . . . Zong, W. X. (2012). Class III PI3K Vps34 plays an essential role in autophagy and in heart and liver function. *Proc Natl Acad Sci U S A, 109*(6), 2003-2008. doi:10.1073/pnas.1112848109

Jacoby, M., Cox, J. J., Gayral, S., Hampshire, D. J., Ayub, M., Blockmans, M., . . . Schurmans, S. (2009). INPP5E mutations cause primary cilium signaling defects, ciliary instability and ciliopathies in human and mouse. *Nat Genet, 41*(9), 1027-1031. doi:10.1038/ng.427

Janne, P. A., Suchy, S. F., Bernard, D., MacDonald, M., Crawley, J., Grinberg, A., . . . Nussbaum, R. L. (1998). Functional overlap between murine Inpp5b and Ocrl1 may explain why deficiency of the murine ortholog for OCRL1 does not cause Lowe syndrome in mice. *Journal of Clinical Investigation, 101*(10), 2042-2053. doi:10.1172/jci2414

Jefferson, A. B., & Majerus, P. W. (1995). Properties of type II inositol polyphosphate 5-phosphatase. *J Biol Chem, 270*(16), 9370-9377. doi:10.1074/jbc.270.16.9370

Jefferson, A. B., & Majerus, P. W. (1996). Mutation of the conserved domains of two inositol polyphosphate 5-phosphatases. *Biochemistry, 35*(24), 7890-7894. doi:10.1021/bi9602627

Jiang, M., Wei, Q., Dong, G., Komatsu, M., Su, Y., & Dong, Z. (2012). Autophagy in proximal tubules protects against acute kidney injury. *Kidney Int, 82*(12), 1271-1283.

Jimeno, A., Rudek, M. A., Kulesza, P., Ma, W. W., Wheelhouse, J., Howard, A., . . . Hidalgo, M. (2008). Pharmacodynamic-guided modified continuous reassessment method-based, dose-finding study of rapamycin in adult patients with solid tumors. *J Clin Oncol, 26*(25), 4172-4179. doi:10.1200/JCO.2008.16.2347

Johnston, J. A., Ward, C. L., & Kopito, R. R. (1998). Aggresomes: a cellular response to misfolded proteins. *J Cell Biol, 143*(7), 1883-1898. doi:10.1083/jcb.143.7.1883

Joubert, M., Eisenring, J. J., & Andermann, F. (1968). Familial dysgenesis of the vermis: a syndrome of hyperventilation, abnormal eye movements and retardation. *Neurology, 18*(3), 302-303.

Juhász, G., Hill, J. H., Yan, Y., Sass, M., Baehrecke, E. H., Backer, J. M., & Neufeld, T. P. (2008). The class III PI(3)K Vps34 promotes autophagy and endocytosis but not TOR signaling in Drosophila. *J Cell Biol, 181*(4), 655-666. doi:10.1083/jcb.200712051

Kaibuchi, K., Kuroda, S., & Amano, M. (1999). Regulation of the cytoskeleton and cell adhesion by the Rho family GTPases in mammalian cells. *Annu Rev Biochem, 68*, 459-486. doi:10.1146/annurev.biochem.68.1.459

Kanlaya, R., Sintiprungrat, K., Chaiyarit, S., & Thongboonkerd, V. (2013). Macropinocytosis is the major mechanism for endocytosis of calcium oxalate crystals into renal tubular cells. *Cell Biochem Biophys, 67*(3), 1171-1179. doi:10.1007/s12013-013-9630-8

Kerr, W. G., Park, M. Y., Maubert, M., & Engelman, R. W. (2011). SHIP deficiency causes Crohn's disease-like ileitis. *Gut, 60*(2), 177-188. doi:10.1136/gut.2009.202283

Khvotchev, M., & Südhof, T. C. (1998). Developmentally regulated alternative splicing in a novel synaptojanin. *J Biol Chem, 273*(4), 2306-2311. doi:10.1074/jbc.273.4.2306

Kieras, F. J., Houck, G. E., French, J. H., & Wisniewski, K. (1984). Low sulfated glycosaminoglycans are excreted in patients with the Lowe syndrome. *Biochem Med, 31*(2), 201-210. doi:10.1016/0006-2944(84)90024-3

Kimura, T., Takabatake, Y., Takahashi, A., Kaimori, J. Y., Matsui, I., Namba, T., . . . Isaka, Y. (2011). Autophagy protects the proximal tubule from degeneration and acute ischemic injury. *J Am Soc Nephrol, 22*(5), 902-913.

Kisseleva, M. V., Cao, L., & Majerus, P. W. (2002). Phosphoinositide-specific inositol polyphosphate 5-phosphatase IV inhibits Akt/protein kinase B phosphorylation and leads to apoptotic cell death. *Journal of Biological Chemistry, 277*(8), 6266-6272. doi:10.1074/jbc.M105969200

Kisseleva, M. V., Wilson, M. P., & Majerus, P. W. (2000). The isolation and characterization of a cDNA encoding phospholipid-specific inositol polyphosphate 5-phosphatase. *Journal of Biological Chemistry, 275*(26), 20110-20116. doi:10.1074/jbc.M910119199

Kleta, R. (2008). Fanconi or not Fanconi? Lowe syndrome revisited. *Clin J Am Soc Nephrol, 3*(5), 1244-1245. doi:10.2215/CJN.02880608

Kohjimoto, Y., Ebisuno, S., Tamura, M., & Ohkawa, T. (1996a). Adhesion and endocytosis of calcium oxalate crystals on renal tubular cells. *Scanning Microsc, 10*(2), 459-468; discussion 468-470.

Kohjimoto, Y., Ebisuno, S., Tamura, M., & Ohkawa, T. (1996b). Interactions between calcium oxalate monohydrate crystals and Madin-Darby canine kidney cells: endocytosis and cell proliferation. *Urol Res, 24*(4), 193-199. doi:10.1007/bf00295892

Kong, A. M., Speed, C. J., O'Malley, C. J., Layton, M. J., Meehan, T., Loveland, K. L., . . . Mitchell, C. A. (2000). Cloning, and characterization of a 72-kDa inositol-polyphosphate 5-phosphatase localized to the Golgi network. *Journal of Biological Chemistry, 275*(31), 24052-24064. doi:10.1074/jbc.M000874200

Kopito, R. R. (2000). Aggresomes, inclusion bodies and protein aggregation. *Trends Cell Biol, 10*(12), 524-530. doi:10.1016/s0962-8924(00)01852-3

Kopito, R. R., & Ron, D. (2000). Conformational disease. *Nat Cell Biol, 2*(11), E207-209. doi:10.1038/35041139

Kou, R., Sartoretto, J., & Michel, T. (2009). Regulation of Rac1 by simvastatin in endothelial cells: differential roles of AMP-activated protein kinase and calmodulin-dependent kinase kinase-beta. *J Biol Chem, 284*(22), 14734-14743. doi:10.1074/jbc.M808664200

Kuo, J. C. (2013). Mechanotransduction at focal adhesions: integrating cytoskeletal mechanics in migrating cells. *J Cell Mol Med, 17*(6), 704-712.

Lang, F., Stournaras, C., & Alesutan, I. (2014). Regulation of transport across cell membranes by the serum- and glucocorticoid-inducible kinase SGK1. *Mol Membr Biol, 31*(1), 29-36. doi:10.3109/09687688.2013.874598

Lasne, D., Baujat, G., Mirault, T., Lunardi, J., Grelac, F., Egot, M., . . . Bachelot-Loza, C. (2010). Bleeding disorders in Lowe syndrome patients: evidence for a link between OCRL mutations and primary haemostasis disorders. *British Journal of Haematology, 150*(6), 685-688. doi:10.1111/j.1365-2141.2010.08304.x

Lawson, C. D., & Burridge, K. (2014). The on-off relationship of Rho and Rac during integrin-mediated adhesion and cell migration. *Small GTPases, 5*, e27958. doi:10.4161/sgtp.27958

Laxminarayan, K. M., Chan, B. K., Tetaz, T., Bird, P. I., & Mitchell, C. A. (1994). Characterization of a cDNA encoding the 43-kDa membrane-associated inositol-polyphosphate 5-phosphatase. *J Biol Chem, 269*(25), 17305-17310.

Leahey, A. M., Charnas, L. R., & Nussbaum, R. L. (1993). Nonsense mutations in the OCRL-1 gene in patients with the oculocerebrorenal syndrome of Lowe. *Hum Mol Genet, 2*(4), 461-463. doi:10.1093/hmg/2.4.461

Lee, C. S., Hanna, A. D., Wang, H., Dagnino-Acosta, A., Joshi, A. D., Knoblauch, M., . . . Hamilton, S. L. (2017). A chemical chaperone improves muscle function in mice with a RyR1 mutation. *Nat Commun, 8*, 14659. doi:10.1038/ncomms14659

Lee, E. J., Shin, S.H, Chun, J, Hyun, S, Kim,, & Y, K., S.S. (2010). The modulation of TRPV4 channel activity

through its Ser 824 residue phosphorylation by SGK1. *Animal Cells and Systems, 14*, 99-114.

Lee, Y. S., Ehninger, D., Zhou, M., Oh, J. Y., Kang, M., Kwak, C., . . . Silva, A. J. (2014). Mechanism and treatment for learning and memory deficits in mouse models of Noonan syndrome. *Nat Neurosci, 17*(12), 1736-1743. doi:10.1038/nn.3863

Leung, W. H., Tarasenko, T., & Bolland, S. (2009). Differential roles for the inositol phosphatase SHIP in the regulation of macrophages and lymphocytes. *Immunol Res, 43*(1-3), 243-251. doi:10.1007/s12026-008-8078-1

Li, J., Kim, S. G., & Blenis, J. (2014). Rapamycin: one drug, many effects. *Cell Metab, 19*(3), 373-379. doi:10.1016/j.cmet.2014.01.001

Lin, T., Orrison, B. M., Leahey, A. M., Suchy, S. F., Bernard, D. J., Lewis, R. A., & Nussbaum, R. L. (1997). Spectrum of mutations in the OCRL1 gene in the Lowe oculocerebrorenal syndrome. *Am J Hum Genet, 60*(6), 1384-1388. doi:10.1086/515471

Lioubin, M. N., Algate, P. A., Tsai, S., Carlberg, K., Aebersold, A., & Rohrschneider, L. R. (1996). p150Ship, a signal transduction molecule with inositol polyphosphate-5-phosphatase activity. *Genes Dev, 10*(9), 1084-1095. doi:10.1101/gad.10.9.1084

Liu, Q., Huang, S., Yin, P., Yang, S., Zhang, J., Jing, L., . . . Li, S. (2020). Cerebellum-enriched protein INPP5A contributes to selective neuropathology in mouse model of spinocerebellar ataxias type 17. *Nat Commun, 11*(1), 1101. doi:10.1038/s41467-020-14931-8

Liu, T., Yue, Z., Wang, H., Tong, H., & Sun, L. (2015). Novel mutation of OCRL1 in Lowe syndrome. *Indian J Pediatr, 82*(1), 89-92. doi:10.1007/s12098-014-1581-6

Liu, X., Shi, Y., Woods, K. W., Hessler, P., Kroeger, P., Wilsbacher, J., . . . Luo, Y. (2008). Akt inhibitor A-443654 interferes with mitotic progression by regulating Aurora A kinase expression. *Neoplasia, 10*(8), 828-837. doi:10.1593/neo.08408

Livingston, M. J., & Dong, Z. (2014). Autophagy in acute kidney injury. *Semin Nephrol, 34*(1), 17-26.

Loi, M. (2006). Lowe syndrome. *Orphanet J Rare Dis, 1*, 16.

Loi, M. (2006). Lowe syndrome. *Orphanet Journal of Rare Diseases, 1*. doi:16

10.1186/1750-1172-1-16

Loovers, H. M., Kortholt, A., de Groote, H., Whitty, L., Nussbaum, R. L., & van Haastert, P. J. M. (2007). Regulation of phagocytosis in Dictyostelium by the inositol 5-phosphatase OCRL homolog Dd5P4. *Traffic, 8*(5), 618-628. doi:10.1111/j.1600-0854.2007.00546.x

Lopez-Rios, J., Speziale, D., Robay, D., Scotti, M., Osterwalder, M., Nusspaumer, G., . . . Zeller, R. (2012). GLI3 Constrains Digit Number by Controlling Both Progenitor Proliferation and BMP-Dependent Exit to Chondrogenesis. *Developmental Cell, 22*(4), 837-848. doi:10.1016/j.devcel.2012.01.006

LOWE, C. U., TERREY, M., & MacLACHLAN, E. A. (1952). Organic-aciduria, decreased renal ammonia production, hydrophthalmos, and mental retardation; a clinical entity. *AMA Am J Dis Child, 83*(2), 164-184.

Lowe, M. (2005). Structure and function of the Lowe syndrome protein OCRL1. *Traffic, 6*(9), 711-719. doi:10.1111/j.1600-0854.2005.00311.x

Luo, N., Conwell, M. D., Chen, X., Kettenhofen, C. I., Westlake, C. J., Cantor, L. B., . . . Sun, Y. (2014). Primary cilia signaling mediates intraocular pressure sensation. *Proc Natl Acad Sci U S A, 111*(35), 12871-12876. doi:10.1073/pnas.1323292111

Luo, N., Conwell, M. D., Chen, X., Kettenhofen, C. I., Westlake, C. J., Cantor, L. B., . . . Sun, Y. (2014). Primary cilia signaling mediates intraocular pressure sensation. *Proceedings of the National Academy of Sciences of the United States of America, 111*(35), 12871-12876. doi:10.1073/pnas.1323292111

Luo, N., Lu, J., & Sun, Y. (2012). Evidence of a role of inositol polyphosphate 5-phosphatase INPP5E in cilia formation in zebrafish. *Vision Research, 75*, 98-107. doi:10.1016/j.visres.2012.09.011

Luo, N., West, C. C., Murga-Zamalloa, C. A., Sun, L., Anderson, R. M., Wells, C. D., . . . Sun, Y. (2012). OCRL localizes to the primary cilium: a new role for cilia in Lowe syndrome. *Human Molecular Genetics, 21*(15). doi:10.1093/hmg/dds163

Madhivanan, K., & Aguilar, R. C. (2014). Ciliopathies: The Trafficking Connection. *Traffic, 15*(10), 1031-1056. doi:10.1111/tra.12195

Madhivanan, K., Mukherjee, D., & Aguilar, R. C. (2012). Lowe syndrome: Between primary cilia assembly and Rac1-mediated membrane remodeling. *Communicative & integrative biology, 5*(6).

Madhivanan, K., Ramadesikan, S., & Aguilar, R. C. (2015). Role of Ocrl1 in primary cilia assembly. *Int Rev Cell Mol Biol, 317*, 331-347. doi:10.1016/bs.ircmb.2015.02.003

Madhivanan, K., Ramadesikan, S., Hsieh, W. C., Aguilar, M. C., Hanna, C. B., Bacallao, R. L., & Aguilar, R. C. (2020). Lowe syndrome patient cells display mTOR- and RhoGTPase-dependent phenotypes alleviated by rapamycin and statins. *Hum Mol Genet*. doi:10.1093/hmg/ddaa086

Madhivanan K, R. S., Aguilar RC. (2016). Role of Ocrl1 and Inpp5E in primary cilia assembly and maintainence: a phosphatidylinositol phosphatase relay system? *Research and Reports in Biology, 7*, 15-29.

Maji, D., Shaikh, S., Solanki, D., & Gaurav, K. (2013). Safety of statins. *Indian J Endocrinol Metab, 17*(4), 636-646. doi:10.4103/2230-8210.113754

Manji, S. S., Williams, L. H., Miller, K. A., Ooms, L. M., Bahlo, M., Mitchell, C. A., & Dahl, H. H. (2011). A mutation in synaptojanin 2 causes progressive hearing loss in the ENU-mutagenised mouse strain Mozart. *PLoS One, 6*(3), e17607. doi:10.1371/journal.pone.0017607

Mao, Y., Balkin, D. M., Zoncu, R., Erdmann, K. S., Tomasini, L., Hu, F., . . . De Camilli, P. (2009). A PH domain within OCRL bridges clathrin-mediated membrane trafficking to phosphoinositide metabolism. *Embo Journal, 28*(13), 1831-1842. doi:10.1038/emboj.2009.155

Marion, S., Mazzolini, J., Herit, F., Bourdoncle, P., Kambou-Pene, N., Hailfinger, S., . . . Niedergang, F. (2012). The NF-kappa B Signaling Protein Bcl10 Regulates Actin Dynamics by Controlling AP1 and OCRL-Bearing Vesicles. *Developmental Cell, 23*(5), 954-967. doi:10.1016/j.devcel.2012.09.021

Marioni, R. E., McRae, A. F., Bressler, J., Colicino, E., Hannon, E., Li, S., . . . Deary, I. J. (2018). Meta-analysis of epigenome-wide association studies of cognitive abilities. *Mol Psychiatry, 23*(11), 2133-2144. doi:10.1038/s41380-017-0008-y

Martínez-Menárguez, J., Tomás, M., Martínez-Martínez, N., & Martínez-Alonso, E. (2019). Golgi Fragmentation in Neurodegenerative Diseases: Is There a Common Cause? *Cells, 8*(7). doi:10.3390/cells8070748

Matzaris, M., Jackson, S. P., Laxminarayan, K. M., Speed, C. J., & Mitchell, C. A. (1994). Identification and characterization of the phosphatidylinositol-(4, 5)-bisphosphate 5-phosphatase in human platelets. *J Biol Chem, 269*(5), 3397-3402.

Maxwell, M. J., Srivastava, N., Park, M. Y., Tsantikos, E., Engelman, R. W., Kerr, W. G., & Hibbs, M. L. (2014). SHIP-1 deficiency in the myeloid compartment is insufficient to induce myeloid expansion or chronic inflammation. *Genes Immun, 15*(4), 233-240. doi:10.1038/gene.2014.9

May-Simera, H., Nagel-Wolfrum, K., & Wolfrum, U. (2017). Cilia - The sensory antennae in the eye. *Prog Retin Eye Res, 60*, 144-180. doi:10.1016/j.preteyeres.2017.05.001

McCrea, H. J., Paradise, S., Tomasini, L., Addis, M., Melis, M. A., De Matteis, M. A., & De Camilli, P. (2008). All known patient mutations in the ASH-RhoGAP domains of OCRL affect targeting and APPL1 binding. *Biochemical and Biophysical Research Communications, 369*(2), 493-499. doi:10.1016/j.bbrc.2008.02.067

McFarland, A. J., Anoopkumar-Dukie, S., Arora, D. S., Grant, G. D., McDermott, C. M., Perkins, A. V., & Davey, A. K. (2014). Molecular mechanisms underlying the effects of statins in the central nervous system. *Int J Mol Sci, 15*(11), 20607-20637. doi:10.3390/ijms151120607

McPherson, P. S., Garcia, E. P., Slepnev, V. I., David, C., Zhang, X., Grabs, D., . . . De Camilli, P. (1996). A presynaptic inositol-5-phosphatase. *Nature, 379*(6563), 353-357. doi:10.1038/379353a0

Mehta, Z. B., Pietka, G., & Lowe, M. (2014). The cellular and physiological functions of the Lowe syndrome protein OCRL1. *Traffic, 15*, 471-487. doi:10.1111/tra.12160

Mekahli, D., Decuypere, J. P., Sammels, E., Welkenhuyzen, K., Schoeber, J., Audrezet, M. P., . . . De Smedt, H. (2014). Polycystin-1 but not polycystin-2 deficiency causes upregulation of the mTOR pathway and can be synergistically targeted with rapamycin and metformin. *Pflugers Arch, 466*(8), 1591-1604. doi:10.1007/s00424-013-1394-x

Mengubas, K., Jabbar, S. A., Nye, K. E., Wilkes, S., Hoffbrand, A. V., & Wickremasinghe, R. G. (1994). Inactivation of calcium ion-regulating inositol polyphosphate second messengers is impaired in subpopulations of human leukemia cells. *Leukemia, 8*(10), 1718-1725.

Meshki, J., Douglas, S. D., Hu, M., Leeman, S. E., & Tuluc, F. (2011). Substance P induces rapid and transient membrane blebbing in U373MG cells in a p21-activated kinase-dependent manner. *PLoS One, 6*(9), e25332. doi:10.1371/journal.pone.0025332

Milinkovic, V., Bankovic, J., Rakic, M., Stankovic, T., Skender-Gazibara, M., Ruzdijic, S., & Tanic, N. (2013). Identification of novel genetic alterations in samples of malignant glioma patients. *PLoS One, 8*(12), e82108. doi:10.1371/journal.pone.0082108

Mills, S. J., Silvander, C., Cozier, G., Trésaugues, L., Nordlund, P., & Potter, B. V. (2016). Crystal Structures of Type-II Inositol Polyphosphate 5-Phosphatase INPP5B with Synthetic Inositol Polyphosphate Surrogates Reveal New Mechanistic Insights for the Inositol 5-Phosphatase Family. *Biochemistry, 55*(9), 1384-1397.

Mitchell, C. A., Connolly, T. M., & Majerus, P. W. (1989). Identification and isolation of a 75-kDa inositol polyphosphate-5-phosphatase from human platelets. *J Biol Chem, 264*(15), 8873-8877.

Mochizuki, Y., & Takenawa, T. (1999). Novel inositol polyphosphate 5-phosphatase localizes at membrane ruffles. *J Biol Chem, 274*(51), 36790-36795. doi:10.1074/jbc.274.51.36790

Mondin, V. E., Ben El Kadhi, K., Cauvin, C., Jackson-Crawford, A., Bélanger, E., Decelle, B., . . . Carréno, S. (2019). PTEN reduces endosomal PtdIns(4,5)P. *J Cell Biol, 218*(7), 2198-2214. doi:10.1083/jcb.201805155

Montjean, R., Aoidi, R., Desbois, P., Rucci, J., Trichet, M., Salomon, R., . . . Dorseuil, O. (2015). OCRL-mutated fibroblasts from patients with Dent-2 disease exhibit INPP5B-independent phenotypic variability relatively to Lowe syndrome cells. *Human Molecular Genetics, 24*(4), 994-1006. doi:10.1093/hmg/ddu514

Mukhopadhyay, S., Wen, X., Chih, B., Nelson, C. D., Lane, W. S., Scales, S. J., & Jackson, P. K. (2010). TULP3 bridges the IFT-A complex and membrane phosphoinositides to promote trafficking of G protein-coupled receptors into primary cilia. *Genes Dev, 24*(19), 2180-2193. doi:10.1101/gad.1966210

Mukhopadhyay, S., Wen, X., Ratti, N., Loktev, A., Rangell, L., Scales, S. J., & Jackson, P. K. (2013). The Ciliary G-Protein-Coupled Receptor Gpr161 Negatively Regulates the Sonic Hedgehog Pathway via cAMP Signaling. *Cell, 152*(1-2), 210-223. doi:10.1016/j.cell.2012.12.026

Nakamura, S., Hasegawa, J., & Yoshimori, T. (2016). Regulation of lysosomal phosphoinositide balance by INPP5E is essential for autophagosome-lysosome fusion. *Autophagy, 12*(12), 2500-2501. doi:10.1080/15548627.2016.1234568

Nalepa, G., Enzor, R., Sun, Z., Marchal, C., Park, S. J., Yang, Y., . . . Clapp, D. W. (2013). Fanconi anemia signaling network regulates the spindle assembly checkpoint. *J Clin Invest, 123*(9), 3839-3847. doi:10.1172/JCI67364

Nandez, R., Balkin, D. M., Messa, M., Liang, L., Paradise, S., Czapla, H., . . . De Camilli, P. (2014). A role of OCRL in clathrin-coated pit dynamics and uncoating revealed by studies of Lowe syndrome cells. *Elife, 3*, e02975. doi:10.7554/eLife.02975

Nandez, R., Balkin, D. M., Messa, M., Liang, L., Paradise, S., Czapla, H., . . . De Camilli, P. (2014). A role of OCRL in clathrin-coated pit dynamics and uncoating revealed by studies of Lowe syndrome cells. *eLife, 3*, e02975-e02975. doi:10.7554/eLife.02975

Nelson, N., Wundenberg, T., Lin, H., Rehbach, C., Horn, S., Windhorst, S., & Jücker, M. (2020). Characterization of the substrate specificity of the inositol 5-phosphatase SHIP1. *Biochem Biophys Res Commun, 524*(2), 366-370. doi:10.1016/j.bbrc.2020.01.012

Nemoto, Y., Arribas, M., Haffner, C., & DeCamilli, P. (1997). Synaptojanin 2, a novel synaptojanin isoform with a distinct targeting domain and expression pattern. *J Biol Chem, 272*(49), 30817-30821. doi:10.1074/jbc.272.49.30817

Noakes, C. J., Lee, G., & Lowe, M. (2011). The PH domain proteins IPIP27A and B link OCRL1 to receptor recycling in the endocytic pathway. *Molecular Biology of the Cell, 22*(5), 606-623. doi:10.1091/mbc.E10-08-0730

Nobes, C. D., & Hall, A. (1995). Rho, rac, and cdc42 GTPases regulate the assembly of multimolecular focal complexes associated with actin stress fibers, lamellipodia, and filopodia. *Cell, 81*(1), 53-62. doi:10.1016/0092-8674(95)90370-4

Norden, A. G., Lapsley, M., Igarashi, T., Kelleher, C. L., Lee, P. J., Matsuyama, T., . . . Moestrup, S. K. (2002). Urinary megalin deficiency implicates abnormal tubular endocytic function in Fanconi syndrome. *J Am Soc Nephrol, 13*(1), 125-133.

Oltrabella, F., Pietka, G., Ramirez, I. B.-R., Mironov, A., Starborg, T., Drummond, I. A., . . . Lowe, M. (2015). The Lowe Syndrome Protein OCRL1 Is Required for Endocytosis in the Zebrafish Pronephric Tubule. *Plos Genetics, 11*(4). doi:10.1371/journal.pgen.1005058

Olzmann, J. A., Li, L., & Chin, L. S. (2008). Aggresome formation and neurodegenerative diseases: therapeutic implications. *Curr Med Chem, 15*(1), 47-60. doi:10.2174/092986708783330692

Ooms, L. M., Binge, L. C., Davies, E. M., Rahman, P., Conway, J. R., Gurung, R., . . . Mitchell, C. A. (2015). The Inositol Polyphosphate 5-Phosphatase PIPP Regulates AKT1-Dependent Breast Cancer Growth and Metastasis. *Cancer Cell, 28*(2), 155-169. doi:10.1016/j.ccell.2015.07.003

Ooms, L. M., Fedele, C. G., Astle, M. V., Ivetac, I., Cheung, V., Pearson, R. B., . . . Mitchell, C. A. (2006). The inositol polyphosphate 5-phosphatase, PIPP, Is a novel regulator of phosphoinositide 3-kinase-dependent neurite elongation. *Mol Biol Cell, 17*(2), 607-622. doi:10.1091/mbc.e05-05-0469

Ooms, L. M., Horan, K. A., Rahman, P., Seaton, G., Gurung, R., Kethesparan, D. S., & Mitchell, C. A. (2009). The role of the inositol polyphosphate 5-phosphatases in cellular function and human disease. *Biochemical Journal, 419*, 29-49. doi:10.1042/bj20081673

Osborn, D. P. S., Pond, H. L., Mazaheri, N., Dejardin, J., Munn, C. J., Mushref, K., . . . Manzini, M. C. (2017). Mutations in INPP5K Cause a Form of Congenital Muscular Dystrophy Overlapping Marinesco-Sjögren Syndrome and Dystroglycanopathy. *Am J Hum Genet, 100*(3), 537-545. doi:10.1016/j.ajhg.2017.01.019

Palamidessi, A., Frittoli, E., Garré, M., Faretta, M., Mione, M., Testa, I., . . . Di Fiore, P. P. (2008). Endocytic trafficking of Rac is required for the spatial restriction of signaling in cell migration. *Cell, 134*(1), 135-147. doi:10.1016/j.cell.2008.05.034

Park, J., Park, Y., Ryu, I., Choi, M. H., Lee, H. J., Oh, N., . . . Kim, Y. K. (2017). Misfolded polypeptides are selectively recognized and transported toward aggresomes by a CED complex. *Nat Commun, 8*, 15730. doi:10.1038/ncomms15730

Patel, A. B., Mangold, A. R., Costello, C. M., Nagel, T. H., Smith, M. L., Hayden, R. E., & Sekulic, A. (2018). Frequent loss of inositol polyphosphate-5-phosphatase in oropharyngeal squamous cell carcinoma. *J Eur Acad Dermatol Venereol, 32*(1), e36-e37. doi:10.1111/jdv.14462

Pema, M., Drusian, L., Chiaravalli, M., Castelli, M., Yao, Q., Ricciardi, S., . . . Boletta, A. (2016). mTORC1-mediated inhibition of polycystin-1 expression drives renal cyst formation in tuberous sclerosis complex. *Nat Commun, 7*, 10786. doi:10.1038/ncomms10786

Peng, F., Wu, D., Gao, B., Ingram, A. J., Zhang, B., Chorneyko, K., . . . Krepinsky, J. C. (2008). RhoA/Rho-kinase contribute to the pathogenesis of diabetic renal disease. *Diabetes, 57*(6), 1683-1692. doi:10.2337/db07-1149

Pesesse, X., Moreau, C., Drayer, A. L., Woscholski, R., Parker, P., & Erneux, C. (1998). The SH2 domain containing inositol 5-phosphatase SHIP2 displays phosphatidylinositol 3,4,5-trisphosphate and inositol 1,3,4,5-tetrakisphosphate 5-phosphatase activity. *FEBS Lett, 437*(3), 301-303. doi:10.1016/s0014-5793(98)01255-1

Peverall, J., Edkins, E., Goldblatt, J., & Murch, A. (2000). Identification of a novel deletion of the entire OCRL1 gene detected by FISH analysis in a family with Lowe syndrome. *Clin Genet, 58*(6), 479-482. doi:10.1034/j.1399-0004.2000.580609.x

Pirruccello, M., & De Camilli, P. (2012). Inositol 5-phosphatases: insights from the Lowe syndrome protein OCRL. *Trends Biochem Sci, 37*(4), 134-143. doi:10.1016/j.tibs.2012.01.002

Pirruccello, M., Swan, L. E., Folta-Stogniew, E., & De Camilli, P. (2011). Recognition of the F&H motif by the Lowe syndrome protein OCRL. *Nat Struct Mol Biol, 18*(7), 789-795. doi:10.1038/nsmb.2071

Pirruccello, M., Swan, L. E., Folta-Stogniew, E., & De Camilli, P. (2011). Recognition of the F&H motif by the Lowe syndrome protein OCRL. *Nature Structural & Molecular Biology, 18*(7), 789-U763. doi:10.1038/nsmb.2071

Piwon, N., Gunther, W., Schwake, M., Bosl, M. R., & Jentsch, T. J. (2000). CIC-5Cl(-)-channel disruption impairs endocytosis in a mouse model for Dent's disease. *Nature, 408*(6810), 369-373.

Plotnikova, O. V., Seo, S., Cottle, D. L., Conduit, S., Hakim, S., Dyson, J. M., . . . Smyth, I. M. (2015). INPP5E interacts with AURKA, linking phosphoinositide signaling to primary cilium stability. *Journal of Cell Science, 128*(2), 364-372. doi:10.1242/jcs.161323

Ponting, C. P. (2006). A novel domain suggests a ciliary function for ASPM, a brain size determining gene. *Bioinformatics, 22*(9), 1031-1035. doi:10.1093/bioinformatics/btl022

Price, L. S., Leng, J., Schwartz, M. A., & Bokoch, G. M. (1998). Activation of Rac and Cdc42 by integrins mediates cell spreading. *Mol Biol Cell, 9*(7), 1863-1871. doi:10.1091/mbc.9.7.1863

Prosseda, P. P., Luo, N., Wang, B., Alvarado, J. A., Hu, Y., & Sun, Y. (2017). Loss of OCRL increases ciliary PI(4,5)P. *J Cell Sci, 130*(20), 3447-3454. doi:10.1242/jcs.200857

Pugacheva, E. N., Jablonski, S. A., Hartman, T. R., Henske, E. P., & Golemis, E. A. (2007). HEF1-dependent Aurora A activation induces disassembly of the primary cilium. *Cell, 129*(7), 1351-1363. doi:10.1016/j.cell.2007.04.035

Ramirez, I. B., Pietka, G., Jones, D. R., Divecha, N., Alia, A., Baraban, S. C., . . . Lowe, M. (2012). Impaired neural development in a zebrafish model for Lowe syndrome. *Hum Mol Genet, 21*(8), 1744-1759. doi:10.1093/hmg/ddr608

Ramos, A. R., Ghosh, S., Suhel, T., Chevalier, C., Obeng, E. O., Fafilek, B., . . . Erneux, C. (2020). Phosphoinositide 5-phosphatases SKIP and SHIP2 in ruffles, the endoplasmic reticulum and the nucleus: An update. *Adv Biol Regul, 75*, 100660. doi:10.1016/j.jbior.2019.100660

Rbaibi, Y., Cui, S., Mo, D., Carattino, M., Rohatgi, R., Satlin, L. M., . . . Weisz, O. A. (2012). OCRL1 Modulates Cilia Length in Renal Epithelial Cells. *Traffic (Copenhagen, Denmark), 13*(9). doi:10.1111/j.1600-0854.2012.01387.x

Recker, F., Heutter, R., & Ludwig, M. (2013). Lowe syndrome/Dent-2 disease: A comprehensive review of known and novel aspects. *Journal of Pediatric Genetics, 2*(2).

Recker, F., Zaniew, M., Boeckenhauer, D., Miglietti, N., Bokenkamp, A., Moczulska, A., . . . Ludwig, M. (2015). Characterization of 28 novel patients expands the mutational and phenotypic spectrum of Lowe syndrome. *Pediatric Nephrology, 30*(6), 931-943. doi:10.1007/s00467-014-3013-2

Recker, F., Zaniew, M., Böckenhauer, D., Miglietti, N., Bökenkamp, A., Moczulska, A., . . . Ludwig, M. (2015). Characterization of 28 novel patients expands the mutational and phenotypic spectrum of Lowe syndrome. *Pediatr Nephrol, 30*(6), 931-943. doi:10.1007/s00467-014-3013-2

Reiter, J. F., & Leroux, M. R. (2017). Genes and molecular pathways underpinning ciliopathies. *Nat Rev Mol Cell Biol, 18*(9), 533-547. doi:10.1038/nrm.2017.60

Roberts, M. W., Blakey, G. H., Jacoway, J. R., Chen, S. C., & Morris, C. R. (1994). Enlarged dental follicles, a follicular cyst, and enamel hypoplasia in a patient with Lowe syndrome. *Oral Surg Oral Med Oral Pathol, 77*(3), 264-265. doi:10.1016/0030-4220(94)90296-8

Robles, E., & Gomez, T. M. (2006). Focal adhesion kinase signaling at sites of integrin-mediated adhesion controls axon pathfinding. *Nat Neurosci, 9*(10), 1274-1283. doi:10.1038/nn1762

Romani, M., Micalizzi, A., & Valente, E. M. (2013). Joubert syndrome: congenital cerebellar ataxia with the molar tooth. *Lancet Neurol, 12*(9), 894-905. doi:10.1016/S1474-4422(13)70136-4

Ronan, B., Flamand, O., Vescovi, L., Dureuil, C., Durand, L., Fassy, F., . . . Pasquier, B. (2014). A highly potent and selective Vps34 inhibitor alters vesicle trafficking and autophagy. *Nat Chem Biol, 10*(12), 1013-1019. doi:10.1038/nchembio.1681

Ross, T. S., Jefferson, A. B., Mitchell, C. A., & Majerus, P. W. (1991). Cloning and expression of human 75-kDa inositol polyphosphate-5-phosphatase. *J Biol Chem, 266*(30), 20283-20289.

Rubenstein, R. C., Egan, M. E., & Zeitlin, P. L. (1997). In vitro pharmacologic restoration of CFTR-mediated chloride transport with sodium 4-phenylbutyrate in cystic fibrosis epithelial cells containing delta F508-CFTR. *J Clin Invest, 100*(10), 2457-2465. doi:10.1172/JCI119788

Ruellas, A. C., Pithon, M. M., Oliveira, D. D., & Oliveira, A. M. (2008). Lowe syndrome: literature review and case report. *J Orthod, 35*(3), 156-160. doi:10.1179/146531207225022599

Röschinger, W., Muntau, A. C., Rudolph, G., Roscher, A. A., & Kammerer, S. (2000). Carrier assessment in families with lowe oculocerebrorenal syndrome: novel mutations in the OCRL1 gene and correlation of direct DNA diagnosis with ocular examination. *Mol Genet Metab, 69*(3), 213-222. doi:10.1006/mgme.1999.2955

Satir, P., Pedersen, L. B., & Christensen, S. T. (2010). The primary cilium at a glance. *J Cell Sci, 123*(Pt 4), 499-503. doi:10.1242/jcs.050377

Schmid, A. C., Wise, H. M., Mitchell, C. A., Nussbaum, R., & Woscholski, R. (2004). Type II phosphoinositide 5-phosphatases have unique sensitivities towards fatty acid composition and head group phosphorylation. *FEBS Lett, 576*(1-2), 9-13. doi:10.1016/j.febslet.2004.08.052

Schmidt-Ott, K. M., & Barasch, J. (2008). WNT/beta-catenin signaling in nephron progenitors and their epithelial progeny. *Kidney Int, 74*(8), 1004-1008. doi:10.1038/ki.2008.322

Schneider, L., Cammer, M., Lehman, J., Nielsen, S. K., Guerra, C. F., Veland, I. R., . . . Christensen, S. T. (2010). Directional cell migration and chemotaxis in wound healing response to PDGF-AA are coordinated by the primary cilium in fibroblasts. *Cell Physiol Biochem, 25*(2-3), 279-292. doi:10.1159/000276562

Schneider, L., Clement, C. A., Teilmann, S. C., Pazour, G. J., Hoffmann, E. K., Satir, P., & Christensen, S. T. (2005). PDGFR alpha alpha signaling is regulated through the primary cilium in fibroblasts. *Current Biology, 15*(20), 1861-1866. doi:10.1016/j.cub.2005.09.012

Schramm, L., Gal, A., Zimmermann, J., Netzer, K. O., Heidbreder, E., Lopau, K., . . . Wanner, C. (2004). Advanced renal insufficiency in a 34-year-old man with Lowe syndrome. *Am J Kidney Dis, 43*(3), 538-543. doi:10.1053/j.ajkd.2003.11.013

Segawa, T., Hazekil, K., Nigorikawa, K., Morioka, S., Guo, Y., Takasuga, S., . . . Hazeki, O. (2014). Inpp5e increases the Rab5 association and phosphatidylinositol 3-phosphate accumulation at the phagosome through an interaction with Rab20. *Biochemical Journal, 464*, 365-375. doi:10.1042/bj20140916

Sekulic, A., Kim, S. Y., Hostetter, G., Savage, S., Einspahr, J. G., Prasad, A., . . . Bittner, M. (2010). Loss of inositol polyphosphate 5-phosphatase is an early event in development of cutaneous squamous cell carcinoma. *Cancer Prev Res (Phila), 3*(10), 1277-1283. doi:10.1158/1940-6207.CAPR-10-0058

Seow, W. J., Pan, W. C., Kile, M. L., Tong, L., Baccarelli, A. A., Quamruzzaman, Q., . . . Christiani, D. C. (2015). A distinct and replicable variant of the squamous cell carcinoma gene inositol polyphosphate-5-phosphatase modifies the susceptibility of arsenic-associated skin lesions in Bangladesh. *Cancer, 121*(13), 2222-2229. doi:10.1002/cncr.29291

Sharpe, C. C., & Hendry, B. M. (2003). Signaling: focus on Rho in renal disease. *J Am Soc Nephrol, 14*(1), 261-264. doi:10.1097/01.asn.0000048223.05219.e4

Shetty, M., Ramdas, N., Sahni, S., Mullapudi, N., & Hegde, S. (2017). A Homozygous Missense Variant in. *Mol Syndromol, 8*(6), 313-317. doi:10.1159/000479673

Shillingford, J. M., Leamon, C. P., Vlahov, I. R., & Weimbs, T. (2012). Folate-conjugated rapamycin slows progression of polycystic kidney disease. *J Am Soc Nephrol, 23*(10), 1674-1681. doi:10.1681/ASN.2012040367

Shrimpton, A. E., Hoopes, R. R., Jr., Knohl, S. J., Hueber, P., Reed, A. A. C., Christie, P. T., . . . Scheinman, S. J. (2009). OCRL1 Mutations in Dent 2 Patients Suggest a Mechanism for Phenotypic Variability. *Nephron Physiology, 112*(2), 27-36. doi:10.1159/000213506

Sierra Potchanant, E. A., Cerabona, D., Sater, Z. A., He, Y., Sun, Z., Gehlhausen, J., & Nalepa, G. (2017). INPP5E Preserves Genomic Stability through Regulation of Mitosis. *Mol Cell Biol, 37*(6). doi:10.1128/MCB.00500-16

Somasundaram, R., Fernandes, S., Deuring, J. J., de Haar, C., Kuipers, E. J., Vogelaar, L., . . . Fuhler, G. M. (2017). Analysis of SHIP1 expression and activity in Crohn's disease patients. *PLoS One, 12*(8), e0182308. doi:10.1371/journal.pone.0182308

Speed, C. J., Little, P. J., Hayman, J. A., & Mitchell, C. A. (1996). Underexpression of the 43 kDa inositol polyphosphate 5-phosphatase is associated with cellular transformation. *EMBO J, 15*(18), 4852-4861.

Stallone, G., Infante, B., Grandaliano, G., Bristogiannis, C., Macarini, L., Mezzopane, D., . . . Gesualdo, L. (2012). Rapamycin for treatment of type I autosomal dominant polycystic kidney disease (RAPYD-study): a randomized, controlled study. *Nephrol Dial Transplant, 27*(9), 3560-3567. doi:10.1093/ndt/gfs264

Suarez-Artiles, L., Perdomo-Ramirez, A., Ramos-Trujillo, E., & Claverie-Martin, F. (2018). Splicing Analysis of Exonic OCRL Mutations Causing Lowe Syndrome or Dent-2 Disease. *Genes (Basel), 9*(1). doi:10.3390/genes9010015

Suchy, S. F., & Nussbaum, R. L. (2002). The deficiency of PIP2 5-phosphatase in Lowe syndrome affects actin polymerization. *American Journal of Human Genetics, 71*(6). doi:10.1086/344517

Suchy, S. F., Olivos-Glander, I. M., & Nussabaum, R. L. (1995). Lowe syndrome, a deficiency of phosphatidylinositol 4,5-bisphosphate 5-phosphatase in the Golgi apparatus. *Hum Mol Genet, 4*(12), 2245-2250.

Suruda, C., Tsuji, S., Yamanouchi, S., Kimata, T., Huan, N. T., Kurosawa, H., . . . Kaneko, K. (2017). Decreased urinary excretion of the ectodomain form of megalin (A-megalin) in children with OCRL gene mutations. *Pediatr Nephrol, 32*(4), 621-625. doi:10.1007/s00467-016-3535-x

Swan, L. E., Tomasini, L., Pirruccello, M., Lunardi, J., & De Camilli, P. (2010). Two closely related endocytic proteins that share a common OCRL-binding motif with APPL1. *Proceedings of the National Academy of Sciences of the United States of America, 107*(8), 3511-3516. doi:10.1073/pnas.0914658107

Takabatake, Y., Kimura, T., Takahashi, A., & Isaka, Y. (2014). Autophagy and the kidney: health and disease. In *Nephrol Dial Transplant* (Vol. 29, pp. 1639-1647). England: The Author 2014. Published by Oxford University Press on behalf of ERA-EDTA.

Tasic, V., Lozanovski, V. J., Korneti, P., Ristoska-Bojkovska, N., Sabolic-Avramovska, V., Gucev, Z., & Ludwig, M. (2011). Clinical and laboratory features of Macedonian children with OCRL mutations. *Pediatr Nephrol, 26*(4), 557-562. doi:10.1007/s00467-010-1758-9

Taylor, J. R. (1997). *An introduction to error analysis: The Study of Uncertainties in Physical Measurements* (2nd ed.): University Science Books, 2nd edn.

Teachey, D. T. (2012). New advances in the diagnosis and treatment of autoimmune lymphoproliferative syndrome. *Curr Opin Pediatr, 24*(1), 1-8. doi:10.1097/MOP.0b013e32834ea739

Thomas, M. P., Erneux, C., & Potter, B. V. (2017). SHIP2: Structure, Function and Inhibition. *Chembiochem, 18*(3), 233-247. doi:10.1002/cbic.201600541

Thomas, S., Wright, K. J., Le Corre, S., Micalizzi, A., Romani, M., Abhyankar, A., . . . Attie-Bitach, T. (2014). A Homozygous PDE6D Mutation in Joubert Syndrome Impairs Targeting of Farnesylated INPP5E Protein to the Primary Cilium. *Human Mutation, 35*(1), 137-146. doi:10.1002/humu.22470

Tobin, J. L., Di Franco, M., Eichers, E., May-Simera, H., Garcia, M., Yan, J., . . . Beales, P. L. (2008). Inhibition of neural crest migration underlies craniofacial dysmorphology and Hirschsprung's disease in Bardet-Biedl syndrome. *Proceedings of the National Academy of Sciences of the United States of America, 105*(18), 6714-6719. doi:10.1073/pnas.0707057105

Totsukawa, G., Wu, Y., Sasaki, Y., Hartshorne, D. J., Yamakita, Y., Yamashiro, S., & Matsumura, F. (2004). Distinct roles of MLCK and ROCK in the regulation of membrane protrusions and focal adhesion dynamics during cell migration of fibroblasts. *J Cell Biol, 164*(3), 427-439. doi:10.1083/jcb.200306172

Totsukawa, G., Yamakita, Y., Yamashiro, S., Hartshorne, D. J., Sasaki, Y., & Matsumura, F. (2000). Distinct roles of ROCK (Rho-kinase) and MLCK in spatial regulation of MLC phosphorylation for assembly of stress fibers and focal adhesions in 3T3 fibroblasts. *J Cell Biol, 150*(4), 797-806.

Travaglini, L., Brancati, F., Silhavy, J., Iannicelli, M., Nickerson, E., Elkhartoufi, N., . . . Int, J. S. G. (2013). Phenotypic spectrum and prevalence of INPP5E mutations in Joubert Syndrome and related disorders. *European Journal of Human Genetics, 21*(10), 1074-1078. doi:10.1038/ejhg.2012.305

Tresaugues, L., Silvander, C., Flodin, S., Welin, M., Nyman, T., Graslund, S., . . . Nordlund, P. (2014). Structural basis for phosphoinositide substrate recognition, catalysis, and membrane interactions in human inositol polyphosphate 5-phosphatases. In *Structure* (Vol. 22, pp. 744-755). United States: 2014 Elsevier Ltd.

Tresaugues, L., Silvander, C., Flodin, S., Welin, M., Nyman, T., Graslund, S., . . . Nordlund, P. (2014). Structural Basis for Phosphoinositide Substrate Recognition, Catalysis, and Membrane Interactions in Human Inositol Polyphosphate 5-Phosphatases. *Structure, 22*(5), 744-755. doi:10.1016/j.str.2014.01.013

Tripathi, R. C., Cibis, G. W., & Tripathi, B. J. (1986). Pathogenesis of cataracts in patients with Lowe's syndrome. *Ophthalmology, 93*(8), 1046-1051. doi:10.1016/s0161-6420(86)33622-4

Tsai, S. J., & O'Donnell, D. (1997). Dental findings in an adult with Lowe's syndrome. *Spec Care Dentist, 17*(6), 207-210. doi:10.1111/j.1754-4505.1997.tb00898.x

Tsujishita, Y., Guo, S. L., Stolz, L. E., York, J. D., & Hurley, J. H. (2001). Specificity determinants in phosphoinositide dephosphorylation: Crystal structure of an archetypal inositol polyphosphate 5-phosphatase. *Cell, 105*(3), 379-389. doi:10.1016/s0092-8674(01)00326-9

Ueno, T., Falkenburger, B. H., Pohlmeyer, C., & Inoue, T. (2011). Triggering actin comets versus membrane ruffles: distinctive effects of phosphoinositides on actin reorganization. *Sci Signal, 4*(203), ra87. doi:10.1126/scisignal.2002033

Ungewickell, A., Ward, M. E., Ungewickell, E., & Majerus, P. W. (2004). The inositol polyphosphate 5-phosphatase Ocrl associates with endosomes that are partially coated with clathrin. *Proc Natl Acad Sci U S A, 101*(37), 13501-13506. doi:10.1073/pnas.0405664101

Ungewickell, A. J., & Majerus, P. W. (1999). Increased levels of plasma lysosomal enzymes in patients with Lowe syndrome. *Proceedings of the National Academy of Sciences of the United States of America, 96*(23), 13342-13344. doi:10.1073/pnas.96.23.13342

Utsch, B., Bökenkamp, A., Benz, M. R., Besbas, N., Dötsch, J., Franke, I., . . . Ludwig, M. (2006). Novel OCRL1 mutations in patients with the phenotype of Dent disease. *Am J Kidney Dis, 48*(6), 942.e941-914. doi:10.1053/j.ajkd.2006.08.018

Valente, E. M., Brancati, F., Boltshauser, E., & Dallapiccola, B. (2013). Clinical utility gene card for: Joubert syndrome--update 2013. *Eur J Hum Genet, 21*(10). doi:10.1038/ejhg.2013.10

Valente, E. M., Brancati, F., & Dallapiccola, B. (2008). Genotypes and phenotypes of Joubert syndrome and related disorders. *Eur J Med Genet, 51*(1), 1-23. doi:10.1016/j.ejmg.2007.11.003

Valente, E. M., Dallapiccola, B., & Bertini, E. (2013). Joubert syndrome and related disorders. *Handb Clin Neurol, 113*, 1879-1888. doi:10.1016/B978-0-444-59565-2.00058-7

van Rahden, V. A., Brand, K., Najm, J., Heeren, J., Pfeffer, S. R., Braulke, T., & Kutsche, K. (2012). The 5-phosphatase OCRL mediates retrograde transport of the mannose 6-phosphate receptor by regulating a Rac1-cofilin signalling module. *Human Molecular Genetics, 21*(23), 5019-5038. doi:10.1093/hmg/dds343

Verdier, P., Morthorst, S. K., & Pedersen, L. B. (2016). Targeting of ASH Domain-Containing Proteins to the Centrosome. *Methods Mol Biol, 1454*, 15-33. doi:10.1007/978-1-4939-3789-9_2

Vicinanza, M., Di Campli, A., Polishchuk, E., Santoro, M., Di Tullio, G., Godi, A., . . . De Matteis, M. A. (2011). OCRL controls trafficking through early endosomes via PtdIns4,5P(2)-dependent regulation of endosomal actin. *Embo Journal, 30*(24), 4970-4985. doi:10.1038/emboj.2011.354

Vora, S. M., & Phillips, B. T. (2016). The benefits of local depletion: The centrosome as a scaffold for ubiquitin-proteasome-mediated degradation. *Cell Cycle, 15*(16), 2124-2134. doi:10.1080/15384101.2016.1196306

Voronov, S. V., Frere, S. G., Giovedi, S., Pollina, E. A., Borel, C., Zhang, H., . . . Di Paolo, G. (2008). Synaptojanin 1-linked phosphoinositide dyshomeostasis and cognitive deficits in mouse models of Down's syndrome. *Proc Natl Acad Sci U S A, 105*(27), 9415-9420. doi:10.1073/pnas.0803756105

Voth, K. A., Chung, I. Y. W., van Straaten, K., Li, L., Boniecki, M. T., & Cygler, M. (2019). The structure of Legionella effector protein LpnE provides insights into its interaction with Oculocerebrorenal syndrome of Lowe (OCRL) protein. *FEBS J, 286*(4), 710-725. doi:10.1111/febs.14710

Wang, F., Ijuin, T., Itoh, T., & Takenawa, T. (2011). Regulation of IGF-1/PI3K/Akt signalling by the phosphoinositide phosphatase pharbin. *Journal of Biochemistry, 150*(1), 83-93. doi:10.1093/jb/mvr037

Warner, H., Wilson, B. J., & Caswell, P. T. (2019). Control of adhesion and protrusion in cell migration by Rho GTPases. *Curr Opin Cell Biol, 56*, 64-70. doi:10.1016/j.ceb.2018.09.003

Waugh, M. G. (2016). Chromosomal Instability and Phosphoinositide Pathway Gene Signatures in Glioblastoma Multiforme. *Mol Neurobiol, 53*(1), 621-630. doi:10.1007/s12035-014-9034-9

Weber, S. S., Ragaz, C., & Hilbi, H. (2009). The inositol polyphosphate 5-phosphatase OCRL1 restricts intracellular growth of Legionella, localizes to the replicative vacuole and binds to the bacterial effector LpnE. *Cell Microbiol, 11*(3), 442-460. doi:10.1111/j.1462-5822.2008.01266.x

Weissgerber, T. L., Milic, N. M., Winham, S. J., & Garovic, V. D. (2015). Beyond bar and line graphs: time for a new data presentation paradigm. *PLoS Biol, 13*(4), e1002128. doi:10.1371/journal.pbio.1002128

Whisstock, J. C., Romero, S., Gurung, R., Nandurkar, H., Ooms, L. M., Bottomley, S. P., & Mitchell, C. A. (2000). The inositol polyphosphate 5-phosphatases and the apurinic/apyrimidinic base excision repair endonucleases share a common mechanism for catalysis. *Journal of Biological Chemistry, 275*(47), 37055-37061. doi:10.1074/jbc.M006244200

Wiessner, M., Roos, A., Munn, C. J., Viswanathan, R., Whyte, T., Cox, D., . . . Senderek, J. (2017). Mutations in INPP5K, Encoding a Phosphoinositide 5-Phosphatase, Cause Congenital Muscular Dystrophy with Cataracts and Mild Cognitive Impairment. *Am J Hum Genet, 100*(3), 523-536. doi:10.1016/j.ajhg.2017.01.024

Williams, C., Choudhury, R., McKenzie, E., & Lowe, M. (2007). Targeting of the type II inositol polyphosphate 5-phosphatase INPP5B to the early secretory pathway. *Journal of Cell Science, 120*(22), 3941-3951. doi:10.1242/jcs.014423

Wisniewski, K. E., Kieras, F. J., French, J. H., Houck, G. E., & Ramos, P. L. (1984). Ultrastructural, neurological, and glycosaminoglycan abnormalities in lowe's syndrome. *Ann Neurol, 16*(1), 40-49. doi:10.1002/ana.410160109

Wu, G., Zhang, W., Na, T., Jing, H., Wu, H., & Peng, J. B. (2012). Suppression of intestinal calcium entry channel TRPV6 by OCRL, a lipid phosphatase associated with Lowe syndrome and Dent disease. *Am J Physiol Cell Physiol, 302*(10), C1479-1491. doi:10.1152/ajpcell.00277.2011

Xu, W., Jin, M., Hu, R., Wang, H., Zhang, F., Yuan, S., & Cao, Y. (2017). The Joubert Syndrome Protein Inpp5e Controls Ciliogenesis by Regulating Phosphoinositides at the Apical Membrane. *J Am Soc Nephrol, 28*(1), 118-129. doi:10.1681/ASN.2015080906

Yang, A. W., Sachs, A. J., & Nystuen, A. M. (2015). Deletion of Inpp5a causes ataxia and cerebellar degeneration in mice. *Neurogenetics, 16*(4), 277-285. doi:10.1007/s10048-015-0450-4

Yousaf, S., Sheikh, S. A., Riazuddin, S., Waryah, A. M., & Ahmed, Z. M. (2018). INPP5K variant causes autosomal recessive congenital cataract in a Pakistani family. *Clin Genet, 93*(3), 682-686. doi:10.1111/cge.13143

Yu, K., Shi, C., Toral-Barza, L., Lucas, J., Shor, B., Kim, J. E., . . . Gibbons, J. J. (2010). Beyond rapalog therapy: preclinical pharmacology and antitumor activity of WYE-125132, an ATP-competitive and specific inhibitor of mTORC1 and mTORC2. *Cancer Res, 70*(2), 621-631. doi:10.1158/0008-5472.CAN-09-2340

Zaniew, M., Bökenkamp, A., Kolbuc, M., La Scola, C., Baronio, F., Niemirska, A., . . . Bockenhauer, D. (2018). Long-term renal outcome in children with OCRL mutations: retrospective analysis of a large international cohort. *Nephrol Dial Transplant, 33*(1), 85-94. doi:10.1093/ndt/gfw350

Zeng, L. H., Xu, L., Gutmann, D. H., & Wong, M. (2008). Rapamycin prevents epilepsy in a mouse model of tuberous sclerosis complex. *Ann Neurol, 63*(4), 444-453. doi:10.1002/ana.21331

Zhang, H., Dou, J., Yu, Y., Zhao, Y., Fan, Y., Cheng, J., . . . Yang, J. (2015). mTOR ATP-competitive inhibitor INK128 inhibits neuroblastoma growth via blocking mTORC signaling. *Apoptosis, 20*(1), 50-62. doi:10.1007/s10495-014-1066-0

Zhang, X., Jefferson, A. B., Auethavekiat, V., & Majerus, P. W. (1995). The protein deficient in Lowe syndrome is a phosphatidylinositol-4,5-bisphosphate 5-phosphatase. *Proc Natl Acad Sci U S A, 92*(11), 4853-4856.

Zhang, X. L., Hartz, P. A., Philip, E., Racusen, L. C., & Majerus, P. W. (1998). Cell lines from kidney proximal tubules of a patient with Lowe syndromelack OCRL inositol polyphosphate 5-phosphatase and accumulate phosphatidylinositol 4,5-bisphosphate. *Journal of Biological Chemistry, 273*(3). doi:10.1074/jbc.273.3.1574

Zhong, S., Zhang, X., Chen, L., Ma, T., Tang, J., & Zhao, J. (2015). Statin use and mortality in cancer patients: Systematic review and meta-analysis of observational studies. *Cancer Treat Rev, 41*(6), 554-567. doi:10.1016/j.ctrv.2015.04.005

Zullo, A., Iaconis, D., Barra, A., Cantone, A., Messaddeq, N., Capasso, G., . . . Franco, B. (2010). Kidney-specific inactivation of Ofd1 leads to renal cystic disease associated with upregulation of the mTOR pathway. *Hum Mol Genet, 19*(14), 2792-2803. doi:10.1093/hmg/ddq180

# VITA

Swetha Ramadesikan was born in Chennai, India. She obtained her bachelor's degree in Bioengineering at SASTRA University, Tanjore India in 2012. She spent a year as a research intern at the Brigham and Women's Hospital, Boston studying the molecular mechanisms of kidney injury and renal cell carcinoma. In 2013, she joined Purdue University as a graduate student in the Dept. of Biological Sciences. She joined the Aguilar lab in June 2014. Swetha will continue her research career as a postdoctoral research fellow at the Institute for Genomic Medicine at Nationwide Children's Hospital, Columbus OH.